INFORMATION TO USERS

This manuscript has been reproduced from the microfilm master. UMI films the text directly from the original or copy submitted. Thus, some thesis and dissertation copies are in typewriter face, while others may be from any type of computer printer.

The quality of this reproduction is dependent upon the quality of the copy submitted. Broken or indistinct print, colored or poor quality illustrations and photographs, print bleedthrough, substandard margins, and improper alignment can adversely affect reproduction.

In the unlikely event that the author did not send UMI a complete manuscript and there are missing pages, these will be noted. Also, if unauthorized copyright material had to be removed, a note will indicate the deletion.

Oversize materials (e.g., maps, drawings, charts) are reproduced by sectioning the original, beginning at the upper left-hand corner and continuing from left to right in equal sections with small overlaps.

ProQuest Information and Learning
300 North Zeeb Road, Ann Arbor, MI 48106-1346 USA
800-521-0600

FINITE ELEMENT MODELING AND ANALYSIS OF ROTOR-BEARING SYSTEMS

BY

Akram Awni Mohammed Hamad Rabayah

A Thesis Presented to the

DEANSHIP OF GRADUATE STUDIES

KING FAHD UNIVERSITY OF PETROLEUM & MINERALS

DHAHRAN, SAUDI ARABIA

In Partial Fulfillment of the
Requirements for the Degree of

MASTER OF SCIENCE

In

MECHANICAL ENGINEERING

OCTOBER 2002

ProQuest Information and Learning Company
300 North Zeeb Road
P.O. Box 1346
Ann Arbor, MI 48106-1346

DEANSHIP OF GRADUATE STUDIES

This thesis, written by Akram Awni Hamad under the direction of his thesis adviser and approved by his thesis committee, has been presented and accepted by the Dean of Graduate Studies, in partial fulfillment of the requirements for the degree of MASTER OF SCIENCE IN MECHANICAL ENGINEERING

Thesis Committee

Dr. Bassem Al-Bedoor, Associate Professor

Thesis Adviser

Dr. Mehemt Sunar, Associate Professor

Co-Chairman

Department Chairman

Dr. Yehia Khulief, Professor

Member

Dean of Graduate Studies
Dr. Osama A. Jannadi

Dr. Saif Al-Kaabi, Assistant Professor

Memebr

9 March 2003
Date

Dr. B. S. Yilbas, Professor

Memebr

عمادة الدراسات العليا
DEANSHIP OF GRADUATE STUDIES

THESIS ABSTRACT

NAME: **Akram Awni Mohammed Hamad Rabayah**

TITLE: **Finite Element Modeling and Analysis of Rotor-Bearing Systems**

MAJOR: **Mechanics – Mechanical Engineering**

DATE: **6 October 2002**

In this study, a finite element dynamic model of rotor-disk-bearing system was developed using Timoshenko beam theory to incorporate shear deformation and rotary inertia. Each shaft element includes unbalance and gyroscopic effects as well as structural damping. The hydrodynamic bearing system was modeled, damping and stiffness parameters were obtained, using standard Reynolds equation solution for short bearing with half film pressure profile and Sommerfeld static eccentricity. The Reynolds equation was then solved for the case of dynamic loading for which a closed loop interaction between the shaft center position and bearing equations was derived. Lastly, the whole bearing system of equations was solved using finite series solution in rotating coordinate system that rotates at fluid circumferential velocity. With this solution the study included the effects of fluid inertia as well as dynamic eccentricity or shaft position. The study showed that bearing displacements have much slower decay rate and clearer effect of disk unbalance when dynamic eccentricity and fluid inertia are included in the closed loop rotor-bearing system.

Masters of Science Degree
King Fahd University of Petroleum and Minerals
Dhahran, Saudi Arabia

ملخص الرسالة

الاسم : اكرم عوني حمد ربايعه

عنوان الدراسة : تطوير وتحليل نموذج عنصر محدود لنظام محور وحامل مشحم

التخصص : الهندسة الميكانيكية

التاريخ : أكتوبر ٢٠٠٢م

في هذه الدراسة تم تطوير نموذج عنصر محدود ديناميكي باستخدام نظريه عتبة تيمشنكو والتي تأخذ في الحسبان قوة القطع والعزم الدوراني . كل من عناصر المحور يتضمن خاصية عدم الاتزان والتأثيرات الجيروسكوبيه بالاضافه إلى خاصية الانخماد للمادة المستخدمة . أما نظام الحوامل المشحمة هيدروليكيا فقد طور النموذج باستخدام معادلة رينولد كمحل لحامل مُشحم له ضغط موائع في نصف المجال فقط . هذا الحل لاستخراج خواص الاخماد والقسوة للحامل المشحم اعتمد على معادلة سومرفلد لتخمين خاصية عدم مقابله المراكز الاستاتيكيه .كما تم حل أيضا معادلة رينولد لحاله التحميل الديناميكي والذي كشف لنا كيفيه ترابط معادلات منتصف المحور والحوامل المشحمة وأخيرا تم حل كامل نظام المعادلات للحامل المعادلات المشحم باستخدام حل السلسلة المحددة داخل إطار دوار الأبعاد يدور بسرعة المائع المحيطية . بهذا الحل الدراسة آخذت أيضا خواص عزم المائع المستخدم في الحوامل المتشحمه و عدم مقابله المراكز في الحالة الديناميكية . استنتجت الدراسة أن اهتزاز وتحرك الحوامل المشحمة لها معدل اضمحلال تنازلي بطيء و ظهور تأثير عالي لعدم اتزان أقراص المحور عندما يتم أخذ خواص عزم المائع وعدم مقابلة المراكز في الحسبان .

درجه الماجستير في العلوم

جامعه الملك فهد للبترول والمعادن

الظهران – المملكة العربية السعودية

DEDICATION

To my BMW and the three monkeys.

ACKNOWLEDGMENT

Acknowledgment is due to the King Fahd University of Petroleum & Minerals for supporting this research. Also acknowledgement is due to Bently Nevada for supporting my study by providing financial support, research advise, data and research material and equipment.

I wish to express my appreciation to Dr. Bassem Al-Bedoor who served as my major advisor. Also I would like to express my appreciation for Dr. Mehemt Sunar, Dr. Yehia Khulief, Dr. Saif Al-Kaabi and Dr. B. Yilbas for their guidance while serving in my thesis committee. My appreciation also goes to Dr. Yagoub Al-Nassar for his guidance and involvement during the course of the thesis work.

TABLE OF CONTENTS

LIST OF FIGURES

LIST OF TABLES

CHAPTER 1

INTRODUCTION TO ROTORDYNAMICS

The steadily increasing demand on improving the performance of high-speed machinery have led to a considerable interest in the use of well-designed rotor-bearing systems. Rotor-bearing Models are used to predict the operational behavior as well as the rated performance of proposed machine configurations and adjust designs by testing the proposed configurations. Accurate modeling of the dynamic behavior of turbomachinery during design stage and even in later stages influence the performance of such machinery to either produce or absorb an amazing amount of power through high speed rotating shafts/rotors without unpredicted problems.

The rotordynamics of rotating machinery are heavily influenced by the bearings system dynamics, predominantly the rotor stiffness and damping depend strongly on the bearing/support stiffness and damping. For accurate predication the rotor-bearing system, the complete system should be modeled to account for the closed loop relation between the rotor dynamics and the bearing fluid dynamics. Late 18^{th} century and early 19^{th} century when modern industrial revolution started with the steam engine generating motion, shafts used to translate such motion were believed to have infinite stiffness. The common understanding of such motion was that machinery cannot go beyond the first natural frequency and as such it is called until date "critical speed". With the invention of fluid lubricated bearings, the shaft disk system now have a source of damping which enabled designers to go in speeds beyond the "critical" and hence increase machinery throughput.

1.1 LITERATURE SURVEY

The subject of rotordynamics have been treated by a number of textbooks, hundreds of published papers and a number of commercial and academic software packages that produce simulation results for rotor and bearing design configurations. Fundamental understanding of lateral vibrations of rotating machinery is attributed to Jeffcot 1919 as reported by Ruhl, et al, [1]. Various configurations have been used to model machinery extending from the simple Jeffcot rotor model mounted on two support bearings to multi-disk multi-rotor with bearings in recent research, prior to 1960 lumped parameter models were used. Ruhl, et al, [1] used rotor discretization into finite disk elements or Finite Elements Modeling (FEM). In his work Ruhl introduced a FEM model that included translational inertia and bending stiffness only. In 1970's researchers used Rayleigh beam based FEM accounting for translational and rotational inertia, gyroscopic moments, bending and shear deformations as well as axial load. Nelson and McVaugh, [2] later introduced axial torque as well. The solution procedures to FEM vary from transfer matrix to modal analysis to impedance and finite element simulation.

Stodola 1925 and Smith 1933 experiments as reported by Ruhl, et al, [1] showed negative energy drain effects, such as instabilities associated with fluid film bearings. Considerable attention in the literature for fluid instabilities started by the works of Newkrik 1925, Robertson 1933, Hagg 1946 and Orbeck 1958, as reported by Lund [3], research nowadays pay attention mainly to system stability and control research as opposed to determining critical speeds, mode shapes and unbalance response. Few research projects do

address machinery components interaction such as Rotor-Bearing and Rotor-Disk–Blade and Rotor-Housing interactions.

1.2 FINITE ELEMENT METHOD

Ruhl applied the finite element approach developed initially for structural vibration analysis, to rotating machinery in 1972. The method uses the approach of discretizing a shape into finite number of elements with degrees of freedom at each element node, an assumed shape function or element behavior to represent the motion of particles in each element is used to derive an interpolation between element nodal parameters and the global or full body parameters such as displacement, velocity, etc. Procedures using numerical methods are utilized to derive the system time and frequency based response as well as natural frequencies and mode shapes. Lund, [3] included hysteretic internal damping and aerodynamic forces in the formulation of shaft elements. He used bearing flexibility effect to reduce critical speeds utilizing Prohl's method, which is based on Holzer eigen-values computational procedure. Nelson, et al. [2, 4] presented a rotor/bearing model using the FEM accounting for the effects of rotary inertia, gyroscopic moments and axial load. They did not include however shear deformation, axial torque or internal damping. Nelson [4] used Timoshenko beam theory to establish the shape functions to interpolate shaft finite element coordinates into global system coordinates. The Timoshenko beam model [1] accounts for transverse shear effects, Nelson [4] did not include internal damping in this work. Abduljabbar, et al. [5], presented a FEM of a rotor/bearing systems incorporating the effects of rotary inertia, gyroscopic moments of disks, internal viscous and hysteretic damping. Mohiuddin and Khulief [6, 7] developed a FEM for a conical Timoshenko beam that included coupling between bending and torsional motions. Inertia coupling between pending and torsional deformations as well as shear deformations were studied up to the tenth mode. Shear deformation was shown to have significant effects at higher modes.

1.3 ROTOR-BEARING SYSTEM

Most of the early research work in rotor dynamics treated rotor and bearings as separate systems, it was not until the 1970's when research work started to consider the effects of bearings and/or flexible supports and the fluid dynamics effects on rotor-bearing dynamics. At the same time fluid film hydrodynamic bearings research have been addressing fluid film dynamic instabilities as well as various methods of solution for the Navier-Stocks/Reynolds equations without considering the rotor-bearing system on fluid dynamics.

Some research work did address Rotor-Bearing-Fluid dynamic interaction partially. Dubois, et al, [8]. presented short bearing analytical solution of the Reynolds equation which included the effect of end leakage and end wise flow from the oil film, in their work the effect of film pressure on circumferential flow was neglected. Hori [9] investigated the oil whip instability phenomenon both theoretically and experimentally; in his work he presented a long bearing solution of the Reynolds equation under static loading condition and tried to explain the inertia effect of the fluid. Hori's work neglected negative pressure in order to account for cavitation effects. Lund, [3] analyzed self-excited oscillation by using non linear equations of motion, he solved the equations using an averaging method and analyzed the stability of the system. Kirk & Gunter [10] studied the stability of rotor systems with non-linear fluid film bearings and included the whip instability phenomenon by accounting for shaft flexibility. Zorzi and Nelson [11] included the effect of internal viscous and hysteretic damping effects of anistropic bearings. Hashish, et al., [12, 13] used the full/partial film cases solution of a linearized Reynolds equation to separate wedge and squeeze pressure components and at later stages modeled rotor/bearing system with non-linear stiffness & damping for finite bearings and flexible bearing supports.

Modern research in rotor-bearing dynamics and contributions of rotor bearing system interaction are attributed to some key organizations. Texas A&M Turbomachinery Lab did extensive work on squeeze film dampers in association with NASA to address instabilities in fluid film bearings used on cryogenic space shuttle fuel pumps. Bently Rotor Dynamics Research Corp (BRDRC[1]) conducted numerous experimental and numerical work mid 1980's – 2002 to identify fluid/solid interaction in rotor-bearing systems in order to eliminate fluid film bearings instability phenomena [14, 15, 16, 17, 18, 19, 20, 21].

BRDRC used system perturbation and identification techniques to arrive at rotor-bearing model equations and extract empirical relations between fluid parameters and shaft eccentricity. Their work covered a wide range of rotor-bearing system configurations of unloaded/loaded, isotropic and anistropic rotors. They investigated first to multi bending mode and used variation of perturbation sweep frequency circular forces to verify the research results. Their work in this area led to the identification of fluid average circumferential velocity as a varying parameter contrary to the traditionally assumed one half running speed. They also identified the threshold of rotor-bearing system instability after which the rotor-bearing system enters into oil whirl and oil whip. BRDRC and NASA conducted joint research work, Tam, et al., [22] to solve numerically a three-dimensional Navier-Stocks conservative equations for a lumped fluid model in a bearing, the simulation was used to identify fluid flow injection effects on axial flow as a mean to eliminate fluid induced instabilities.

[1] Bently Rotor Dynamics Research Corp. (BRDRC), is a research facility lead by Mr. Don Bently owner and founder of Bently Nevada Corporation to conduct research in various rotordynamics subjects.

1.4 SYSTEM NON-LINEAR INTERACTION MODELING

Rotating machinery nowadays operate at high speeds, for example air compressors running at 30,000 rpm[2] and as such rotor-bearing system modeling is increasing in complexity due to the presence of non-linear interaction between various machine components at such high speeds. Smith 1964, Lund 1975 and Tecza 1983 all in their works showed the presence of fluid inertia effect to various degrees and tried to quantify or model it, as reported by Elshafei [24]. Elshafei modeled fluid inertia effect on bearing stiffness and damping in short journal bearings by using energy approximation method. However, the analysis was limited to the bearing system only and attention to the rotordynamics was not given. The same observations have been reported and investigated by Bently, et al., [14] for lightly loaded journal bearings. Modern research work by Barret, et al., [25], Berger, et al, [26], Rieger and Zhou, [27], Shabanah, and Zu, [28] on system non-linear interaction between elastic support to bearing, thrust to radial bearings, viscoelastic support to rotor, disk blades to rotor and squeeze film dampers to rotor did emphasize the non-linear system interaction effects at higher speeds and modes. Most of the recent research in rotordynamics nowadays is directed towards vibration control using flexible dampers, magnetic bearings, piezoelectric shaft material and recently externally pressurized fluid bearings. Other areas of research address specific phenomenons such as aerodynamic instabilities, crack shaft dynamics and torsional/bending vibration coupling. Wong, [29] transformed non-linear partial differential equations in order to solve for beam bending/torsional vibration using Chebyshev series. Mohiuddin and Khulief, [6, 7] as mentioned earlier used modal truncation on a conical beam element to study torsional/bending deformations at high modes.

---

[2] Rotations Per Minute

1.5 RESEARCH CONTRIBUTIONS

None of the recent work in the area of rotor-bearing interaction investigated the effect of instantaneous dynamic eccentricity[3] on bearing stiffness and damping characteristics, nor any of the work in this area addressed fluid film inertia effects on rotor-bearing systems dynamics. The objective of this study based on the current status of the work as presented in the previous sections is to produce reliable and accurate rotor-disk-bearing system FEM model, which address the following points.

- The interaction of rotor and bearing as one integrated system.
- Instantaneous calculation of dynamic eccentricity to be used for calculating the bearing stiffness and damping parameters.
- Fluid inertia terms addition to the system model.

The approach to the work is to derive rotor and disk equations along with the bearing equations using the most current available models and then transform it into rotating cylindrical coordinate system to facilitate the addition of fluid inertia terms. The model will be validated using MATLAB® simulation for the simple case of a Jeffcot rotor. The FEM model will be then simulated for steady state speeds with the inclusion of dynamic instantaneous eccentricity as well as fluid inertia terms. These runs will be compared to current available models. The simulation work will be presented in graphical formats to demonstrate the effect of both terms on Rotor-Disk-Bearing system dynamics.

[3] Instantaneous shaft position measurement within the bearing radial clearance

CHAPTER 2

FINITE ELEMENT MODEL OF A SHAFT-DISK-BEARING SYSTEM, FORMULATION AND ASSEMBLY

The most common and damaging behavior in a shaft-disk-bearing system is it's vibration. Vibration in shafts can be longitudinal, lateral or Torsional or combination of some or all. Vibration is usually classified as transient, forced and self-excited. The self-excited vibration is one type that can result from bearing fluid instability. In order to effectively estimate the system dynamic behavior and hence be able to study the vibration, the shaft, disk and bearing element equations of motion are developed for this purpose.

2.1 INTRODUCTION

In the course of developing the kinetic and potential energy expressions, a reference frame is chosen first and then displacement and velocity vectors along with angular rotation vectors are derived. The vectors are used to derive a shaft element force and momentum balance equation incorporating shear deformation and rotary inertia effects. Applicable equations of internal damping effect on shaft element are incorporated into the model. Internal material damping is a material property that causes shaft whirling resulting in self-excited instability [4]. The system model will also account for external damping from the bearings as well as structural or internal damping. Foundation stiffness and damping act like a bearing except that it has a constant stiffness and damping coefficients, foundation effect

plays a role in amending the first and last stations stiffness and damping matrices [28]. If the foundation stiffness is low as in the case of lightly frame bearing in gas turbines, it could present a significant amount of instability to the system and asymmetry. Gyroscopic inertia is included which will play effect when the shaft is excited by spin. In this chapter the equations governing the behavior of shaft element with internal damping, the equations of motion for a rigid disk as well as the inclusion of foundation effect in the system equations will be developed.

Rotating machinery are supported by bearing(s) which play a vital role in the behavior of the system under static and dynamic load conditions. Fluid film journal bearings consist of the circular section of the shaft (Journal) rotating inside a bearing bush. The journal diameter is usually 99.8-99.9 % of the bush; the bearing clearance is filled with lubricating fluid. The shaft weight force under static loading conditions i.e., no shaft spin, acts on fluid film, the shaft in this case will rest on the bottom of the bearing. At start up and as the shaft starts speeding from zero to its normal operating speeds, it will exhibit a dynamic load on the fluid film and move from its static position to an eccentric position. The fluid film will exhibit a reaction force to this dynamic load. Under this condition with the fluid being dragged into motion with the journal and the pressure building up, fluid film will build between the journal and the bearing and there will be no surface-to-surface contact. Traditionally eccentricity ratio in journal bearings is defined as journal eccentricity to radial clearance ratio $\varepsilon = e/c$ as shown in *Figure 2.1*. Eccentricity ration is normally set in journal bearings design between 0.6 - 0.7 so this ratio would accommodate for various loads the machine might have to operate with during it's life cycle and develop immunity to self excited vibrations due to fluid film interactions (Oil Whirl and Whip).

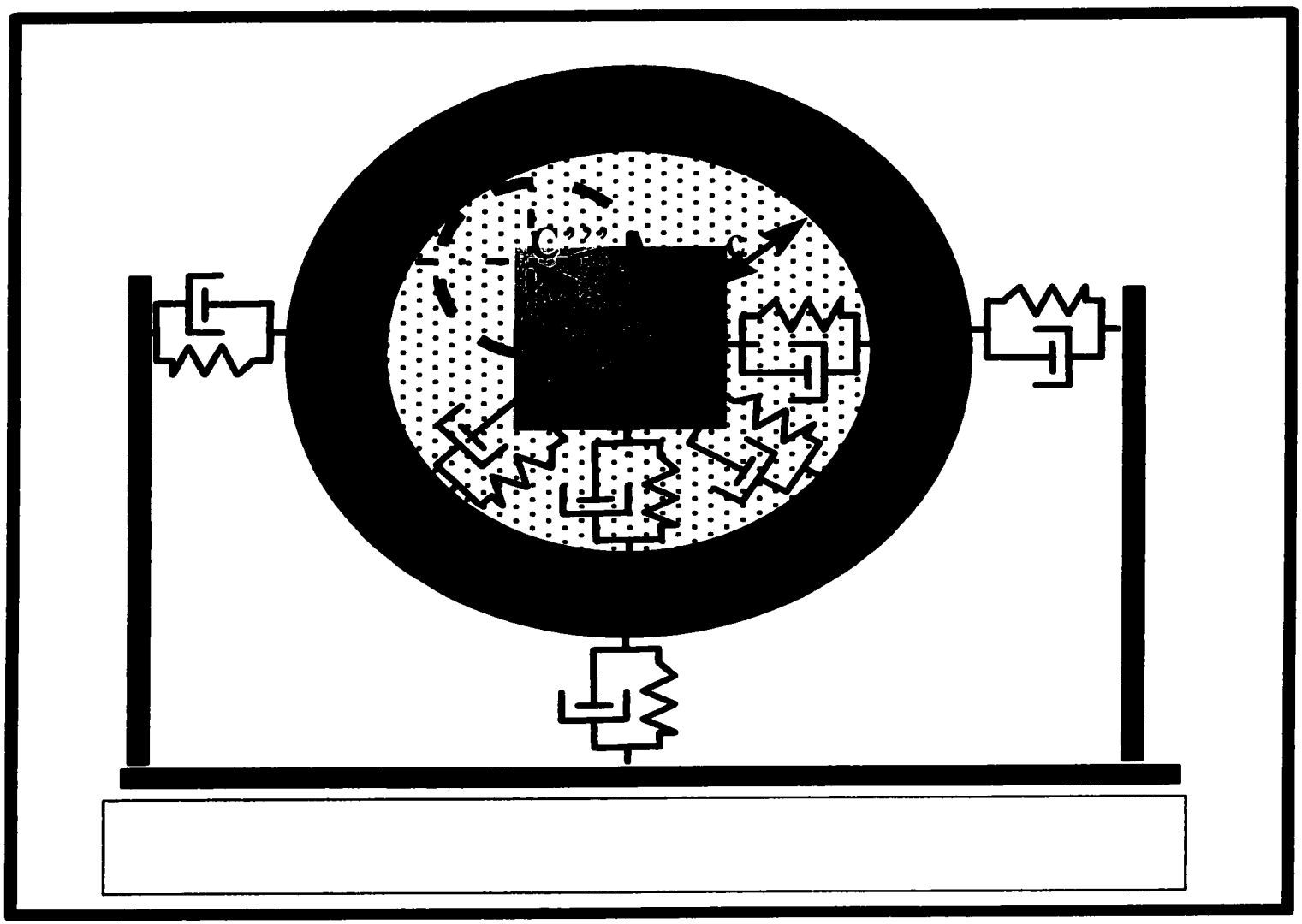

Figure 2.1 Bearing Housing with flexible supports

In the linearized fluid mechanics representation of the fluid film properties, the fluid, which is normally oil, behaves like a complicated set of springs and dampers and thus influences the machine critical speed or natural frequency and unbalance response. In the traditional representation of fluid film behavior as a set of springs and dampers, a linearized model is utilized. This linearized model does not take into account the effect of Quadrature stiffness and fluid average velocity effect [14, 15, 16, 17, 18, 19, 20, 21, 22], which do create a cross stiffness and damping effect. In this chapter the matrices for shaft element, disk and bearing equations incorporating translational, rotational, gyroscopic, internal damping are presented.

2.2 SYSTEM DESCRIPTIONS AND MODELING APPROACH

A flexible rotor is used as the basis for the research, which includes gyroscopic effects, internal material viscous damping and hysteretic damping. Short bearing with Length to Diameter ratio[1] of less than one is used to provide support and damping for the system. The shaft is divided into shaft elements. Third order polynomial interpolation equation is used to develop shape function transformation from local translation coordinates into global or FEM coordinates. Each shaft element is modeled based on a rotating Timoshenko beam, which accounts for Shear deformation and rotary inertia. Shear correction terms arise in the derivation of system stiffness matrix are included. Disk is assumed as rigid as shown in *Figure 2.2* and modeled accordingly with gyroscopic effects, unbalance mass added.

[1] L/D Ratio < 1

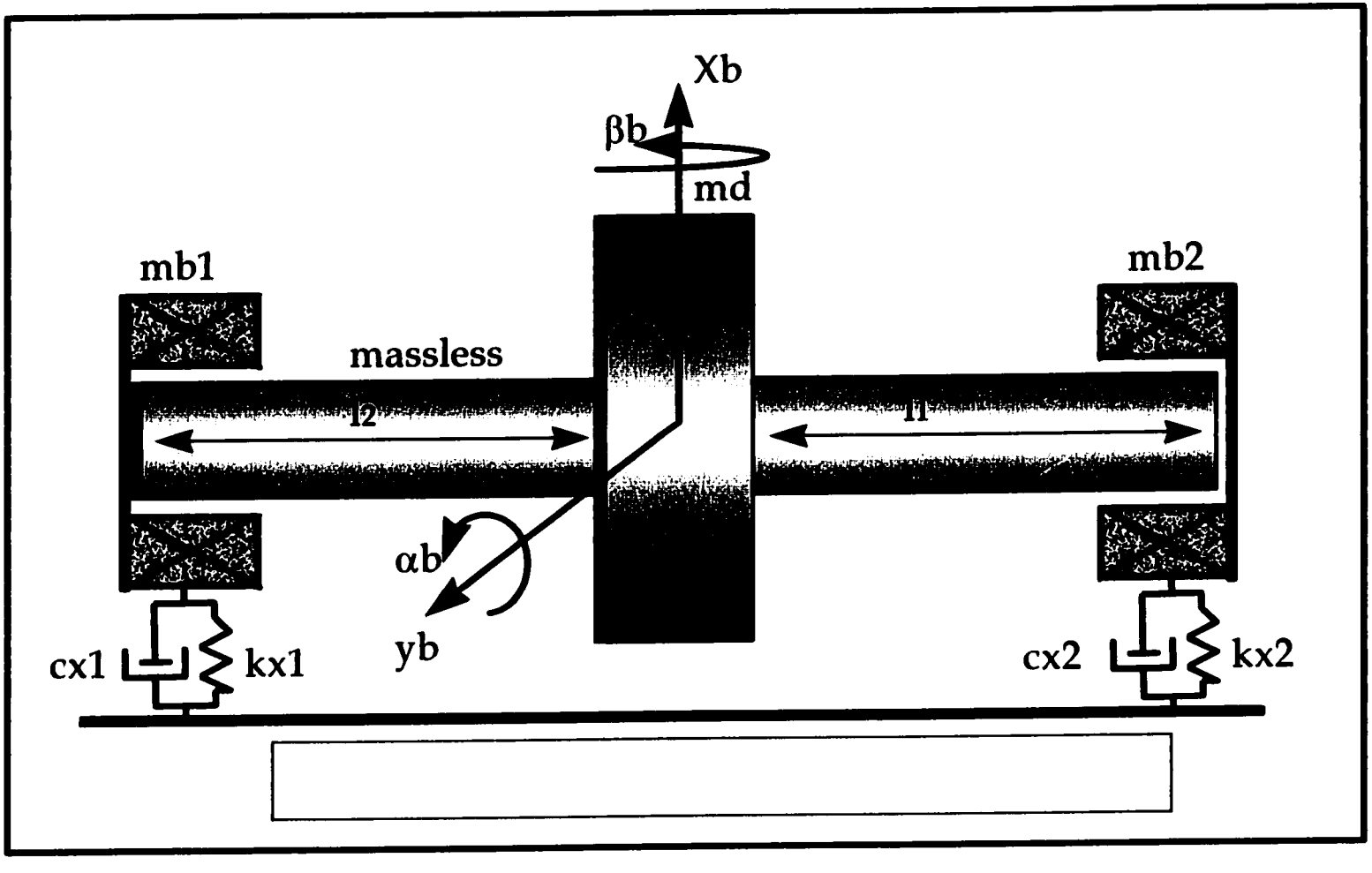

Figure 2.2 – Flexible Foundation Effect on Shaft Motion

Bearings are modeled using a linearized short bearing approximation of Reynolds equation to arrive at oil film pressure distribution. In chapter 2 the study provides a discussion on the set of assumptions used to derive Reynolds equation from the three dimensional Navier-Stocks equations into Reynolds. To achieve the objective of this research the Reynolds equation is transformed into cylindrical coordinates and a finite series solution is used to solve the general case. The series solution results in system stiffness and damping parameters that use a model based on fluid forces rotating at the rate of $\lambda\Omega$ where λ is the fluid average circumferential flow rate [14] and Ω is the rotor speed. The parameters that result from the infinite series solution for damping, stiffness and fluid inertia are inserted into the rotating fluid model and then incorporated into the system equations. Shaft position within the bearing at the first and last element deflections is used to calculate the dynamic eccentricity instead of the standard 4^{th} order equation solution that relates eccentricity and Sommerfeld number. Simulation using MATLAB is used to verify the basic model and then to show the results of incorporating fluid inertia and dynamic eccentricity.

2.3 DISPLACEMENT AND VELOCITY VECTORS

In this section, the formulation of transformations from the fixed coordinates system to the rotating coordinates "*Whirl Frame Coordinates*" are derived. The bearing housing in this case is considered as fixed to the foundation and hence is used as inertial frame Xr Yr Zr. The frame Xj Yj Zj is defined also in the study, which is the journal (body) coordinate system with the origin attached to the center of the journal. At rest, the shaft will be resting in a certain location within the bearing (Static Equilibrium position). In *Figure 2.3* when the shaft gets its power from the driver, the shaft will:

- First spin ϕ with rate of change $\dot{\phi} = \Omega$ which is the rotational speed.
- Second it will go through torsion angles, which is not addressed in this study due to minimal effect, expected on fluid inertia and dynamic eccentricity which are the objectives of this research.
- It will also deform in the lateral and longitudinal directions as a result of shear and bending with angles θ around Xj and ψ around Yj.
- The shaft will also move or translate in the lateral, longitudinal (R_{jx} and R_{jy}).

In *Figure 2.2* ω is defined as the angular velocity vector of the journal. r_J is global position vector of a shaft particle point while R_J is a position vector to describe shaft center translation. The position vector for the shaft material point is defined as

$$r_J = R_J + u_J \tag{2.1}$$

Also $\bar{u}^t$ is defined as the particle position within the shaft. Notice that as shaft is undeformable, components of $\bar{u}^t$ remain constant.

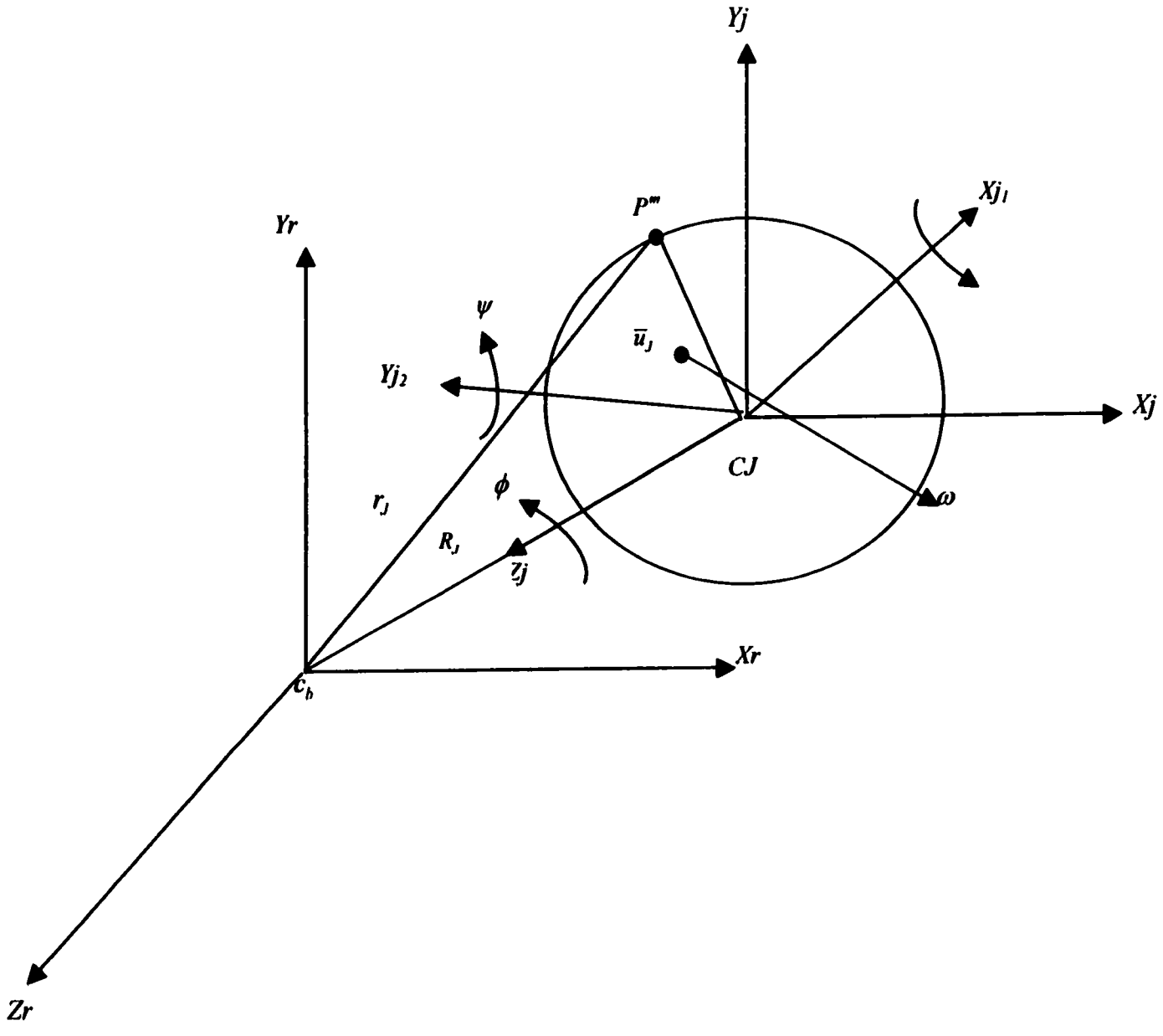

Figure 2.3 – Journal Motion (Translational & Rotational) within bearing sleeve

In *Figure 2.4* if the shaft material point position is traced, the following changes will occur;

- Rotation around Zj, ϕ with $P \rightarrow P'$ $(-\Delta Y', -\Delta X')$ and new coordinate system $Xj_1 Yj_1 Zj_1$
- Rotation around Xj_1, θ with $P' \rightarrow P''$ $(\Delta Z', -\Delta X'')$ and new coordinate system $Xj_2 Yj_2 Zj_2$
- Rotation around Yj_2, ψ with $P'' \rightarrow P'''$ $(\Delta Z'', -\Delta Y'')$.

The angles θ and ψ are considered small such that $\cos\theta = \cos\psi = 1$, $\sin\theta = \theta$, $\sin\psi = \psi$ and all rotations are counterclockwise[1]. The body coordinate system obviously will change due to the consecutive rotations from stationary body coordinates Xj, Yj, Zj with i_k, $k = 1,2,3$ representing the three different rotational deformations. The end result is a rotating body coordinate system Xj_3, Yj_3, Zj_3 with i_{k3}, $k = 1,2,3$. The orientation of the disk is to be defined in order to express $\bar{u}'$ in terms of global coordinate system. The transformation, which is given in more details in multi-body dynamics textbooks, takes the form [1]

$$u_J = A_J \bar{u}_J$$

$$A_J = \begin{bmatrix} \cos\phi - \theta\psi\sin\phi & \sin\phi + \psi\theta\cos\phi & -\psi \\ -\sin\phi & \cos\phi & \theta \\ \theta\sin\phi + \psi\cos\phi & -\theta\cos\phi + \psi\sin\phi & 1 \end{bmatrix} \qquad (2.2)$$

[1] In standard text books and research papers, the lateral deformation angle is normally taken as clockwise and hence would have a sign difference from the angles used here

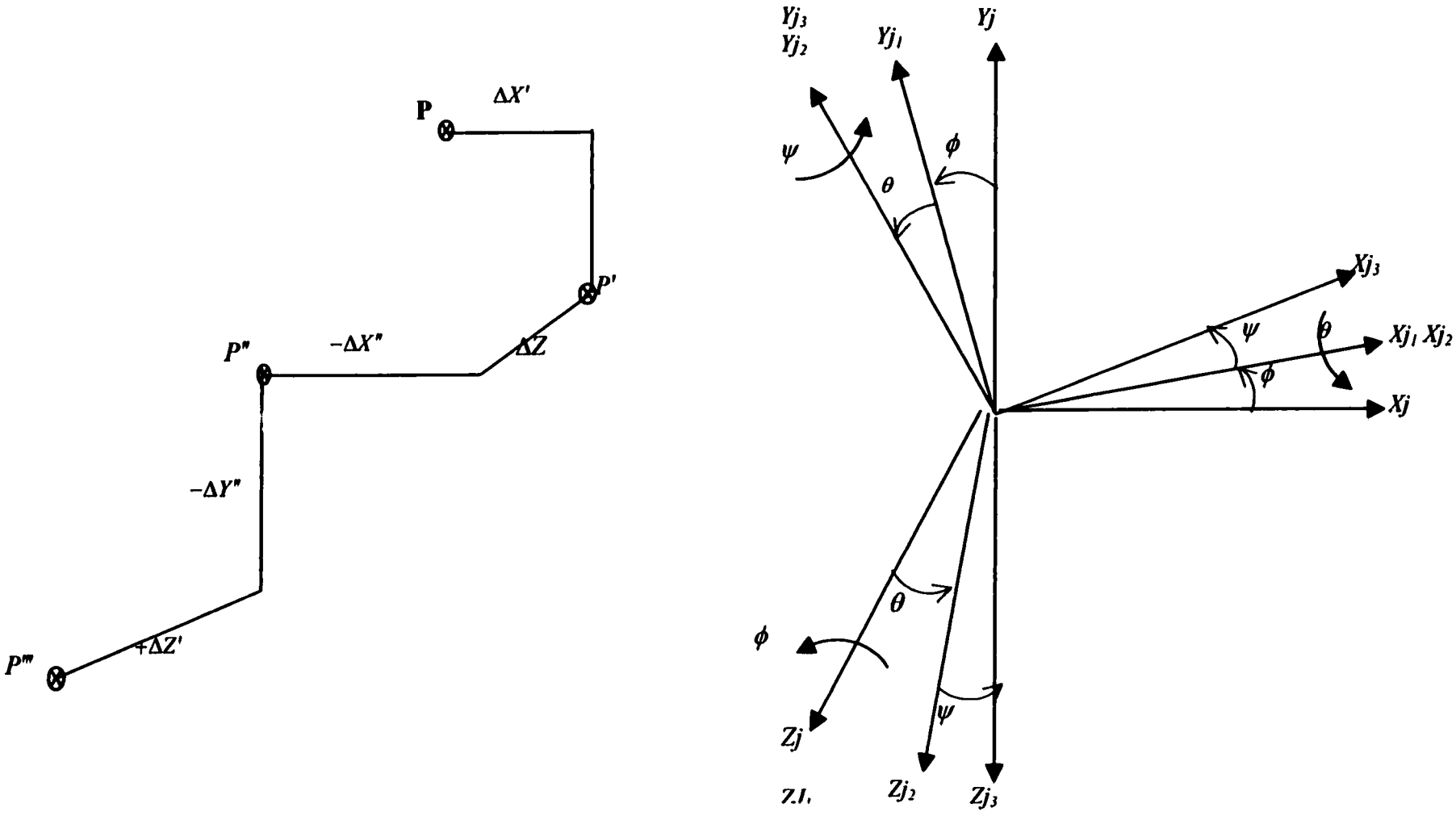

Figure 2.4 Shaft Material Point Position Changes and coordinate system transformations

With the sequence of rotations ϕ rotation around Zj $v=[0 \quad 0 \quad v_3]^T$, θ rotation around Xj_1 $v=[v_1 \quad 0 \quad 0]^T$ and ψ rotation around Yj_2 $v=[0 \quad v_2 \quad 0]^T$ the intermediate transformation matrices are given as

$$A_1=\begin{bmatrix}\cos\phi & \sin\phi & 0\\ -\sin\phi & \cos\phi & 0\\ 0 & 0 & 1\end{bmatrix} \quad A_2=\begin{bmatrix}1 & 0 & 0\\ 0 & \cos\theta & \sin\theta\\ 0 & -\sin\theta & \cos\theta\end{bmatrix}=\begin{bmatrix}1 & 0 & 0\\ 0 & 1 & \theta\\ 0 & -\theta & 1\end{bmatrix} \quad A_3=\begin{bmatrix}1 & 0 & -\psi\\ 0 & 1 & 0\\ \psi & 0 & 1\end{bmatrix}$$

with position vectors related by ;

$$\begin{aligned} r_1 &= A_1\bar{r}\\ r_2 &= A_2 r_1 = A_2A_1\bar{r}\\ r_3 &= A_3 r_2 = A_3A_2A_1\bar{r}\end{aligned} \qquad (2.3)$$

$$A_2A_1=\begin{bmatrix}\cos\phi & \sin\phi & 0\\ -\sin\phi & \cos\phi & \theta\\ \theta\sin\phi & -\theta\cos\phi & 1\end{bmatrix} \quad A_J=\begin{bmatrix}\cos\phi-\theta\psi\sin\phi & \sin\phi+\psi\theta\cos\phi & -\psi\\ -\sin\phi & \cos\phi & \theta\\ \theta\sin\phi+\psi\cos\phi & -\theta\cos\phi+\psi\sin\phi & 1\end{bmatrix}$$

With the transformation matrix Aj derived, one can write the position vector in terms of

$$r_J = R_J + A_J\bar{u}_J \qquad (2.4)$$

Differentiating to get absolute velocity of shaft material point [1] P_i

$$\dot{r}_J = \dot{R}_J + \dot{A}_J\bar{u}_J \qquad \dot{A}_J\bar{u}_J = \tilde{\omega}_J A_J\bar{u}_J = A_J(\bar{\omega}_J\times\bar{u}_J) \qquad (2.5)$$

It is important to note that the shaft material is considered finite line element and hence $A_J\dot{\bar{u}}_J=0$, with $\dot{R}_J$ is absolute velocity of frame which gives from 2.5 above,

$$\dot{r}_J = \dot{R}_J + A_J(\bar{\omega}_J\times\bar{u}_J)$$

Differentiating again to obtain the acceleration vector as

$$\ddot{r}_J = \ddot{R}_J + A_J\left[\bar{\omega}_J\times(\bar{\omega}_J\times\bar{u}_J)\right] + A_J(\bar{\alpha}_F\times\bar{u}_J) \qquad (2.6)$$

Relative acceleration of P and coriolis acceleration are zero. In 2.6 the 2nd term represents centripetal acceleration and 3rd term representing angular acceleration of moving frame, $\alpha_{F_r}\big|_{\bar{x}_k^*} = \dot{\omega}_{F_r}\big|_{\bar{x}_k^*}$.

The transformation from rotating to stationary body coordinate system is given by

$$\begin{aligned}
\left[\bar{i}_{k1}\right] &= A_1\left[i_k\right] \\
\left[\bar{i}_{k2}\right] &= A_2\left[\bar{i}_{k1}\right] = A_2A_1\left[\bar{i}_k\right] \\
\left[\bar{i}_{k3}\right] &= A_3A_2A_1\left[\bar{i}_k\right] = A_J\left[\bar{i}_k\right]
\end{aligned} \tag{2.7}$$

And in similar fashion, transformation from stationary to rotating boundary conditions

$$\begin{aligned}
\left[\bar{i}_k\right] &= A_1^T\left[\bar{i}_{k1}\right] = A_1^TA_2^TA_3^T\left[\bar{i}_{k3}\right] \\
\left[\bar{i}_{k1}\right] &= A_2^T\left[\bar{i}_{k2}\right] = A_2^TA_3^T\left[\bar{i}_{k3}\right] \\
\left[\bar{i}_{k2}\right] &= A_3^T\left[\bar{i}_{k3}\right]
\end{aligned} \tag{2.8}$$

With the transformation matrices given as below,

$$A_3^T = \begin{bmatrix} 1 & 0 & \psi \\ 0 & 1 & 0 \\ -\psi & 0 & 1 \end{bmatrix} \qquad A_2^TA_3^T = \begin{bmatrix} 1 & 0 & \psi \\ \theta\psi & 1 & -\theta \\ -\psi & \theta & 1 \end{bmatrix}$$

$$A_1^TA_2^TA_3^T = A_J^T = \begin{bmatrix} \cos\phi - \theta\psi\sin\phi & -\sin\phi & \theta\sin\phi + \psi\cos\phi \\ \sin\phi + \psi\theta\cos\phi & \cos\phi & -\theta\cos\phi + \psi\sin\phi \\ -\psi & \theta & 1 \end{bmatrix}$$

To obtain the angular velocity vector, the instantaneous angular velocity considering the shaft sequence of rotations as shown in *Figure 2.5* is given below along with the required unit vector transformations to rotating body coordinate system,

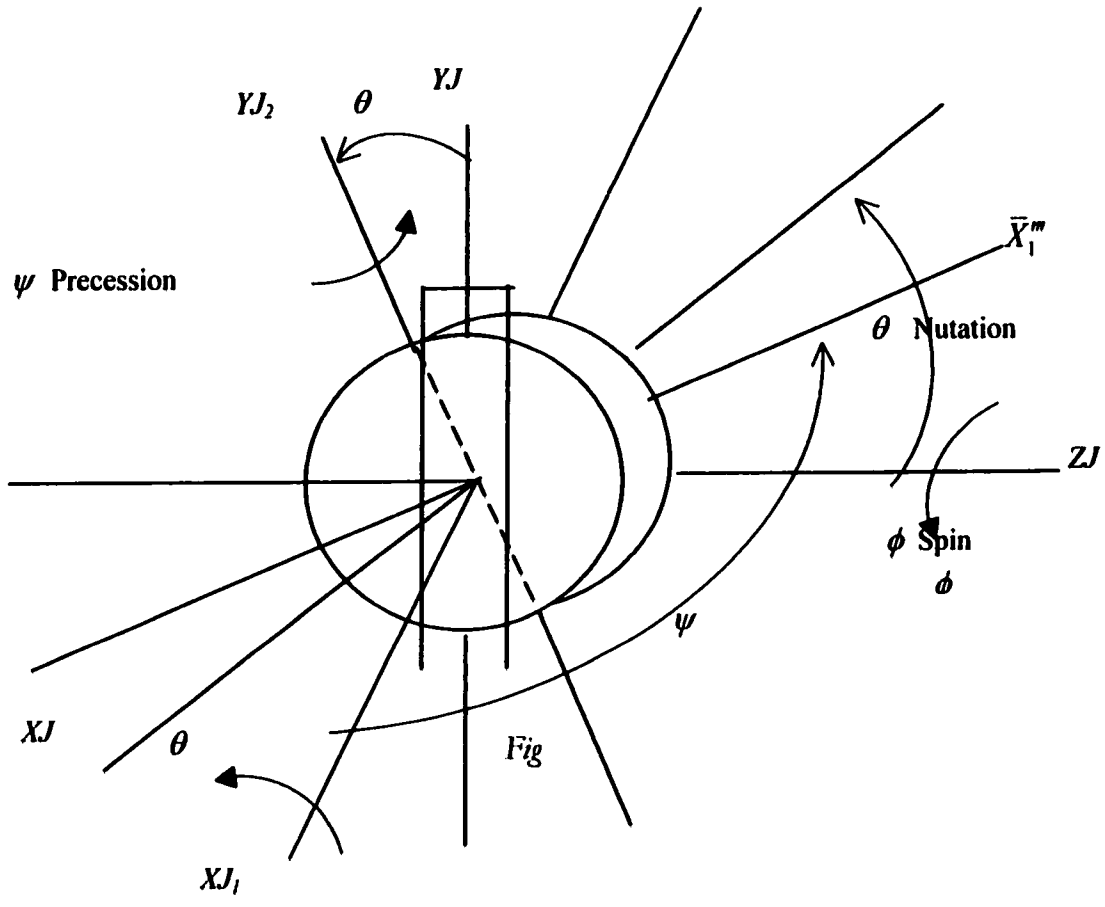

Figure 2.5 – Instantaneous Angular Velocity of Shaft

$$
\begin{aligned}
&\omega = \dot{\theta}\bar{i}_{11} + \dot{\psi}\bar{i}_{22} + \dot{\phi}\bar{i}_3 \\
&\bar{i}_3 = -\psi\bar{i}_{13} + \theta\bar{i}_{23} + \bar{i}_{33} \\
&\bar{i}_{11} = \bar{i}_{13} + \psi\bar{i}_{23} \\
&\bar{i}_{11} = \cos\phi\bar{i}_1 + \sin\phi\bar{i}_2 \\
&\bar{i}_{22} = -\sin\phi\bar{i}_1 + \cos\phi\bar{i}_2 + \theta\bar{i}_3, \quad \bar{i}_{22} = \bar{i}_{22}
\end{aligned}
\tag{2.9}
$$

The transformations above is used to obtain the stationary and the rotating angular velocity vectors as given below

$$
\begin{aligned}
&\omega = \dot{\theta}\cos\phi\bar{i}_1 + \dot{\theta}\sin\phi\bar{i}_2 - \dot{\psi}\sin\phi\bar{i}_1 + \dot{\psi}\cos\phi\bar{i}_2 + \dot{\psi}\phi\bar{i}_3 + \dot{\phi}\bar{i}_3 \\
&\bar{\omega} = \dot{\theta}\bar{i}_{13} + \dot{\theta}\psi\bar{i}_{33} + \dot{\psi}\bar{i}_{23} - \dot{\phi}\psi\bar{i}_{13} + \dot{\phi}\theta\bar{i}_{23} + +\dot{\phi}\bar{i}_{33}
\end{aligned}
$$

$$
\omega_J = \begin{bmatrix} \dot{\theta}\cos\phi - \dot{\psi}\sin\phi \\ \dot{\theta}\sin\phi + \dot{\psi}\cos\phi \\ \dot{\psi}\theta + \dot{\phi} \end{bmatrix}, \qquad \bar{\omega}_J = \begin{bmatrix} \dot{\theta} - \dot{\phi}\psi \\ \theta\dot{\phi} + \dot{\psi} \\ \psi\dot{\theta} + \dot{\phi} \end{bmatrix} \tag{2.10}
$$

ω_{J2} is defined with respect to stationary body coordinates and $\bar{\omega}_J$ is with respect to rotating body coordinates.

[2] Note: In standard textbook of rotordynamics, θ is around YJ then ψ around XJ, then spin ϕ is around ZJ_2.

To derive ω_{F_r}, subtract $\bar{\omega}_F - \Omega\bar{i}_{33}$

2.4 SHAFT ELEMENT FORMULATION

The model kinetic energy equation is formulated using the velocity vector of a material point on the deformed shaft. The bearing sleeve will be taken as our inertial frame for the purpose of developing the force and moment balance equations. In *Figure 2.6* taking a small cross section of a deformed shaft under shear deformation and bending moment effects

Shear angle can be expressed as [1] $\gamma = \left(\theta - \frac{\partial Y_{J1}}{\partial Z_{J1}}\right)$ using Timoshenko beam theory and moment-curvature relations which can be found in standard structural mechanics and vibration text books. To summarize, position, velocity and acceleration vectors with respect to journal, we have developed so far;

$$r_J = r_{XJ}\bar{i}_{13} + r_{YJ}\bar{i}_{23} + r_{ZJ}\bar{i}_{33}$$

$$\bar{u}_J = u_{XJ}\bar{i}_{11} + u_{YJ}\bar{i}_{21} + u_{ZJ}\bar{i}_{31}$$

$$\bar{R}_J = R_{XJ}\bar{i}_{11} + R_{YJ}\bar{i}_{21} + R_{ZJ}\bar{i}_{31}$$

With large $\dot{\phi}$ spin velocity, applying P_{X3} force will cause torque; the force in the normal direction P_{Y3} introduces change in momentum. The angular moment vector of a rotating disk, where G is the mass center, is [11]

$$H_{GJ}\big|_{\bar{X}_{k1}} = \begin{bmatrix} I_d & & \\ & I_d & \\ & & I_a \end{bmatrix} \left(\left[\omega_{fr}\right] + \left[\Omega \bar{i}_{31}\right] \right) \tag{2.11}$$

Given that

$$\left[\bar{i}_{k3}\right] = A_3\left[\bar{i}_{k2}\right] = A_3A_2\left[\bar{i}_{k1}\right] = A_3A_3A_1\left[\bar{i}_k\right] \text{ with } \bar{i}_{22} = \bar{i}_{21} + \theta\bar{i}_{31} \text{ and } \omega_{fr} = \dot{\theta}\bar{i}_{11} + \dot{\psi}\bar{i}_{22}$$

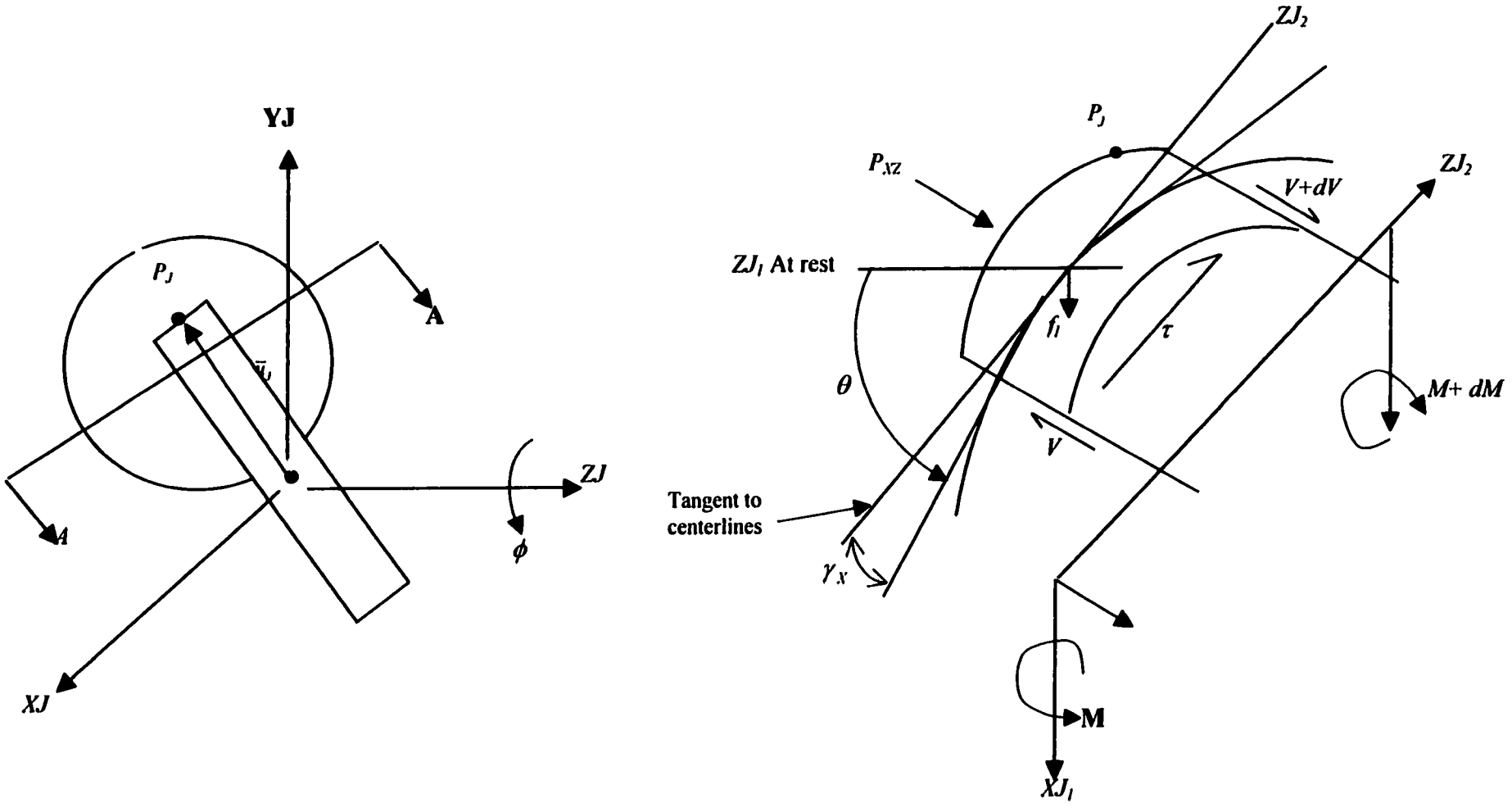

Figure 2.6 – Cross Section of Shaft in Deformed State with Shear & bending moment effects

The frame angular velocity vectors is given by [4]

$$\omega_{fr} = \begin{bmatrix} \dot{\theta} \\ \dot{\psi} \\ \dot{\psi}\theta \end{bmatrix} \tag{2.12}$$

Our angular momentum equation becomes

$$H_{GJ}\big|_{\bar{X}_{k1}} = \begin{bmatrix} I_d\dot{\theta} \\ I_d\dot{\psi} \\ I_a(\dot{\psi}\theta + \Omega) \end{bmatrix}$$

The disk is treated as axisymmetric, with diameteral and polar moment of inertia given by

$$I_d = \tfrac{1}{4}mr^2, \qquad I_a = \tfrac{1}{2}mr^2.$$

Conservation of momentum principal states

$$M_{GJ}\big|_{\bar{X}_{k1}} = \dot{H}_{GJ} = \dot{H}_{GJ}\big|_{\bar{X}_{k1}} + \omega_{fr}^{(*)} \times H_{GJ} \tag{2.13}$$

Bearing rotational deformation is assumed to have negligible effect on angular moment due to fluid in journal bearing. Referring to standard moment-curvature relations, one can write

$$M_{GJ} = \dot{H}_{GJ}\big|_{\bar{X}_{k1}} + \tilde{\omega}_{fr}(H_{GJ})$$

Where the angular velocity transform matrix is given by

$$\tilde{\omega}_{fr} = \begin{bmatrix} 0 & -\omega_3 & \omega_2 \\ \omega_3 & 0 & -\omega_1 \\ -\omega_3 & \omega_1 & 0 \end{bmatrix} = \begin{bmatrix} 0 & -\dot{\psi}\theta & \dot{\psi} \\ \dot{\psi}\theta & 0 & \dot{\theta} \\ -\dot{\psi} & \dot{\theta} & 0 \end{bmatrix}$$

And the second & first terms in 2.13 can be obtained as follows

$$\tilde{\omega}_{fr}[H_{GJ}]_{\bar{X}_{k1}} = \begin{bmatrix} -\dot{\psi}^2\theta I_d + \dot{\psi}^2\theta I_a + \dot{\psi}\Omega I_a \\ \dot{\psi}\dot{\theta}\theta I_d + \dot{\psi}\dot{\theta}\theta I_a + \dot{\theta}\Omega I_a \\ -\dot{\psi}^2\dot{\theta} I_d - \dot{\psi}^2 I_d \end{bmatrix}$$

$$\dot{H}_{GJ}\big|_{\bar{X}_{k1}} = \begin{bmatrix} \ddot{\theta} I_d \\ \ddot{\psi} I_d \\ I_a\left(\ddot{\psi}\dot{\theta} + \dot{\psi}\dot{\theta} + \dot{\Omega}\right) \end{bmatrix}$$

Using 2.13 the moment equations in X, Y & Z stationary coordinates, while utilizing Linearization of angles ψ and θ which are assumed to be very small angles, and hence their products are negligible, one gets

$$M_{XJ}\big|_{\bar{X}_{k1}} = I_d\ddot{\theta} + \left(I_a - I_d\right)\dot{\psi}^2\theta + I_a\dot{\psi}\Omega \tag{2.14a}$$

$$M_{YJ}\big|_{\bar{X}_{k1}} = I_d\ddot{\psi} + \left(I_d + I_a\right)\dot{\psi}\dot{\theta}\theta + I_a\dot{\theta}\Omega \tag{2.14b}$$

$$M_{ZJ}\big|_{\bar{X}_{k1}} = I_a\dot{\Omega} + \left(I_a - I_d\right)\dot{\psi}\dot{\theta} - I_d\ddot{\psi}^2 \tag{2.14c}$$

In this study one is interested in $M_{GJ}\big|_{\bar{X}_{k2}}$ referencing rotating body coordinates (without spin $\bar{X}_{k3}$), using the transformations developed in section 2.1

$$\left[\bar{i}_k\right] = A_1^T\left[\bar{i}_{k1}\right] = A_1^T A_2^T\left[\bar{i}_{k2}\right] = A_1^T A_2^T A_3^T\left[\bar{i}_{k3}\right] \quad \left[\bar{i}_{k2}\right] = A_3 A_2\left[\bar{i}_{k1}\right]$$

With the linearized matrices are given below

$$A_2 = \begin{bmatrix} 1 & 0 & 0 \\ 0 & 1 & \theta \\ 0 & -\theta & 1 \end{bmatrix} \quad A_2 = \begin{bmatrix} 1 & 0 & -\psi \\ 0 & 1 & 0 \\ \psi & 0 & 1 \end{bmatrix} \quad A_3A_2 = \begin{bmatrix} 1 & \theta\psi & -\psi \\ 0 & 1 & \theta \\ \psi & -\theta & 1 \end{bmatrix}$$

One can get $M_{GJ}\big|_{\bar{X}_{k2}}$ as

$$M_{GJ}\big|_{\bar{X}_{k2}} = \left[A_3A_2\right]\begin{bmatrix} I_d & 0 & 0 \\ 0 & I_d & 0 \\ 0 & 0 & 0 \end{bmatrix}\begin{bmatrix} \ddot{\theta} \\ \ddot{\psi} \\ \dot{\Omega} \end{bmatrix} + \left[A_3A_2\right]\begin{bmatrix} 0 & I_d\Omega & 0 \\ I_d\Omega & 0 & 0 \\ 0 & 0 & I_a \end{bmatrix}\begin{bmatrix} \dot{\theta} \\ \dot{\psi} \\ \dot{\Omega} \end{bmatrix}$$

$$= \begin{bmatrix} 1 & \theta\psi & -\psi \\ 0 & 1 & \theta \\ \psi & -\theta & 1 \end{bmatrix}\begin{bmatrix} I_d & 0 & 0 \\ 0 & I_d & 0 \\ 0 & 0 & 0 \end{bmatrix}\begin{bmatrix} \ddot{\theta} \\ \ddot{\psi} \\ \dot{\Omega} \end{bmatrix} + \begin{bmatrix} 1 & \theta\psi & -\psi \\ 0 & 1 & \theta \\ \psi & -\theta & 1 \end{bmatrix}\begin{bmatrix} 0 & I_d\Omega & 0 \\ I_d\Omega & 0 & 0 \\ 0 & 0 & I_a \end{bmatrix}\begin{bmatrix} \dot{\theta} \\ \dot{\psi} \\ \dot{\Omega} \end{bmatrix} \tag{2.15}$$

Using the approximations of angles θ, ψ and $\dot{\theta}$, $\dot{\psi}$ which equates them to zero after conversion are performed, the moments in rotating body coordinates can be written as

$$M_{XJ_2} = I_d\left(\ddot{\theta} + 2\dot{\psi}\Omega - 2\psi\dot{\Omega}\right) \quad (2.16a)$$

$$M_{YJ_2} = I_d\left(\ddot{\psi} + 2\dot{\theta}\Omega + 2\theta\dot{\Omega}\right) \quad (2.16b)$$

$$M_{ZJ_2} = 2I_d\dot{\Omega} \quad (2.16c)$$

The terms on the right of equations 2.16 when reversed in sign represent the inertia torques acting on the shaft element, the first term on the right of equations 2.16a, b provide the angular acceleration inertia torques, the second terms provide the gyroscopic torques which their strength is proportional to the axial angular momentum $I_d\Omega$. The third terms account for cross-coupling between torque in one direction and angular velocity in the other direction. The standard Moment-Curvature equations gives Moment and Shear as ,

$$M = EI\frac{\partial\theta}{\partial ZJ_2}$$

$$V = \frac{\partial M}{\partial \bar{X}_3} = \kappa AG\gamma \quad (2.17\ a,b)$$

Hence the total bending angle will be written as

$$\theta = \gamma_X + \frac{\partial YJ_1}{\partial YJ_1} \quad (2.18a)$$

$$\psi = \gamma_Y + \frac{\partial XJ_2}{\partial ZJ_2} \quad (2.18b)$$

From the free body diagram in *Figure 2.7*, with inertia force due to acceleration $f_I = m\ddot{r}_f$, the forces and moments balance equations on the element can be written as ;

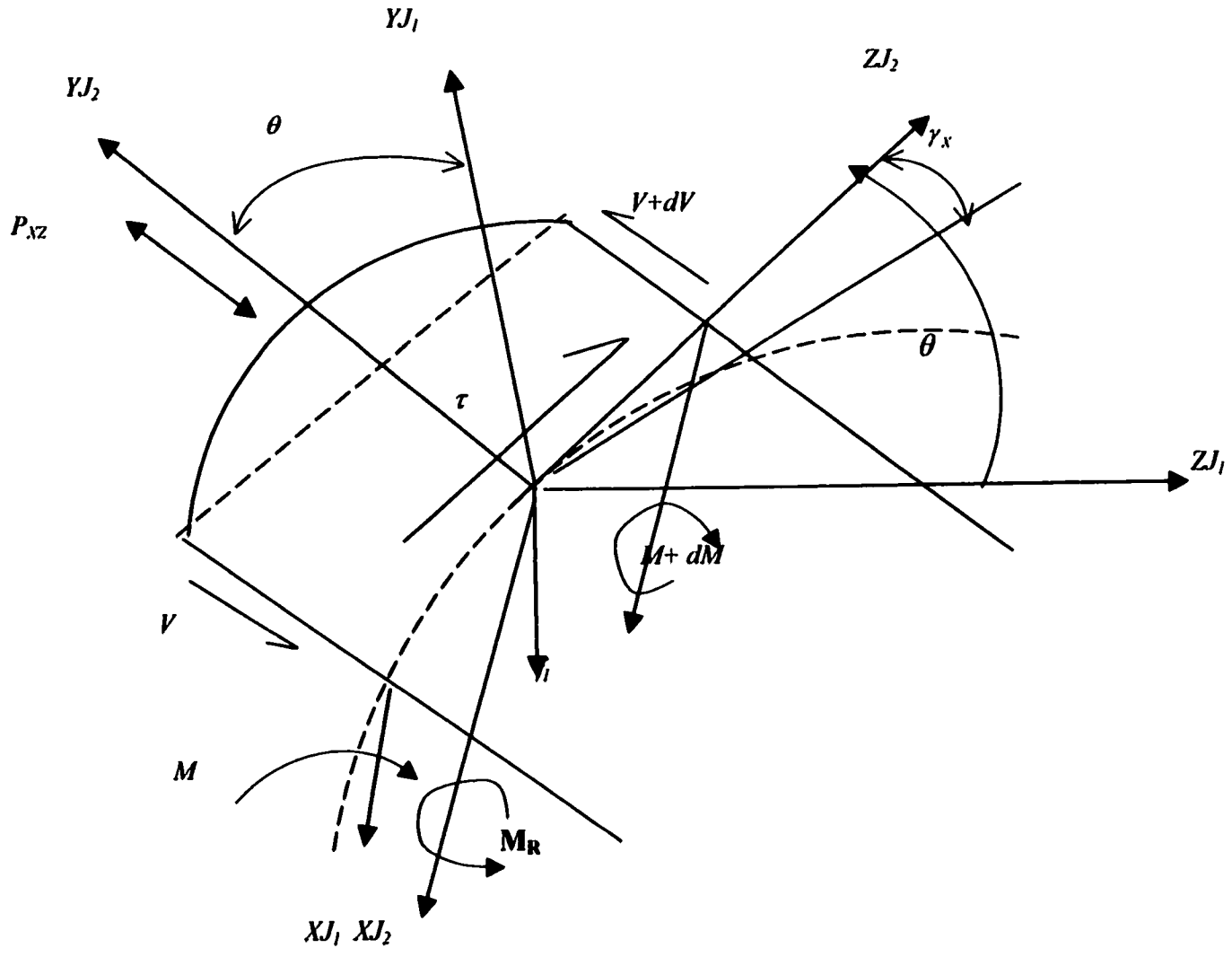

Figure 2.7 – Free Body Diagram of a shaft element

The balance of forces $f_l = P_{XZ} + V - (V + dV)$ is given by;

$$\rho A \frac{\partial^2 r_{XJ}}{\partial t^2} = P_{X1} + \frac{\partial V}{\partial ZJ_2} \tag{2.19}$$

Lateral vibration is associated with time variation of beam slope, which resists rotational acceleration with rotary inertia, which we calculated as M_{XJ_2}, M_{YJ_2}, M_{ZJ_2}. The balance of moments about center point of the element is $-M + \left(M + \frac{\partial M}{\partial ZJ_2}\right) - V = M_{XJ_2}$ In which the force P_{XZ} multiplied by $\partial Z_{J_2^1}$ is neglected.

When substituting using moment-curvature and shear relations the moment balance equation will be

$$EI \frac{\partial^2 \theta}{\partial ZJ_2^2} - V = M_{XJ_2},$$
$$EI \frac{\partial^2 \theta}{\partial ZJ_2^2} - \kappa AG\left(\theta - \frac{\partial YJ_1}{\partial ZJ_1}\right) = M_{XJ_2} \tag{2.20}$$

Using the moments equations 2.16, the shaft element equations considering that lateral moment of inertia: $J_d = \rho I_d$ are given below for translational and rotational motion,

Xj_2 direction -

$$\rho A \frac{\partial^2 r_{XJ}}{\partial t^2} = P_{X_2} + \kappa AG \frac{\partial^2 r_{YJ_1}}{\partial ZJ_2^2} - \kappa AG \frac{\partial \theta}{\partial ZJ_2} \tag{2.21a}$$

$$J_d\left(\ddot{\theta} + 2\dot{\psi}\Omega - 2\psi\dot{\Omega}\right) = EI_d \frac{\partial^2 \theta}{\partial ZJ_2^2} + \kappa AG \frac{\partial r_{YJ_1}}{\partial ZJ_2} - \kappa AG\theta \tag{2.21b}$$

Yj_2 direction:

$$\rho A \frac{\partial^2 r_{YJ}}{\partial t^2} = P_{Y_1} + \kappa AG \frac{\partial^2 r_{XJ_2}}{\partial ZJ_2^2} - \kappa AG \frac{\partial \psi}{\partial ZJ_2} \tag{2.21c}$$

$$J_d \left(\ddot{\psi} + 2\dot{\psi}\Omega + 2\psi\dot{\Omega} \right) = EI_d \frac{\partial^2 \psi}{\partial ZJ_2^2} + \kappa AG \frac{\partial r_{XJ_2}}{\partial ZJ_2} - \kappa AG\psi \tag{2.21d}$$

Zj_2 direction

$$M_{ZJ^*} = 2J_d\Omega \tag{2.21e}$$

With P_Z acts at the center, this implies $P_Z = 0$ as shown in *Figure 2.8*. With constant spin, we get $2J_d\Omega = 0, \qquad \dot{\Omega} = 0$

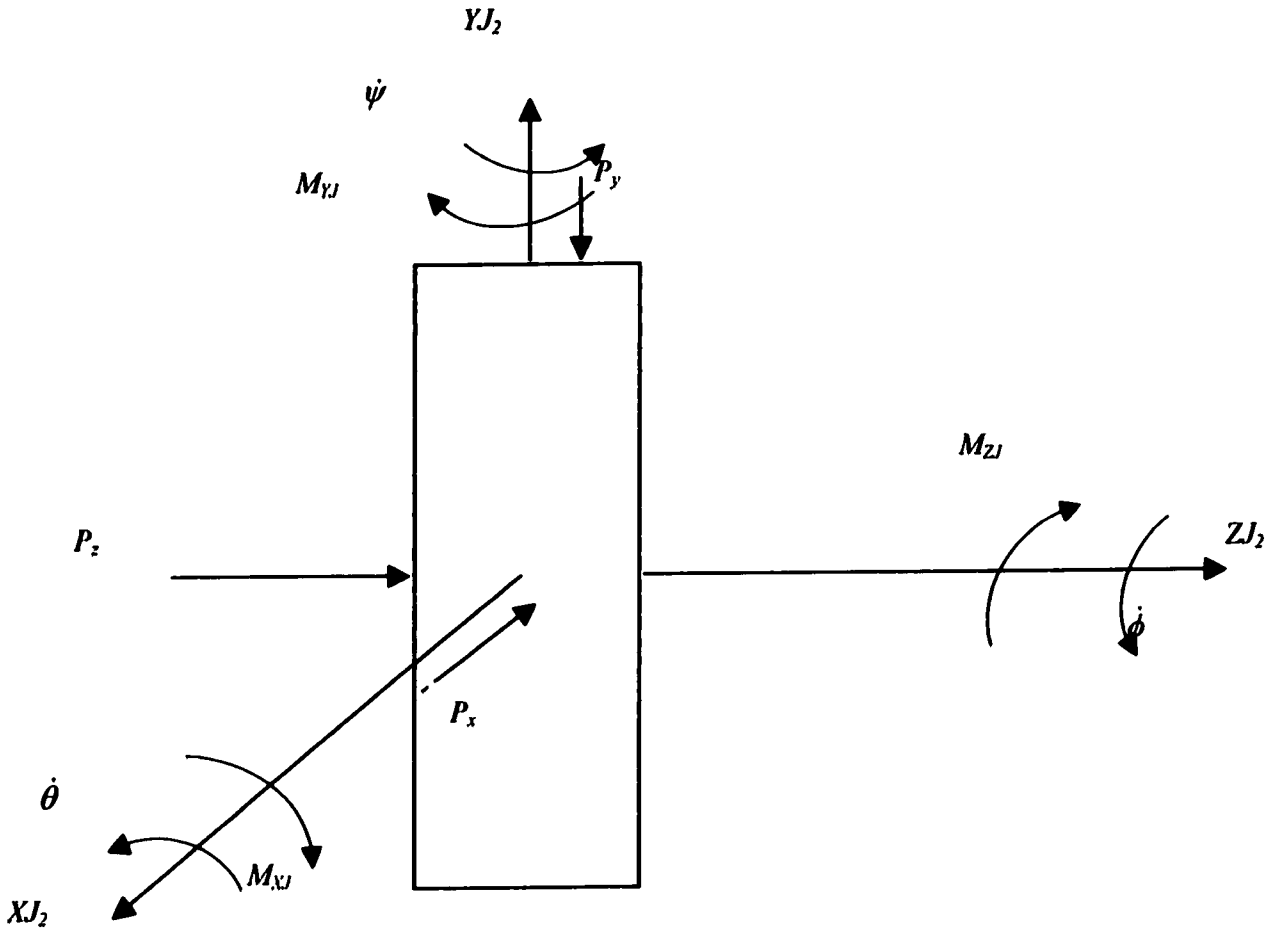

Figure 2.8 Forces and Moments in shaft element

2.5 SHAFT FINITE ELEMNT MODEL

To solve the shaft element equations and put them into matrix form FEM is used. The procedure is to discretize the shaft into elements with each element having two nodes. The element equation of motion is derived and interpolation utilizing an assumed motion shape function is used to transform the element local or nodal equations to global or FEM coordinates. Kinetic and potential energy expressions are then developed using the global coordinates which enables the construction of mass, stiffness, damping matrices and forces matrices in global coordinates. Assembly process further takes place, taking into consideration overlapping nodal coordinates at elements common nodal points. This gives us the final global shaft linear & discretized equations of motion. The boundary conditions for each element as shown in *Figure 2.9* is set to

$$r_{XJ}(0)=1, \qquad \theta(0)=0$$
$$r_{XJ}(1)=0, \qquad \theta(1)=0$$

The basics of the solution to a shaft element is that system deflections (two rotational and two translation) will assume the form given in (2.22) below such that displacement at any point inside the element is assumed to follow a shape function defined by $N_i(Z_J)$ for the i^{th} element. This same strategy applies to r_{Yf} as well as θ and ψ.

$$r_{XJ}(Z_j,t)=\sum_{i=1}^{4} N_i(Z_J)\begin{Bmatrix} r^1_{XJ}(i) \\ r^2_{XJ}(i) \end{Bmatrix} \tag{2.22}$$

Denoting $\frac{\partial}{\partial Z_J}$ as $\left(\,'\right)$ and $\frac{\partial}{\partial t}$ as $\left(\dot{}\right)$ the shaft element equations as derived previously are given below;

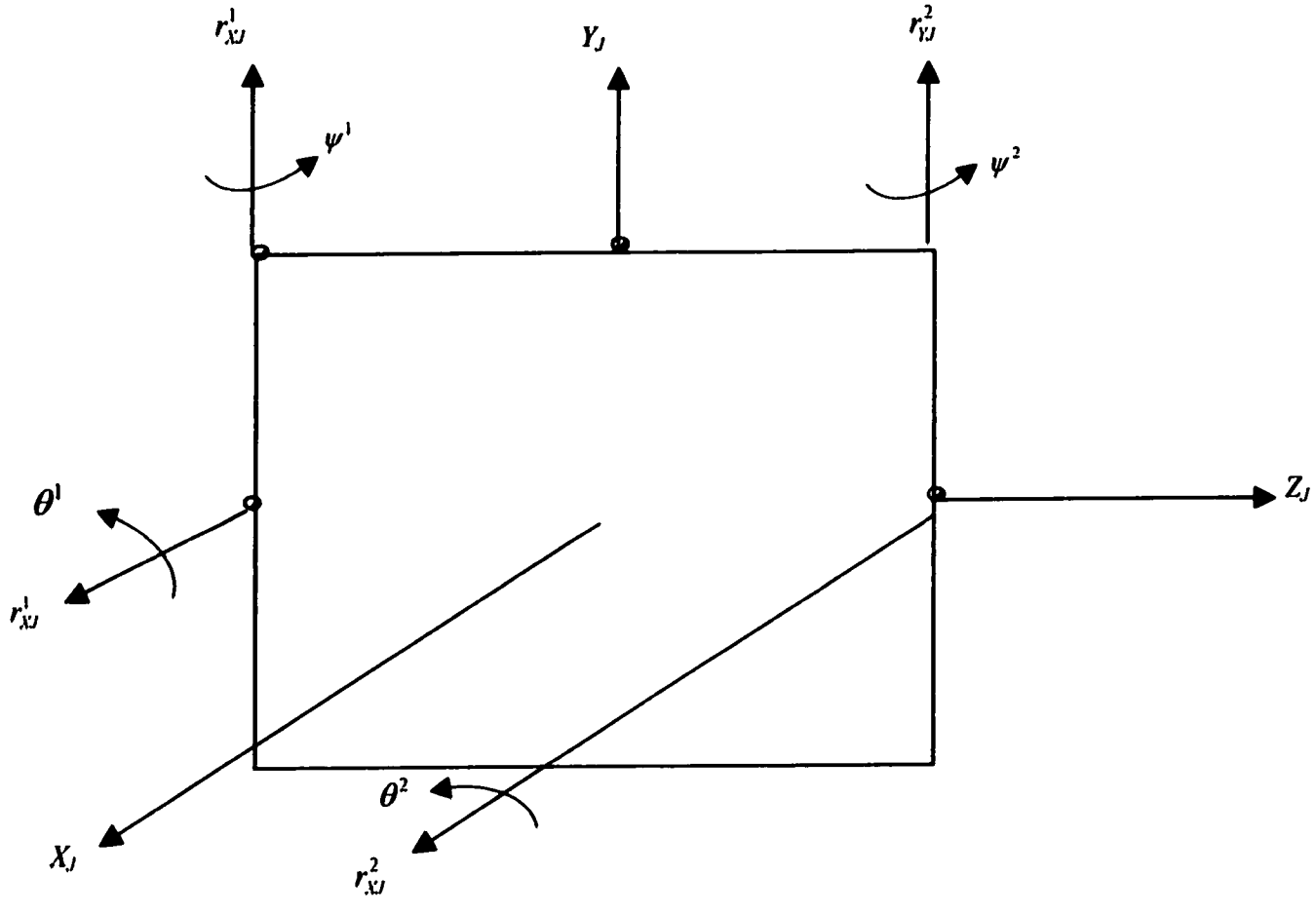

Figure 2.9 Shaft Finite Element Nodal Coordinates

X_J direction:

$$\rho A\ddot{r}_{XJ} = P_X + \kappa AGr''_{YJ} - \kappa AG\theta'$$

$$J_d\left(\ddot{\theta} + 2\psi\Omega - 2\psi\dot{\Omega}\right) = EI_d\theta'' + \kappa AGr'_{YJ} - \kappa AG\theta$$

Y_J direction:

$$\rho A\ddot{r}_{YJ} = P_Y + \kappa AGr''_{XJ} - \kappa AG\psi'$$

$$J_d\left(\ddot{\psi} + 2\dot{\theta}\Omega + 2\theta\dot{\Omega}\right) = EI_d\psi'' + \kappa AGr'_{XJ} - \kappa AG\psi$$

Combining each two equations in each direction in Xj we get $\rho I_d M_{XJ_2} = EI_d\theta''' + \rho A\ddot{r}_{XJ} - P_X$ or in a different from as ;

$$\rho I_d M_{XJ_2} = -\frac{EI_d\rho}{\kappa G}\ddot{r}''_{XJ} + \frac{EI_d}{\kappa AG}P''_X + EI_d r'''_{YJ} + \rho A\ddot{r}_{XJ} - P_X \qquad (2.23)$$

To solve for the static problem, t=0, $\frac{\partial}{\partial t} = 0$, $P_X = P_Y = 0$ which gives a fourth order equation for Translational deformations and a third order equation for rotational deformations;

$$EI_d\theta''' = 0$$

$$EI_d r''' = 0$$

Integrating each we get our shape interpolation equations as

$$r_{YJ} = a + bz + cz^2 + cz^3$$

$$\theta = e + fz + gz^2$$

Where a,b,c,d,e,f and g are to be determined using geometric boundary conditions assuming a unity displacement for the beginning of each element. Using [4] $V = \kappa AG\left(r_{YJ} - \theta\right) = M' = EI\theta''$ and differentiating the two equations above

$$\kappa AG(b+2cz+3dz^2-e-fz-gz^2)=EI2g$$

Solving we get

$$\text{g=3d} \quad \text{and} \quad \text{f=2c} \quad \text{and} \quad \text{e=b-}\frac{6EI}{\kappa AG}d=b-\tfrac{1}{2}\Phi d\ l^2$$

Where $\Phi=\dfrac{12EI}{\kappa AGl^2}$, l is the length of the element, Φ is called the transverse shear effect

$$r_{Yj}=a+bz+cz^2+dz^3$$
$$\theta=\text{b-}\tfrac{1}{2}\Phi d\ l^2+2cz+3dz^2$$

Application of the geometric boundary conditions for a free-free beam for which the beginning node displacement have unity value, end node displacement is zero and both the beginning and end node deformation angles =0 the following is obtained:

$r_{Y_j}(0)=1$ a=1

$r_{Y_j}(l)=0$ $1+\text{bl}+\text{cl}^2+dl^3=0$

$\theta(0)=0$ $\text{b-}\dfrac{\Phi}{2}l^2d=0$

$\theta(l)=0$ $\text{b+2cl+}\left(3-\dfrac{\Phi}{2}\right)l^2d=0;$

for convenience, the J subscript is dropped in matrix format

$$\begin{bmatrix} 1 & 0 & 0 & 0 \\ 0 & 1 & 0 & \frac{\Phi}{2}l^2 \\ 1 & l & l^2 & l^3 \\ 0 & 1 & 2l & \left(3-\frac{\Phi}{2}\right)l^2 \end{bmatrix} \begin{Bmatrix} a \\ b \\ c \\ d \end{Bmatrix} = \begin{Bmatrix} r_Y^1 \\ \theta^1 \\ r_Y^2 \\ \theta^2 \end{Bmatrix} \tag{2.24}$$

Inverting the above matrix

$$\begin{Bmatrix} a \\ b \\ c \\ d \end{Bmatrix} = [Co]^{-1} \{Nodal \text{ displacements}\}$$

The above when substituted back into the fixed coordinate global displacement assumed function shape will give an interpolation between the global coordinates and the nodal coordinates

$$\begin{Bmatrix} r_Y \\ \theta \end{Bmatrix} = [N] \begin{Bmatrix} r_Y^1 \\ \theta^1 \\ r_Y^2 \\ \theta^2 \end{Bmatrix} \quad \text{denoted in this report by } \{d\} = [N]\{q\}$$

The same applies to the Y-axis and the general interpolation relation is given below in (2.25).

As N is symmetric, we interchange variables

$$\begin{Bmatrix} r_X \\ \theta \\ r_Y \\ \psi \end{Bmatrix} = \begin{bmatrix} \Psi_1 & \Psi_2 & \Psi_3 & \Psi_4 & 0 & 0 & 0 & 0 \\ \Psi_5 & \Psi_6 & \Psi_7 & \Psi_8 & 0 & 0 & 0 & 0 \\ 0 & 0 & 0 & 0 & \Psi_1 & \Psi_2 & \Psi_3 & \Psi_4 \\ 0 & 0 & 0 & 0 & \Psi_5 & \Psi_6 & \Psi_7 & \Psi_8 \end{bmatrix} \begin{Bmatrix} r_X^1 \\ \theta^1 \\ r_X^2 \\ \theta^2 \\ r_Y^1 \\ \psi^1 \\ r_Y^2 \\ \psi^2 \end{Bmatrix} \tag{2.25}$$

Where

$$\Psi_1 = \frac{1}{1+\Phi}(1 + \Phi - \Phi\bar{z} - 3\bar{z}^2 + 2\bar{z}^3) \tag{2.26a}$$

$$\Psi_2 = \frac{1}{2(1+\Phi)}(2\bar{z} + \Phi\bar{z} - 4\bar{z}^2 - \Phi\bar{z}^2 + 2\bar{z}^3) \tag{2.26b}$$

$$\Psi_3 = \frac{1}{1+\Phi}(\Phi\bar{z} + 3\bar{z}^2 - 2\bar{z}^3) \tag{2.26c}$$

$$\Psi_4 = \frac{l}{2(1+\Phi)}(-\Phi\bar{z} - 2\bar{z}^2 + \Phi\bar{z}^2 + 2\bar{z}^3) \tag{2.26d}$$

$$\Psi_5 = \frac{1}{l(1+\Phi)}(-6\bar{z} + 6\bar{z}^2) \tag{2.26e}$$

$$\Psi_6 = \frac{1}{(1+\Phi)}(1 + \Phi - 4\bar{z} - \Phi\bar{z} + 3\bar{z}^2) \tag{2.26f}$$

$$\Psi_7 = \frac{1}{l(1+\Phi)}(6\bar{z} - 6\bar{z}^2) \tag{2.26g}$$

$$\Psi_8 = \frac{1}{(1+\Phi)}(-2\bar{z} + \Phi\bar{z} + 3\Phi\bar{z}^2) \tag{2.26h}$$

The above shape functions which describe the displacement of the shaft finite elements are used to represent the element as degrees of freedom in terms of the finite nodal degrees of freedom.

2.6 CONSTITUTIVE RELATIONS IN ROTATING COORDINATES

In this section we will use standard constitutive relations for solid material between stress and strain and transform them into rotating coordinates. Standard advanced materials science textbooks give details about the derivation of constitutive relations and the basic moment curvature equation. Using basic material mechanics relations and rotation transformation matrix as well as the rotational deformation relation with shear angle and bending moment as we get,

$$\sigma = E \in, \qquad \tau = G\gamma, \qquad G = \frac{E}{1+\nu}$$

Transformation matrix

$$A_3 A_2 = \begin{bmatrix} 1 & \theta\psi & -\psi \\ 0 & 1 & \theta \\ \psi & -\theta & 1 \end{bmatrix}$$

Deformation angles

$$\psi = \frac{\partial r_{YJ}}{\partial Z_J}, \qquad \theta = \frac{\partial r_{XJ}}{\partial Z_J}$$

Position vector

$$r_{fJ} = r_{JX}\bar{i}_{11} + r_{JY}\bar{i}_{21} + (\psi r_{JX} - \theta r_{JY})\bar{i}_{33}$$

The strain tensor is given by standard textbooks

$$\in_{ij} = \begin{bmatrix} \in_X & \gamma_{XY}/2 & \gamma_{XZ}/2 \\ & \in_Y & \gamma_{YZ}/2 \\ Sym & & \in_Z \end{bmatrix}$$

The shear angles can be expressed as

$$\gamma_X = \theta - \frac{\partial r_{YJ}}{\partial Z_J}, \qquad \gamma_Y = \psi - \frac{\partial r_{XJ}}{\partial Z_J}$$

Since $\epsilon_X = y\frac{M_X}{EI} = y\frac{\partial^2 r_{YJ}}{\partial Z_J}$, one can write

$$\begin{bmatrix} M_X \\ M_Y \end{bmatrix} = EI \begin{bmatrix} 1 & \\ & 1 \end{bmatrix} \begin{bmatrix} \theta' \\ \psi' \end{bmatrix} \tag{2.27}$$

As such we can obtain the Z-coordinate strain as

$$\epsilon_Z = \frac{\partial r_{ZJ}}{\partial Z_J} = r_{JX}\frac{\partial^2 r_{YJ}}{\partial Z^2} + r_{JY}\frac{\partial^2 r_{XJ}}{\partial Z^2} \tag{2.28}$$

The corresponding potential energy equation can be written as

$$U_1 = \frac{1}{2}\int_V \varepsilon\sigma dV = \frac{1}{2}E\int_V \varepsilon^2 \sigma dV = \frac{1}{2}E\int_V \left[r_{JX}^2 \left(r''_{YJ}\right)^2 + r_{JY}^2 \left(r''_{XJ}\right)^2 - 2r_{JX}r_{JY}r''_{YJ}r''_{XJ} \right] dAdZ \tag{2.29}$$

The third term is zero due to symmetry of shaft. Also one can write $\int_A r_{JX}^2 dA = \int_A r_{JY}^2 dA = I$

$$U_1 = \frac{1}{2}EI\int_0^\ell \left(\left(r''_{YJ}\right)^2 + \left(r''_{XJ}\right)^2 \right) dZ = \frac{1}{2}EI\int_0^\ell \left(\left(\psi'\right)^2 + \left(\theta'\right)^2 \right) dZ \tag{2.30}$$

In *Figure 2.10* which shows a shaft material under rotation, one can use the transformation below to obtain the strain energy in rotating coordinates

$$A_1 = \begin{bmatrix} \cos\phi & \sin\phi \\ -\sin\phi & \cos\phi \end{bmatrix} \tag{2.31}$$

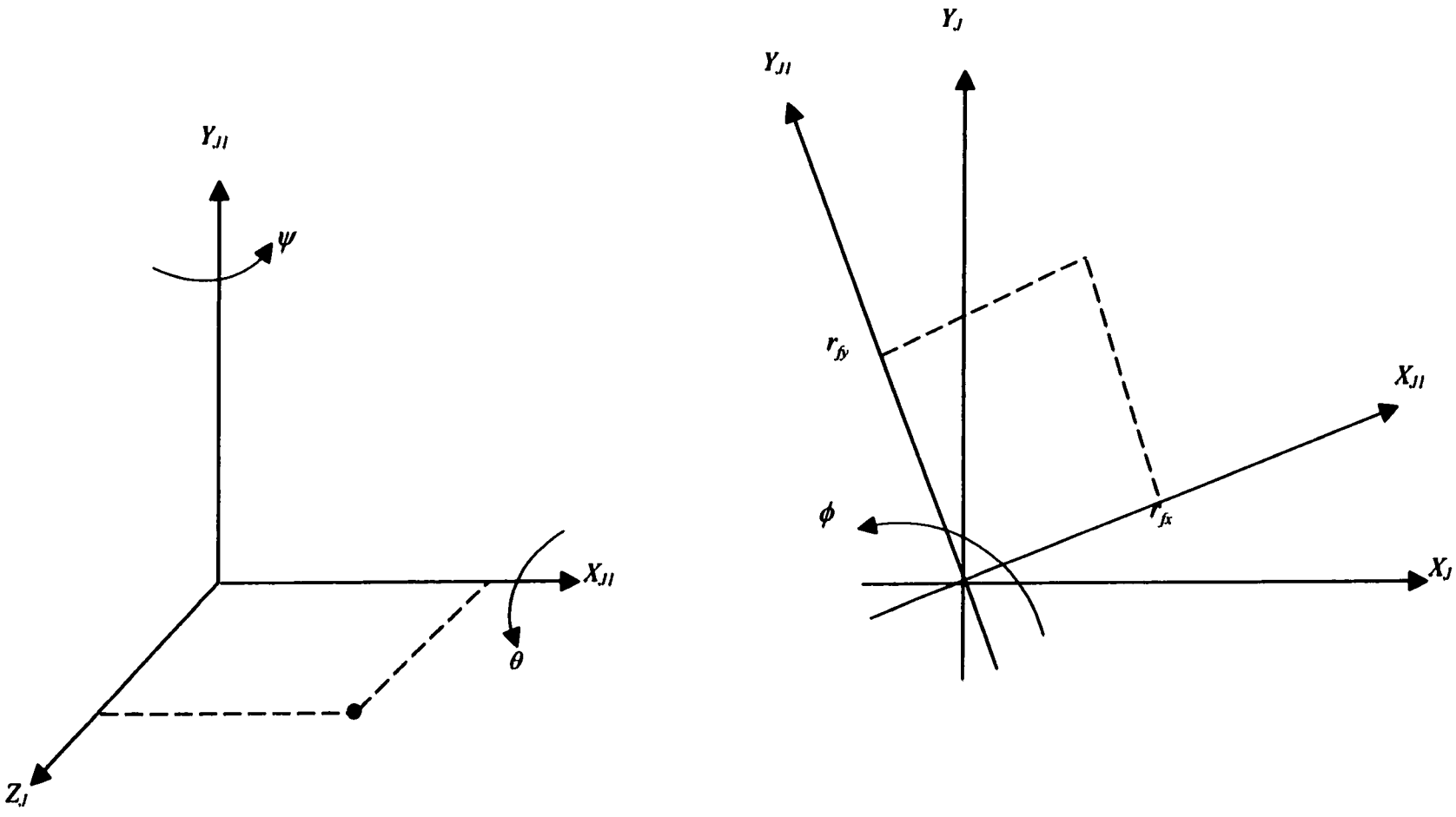

Figure 2.10 Shaft Material under rotation

While in the XZ plane and YZ plane we have shear strain given in standard mechanics of materials textbooks as

$$\tau_{XZ} = G\gamma_{XZ} = \frac{G}{2}(-\gamma_X - \gamma_Y) = \tau_{YZ} \tag{2.32}$$

The corresponding strain energy equation is

$$U_2 = \int \frac{\kappa}{GA} V^2 dZ = \int_V (\tau_{XZ} V_{XZ} + \tau_{YZ} V_{YZ}) dV \tag{2.33}$$

Using

$$V_{XZ} = \kappa A G \tau_{XZ} \tag{2.34}$$

$$\kappa = \frac{6(1+\nu)}{6\nu + 7} \tag{2.35}$$

We obtain

$$U_2 = \frac{1}{2} \int_0^{\ell} \kappa AG \left\{ (r'_{XJ} - \psi)^2 + (r'_{YJ} - \theta)^2 \right\} dZ \tag{2.35}$$

The shape correction factor is to account for shear strain variation over the cross section.

2.7 EQUATIONS OF MOTION FOR A TYPICAL SHAFT ELEMENT

The kinetic and potential energy expressions for the shaft element with angular velocity in rotating body coordinate will be developed in this section. The angular velocity vector was derived in 2.3 as given below

$$\omega_J|_{\bar{X}_{k3}} = \begin{bmatrix} \dot{\theta}\cos\phi - \dot{\psi}\sin\phi \\ \dot{\theta}\sin\phi + \dot{\psi}cos\phi \\ \dot{\psi}\theta + \dot{\phi} \end{bmatrix}, \qquad \bar{X}_{k3} = XJ_3,\ YJ_3,\ ZJ_3$$

Standard disk or shaft element kinetic energy function is given by

$$T = \frac{1}{2} m_s \left(\dot{r}_{JX}^2 + \dot{r}_{JY}^2 \right) + \frac{1}{2} I_a \left(\omega_X^2 + \omega_Y^2 + \omega_Z^2 \right)$$

$$T|_{\bar{X}_{k3}} = \frac{1}{2} \int_0^{\ell} \left\{ \rho I \left(\dot{r}_{J,x}^2 + \dot{r}_{J,Y}^2 \right) + \rho I_d \left(\dot{\theta}^2 + \dot{\psi}^2 \right) + 2 I_d \Omega \dot{\psi} \theta + \Omega^2 \int_0^{\ell} I_d \right\} dZ_J \text{ [1]}$$

(2.36)

Where first term is rectilinear inertia, second term is rotary inertia, third term is gyroscopic inertia and the last term is spin axis inertia. In rotating body coordinates the expression for strain energy developed in previous section is

$$V|_{\bar{X}_{k3}} = \frac{1}{2} \int_0^{\ell} EI \left(\theta'^2 + \psi'^2 \right) dZ + \frac{1}{2} \int_0^{\ell} \kappa AG \left\{ \left(r'_{XJ} - \psi \right)^2 + \left(r'_{YJ} - \theta \right)^2 \right\} dZ$$

(2.37)

The global coordinates will be transformed by use of shape functions to nodal coordinates, $J = \rho I$. In terms of the global coordinates, we have

[1] The reader might notice that the equation have sign differences from standard textbooks equation. This is due to the fact that notation deformation is counterclockwise similar to other angular deformations as used in this study.

$$T = \frac{1}{2}\int_0^{\ell} \rho\{\dot{d}\}^T [m_1]\{\dot{d}\}dz + \Omega^2 J \int_0^{\ell} dz + 2J\Omega \int_0^{\ell} \rho\{\dot{d}\}^T [g_1]\{\dot{d}\}dz$$
$$= \frac{1}{2}\{\dot{q}\}^T \int_0^{\ell} \rho[N]^T [m_1][N]dz\{\dot{q}\} + \Omega^2 JM + 2J\Omega\{\dot{q}\}^T \int_0^{\ell} \rho[N]^T [g_1][N]dz\{\dot{q}\}$$

(2.38a)

$$V = \frac{1}{2}\int_0^{\ell} \{d'\}^T [k_1]\{d'\}dz + \frac{1}{2}\int_0^{\ell} \{d\}^T [k_2]\{d\}dz$$
$$= \frac{1}{2}\{q\}^T \int_0^{\ell} [N']^T [k_1][N']dz\{q\} + \frac{1}{2}\{q\}^T \int_0^{\ell} [N]^T [k_2][N]dz\{q\}$$

(2.38b)

The matrices above are computed as follows

$$[m_1] = \begin{bmatrix} A & & & \\ & I & & \\ & & A & \\ & & & I \end{bmatrix} \qquad [g_1] = \begin{bmatrix} 0 & & & \\ & 0 & & 1 \\ & & 0 & \\ & & & 0 \end{bmatrix}$$

$$[k_1] = \begin{bmatrix} \kappa AG & & & \\ & EI & & \\ & & \kappa AG & \\ & & & EI \end{bmatrix} \qquad [k_2] = \begin{bmatrix} 0 & & & \\ -\kappa AG & 0 & & \\ & & 0 & \\ & & & -\kappa AG \end{bmatrix}$$

Due to the fact that mass center in shafts is typically away from the geometric center and each shaft element has its weight, this results in tangential and centrifugal inertia forces causing element internal unbalance as well as gravity forces associated with each shaft element. If the unbalance is located (mass center eccentricity) at a_{x3} and a_{y3} considering rotating body coordinates, the equation for mass unbalance force is obtained using the principal of virtual work as [3]

$$\delta W_{im} = -\Omega^2 m_{us} \int_0^l \left(a_{x3} \delta r_{jx} + a_{y3} \delta r_{jy} \right) dz \tag{2.39}$$

Such that $a_{x3} = a_x \cos(\Omega t) - a_y \sin(\Omega t)$ and $a_{y3} = a_x \sin(\Omega t) + a_y \cos(\Omega t)$

The non-conservative force can be written as

$$\boxed{\delta W_{im} = -\Omega^2 m_{us} \left[\cos(\Omega t)[m_2]\{q\} + \sin(\Omega t)[m_3]\{q\} \right]} \tag{2.40}$$

With linear distribution of mass center eccentricity given as

$$\begin{aligned} a_x &= a_{x1}(1-\bar{z}) + a_{x2}\bar{z} \\ a_y &= a_{y1}(1-\bar{z}) + a_{y2}\bar{z} \end{aligned} \tag{2.41}$$

and $$\{d_a\} = \begin{pmatrix} a_{x1} \\ a_{x2} \\ a_{y1} \\ a_{y2} \end{pmatrix}$$

The shaft unbalance transformation matrices can be derived as given in Chapter 5. The gravity force is given by [11]

$$\boxed{Q_g = \frac{9.81 \times m_s}{12} [g_2]\{q\}} \tag{2.42}$$

where again a linear distribution of gravity center is assumed and used to obtain the transformation matrix.

2.8 STRUCTURAL DAMPING

Structural or internal material damping is a form of material resistance to change in material configuration as a function of the rate of change. Three types of internal damping are treated in papers and various research topics, these are hysteresis, viscous and shrink fit joints internal friction.

2.8.1 HYSTERESIS DAMPING

The dissipated energy is proportional to the sign of change. As material change sign of strain cycles between tension and compression called hysteresis loop which is a measure of dissipated energy shown in *figure 2.11.* In such a case the stress will lead the strain (Lag in the neutral stress plane from the geometric one) by an angle of α. For every period of vibration, material will go through the hysteresis loop with period $f_n = \frac{\omega_n}{2\pi}$ and speed of $f_\Omega = \frac{\Omega}{2\pi}$. Material will change sign of strain $f_\Omega - f_n$ times per unit time. In viscoelastic material, stress rate raises damping strain rate of $c\dot{\varepsilon}$. Using Taylor expansion $a_0\sigma + a_1\frac{\partial\sigma}{\partial t} + \cdots = b_0 + b_1\frac{\partial\varepsilon}{\partial t} + \cdots$ with cyclic stress/strain of harmonic $(\Omega - \omega_n)t$ the stress and strain will given as [28]

$$\sigma_0 = e^{i(\Omega-\omega_n)t} \qquad \text{and} \qquad \varepsilon_0 = e^{i((\Omega-\omega_n)t-\alpha)} \qquad (2.43\ \text{a,b})$$

and hence

$$\frac{\partial^n\sigma}{\partial t^n} = \left[i(\Omega-\omega_n)\right]^n \sigma_0 e^{i(\Omega-\omega_n)t} \quad \text{and} \quad \frac{\partial^n\varepsilon}{\partial t^n} = \left[i(\Omega-\omega_n)\right]^n \varepsilon_0 e^{i[(\Omega-\omega_n)t-\alpha]}$$

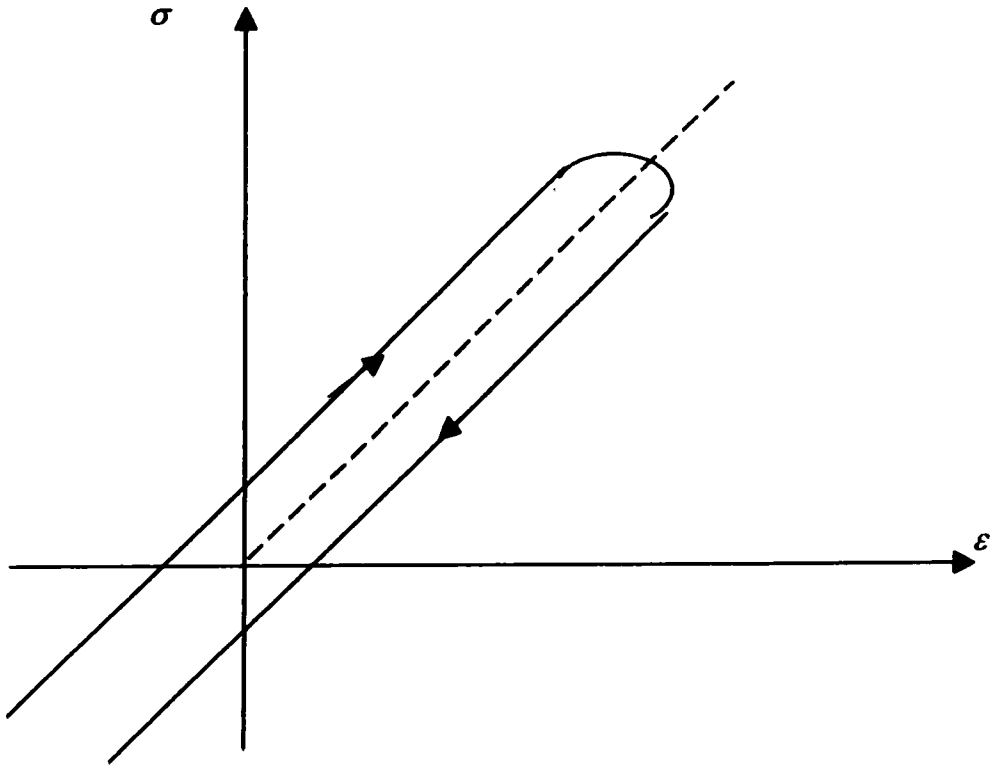

Figure 2.11 Stress-Stain hysteresis damping

Substituting into the Taylor expansion we get

$$\left[a_0 + a_1\left(i(\Omega-\omega_n)\right)+\cdots\right]\sigma_0 = \left[b_0 + b_1\left(i(\Omega-\omega_n)\right)+\cdots\right]\varepsilon_0 e^{-i\alpha}$$

$$\frac{\sigma_0}{\varepsilon_0} = \frac{\bar{b}(\Omega-\omega_n)+i\bar{\bar{b}}(\Omega-\omega_n)}{\bar{a}(\Omega-\omega_n)+i\bar{\bar{a}}(\Omega-\omega_n)}e^{-i\alpha}$$

where $\bar{a},\bar{\bar{a}},\bar{b}$ and $\bar{\bar{b}}$ are functions of $(\Omega-\omega_n)$, $a_0, a_1, b_0, b_1, \cdots\cdots$

$$\frac{\sigma_0}{\varepsilon_0} = \left[A(\Omega-\omega_n)+iB(\Omega-\omega_n)\right]e^{-i\alpha}$$

$$\sigma_0 = E^*\varepsilon_0 \qquad (2.44)$$

This is known in structural mechanics as Kelvin-Veiget constitutive equation [28] where $E^* = E(1+i\eta)$, E^* is complex modulus of elasticity. $\eta = \frac{\delta}{\pi}$ is defined as loss factor. The loss factor is a material property and δ is log decrement of the shaft. Using trigonometric identities and Euler's formula we can get

$$\eta = \frac{\sqrt{1-\sin^2\alpha}}{\sin^2\alpha},\quad \sin\alpha = \frac{\eta}{\sqrt{1+\eta^2}},\quad \cos\alpha = \frac{1+\eta}{\sqrt{1+\eta^2}} \qquad (2.45)$$

2.8.2 INTERNAL VISCOUS DAMPING

This is known as the internal resistance to strain and is given in terms of shaft center velocity [2]as shown in *figure 2.12*

$$D_v = \int_0^{2\pi/\Omega} Pxdt = \pi X^2 c_i \Omega \qquad (2.46)$$

Where X is the amplitude and c_i is the internal viscous damping coefficient.

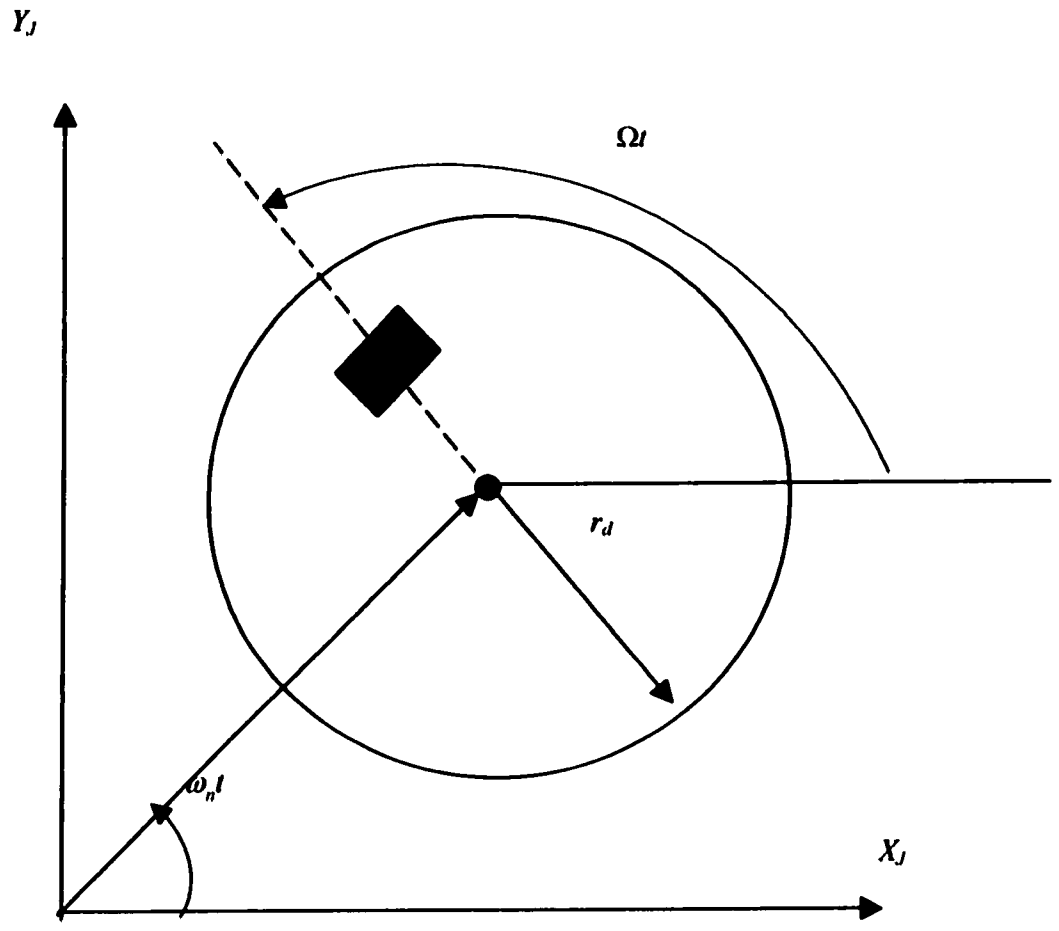

Figure 2.12 – Internal viscous damping in rotating coordinates

2.8.3 ADDING THE EFFECT OF INTERNAL DAMPING

Hysteresis will introduce axis rotation with a transformation matrix due to its effect in producing a lag from neutral or principal axis as shown in *Figure 2.13*. The transformation will be applied to the stress-strain constitutive relations developed in section 2.8.1. Such transformation is given in the following matrix format

$$A_{ID} = \begin{bmatrix} \cos\alpha & \sin\alpha \\ -\sin\alpha & \cos\alpha \end{bmatrix} = \begin{bmatrix} 1 & \alpha \\ -\alpha & 1 \end{bmatrix} \tag{2.47}$$

Which will be applied to moment-curvature relation

$$\begin{bmatrix} M_X \\ M_Y \end{bmatrix} = EI\left[A_{ID}\right]\begin{bmatrix} \theta' \\ \psi' \end{bmatrix} \quad \begin{matrix} M_X = EI\theta' + EI\alpha\psi' \\ M_Y = EI\psi' + EI\alpha\theta' \end{matrix} \tag{2.48 a,b}$$

The effect of internal damping is introduced by the second terms on the right hand side of equation (2.48). Those will result in dissipation energy introduced to the system. Using the principle of virtual work, one can write;

$$\delta w_{id} = \int_0^{\ell} \frac{\partial}{\partial z_J}(EI\alpha\theta')\delta\psi dz = EI\alpha\theta'\Big|_0^{\ell} - \int_0^{\ell} EI\alpha\theta'\delta\psi' dz$$

The first term forms a natural boundary term and vanishes for a free-free beam element while the second term introduces the non-conservative work.

$$\boxed{\delta W^{nc} = -EI\alpha\int_0^{\ell}\delta\{d'\}^T[c_1]\{d'\}dz = -EI\alpha\{q\}^T\int_0^{\ell}[N']^T[c_1][N']dz\{q\}} \tag{2.49}$$

The second effect will be a non-conservative terms introduced in the stress-strain constitutive relations as expressed in rotating body coordinates.

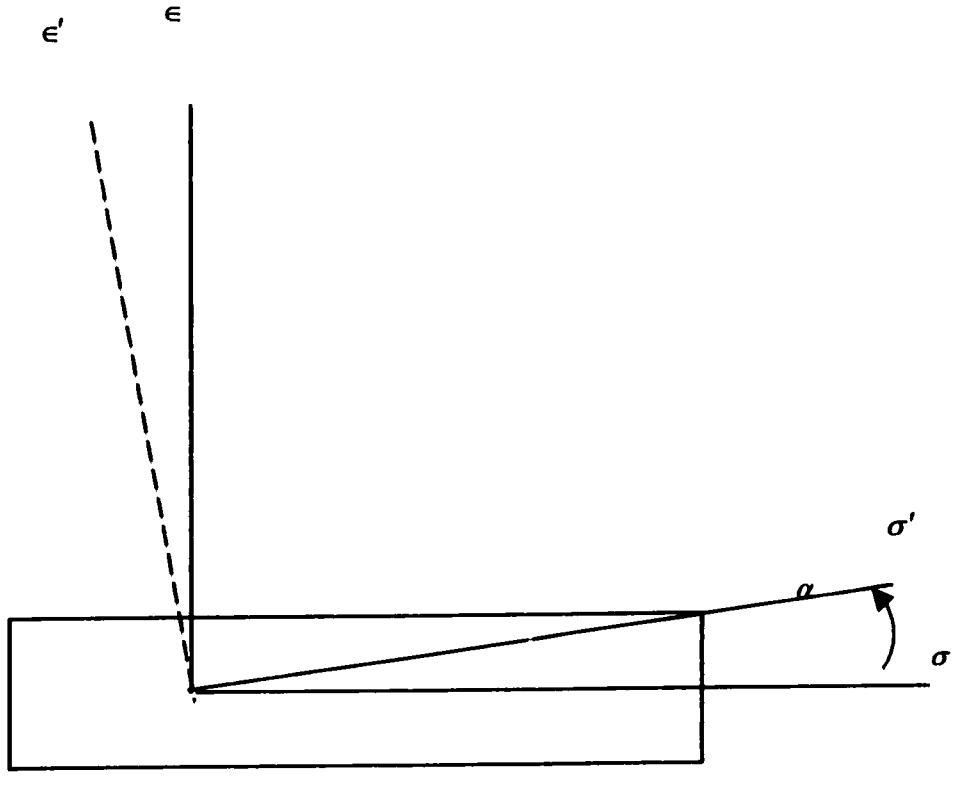

Figure 2.13 Stress-Strain angle lag due to hysteresis damping

The shear angle relation given by $\gamma = V/\kappa AG$ will not be affected and only ϵ_z will introduce a non-conservative term as $\sigma_z^{nc} = -E\alpha\,\epsilon_z$ This term is expressed by the following equation [11].

$$\delta W^{nc} = \int_0^\ell \int_A \delta\epsilon_z\,\sigma_z^{nc}\,dA\,dz = -\frac{1}{2}EI\alpha\int_0^\ell \delta\epsilon_z\,\epsilon_z\,dz = -\frac{1}{2}EI\alpha\int_0^\ell \left(\psi'^2+\theta'^2\right)dz$$
$$= -\frac{1}{2}EI\alpha\int_0^\ell \{d'\}^T[c_2]\{d'\}\,dz \qquad (2.50)$$

To include the effect of internal viscous damping we utilize [11].

$$f_i = e_i\left\{\left(\dot{r}_X - \Omega r_Y\right)\bar{i}_{11} + \left(\dot{r}_Y - \Omega r_X\right)\bar{i}_{21}\right\}$$

The viscous damping force will introduce two matrices into displacement and velocities given below [13]

$$Q = -c_i\int_0^\ell \{\dot{d}\}^T[k_4][N]\,dz - c_d\Omega\int_0^\ell \{\dot{d}\}^T[k_5][N]\,dz$$
$$= \frac{c_i}{\rho A}\{\dot{q}\}^T\int_0^\ell [N]^T[k_4][N]\,dz - \frac{c_d\Omega}{\rho A}\{\dot{q}\}^T\int_0^\ell [N]^T[k_5][N]\,dz \qquad (2.51)$$

The transformation matrices are derived as

$$[k_4] = \begin{bmatrix} 1 & & \\ & 0 & \\ & & 1 \\ & & & 0 \end{bmatrix} \quad [k_5] = \begin{bmatrix} 0 & 1 & & \\ & 0 & & \\ -1 & & 0 & \\ & & & 0 \end{bmatrix} \quad [c_1] = \begin{bmatrix} 0 & & & \\ & 0 & & 2 \\ & & 0 & \\ & & & 0 \end{bmatrix}, \quad [c_2] = \begin{bmatrix} 0 & & & \\ & 1 & & \\ & & 0 & \\ & & & 1 \end{bmatrix}$$

2.9 DISK AND FOUNDATION EQUATIONS

The disk is assumed to be located at a node, rigid, with element unbalance mass m_{ud} of negligible size, located at distance e_x and e_y. In real machinery, turbine and compressor wheels and gears are modeled as disks. The assumption of rigidity of the disk gives the ground to neglect the inertia coupling between longitudinal, torsional and lateral motion. The rigid disk assumption is based on the fact that disk thickness is negligible compared with the disk length. If this is not the case, thick disk treatment is necessary where a shape transformation matrix is used and the disk is treated as a shaft element with varying length. As shown in *Figure 2.14* and using the shaft element angular velocity vector, the disk angular velocity vector can be written as below

$$\omega_J = \begin{Bmatrix} \dot{\theta}\cos\phi - \dot{\psi}\sin\phi \\ \dot{\theta}\sin\phi + \dot{\psi}\cos\phi \\ \dot{\psi}\theta + \dot{\phi} \end{Bmatrix}$$

Using thin disk diameteral and lateral moments of inertia $I_a = 2I_d$, the kinetic energy expression is given as [7].

$$T_D = \frac{1}{2}m_D\left(\dot{r}_{fx}^2 + \dot{r}_{fy}^2\right) + \frac{1}{2}I_a\left(\omega_x^2 + \omega_y^2 + \omega_z^2\right) \tag{2.52}$$

$$T_D = \frac{1}{2}m_D\left(\dot{r}_{fx}^2 + \dot{r}_{fy}^2\right) + \frac{1}{2}I_d\left(\dot{\theta}^2 + \dot{\psi}^2\right) + \frac{1}{2}\Omega^2 I_d + \frac{1}{2}I_a\dot{\psi}^2\theta^2 + I_a\dot{\psi}\theta\Omega$$

In matrix format we get

$$T = \frac{1}{2}\{\dot{d}\}^T \begin{bmatrix} m_d & 0 & 0 & 0 \\ 0 & I_d & 0 & 0 \\ 0 & 0 & m_d & 0 \\ 0 & 0 & 0 & I_d \end{bmatrix} \{\dot{d}\} + 2I_d\dot{\psi}\theta\Omega + I_d\Omega^2 \tag{2.53}$$

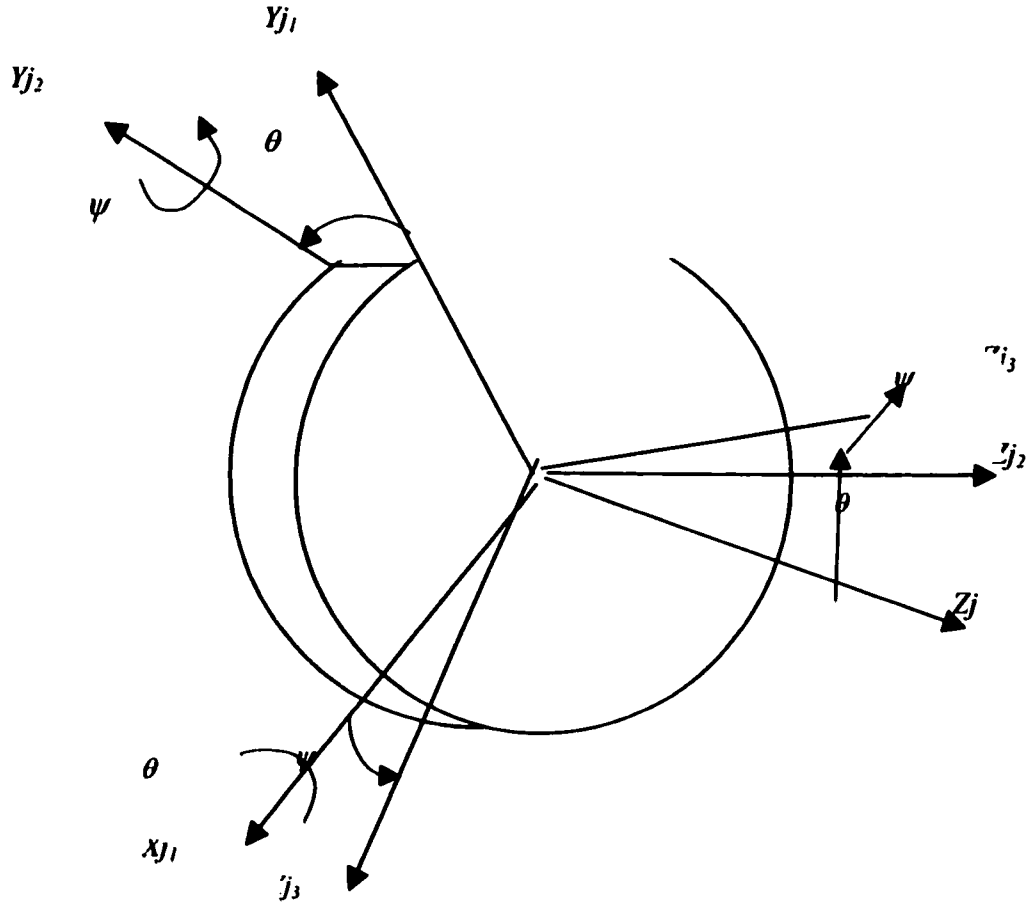

Figure 2.14 – Disk Rotational Deformations

Or expressed as

$$T = \frac{1}{2}\{\dot{d}\}^T \begin{bmatrix} m_d & 0 & 0 & 0 \\ 0 & I_d & 0 & 0 \\ 0 & 0 & m_d & 0 \\ 0 & 0 & 0 & I_d \end{bmatrix} \{\dot{d}\} + \Omega \{\dot{d}\}^T \begin{bmatrix} 0 & 0 & 0 & 0 \\ 0 & 0 & 0 & 2I_d \\ 0 & 0 & 0 & 0 \\ 0 & 2I_d & 0 & 0 \end{bmatrix}$$

Where $I_d\Omega^2$ will be added to unbalance force. Unbalance force, $m_{ud}\ddot{r}_{jx}$, $r_{jx} = e_x \sin\Omega t$ [1]

$$f_{ud} = -e_x m_{ud}\Omega^2 \sin\Omega t \qquad (2.54)$$

$$\{Q\} = \left(m_{us}\Omega^2 \begin{Bmatrix} e_x \\ e_y \\ 0 \\ 0 \end{Bmatrix} \cos(\Omega t) + m_{us}\Omega^2 \begin{Bmatrix} -e_x \\ e_y \\ 0 \\ 0 \end{Bmatrix} \sin(\Omega t) - I_d\Omega^2 \right) + 9.81 \times m_d \begin{Bmatrix} 0 \\ -1 \\ 0 \\ 0 \end{Bmatrix} \qquad (2.55)$$

In equation 2.55, the last term accounts for gravity force.

In some machines the bearings might be mounted on flexible supports as typically the case in gas turbines compressor-turbine section bearing. This flexibility will influence the system motion especially at that location shown in *Figure 2.15*. At such bearings the designer would be able to design for bearing sleeve movement due to foundation flexibility, which is termed absolute motion. The absolute shaft motion is the vector sum of shaft relative displacement (relative to sleeve) and the bearing displacement relative to foundation. To develop the shaft absolute motion position, velocity and acceleration vectors, the reader is recommended to go through the work of Fung, et al [30].

[1] It is worth mentioning that the assumed position for mass unbalance will be compensated by the shaft static and dynamic deflection as a closed loop feed while programming the model.

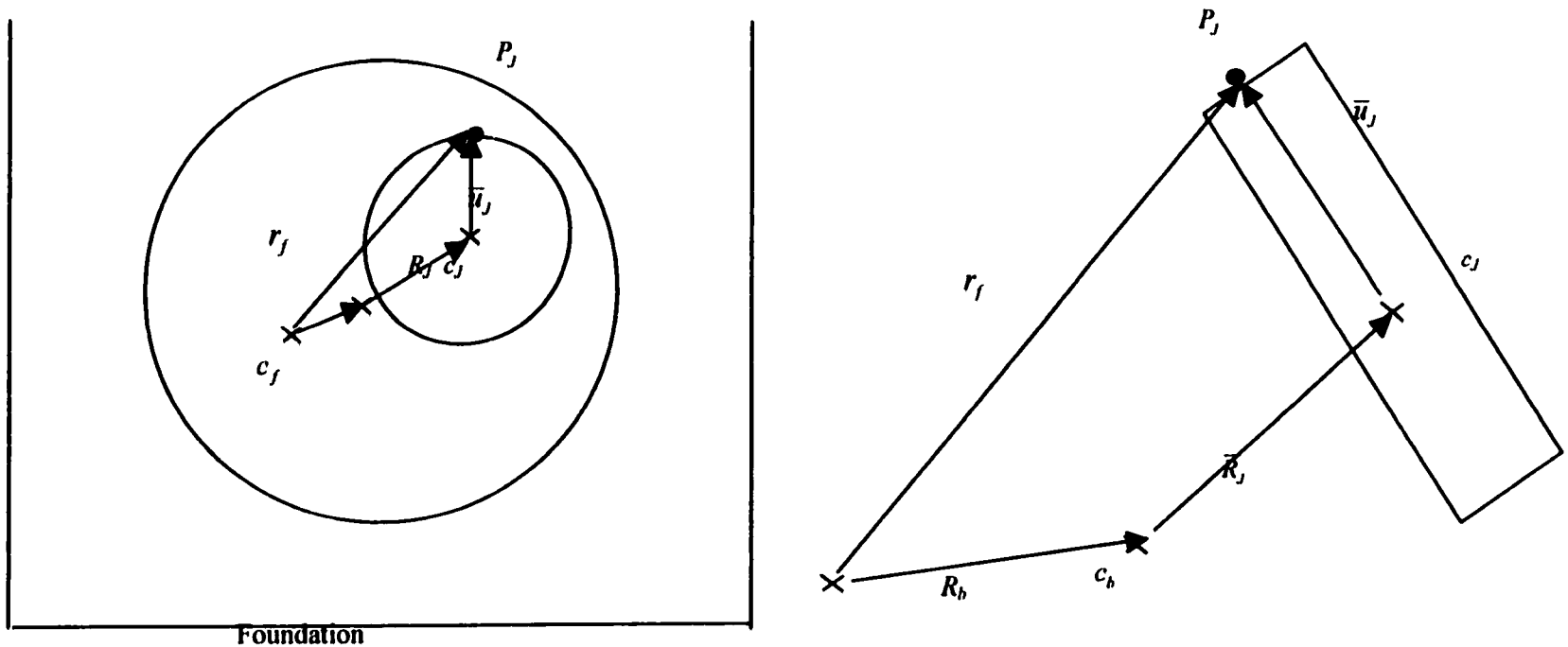

Figure 2.15 – Flexible Foundation Effects

The effect of force transmitted from the bearing on the shaft motion is incorporated as opposed to including the full model of the elastic foundation, which is not in the scope of this study. Shaft material point P_J with respect to foundation using multi-body dynamics relations gives :

$$\dot{A}\bar{r} = \tilde{\omega} A\bar{r} = \omega \times r = A(\bar{\omega} \times r)$$

$$\ddot{A}\bar{r} = \dot{\tilde{\omega}} A\bar{r} + \tilde{\omega}\dot{A}\bar{r} = \dot{\tilde{\omega}} r + \tilde{\omega}\tilde{\omega} r = A(\bar{\alpha} \times \bar{r}) + A\left[\bar{\omega} \times (\bar{\omega} \times \bar{r})\right]$$

$$\begin{aligned} r_f &= R_b + r_J = R_b + R_J + u_J \\ &= R_b + A_b\left[\bar{R}_J + u_J\right] \\ &= R_b + A_b\left[\bar{R}_J + A_J\bar{u}_J\right] \end{aligned} \tag{2.56}$$

$$\begin{aligned} \dot{r}_f &= \dot{R}_b + \dot{R}_J + \dot{u}_J \\ \dot{R}_J &= A_b\dot{\bar{R}}_J + \dot{A}_b\bar{R}_J = A_b\dot{\bar{R}}_J + A_b(\bar{\omega}_b \times \bar{R}_J) \end{aligned} \tag{2.57}$$

Since $u_J = A_bA_J\bar{u}_J$, $\dot{u}_J = \dot{A}_bA_J\bar{u}_J + A_b\dot{A}_J\bar{u}_J + A_bA_J\dot{\bar{u}}_J$. The shaft is treated as non-deformable body, $\dot{\bar{u}}_J = \ddot{\bar{u}}_J = 0$ which gives us

$$\dot{u}_J = \tilde{\omega}_bA_bA_J\bar{u}_J + A_b\tilde{\omega}_JA_J\bar{u}_J = A_b(\tilde{\omega}_b \times A_J\bar{u}_J) + A_bA_J(\tilde{\omega}_J \times \bar{u}_J) = A_bA_J\left[(\bar{\omega}_b \times \bar{u}_J) + (\bar{\omega}_J \times \bar{u}_J)\right]$$

In summary the displacement, velocity and acceleration vectors are as given below

$$r_f = R_b + A_b\left[\bar{R}_J + A_J\bar{u}_J\right] \tag{2.58}$$

$$\dot{r}_f = A_b\dot{\bar{R}}_J + A_b(\bar{\omega}_b \times \bar{R}_J) + A_bA_J\left[(\bar{\omega}_b \times \bar{u}_J) + (\bar{\omega}_J \times \bar{u}_J)\right] \tag{2.59}$$

$$\begin{aligned} \ddot{r}_f = {} & 2A_b(\bar{\omega}_b \times \dot{\bar{R}}_J) + A_b\ddot{\bar{R}}_J + A_b(\bar{\alpha}_b \times \bar{R}_J) + A_b\left[\bar{\omega}_b \times (\bar{\omega}_b \times \bar{R}_J)\right] \\ & + A_bA_J\left\{\left[2\bar{\omega}_b \times (\bar{\omega}_J \times \bar{u}_J)\right] + (\bar{\alpha}_b \times \bar{u}_J) + (\bar{\alpha}_J \times \bar{u}_J) + \left[\bar{\omega}_b \times (\bar{\omega}_b \times \bar{u}_J)\right] + \left[\bar{\omega}_J \times (\bar{\omega}_J \times \bar{u}_J)\right]\right\} \end{aligned} \tag{2.60}$$

The transformation matrices of the foundation frame are given below

$$A_J = \begin{bmatrix} \cos\phi - \theta\psi\sin\phi & \sin\phi + \psi\theta\cos\phi & -\psi \\ -\sin\phi & \cos\phi & \theta \\ \theta\sin\phi + \psi\cos\phi & -\theta\cos\phi + \psi\sin\phi & 1 \end{bmatrix} \qquad \bar{\omega}_J = \begin{bmatrix} \dot{\theta} - \dot{\phi}\psi \\ \theta\dot{\phi} + \dot{\psi} \\ \psi\dot{\theta} + \dot{\phi} \end{bmatrix}$$

$$A_b = \begin{bmatrix} 1 & -\theta_b\psi_b & -\psi_b \\ 0 & 1 & \theta_b \\ \psi_b & \theta_b & 1 \end{bmatrix} \qquad \bar{\omega}_b = \begin{bmatrix} \dot{\theta}_b \\ \dot{\psi}_b \\ \psi_b\dot{\theta}_b \end{bmatrix}$$

Using the assumption that if the shaft was rigid, bearing flexible foundations will cause the system to have two additional rigid body translational degrees of freedom and two additional rigid body rotational degrees of freedom and treating the system as lumped system approach, the flexible foundation stiffness, damping and bearing housing mass will affect the translational nodes at the first and last station. The effect of flexible bearing supports will add a translational vector, a rotational transformation to the original position vector (with respect to bearing coordinates) and also it will add some inertia, stiffness and damping to the system. Below the force and moment balance equations taken at middle of the shaft (disk location) are derived.

$$m_d\ddot{\alpha}_b - l_2 m_{b1}(\ddot{x}_b - l_2\ddot{\alpha}_b) + l_1 m_{b2}(\ddot{x}_b + l_1\ddot{\alpha}_b) + J\ddot{\alpha}_b - l_2 c_{x1}(\dot{x}_b - l_2\dot{\alpha}_b) + l_1 c_{x2}(\dot{x}_b + l_1\dot{\alpha}_b) - l_2 k_{x1}(x_b - l_2\alpha_b) + l_1 k_{x2}(x_b + l_1\alpha_b) = M_{xb1} + M_{xb2} \tag{2.61a}$$

$$m_{b1}(\ddot{x}_b - l_2\ddot{\alpha}_b) + m_{b2}(\ddot{x}_b + l_1\ddot{\alpha}_b) + c_{x1}(\dot{x}_b - l_2\dot{\alpha}_b) + c_{x2}(\dot{x}_b + l_1\dot{\alpha}_b) + k_{x1}(x_b - l_2\alpha_b) + k_{x2}(x_b + l_1\alpha_b) = F_{xb1} + F_{xb2} \tag{2.61b}$$

$$m_d\ddot{\beta}_b + l_2 m_{b1}(\ddot{y}_b + l_2\ddot{\beta}_b) - l_1 m_{b2}(\ddot{y}_b - l_1\ddot{\beta}_b) + J\ddot{\beta}_b + l_2 c_{y1}(\dot{y}_b + l_2\dot{\beta}_b) - l_1 c_{y2}(\dot{y}_b - l_1\dot{\beta}_b) + l_2 k_{y1}(y_b + l_2\beta_b) - l_1 k_{y2}(y_b - l_1\beta_b) = M_{yb1} + M_{yb2} \tag{2.61c}$$

$$m_{b1}(\ddot{y}_b + l_2\ddot{\beta}_b) + m_{b2}(\ddot{y}_b - l_1\ddot{\beta}_b) + c_{y1}(\dot{y}_b + l_2\dot{\beta}_b) + c_{y2}(\dot{y}_b - l_1\dot{\beta}_b) + k_{y1}(y_b + l_2\beta_b) + k_{y2}(y_b - l_1\beta_b) = F_{yb1} + F_{yb2} \tag{2.61d}$$

In matrix format one can write,

$$\begin{bmatrix} m_{b1}+m_{b2} & -l_2m_{b1}+l_1m_{b2} & & \\ -l_2m_{b1}+l_1m_{b2} & m_d+J+l_2^2m_{b1}+l_1^2m_{b2} & & \\ & & m_{b1}+m_{b2} & l_2m_{b1}-l_1m_{b2} \\ & & l_2m_{b1}-l_1m_{b2} & m_d+J+l_2^2m_{b1}+l_1^2m_{b2} \end{bmatrix} \begin{Bmatrix} \ddot{x}_b \\ \ddot{\alpha}_b \\ \ddot{y}_b \\ \ddot{\beta}_b \end{Bmatrix}$$

$$+ \begin{bmatrix} c_{x_1}+c_{x_2} & -l_2c_{x_1}+l_1c_{x_2} & & \\ -l_2c_{x_1}+l_1c_{x_2} & l_2^2c_{x_1}+l_1^2c_{x_2} & & \\ & & c_{y_1}+c_{y_2} & l_2c_{y_1}-l_1c_{y_2} \\ & & l_2c_{y_1}-l_1c_{y_2} & l_2^2c_{y_1}+l_1^2c_{y_2} \end{bmatrix} \begin{Bmatrix} \dot{x}_b \\ \dot{\alpha}_b \\ \dot{y}_b \\ \dot{\beta}_b \end{Bmatrix} +$$

$$\begin{bmatrix} k_{x_1}+k_{x_2} & -l_2k_{x_1}+l_1k_{x_2} & & \\ -l_2k_{x_1}+l_1k_{x_2} & l_2^2k_{x_1}+l_1^2k_{x_2} & & \\ & & k_{y_1}+k_{y_2} & l_2k_{y_1}-l_1k_{y_2} \\ & & l_2k_{y_1}-l_1k_{y_2} & l_2^2k_{y_1}+l_1^2k_{y_2} \end{bmatrix} \begin{Bmatrix} x_b \\ \alpha_b \\ y_b \\ \beta_b \end{Bmatrix} = \begin{Bmatrix} f_{xb_1}+f_{xb_2} \\ M_{xb_1}+M_{xb_2} \\ f_{yb_1}+f_{yb_2} \\ M_{yb_1}+M_{yb_2} \end{Bmatrix}$$

To asses the effect of foundation on the shaft nodal motion, which can be translated to the middle station as

$$\begin{bmatrix} m_b & & & \\ & l^2m_b & & \\ & & m_b & \\ & & & l^2m_b \end{bmatrix} \begin{Bmatrix} \ddot{r}_{jx} \\ \ddot{\theta} \\ \ddot{r}_{jy} \\ \ddot{\psi} \end{Bmatrix} + \begin{bmatrix} c_x & & & \\ & l^2c_x & & \\ & & c_y & \\ & & & l^2c_y \end{bmatrix} \begin{Bmatrix} \ddot{r}_{jx} \\ \ddot{\theta} \\ \ddot{r}_{jy} \\ \ddot{\psi} \end{Bmatrix} + \begin{bmatrix} k_x & & & \\ & l^2k_x & & \\ & & k_y & \\ & & & l^2k_y \end{bmatrix} \begin{Bmatrix} \ddot{r}_{jx} \\ \ddot{\theta} \\ \ddot{r}_{jy} \\ \ddot{\psi} \end{Bmatrix} = \begin{Bmatrix} f_{xb} \\ M_{xb} \\ f_{yb} \\ M_{yb} \end{Bmatrix}$$

(2.62)

The above equations will be super imposed on the original equations of motion for the shaft elements.

2.10 FLUID FILM BEARING EQUATIONS

Fluid mechanics deal with the determination of the forces acting on fluid particles and their responses to these forces. The responses or flow patterns, depend on both the forces acting on the fluid and also on the fluid properties and the flow boundaries. The motion of a fluid in chemical equilibrium can be completely defined by knowing the pressure, temperature and velocity of the fluid as a function of time and space. General flows are flows that can be steady or unsteady, viscous or inviscid, compressible or incompressible. The fundamental laws to solve fluid motion problems utilize are conservation of mass (Continuity Equation), conservation of linear momentum and conservation of energy. By applying Newton's law, which states that the net force acting on a fluid particle is equal to the time rate of change of the linear momentum of the fluid particle, one can develop the equations for the conservation of linear momentum. The principal forces considered were those that act directly on the mass of the fluid (i.e. body forces) and those that act on the fluid surface (i.e. pressure and shear forces). The resultant equations are known as the Navier-Stockes equations. There are no general solutions for the complete Navier-Stockes equations, exact solutions can be obtained for special flows with simplifying assumptions. Other methods implemented to solve the equations utilized three-dimensional FEM as addversed by Tam, et al [22]. The development of equations of motion attributed to Navier-Stockes is generally found in advanced and basic fluid mechanics as well as constitutive relations of stress and strain rate for Newtonian fluids found in continuum mechanics textbooks. Using FEM to arrive at the bearing equations involve addressing fluids rotating between concentric cylinders of which one or both rotate and deform. Researchers reported

difficulties that are encountered in developing FEM for fluid film bearings [20, 22, 23] the most significant ones that current research did not address are

- Shaft will be changing position from one place to the other especially during dynamic loading and/or machine start-up. This makes the film thickness vary according to which side the shaft is translating or deforming. Adaptive mesh is required which takes input from the shaft eccentricity.
- The FEM mesh itself has to rotate starting from Ω at journal boundary to zero at sleeve sides. This is due to the fact that the fluid rotates within the bearing at an average circumferential flow velocity λ.

In this section equations the variables x, y, z are exchanged for r_{jx}, r_{jy}, r_{jz} as is the custom in deriving fluid equations.

2.10.1 NAVIER-STOCKES EQUATIONS OF MOTION

At the beginning of the development of bearing fluid forces theory, it was assumed that the load from the journals was applied directly to the stationary part (bearing case) and the role of the fluid was to reduce friction. Experiments by Tower and Reynolds made it obvious that the load was carried by the fluid and transmitted to the stator through the fluid film. The general equations of motion (Momentum) and Conservation of mass (Continuity) are of the form [22]:

Conservation of mass "Continuity"

$$\frac{D\rho_f}{Dt} + \rho_f \nabla \cdot \bar{V}_f = 0 \qquad (2.64)$$

Conservation of Momentum

$$\rho_f \frac{D\vec{V}_f}{Dt} = \rho_f \vec{g} + \nabla \cdot \sigma'_{ij} - \nabla P \qquad (2.65)$$

Where $\sigma'_{ij} = \underbrace{\mu\left(\frac{\partial u_i}{\partial x_j} + \frac{\partial u_j}{\partial x_i}\right)}_{\text{rate of distortion}} + \underbrace{\mu\delta_{ij} div\vec{V}_f}_{\text{volumetric dialation}}$ and $P = \frac{\partial P_x}{\partial x} + \frac{\partial P_y}{\partial y} + \frac{\partial P_z}{\partial z}$

And $P_x = -\frac{\partial P_x}{\partial x} + \frac{\partial}{\partial x}\left[2\mu\frac{\partial u}{\partial x} - \frac{2}{3}\mu div\vec{V}_f\right] + \frac{\partial}{\partial x}\left[\mu\left(\frac{\partial u}{\partial y} + \frac{\partial v}{\partial x}\right)\right] + \frac{\partial}{\partial z}\left[\mu\left(\frac{\partial w}{\partial x} + \frac{\partial u}{\partial z}\right)\right]$

For incompressible flow the conservation of momentum equation becomes

$$\rho_f \frac{D\vec{V}_f}{Dt} = \rho_f g - \nabla P + \mu\nabla^2\vec{V} \qquad (2.66)$$

Expanding the summarized forms to three-dimensional flow gives us for incompressible flow

$$\rho_f \frac{Du}{Dt} = \rho_f X_a - \frac{\partial P}{\partial x} - \frac{2}{3}\frac{\partial}{\partial y}(\Lambda\mu) + 2\frac{\partial}{\partial x}\left(\mu\frac{\partial u}{\partial y}\right) + \frac{\partial}{\partial y}\left[\mu\left(\frac{\partial u}{\partial y} + \frac{\partial v}{\partial x}\right)\right] + \frac{\partial}{\partial z}\left[\mu\left(\frac{\partial u}{\partial z} + \frac{\partial w}{\partial x}\right)\right]$$

$$\rho_f \frac{Dv}{Dt} = \rho_f Y_a - \frac{\partial P}{\partial y} - \frac{2}{3}\frac{\partial}{\partial y}(\Lambda\mu) + 2\frac{\partial}{\partial y}\left(\mu\frac{\partial v}{\partial y}\right) + \frac{\partial}{\partial x}\left[\mu\left(\frac{\partial u}{\partial y} + \frac{\partial v}{\partial x}\right)\right] + \frac{\partial}{\partial z}\left[\mu\left(\frac{\partial v}{\partial z} + \frac{\partial w}{\partial y}\right)\right]$$

$$\rho_f \frac{Dw}{Dt} = \rho_f Z_a - \frac{\partial P}{\partial z} - \frac{2}{3}\frac{\partial}{\partial z}(\Lambda\mu) + 2\frac{\partial}{\partial z}\left(\mu\frac{\partial u}{\partial z}\right) + \frac{\partial}{\partial x}\left[\mu\left(\frac{\partial u}{\partial z} + \frac{\partial w}{\partial x}\right)\right] + \frac{\partial}{\partial y}\left[\mu\left(\frac{\partial v}{\partial z} + \frac{\partial w}{\partial y}\right)\right]$$

$$\frac{\partial\rho_f}{\partial t} + \frac{\partial}{\partial x}(\rho_f u) + \frac{\partial}{\partial y}(\rho_f v) + \frac{\partial}{\partial z}(\rho_f w) = 0 \qquad (2.67\ a,b,c,d)$$

Where

$$\frac{Du}{Dt} = \frac{\partial u}{\partial t} + u\frac{\partial u}{\partial x} + v\frac{\partial u}{\partial y} + w\frac{\partial u}{\partial z}, \qquad \frac{Dv}{Dt} = \frac{\partial v}{\partial t} + u\frac{\partial v}{\partial x} + v\frac{\partial v}{\partial y} + w\frac{\partial v}{\partial z}$$

$$\frac{Dw}{Dt} = \frac{\partial w}{\partial t} + u\frac{\partial w}{\partial x} + v\frac{\partial w}{\partial y} + w\frac{\partial w}{\partial z} \qquad \Lambda = \frac{\partial u}{\partial x} + \frac{\partial v}{\partial y} + \frac{\partial w}{\partial z}$$

2.10.2 GENERAL REYNOLDS EQUATION DERIVATION

Conservation of energy equations developed on the basis of the conservation of mass and conservation of linear momentum do consider fluids whose temperature could vary in space and/or in time. Variations in temperature would produce changes in density and viscosity. In most of the problems of oil flow in fluid film bearings, temperature is normally assumed to be constant and thus viscosity and density are constant. The flow field solution in such cases is characterized and obtained using the continuity and momentum equations only. If the application involves considerable variations in the fluid temperature so the convective heat transfer is important, the temperature field is obtained by solving the energy equation after the velocity field has been determined through the solution of the continuity and momentum equations. Such solution for a laminar boundary layer is known as Pohlhausen solution. Gravity and magnetic forces are the only body forces treated in lubrication which are characterized by three metrics for Xj axis which are Froud Number $= \frac{Inertia}{Gravity} = \frac{u^2}{gl}$, Euler Number $= \frac{Pressure}{Inertia} = \frac{P}{\rho_f u^2}$ and Reynolds Number $= \frac{Inertia}{Viscous} = \frac{\rho_f u h^2}{\mu l_b}$.

Characteristic parameters denoted with 'o' subscript will be used to get the dimensionless parameters as listed below

$$X = \frac{r_{jx}}{l_o} \quad Y = \frac{r_{jy}}{b_o} \quad Z = \frac{r_{jz}}{h_o} \quad T = \frac{t}{t_o} \quad \bar{u} = \frac{u}{u_o} \quad \bar{v} = \frac{v}{v_o} \quad \bar{w} = \frac{w}{w_o} \quad \bar{\rho} = \frac{\rho_f}{\rho_o}$$

$$\bar{\mu} = \frac{\mu}{\mu_o} \quad P = \frac{h_o^2 p}{\mu_o u_o l_o} \quad R_x = \frac{\rho_o u_o l_o}{\mu_o} = \frac{\rho_o u_o h_o^2}{\mu_o l_o} \quad R_y = \frac{\rho_o v_o h_o^2}{\mu_o b_o} \quad R_z = \frac{\rho_o w_o h_o}{\mu_o} \quad \sigma_s = \frac{\rho_o h_o^2}{t_o \mu_o}$$

The modification in R_x is due to dominance of viscous term in N-S equation $\frac{\partial^2 \bar{u}}{\partial Z^2}$

$$\sigma_s \frac{\partial \bar{u}}{\partial T} + R_X \bar{u} \frac{\partial \bar{u}}{\partial X} + R_Y \bar{v} \frac{\partial \bar{u}}{\partial Y} + R_Z \bar{w} \frac{\partial \bar{u}}{\partial Z} = g \frac{l_o}{u_o^2} R_X - \frac{1}{\bar{\rho}} \frac{\partial P}{\partial X} + \frac{1}{\bar{\rho}} \frac{\partial}{\partial Z}\left(\bar{\mu} \frac{\partial \bar{u}}{\partial Z} \right)$$
$$-\frac{2}{3}\left(\frac{h_o}{l_o}\right)^2 \frac{1}{\bar{\rho}} \frac{\partial}{\partial X}\left[\bar{\mu}\left(\frac{\partial \bar{u}}{\partial X} + \frac{v_o}{u_o}\frac{l_o}{b_o}\frac{\partial \bar{v}}{\partial Y} + \frac{w_o}{u_o}\frac{l_o}{h_o}\frac{\partial \bar{w}}{\partial Z} \right) \right] + \left(\frac{h_o}{b_o}\right)^2 \frac{1}{\bar{\rho}} \frac{\partial}{\partial Y}\left[\bar{\mu}\left(\frac{\partial \bar{u}}{\partial Y} + \frac{v_o}{u_o}\frac{b_o}{l_o}\frac{\partial \bar{v}}{\partial X} \right) \right]$$
$$+2\left(\frac{h_o}{l_o}\right)^2 \frac{1}{\bar{\rho}} \frac{\partial}{\partial Z}\left(\bar{\mu} \frac{\partial \bar{u}}{\partial Z} \right) + \frac{1}{\bar{\rho}} \frac{\partial}{\partial Z}\left(\bar{\mu} \frac{w_o}{u_o}\frac{h_o}{l_o}\frac{\partial \bar{v}}{\partial X} \right)$$

(2.68)

In order to arrive at the General Reynolds equation approximation of N-S equations (2.67), a number of assumptions are made as listed below

1) Neglect body forces, no extra fields of forces acting on fluid
2) Pressure is constant through the thickness of film (side leakage =0) $\frac{\partial P}{\partial Z} = 0$
3) Curvature of surfaces is large compared with film thickness. Surface velocities are not considered as varying in direction
4) No slip at boundaries, velocity of oil layer adjacent to the boundary is the same as the boundary
5) Lubricant is Newtonian, stress is proportional to rate of shear
6) Flow is laminar
7) Fluid inertia is neglected
8) Viscosity is constant
9) $\frac{\partial w}{\partial x} \& \frac{\partial w}{\partial y} << \frac{\partial u}{\partial z} \& \frac{\partial v}{\partial z}$, Velocity in the lateral direction << longitudinal and axial directions.

In equation 2.68 the following relations are observed;

- Inertia and gravity is of the order $\frac{h_o}{l_o}$
- Velocity ration $\frac{w_o}{u_o}$ is of $\frac{h_o}{l_o}$ order.
- Pressure gradient $\frac{\partial P}{\partial X}$ and first viscous terms $\frac{\partial}{\partial Z}\left(\bar{\mu}\frac{\partial \bar{u}}{\partial Z}\right)$ are of order (1)
- The remaining viscous terms are of the orders $\left(\frac{h_o}{l_o}\right)^2$ or $\left(\frac{h_o}{b_o}\right)^2$

Neglecting all $\left(\frac{h_o}{l_o}\right)^2$ or $\left(\frac{h_o}{b_o}\right)^2$ terms considered to be very small as in (7) & (8) in the assumptions above, the following equation is obtained in place of the first and second NS equations, while the third equation according to assumption (2) is zero.

$$\sigma_s \frac{\partial \bar{u}}{\partial T} + R_X \bar{u}\frac{\partial \bar{u}}{\partial X} + R_Y \bar{v}\frac{\partial \bar{u}}{\partial Y} + R_Z \bar{w}\frac{\partial \bar{u}}{\partial Z} = g\frac{l_o}{u_o^2}R_X - \frac{1}{\bar{\rho}}\frac{\partial P}{\partial X} + \frac{1}{\bar{\rho}}\frac{\partial}{\partial Z}\left(\bar{\mu}\frac{\partial \bar{u}}{\partial Z}\right)$$

$$\sigma_s \frac{\partial \bar{v}}{\partial T} + R_X \bar{u}\frac{\partial \bar{v}}{\partial X} + R_Y \bar{v}\frac{\partial \bar{v}}{\partial Y} + R_Z \bar{w}\frac{\partial \bar{v}}{\partial Z} = g\frac{b_o}{v_o^2}R_Y - \frac{1}{\bar{\rho}}\frac{\partial P}{\partial Y} + \frac{1}{\bar{\rho}}\frac{\partial}{\partial Z}\left(\bar{\mu}\frac{\partial \bar{v}}{\partial Z}\right) \qquad (2.69\ a,b)$$

$$\sigma_s \frac{\partial \bar{\rho}}{\partial T} + R_X \frac{\partial}{\partial X}(\bar{\rho}\bar{u}) + R_Y \frac{\partial}{\partial Y}(\bar{\rho}\bar{v}) + R_Z \frac{\partial}{\partial Z}(\bar{\rho}\bar{w}) = 0 \qquad (2.69\ c)$$

Eliminating inertia and gravity terms of order $\frac{h_o}{l_o}$ and $\frac{h_o}{b_o}$ listed below

$$\frac{l_o}{u_o t_o}\frac{\partial \bar{u}}{\partial T}, \quad \frac{l_o}{h_o}\frac{w_o}{u_o}\bar{w}\frac{\partial \bar{u}}{\partial Z}, \quad \frac{l_o}{b_o}\frac{v_o}{u_o}\bar{v}\frac{\partial \bar{u}}{\partial Y}, \quad \frac{l_o}{u_o^2}g$$

gives

$$\frac{\partial P}{\partial x} = \frac{\partial}{\partial z}\left(\mu \frac{\partial u}{\partial z}\right)$$
$$\frac{\partial P}{\partial y} = \frac{\partial}{\partial z}\left(\mu \frac{\partial v}{\partial z}\right) \qquad (2.70\ a,b)$$

Integrating twice

$$u = \frac{z^2}{2\mu}\frac{\partial p}{\partial x} + \tilde{A}\frac{z}{\mu} + \tilde{B}$$
$$v = \frac{z^2}{2\mu}\frac{\partial p}{\partial y} + \tilde{C}\frac{z}{\mu} + \tilde{D}$$

At no slip, the boundary conditions are $\begin{cases} @\, z = h & u = U_2 \text{ and } v = V_2 \\ @z = 0 & u = U_1 \text{ and } v = V_1 \end{cases}$

Solving the above equations gives the velocity profiles as ;

$$u = \frac{\partial P}{2\mu\partial x}\left(z^2 - zh\right) + \left(U_1 - U_2\right)\frac{z}{h} + U_2$$
$$v = \frac{\partial P}{2\mu\partial y}\left(z^2 - zh\right) + \left(V_1 - V_2\right)\frac{z}{h} + V_2 \qquad (2.71)$$

Putting the continuity equation in integral form

$$\int_0^h \left[\frac{\partial \rho}{\partial t} + \frac{\partial}{\partial x}(\rho u) + \frac{\partial}{\partial y}(\rho v) + \frac{\partial}{\partial z}(\rho w)\right] dz = 0 \qquad (2.72)$$

This integral can be performed using the following role for each of the terms :

$$\int_0^h \frac{\partial}{\partial x}[f(x,y,z)]dz = -f(x,y,h)\frac{\partial h}{\partial x} + \frac{\partial}{\partial x}\left[\int_0^h f(x,y,z)dz\right]$$

ρ_f is assumed to be the mean force density across the film, the u-component is given as

$$\int_0^h \frac{\partial}{\partial x}\left(\rho_f u\right)dz = -\left(\rho_f u\right)_{z=h}\frac{\partial h}{\partial x} + \frac{\partial}{\partial x}\int_0^h \left(\rho_f u\right)dz = -\rho_f U_1 \frac{\partial h}{\partial x} + \frac{\partial}{\partial x}\left(\rho_1 \int_0^h u dz\right) \qquad (2.73)$$

And the v-component

$$\int_0^h \frac{\partial}{\partial y}(\rho_f v)dz = -\rho_f V_1 \frac{\partial h}{\partial y} + \frac{\partial}{\partial y}\left(\rho_f \int_0^h v dz\right) \tag{2.74}$$

The w-component

$$\int_0^h \frac{\partial}{\partial z}(\rho_f w)dz = -\rho(W_1 - W_2) \tag{2.75}$$

The integrated continuity equation is given now by

$$h\frac{\partial \rho_f}{\partial t} - \rho_f U_1 \frac{\partial h}{\partial x} + \frac{\partial}{\partial x}\left(\rho_f \int_0^h u dz\right) - \rho_f V_1 \frac{\partial h}{\partial y} + \frac{\partial}{\partial y}\left(\rho \int_0^h v dz\right) + \rho(W_1 - W_2) = 0 \tag{2.76}$$

Fluid flows at rate $q_x = \int_0^h u dz$ **and** $q_y = \int_0^h v dz$ per unit width, the volume flow rate is $q_x dy$.

The rate of flow out per unit width is $q_x + \frac{\partial q_x}{\partial x}dx$ where $\frac{\partial q_x}{\partial x}$ is the rate of change of flow in the x-direction. Same applies to the flow in and out in the y-direction and the actual flow rate in both directions is From *Figure 2.16*

$$\left(q_x + \frac{\partial q_x}{\partial x}dx\right)dy \text{ in the x - direction}, \qquad \left(q_y + \frac{\partial q_y}{\partial y}dy\right)dx \text{ in the y - direction}$$

For the vertical direction, floor moves at V_2 and roof moves up at V_1, volume change is $(V_1 - V_2)dxdy$. If the top and bottom surface are impermeable, one can write $W_1 - W_2 = \frac{\partial h}{\partial t}$ and equation (2.76) becomes

$$\frac{\partial}{\partial x}(q_x) + \frac{\partial}{\partial y}(q_y) + \rho_f(W_1 - W_2) - \rho_f U_1 \frac{\partial h}{\partial x} - \rho_f V_1 \frac{\partial h}{\partial y} + h\frac{\partial \rho_f}{\partial t} = 0 \tag{2.77}$$

Using the velocity profiles equation (4.71), the flow rates are computed as

$$q_x = \frac{-h^3}{12\mu\partial x}\frac{\partial P}{\partial x} + (U_1 - U_2)h/2 \quad \text{and} \quad q_y = \frac{-h^3}{12\mu\partial y}\frac{\partial P}{\partial y} + (V_1 - V_2)h/2$$

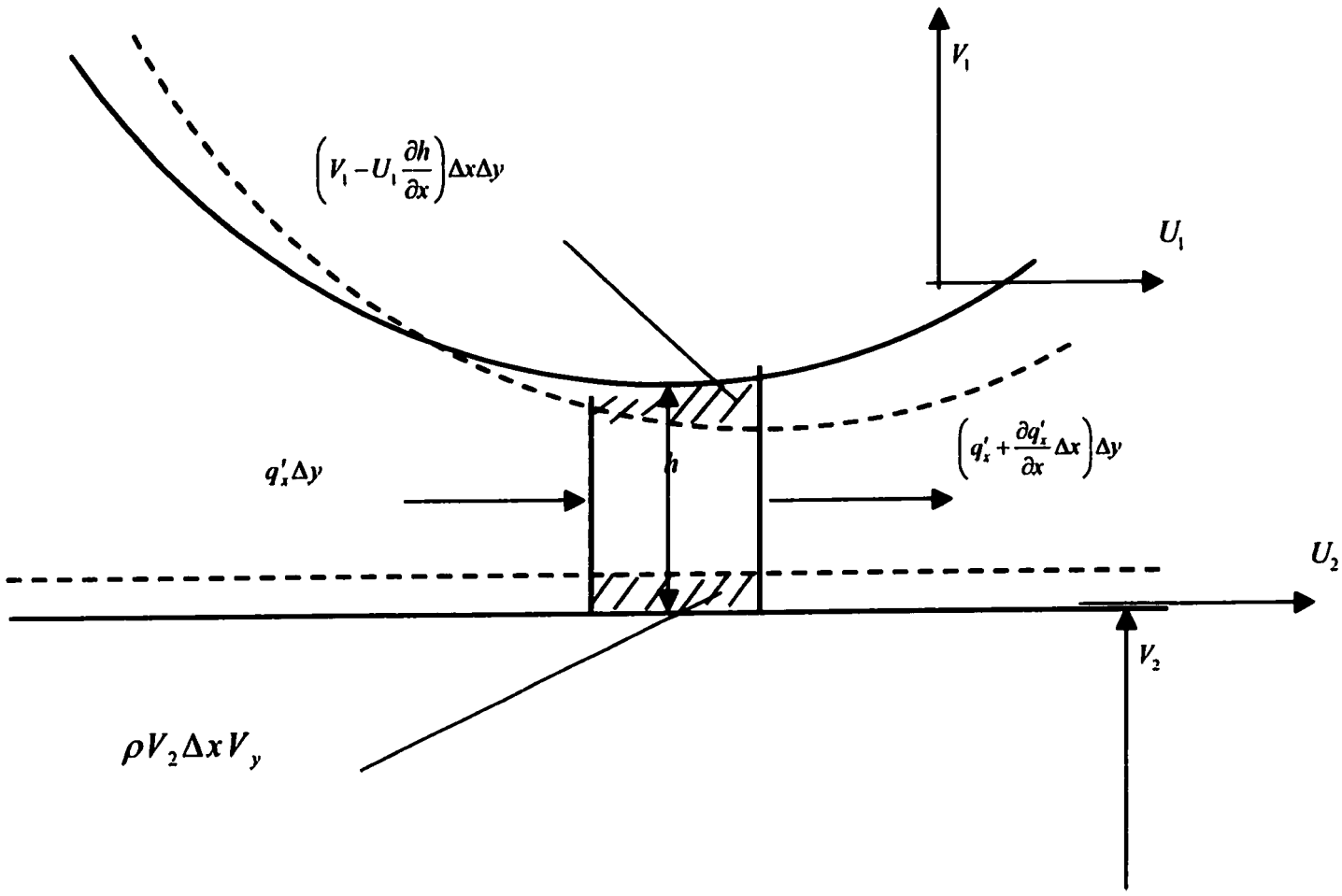

Figure2.16 – Flow Balance

Substituting those into equation (2.77) the General Reynolds Equation becomes

$$\frac{\partial}{\partial x}\left(\frac{-\rho_f h^3}{12\mu}\frac{\partial P}{\partial x}\right)+\frac{\partial}{\partial y}\left(\frac{-\rho_f h^3}{12\mu}\frac{\partial P}{\partial y}\right)+\frac{\partial}{\partial x}\left[\frac{\rho_f h(U_1+U_2)}{2}\right]+\frac{\partial}{\partial y}\left[\frac{\rho_f h(V_1+V_2)}{2}\right]+$$

$$\rho_f(W_1-W_2)-\rho_f U_1\frac{\partial h}{\partial x}-\rho_f V_1\frac{\partial h}{\partial y}+h\frac{\partial \rho_f}{\partial t}=0 \qquad (2.78)$$

Terms from left to right are :

First and second Terms: Poiseville terms, which describe the flow, rate due to pressure gradients within the lubrication area. first term represents Poiseuille (pressure) flow, second term represents Couette (velocity) flow. Both the third and fourth terms describe the net remaining flow rates due to surface velocities which give us the following components in the X & Y directions

Density wedge $\frac{h(U_1+U_2)}{2}\frac{\partial \rho_f}{\partial x}$

Stretch wedge $\frac{\rho_f h}{2}\frac{\partial}{\partial x}(U_1+U_2)$

Physical wedge $\frac{\rho_f(U_1+U_2)}{2}\frac{\partial h}{\partial x}$

Fifth, sixth and seventh terms describe the net flow rates due to squeezing motion . Eighth term give the net flow rate due to local expansion. As ρ decreases, Couette mass flows for each location of the three velocities must differ for continuity of mass flow; generating balancing Poiseuille flow eliminates this discrepancy. Fifth term : Density (Thermal) Wedge which is concerned with the rate at which the lubricant density changes in the sliding direction. Density must decrease in the direction of sliding if positive pressures are to be generated. This effect could be introduced by raising the temperature of the lubricant as it passes through the bearing. The normal squeeze term provides a valuable cushioning effect

when bearing surfaces tend to be pressed together. Positive pressures will be generated when the film thickness is diminishing. In the absence of sliding, the self-acting pressure generating device arises directly from the difference in normal velocities ($W_1 - W_2$). Positive pressure will clearly be achieved if film thickness is decreasing ($W_2 > W_1$). Sixth and Seventh are the translation squeeze term that result from translation of inclined surfaces where local film thickness is squeezed by the sliding of the inclined bearing surface. Pressure is a function of time. The sixth term called the stretch term, which is the rate at which surface velocity changes in the sliding direction. This term is produced if the boundary solids are elastic and the extent to which the surfaces are stretched varies through the bearing. Velocities have to decrease in the sliding direction for the pressure to build. Seventh term called the physical wedge, with Couette volume flow rate which is proportional to the area of the triangle with height h and width u. For positive load carrying capacity the thickness of the lubricant film must decrease in the sliding direction. Eighth term called the local expansion; if heat is supplied to the lubricant, it will expand and the excess volume will have to be expelled. In the absence of surface velocities the excess lubricant volume must be expelled by a pressure (Poiseville) flows action. The General Reynolds Equation is given [20] by

$$\frac{\partial}{\partial x}\left(\frac{\rho h^3}{12\eta}\frac{\partial P}{\partial x}\right)+\frac{\partial}{\partial y}\left(\frac{\rho h^3}{12\eta}\frac{\partial P}{\partial y}\right)=\tilde{u}\frac{\partial(\rho h)}{\partial x}+\tilde{v}\frac{\partial(\rho h)}{\partial y}+\frac{\partial(\rho h)}{\partial t} \qquad (2.79)$$

2.10.3 SHORT BEARING APPROXIMATION OF REYNOLDS EQUATION

There are further simplifications used in order to obtain closed form solution of the Reynolds equation. Those are listed below which simplify the equation and prepare it for being solved by either as a short bearing approximation or as a long bearing approximation. This study address the case of short bearing approximation only. Referring back to *Figure 2.16*, the inflow is given by $q'_y \Delta x$, while the outflow is given by $\left(q'_y + \frac{\partial q'_y}{\partial y}\Delta y\right)\Delta x$ and Mass flow in to the control volume is given by $\rho_f h \Delta x \Delta y$, the rate of mass accumulation becomes $\frac{\partial}{\partial t}(\rho_f h) = \Delta Q = \frac{\partial q_x}{\partial x} + \frac{\partial q_y}{\partial y}$. Using the following expressions below;

1. $\frac{U_1 + U_2}{2} = \tilde{u}$ and $\frac{V_1 + V_2}{2} = \tilde{v}$

2. ρ_f density is constant in z-direction and elsewhere.

One can write $\frac{\partial h}{\partial t} = \frac{\partial q_x}{\partial x} + \frac{\partial q_y}{\partial y}$. Making use of equation (2.76) with constant density given below as $\frac{\partial}{\partial x}(q_x) + \frac{\partial}{\partial y}(q_y) = -(W_1 - W_2) + U_1 \frac{\partial h}{\partial x} + V_1 \frac{\partial h}{\partial y}$

The equation for film thickness becomes

$$\frac{\partial}{\partial t}(\rho h) = \rho \frac{\partial h}{\partial t} + h \frac{\partial \rho}{\partial t} = \rho\left(w_1 - w_2 - u_1 \frac{\partial h}{\partial x} - v_1 \frac{\partial h}{\partial y}\right) + h \frac{\partial \rho}{\partial t}$$

$$\frac{\partial(\rho h)}{\partial t} = \rho(w_h - w_o) - \rho U_1 \frac{\partial h}{\partial x} - \rho V_1 \frac{\partial h}{\partial y} + h \frac{\partial \rho}{\partial t}$$

$$\boxed{\frac{\partial h}{\partial t} = W_2 - W_1 + U_1 \frac{\partial h}{\partial x} + V_1 \frac{\partial h}{\partial y}} \qquad (2.80)$$

Equation (2.80) can be interpreted such that surfaces are impermeable and hence no fluid seeps in or out and they are merely moving relative to each other. This can stated other wise as flow is pure tangential motion or $W_2 = 0, \quad W_1 = u_1 \frac{\partial h}{\partial x} + v_1 \frac{\partial h}{\partial y}$. Following are two approximations, which are;

3. Motion is purely sliding, $\bar{v} = 0$

4. Velocity of a surface does not vary from one point in a bearing to another ($\bar{u}$ is not a function of x. $\frac{\partial}{\partial x} uh \rightarrow u \frac{dh}{dx}$

Reynolds Equation can be written now as

$$\frac{\partial}{\partial x}\left(\frac{h^3}{12\mu}\frac{\partial P}{\partial x}\right) + \frac{\partial}{\partial y}\left(\frac{h^3}{12\mu}\frac{\partial P}{\partial y}\right) = -\bar{u}\frac{\partial h}{\partial x} - \bar{v}\frac{\partial h}{\partial y} - (W_1 - W_2) + U_1\frac{\partial h}{\partial x} + V_1\frac{\partial h}{\partial y}$$

or

$$\frac{\partial}{\partial x}\left(\frac{h^3}{12\mu}\frac{\partial P}{\partial x}\right) + \frac{\partial}{\partial y}\left(\frac{h^3}{12\mu}\frac{\partial P}{\partial y}\right) = -\bar{u}\frac{\partial h}{\partial x} - \bar{v}\frac{\partial h}{\partial y} + \frac{\partial h}{\partial t}$$

Using the assumption below

5. No bearing that slide axially and rotate at the same time $\bar{u}\frac{\partial h}{\partial x} = 0$ or $\bar{v}\frac{\partial h}{\partial y} = 0$.

The axis are arranged so that either of them is zero to prevent wedge so that wedge and velocity are in two perpendicular directions

The General Reynolds Equation takes the form

$$\frac{\partial}{\partial x}\left(\frac{h^3}{\mu}\frac{\partial P}{\partial x}\right) + \frac{\partial}{\partial y}\left(\frac{h^3}{\mu}\frac{\partial P}{\partial y}\right) = 6\left(\bar{u}\frac{dh}{dx} + 2\frac{dh}{dt}\right) \qquad (2.81)$$

In the equation above the right hand side first term represent the normal wedge action while the second term represent the squeeze film term. Further considering the special case for steady state load condition, the normal wedge action $\tilde{v}\frac{dh}{dx}$ and the squeeze film term $2\frac{dh}{dt}$ are zero. With constant viscosity, the special Reynolds Equation can be written as

$$\frac{\partial}{\partial x}\left(h^3\frac{\partial P}{\partial x}\right)+\frac{\partial}{\partial y}\left(h^3\frac{\partial P}{\partial y}\right)=12\tilde{u}\mu\frac{dh}{dx} \tag{2.82}$$

Two types of bearings are typically used in rotordynamic evaluation of bearings, those are Long Bearing (Infinitely Wide) Approximation and Short Bearing Approximation. In the long bearing approximation, the pressure variation in circumferential direction is negligible compared with axial direction (Couette flow term) $\frac{\partial P}{\partial y} >> \frac{\partial P}{\partial x}$. In our study using short bearing approximation or configurations as $\lambda_k = \frac{2r_b}{b} < \frac{1}{2}$, implies that side leakage (flow in y-direction) is zero and Axial pressure is assumed constant. The General Reynolds equations (2.81) is reduced for Short Bearing Approximation to the form

$$\frac{\partial}{\partial x}\left(h^3\frac{\partial P}{\partial x}\right)=12\mu\tilde{u}\frac{\partial}{\partial x}(\rho h) \tag{2.83}$$

2.10.4 SHORT BEARING EQUATIONS

Various boundary conditions are used to solve for short bearing configuration pressure profile. Either full Sommerfeld (2π) lubrication is assumed around the bearing, for which such solution leads to divergent film[1]. The full Sommerfeld boundary condition if ignored leas to a violation of the continuity of mass flow condition at the end of the pressure curve. In this study half Sommerfeld solution (π) boundary condition is used as shown in *Figure 2.17*. The π-film bearing limit the integration of the second part from 0 to π, since pressure is assumed zero from π to 2π. This assumption is taken from the half Sommerfeld condition. In performing the integrals resulting in closed form the resultant forces in such pressure distribution is obtained. Two different relations are need to be explained before solving for the pressure profile, one is the fact that eccentricity adjusts itself until load is balanced by the pressure generated in the converging lubricating film given by $\varepsilon = \frac{e}{c}$. And the other is the relation between eccentricity and fluid film thickness, which is developed for both static and dynamic loading conditions in the Appendix A. The static eccentricity case has [24]

$$h = c(1 + \varepsilon \cos\phi) \qquad (2.84)$$

The attitude angle, Φ, is the angle at which load vector has to be rotated in the direction of journal rotation to bring it into line of centers as shown in *Figure 2.18*.

$$\omega_x' = \int_0^{2\pi} \mathrm{Pr}_b \sin(\pi - \phi) d\phi = \int_0^{2\pi} \mathrm{Pr}_b \sin\phi d\phi = \mathrm{r}_b \int_0^{2\pi} \cos\phi \frac{dP}{d\phi} d\phi$$

$$\omega_z' = \int_0^{2\pi} \mathrm{Pr}_b \cos(\pi - \phi) d\phi = -\int_0^{2\pi} \mathrm{Pr}_b \cos\phi d\phi = \mathrm{r}_b \int_0^{2\pi} \sin\phi \frac{dP}{d\phi} d\phi$$

[1] Divergent film implies lower than atmospheric pressure profile which is not possible in reality Since oil contains 8-12% of dissolved air, this leads to the suggestion that sub-ambient pressures predicted by full Sommerfeld solution should be ignored

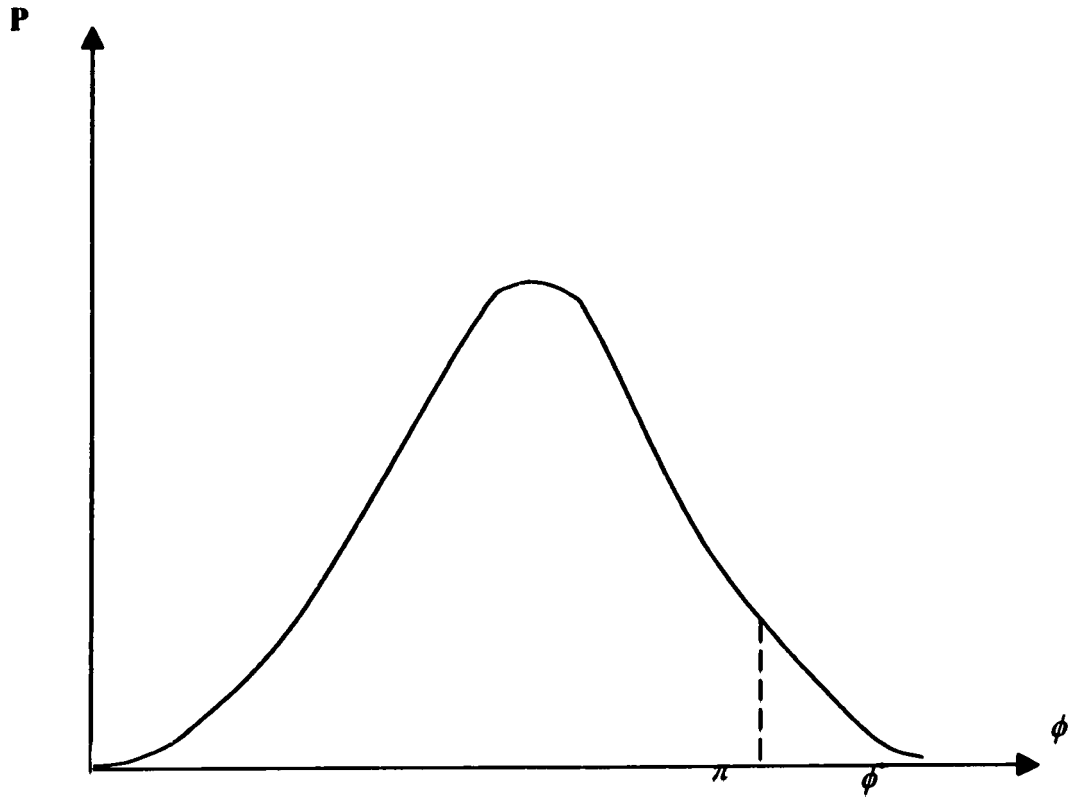

Figure 2.17 – Half Sommerfeld Boundary Condition

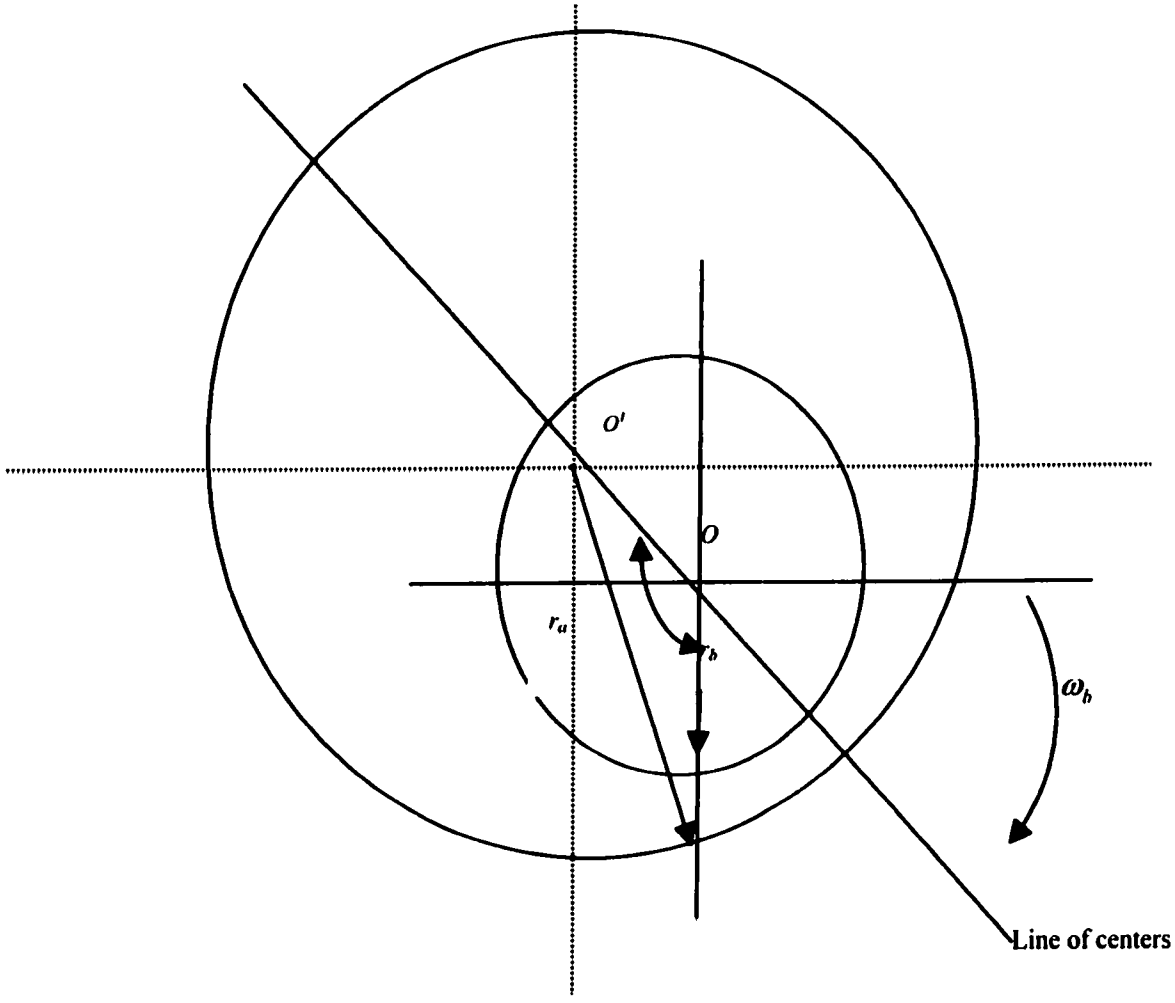

Figure 2.18 – Shaft Line of Centers and Eccentricity

The short bearing pressure equation is transformed into polar coordinates where

$u = \frac{\omega_b + \omega_j}{R} = \frac{\omega}{R}$, ω_b is bearing angular velocity and ω_j is journal angular velocity

$\frac{\partial}{\partial x} = \frac{1}{R}\frac{\partial}{\partial \phi}$ and with $\dot{\phi}$ is angular velocity of line of centers

$$\frac{\partial h}{\partial t} = c\left(\dot{\varepsilon}\cos\phi - \varepsilon\dot{\phi}\sin\phi\right) \tag{2.85}$$

$$\frac{\partial h}{\partial \phi} = -c\varepsilon\sin\phi \tag{2.86}$$

For $U_1 = V_1 = 0$, $\frac{h^3}{12\eta_0 r_b}\frac{\partial P}{\partial \phi} << \frac{hr_b\omega_b}{2}$ and $q'_\phi = \frac{hr_b\omega_b}{2}$. The Poiseuille (pressure) flow is

more significant in the y-direction than in circumferential direction, ϕ, which gives

$$\frac{\partial}{\partial x}\left(h^3\frac{\partial P}{\partial x}\right) + \frac{\partial}{\partial y}\left(h^3\frac{\partial P}{\partial y}\right) = 12\bar{u}\eta_o\frac{\partial h}{\partial x} \Rightarrow \frac{\partial}{\partial y}\left(h^3\frac{\partial P}{\partial y}\right) \approx 6\eta_o\omega_b\frac{\partial h}{\partial \phi}$$

$$\frac{\partial}{\partial x}\left(\frac{\rho h^3}{\eta}\frac{\partial P}{\partial x}\right) \approx 12\bar{u}\frac{\partial}{\partial x}(\rho h)$$

Reynolds equation in polar coordinates becomes

$$\boxed{\frac{\partial}{\partial y}\left[\left(1+\varepsilon\cos\phi\right)^3\frac{\partial P}{\partial y}\right] = -6\eta\left(\frac{1}{c}\right)^2\left[\left(\omega - 2\dot{\phi}\right)\varepsilon\sin\phi - 2\dot{\varepsilon}\cos\phi\right]} \tag{2.87}$$

For steady load conditions $\frac{\partial h}{\partial t} = 0$, the equation (2.87) reduces to the short bearing form

$$\frac{\partial^2 P}{\partial y^2} = 6\eta\left(\frac{1}{c}\right)^2\frac{\omega\varepsilon\sin\phi}{\left(1+\varepsilon\cos\phi\right)^2} = \frac{6\eta\omega}{h^3}\frac{dh}{dx} \tag{2.88}$$

Bearing opens to atmosphere at both ends $z = 0$ and $z = L$ with cavitated fluid film

$P(\phi,0)=P(\phi,L)=P_a$, P_a is atmospheric pressure, $P(0,z)=P(2\pi,z)=P_0$, P_0 is the supply pressure. Integrating twice $P=\frac{3\omega\eta}{h^3}\frac{dh}{dx}y^2+C_1y+C_2$, At $y=0$, $P=P_a$, $C_2=P_a$ and $y=\pm L$, $P=0$, $C_1=-\frac{3\omega\eta}{h^3}\frac{dh}{dx}\frac{L^2}{4}$, one gets

$$P(\phi,y)=\frac{3\omega\eta\varepsilon\sin\phi}{c^2(1+\varepsilon\cos\phi)^3}\left(\frac{L^2}{4}-y^2\right)+P_a \qquad (2.89)$$

$$\frac{\partial}{\partial y}\left(h^3\frac{\partial P}{\partial y}\right)=6\eta_o\omega_b\frac{\partial h}{\partial\phi} \text{ valid for } \lambda_k > z.$$

With no misalignment, film thickness is a function of ϕ and Taking y-axis as center of bearing, $P=0$ at $y=\pm\frac{b}{2}$, $A=0$, $B=-\frac{6\eta_0\omega_b}{h^3}\frac{\partial h}{\partial\phi}\frac{b^2}{8}$, pressure profile becomes

$$P=\frac{6\eta_o\omega_b}{h^3}\frac{\partial h}{\partial\phi}\frac{y^2}{2}+\frac{Ay}{h^3}+B$$

or when re-arranging and considering that $\frac{\partial h}{\partial\phi}=-e\sin\phi$, the equations beocmes

$$\boxed{P=\frac{3\eta_0\omega_b\varepsilon}{c^2}\left(\frac{b^2}{4}-y^2\right)\frac{\sin\phi}{(1+\varepsilon\cos\phi)^3} \qquad 0\le\phi\le\pi} \qquad (2.90)$$

From *Figure 2.19* below

$$\frac{\partial P}{\partial\phi}=0 \text{ at } \phi_m=\cos^{-1}\left[\frac{1-(1+24\varepsilon^2)^{1/2}}{4\varepsilon}\right] \text{ and } P_m=\frac{3\eta_0\omega_b\varepsilon b^2\sin\phi_m}{4c^2(1+\varepsilon\cos\phi_m)^3}$$

$$P-P_0=6\eta_0\left(\frac{r_b}{c}\right)^2\left\{\frac{\varepsilon\sin\phi(2+\varepsilon\cos\phi)}{(2+\varepsilon^2)(1+\varepsilon\cos\phi)^2}\right\} \qquad (2.91a)$$

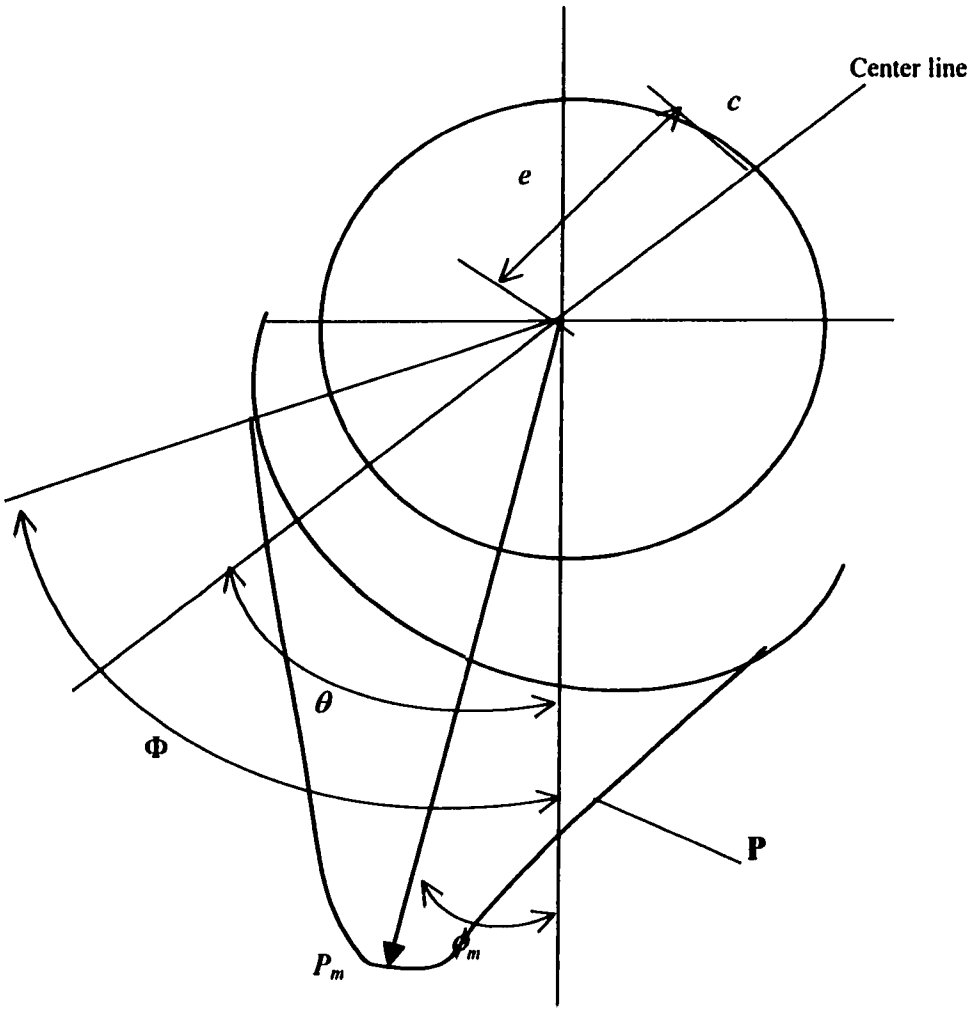

Figure 2.19 – Maximum pressure and Angle for half Sommerfeld Condition

The above gives the pressure distribution in short bearings approximation with static equilibrium conditions. By integrating the above pressure distribution taking directions into account the load carried by the fluid film is obtained. The conditions or directions of integration above have some scenarios. In the first where variation of pressure around a short bearing is given, the half Sommerfeld condition were P=0 is taken for the divergence region $\pi < \theta < 2\pi$ where film pressure is highly negative. In practice the lubricant caviatets. Bearings that cavitate fully over half of their circumference are called π-film bearings. Under static load conditions $\dot{\varepsilon} = \dot{\theta} = 0$, the location of the cavitation is determined by the instantaneous values of $\dot{\varepsilon}$ and $\dot{\theta}$. Uncavitated bearings are called 2π-film bearings. The analysis below will be for the case of π-film or fully cavitated film bearings. The load vectors as derived earlier

$$\omega_x = 2\int_0^{\pi}\int_0^{b/2} Pr_b \sin\phi dy d\phi = \frac{\eta_0\omega_b\varepsilon r_b b^3}{2c^2}\int_0^{\pi}\frac{\sin^2\phi}{(1+\varepsilon\cos\phi)^3}d\phi$$

$$\omega_z = -2\int_0^{\pi}\int_0^{b/2} Pr_b \cos\phi dy d\phi = -\frac{\eta_0\omega_b\varepsilon r_b b^3}{2c^2}\int_0^{\pi}\frac{\sin\phi\cos\phi}{(1+\varepsilon\cos\phi)^3}d\phi$$

Using Sommerfeld substitution given in standard textbooks,

$$\omega_x = \frac{\eta_0\omega_b\varepsilon r_b b^3}{2c^2(1-\varepsilon^2)^{3/2}}\int_0^{\pi}\sin^2\gamma d\gamma = \frac{\eta_0\omega_b\varepsilon r_b b^3\pi}{4c^2(1-\varepsilon^2)^{3/2}}$$

$$\omega_z = -\frac{\eta_0\omega_b\varepsilon r_b b^3}{2c^2(1-\varepsilon^2)^2}\int_0^{\pi}(\sin\gamma\cos\gamma - \varepsilon\sin\gamma)d\gamma = \frac{\eta_0\omega_b\varepsilon^2 r_b b^3}{c^2(1-\varepsilon^2)^{3/2}}$$

The load resultant and attitude angle become

$$\omega_r = \sqrt{\omega_x^2+\omega_z^2} = \frac{\eta_0\omega_b r_b b^3}{4c^2}\frac{\varepsilon}{(1+\varepsilon^2)^2}\left[16\varepsilon^2+\pi^2(1-\varepsilon^2)\right]^{1/2} \quad (2.92)$$

$$\Phi = \tan^{-1}\left(\frac{\omega_x}{\omega_z}\right) = \tan^{-1}\left(\frac{\pi\left(1-\varepsilon^2\right)^{1/2}}{4\varepsilon}\right) \tag{2.93}$$

In dimensionless form

$$W_x = \frac{\omega_x}{\eta_0\omega_b r_b b}\left(\frac{c}{r_b}\right)^2 = \left(\frac{b}{r_b}\right)^2 \frac{\pi\varepsilon}{4\left(1-\varepsilon^2\right)^{3/2}} \tag{2.94a}$$

$$W_z = \frac{\omega_z}{\eta_0\omega_b r_b b}\left(\frac{c}{r_b}\right)^2 = \left(\frac{b}{r_b}\right)^2 \frac{\varepsilon^2}{\left(1-\varepsilon^2\right)^2} \tag{2.94b}$$

$$W_r = \left(\frac{b}{r_b}\right)^2 \frac{\varepsilon}{4\left(1-\varepsilon^2\right)^2}\left[16\varepsilon^2 + \pi^2\left(1-\varepsilon^2\right)\right]^{1/2} \tag{2.94c}$$

In equation (2.90) the film thickness rate of change was given as $\frac{dh}{dx} = -\frac{c\varepsilon\sin\phi}{R}$ and $\frac{dh}{dt} = c\dot{\varepsilon}\cos\phi - c\varepsilon\dot{\phi}\sin\phi$ and since for a small segment of the journal surface, $dF = r_b P d\phi dy$ on small segment $r_b d\phi dy$ with ϕ angle to the line of centers

$$dF_r = -Pr_b\cos\phi d\phi dy, \qquad dF_t = -Pr_b\sin\phi d\phi dy$$

$$F_r = r_b\int_{-L/2}^{L/2}\int_0^{2\pi} P\cos\phi d\phi dy, \qquad F_t = r_b\int_{-L/2}^{L/2}\int_0^{2\pi} P\sin\phi d\phi dy$$

With $\int_{-L/2}^{L/2}\left(\frac{L^2}{4} - y^2\right)dy = \frac{L^3}{6}$ the fluid film forces are given as

$$F_r = -\frac{\eta r_b L^3}{c^2}\left[\left|\omega_b - 2\dot{\phi}\right|\frac{\varepsilon^2}{\left(1-\varepsilon^2\right)^2} + \frac{\dot{\varepsilon}\pi\left(1+2\varepsilon^2\right)}{2\left(1-\varepsilon^2\right)^{5/2}}\right] \tag{2.95a}$$

$$F_t = -\frac{\eta r_b L^3}{c^2}\left[\left(\omega - 2\dot{\phi}\right)\frac{\pi\varepsilon}{4\left(1-\varepsilon^2\right)^{3/2}} + \frac{2\dot{\varepsilon}\varepsilon}{\left(1-\varepsilon^2\right)^2}\right] + 2r_b L P_0 \tag{2.95b}$$

Lubricant films are flexible, when a dynamic load like above is applied, journal is caused to orbit around the static equilibrium position, which it would otherwise take up when carrying only static load. Assuming small displacements ***dx*** and ***dy*** of the journal from its static equilibrium position. Journal center is assumed to possess velocities ***dẋ*** **and** ***dẏ***. When there is no dynamic load , lubricant steady state film forces can be expressed as a function of displacements and velocities. Under steady load:

$$F_x = f_1(x, y, \dot{x}, \dot{y}), \qquad F_y = f_2(x, y, \dot{x}, \dot{y})$$

Under dynamic load the variation in the forces which can be expressed using a truncated Taylor series expansion given by [1]

$$F_x + dF_x = f_1 + \frac{\partial F_x}{\partial x}dx + \frac{\partial F_y}{\partial y}dy + \frac{\partial F_x}{\partial \dot{x}}d\dot{x} + \frac{\partial F_y}{\partial \dot{y}}d\dot{y}$$

$$F_y + dF_y = f_2 + \frac{\partial F_x}{\partial x}dx + \frac{\partial F_y}{\partial y}dy + \frac{\partial F_x}{\partial \dot{x}}d\dot{x} + \frac{\partial F_y}{\partial \dot{y}}d\dot{y}$$

$$dF_x = \frac{\partial F_x}{\partial x}dx + \frac{\partial F_y}{\partial y}dy + \frac{\partial F_x}{\partial \dot{x}}d\dot{x} + \frac{\partial F_y}{\partial \dot{y}}d\dot{y} = k_{xx}dx + k_{xy}dy + C_{xx}d\dot{x} + C_{xy}d\dot{y}$$

$$dF_y = \frac{\partial F_x}{\partial x}dx + \frac{\partial F_y}{\partial y}dy + \frac{\partial F_x}{\partial \dot{x}}d\dot{x} + \frac{\partial F_y}{\partial \dot{y}}d\dot{y} = k_{yx}dx + k_{yy}dy + C_{yx}d\dot{x} + C_{yy}d\dot{y}$$

when dynamic load is applied, journal is caused to orbit around the static equilibrium position, approximation of small displacement *dx* and *dy* of journal from static equilibrium position is utilized. Journal center is assumed to possess velocities *dẋ* and *dẏ*. For static loads $\dot{\varepsilon} = \dot{\phi} = 0$

$$F_r = -\frac{\eta r_b L^3}{c^2}\left[\frac{\omega_b \varepsilon^2}{\left(1-\varepsilon^2\right)^2}\right], \qquad F_t = \frac{\eta r_b L^3}{c^2}\left[\frac{\omega \pi \varepsilon}{4\left(1-\varepsilon^2\right)^{3/2}}\right]$$

The resultant of tangential and radial forces is

$$F = \frac{\eta r_b L^3 \omega_b}{c^2}\left[\frac{\varepsilon^4}{\left(1-\varepsilon^2\right)^4} + \frac{\pi^2\varepsilon^2}{16\left(1-\varepsilon^2\right)^3}\right]^{1/2}$$

Or re-arranged as

$$\frac{\eta r_b^3 \omega_b c^2 L/\pi}{F} = \frac{r_b^2}{\pi L^2}\left[\frac{16\left(1-\varepsilon^2\right)^4}{16\varepsilon^4 + \pi^2\varepsilon^2\left(1-\varepsilon^2\right)}\right]^{1/2} \qquad (2.96)$$

With $R = \frac{\eta N r_b^2}{Pc^2}$, $N = \frac{\omega_b}{2\pi}$, $P = \frac{F}{2Lr_b}$, $D = 2r_b$ and $R = \frac{2\eta\omega_b L r_b^3}{2\pi F c^2}$ one can

define the following constants to solve for eccentricity

$$s = \frac{\left(1-\varepsilon^2\right)}{\pi\varepsilon\left(L/D\right)^2}\left[\frac{1}{\pi^2 + \left(16-\pi^2\right)\varepsilon^2}\right]^{1/2}, \qquad s^2 = \frac{16 r_b^4\left(1-\varepsilon^2\right)^2}{\pi^2\varepsilon^2 L^4\left[\pi^2\left(1-\varepsilon^2\right)+16\varepsilon^2\right]} = \frac{\left(1-2\varepsilon^2+\varepsilon^4\right)A_1}{\pi^2\varepsilon^2 + \varepsilon^4\left(16-\pi^2\right)}$$

$$A_1 = \frac{16 r_b^4}{\pi^2 L^4}, \qquad A_2 = \left[A_1 - s^2\left(16-\pi^2\right)\right], \qquad A_3 = \left[-2A_1 - s^2\pi^2\right]$$

$$A_2\varepsilon_1^2 + A_3\varepsilon_1 + A_1 = 0$$

$$\varepsilon = \left[\frac{A_3 \pm \left(4A_2A_1\right)}{2A_2}\right]^{1/2}$$

Two methods were used in the study to solve the roots of the static eccentricity equation (2.96) above namely, polynomial and bi-section iteration methods. However both solutions produce different results as explained in Chapter 4. The Cartesian forces can be obtained and by using the Taylor series expansion earlier, the direct and cross-coupled stiffness and damping parameters can be obtained [12]as.

$$\begin{bmatrix} F_x \\ F_y \end{bmatrix} = \begin{bmatrix} \sin\phi & \cos\phi \\ -\cos\phi & \sin\phi \end{bmatrix}\begin{bmatrix} F_r \\ F_t \end{bmatrix}$$

Non-dimensionalizing $k_{ij} = \frac{F}{c} k'_{ij}, \qquad C_{ij} = \frac{F}{c\omega} C'_{ij}$, Let $B = \left[\frac{1}{\pi^2 + \left(16 - \pi^2\right)\varepsilon^2} \right]^{1/2}$

$$k'_{xx} = \frac{4\varepsilon}{\left(1-\varepsilon^2\right)^3}\left[(\pi B)^2\left(1-\varepsilon^2\right)+1-\varepsilon^2\right] \tag{2.97a}$$

$$k'_{xy} = \frac{-\pi}{\left(1-\varepsilon^2\right)^{5/2}}\left[(4B\varepsilon)^2 - 1 + \varepsilon^2\right] \tag{2.97b}$$

$$k'_{yx} = \frac{-\pi}{\left(1-\varepsilon^2\right)^{5/2}}\left[(4B\varepsilon)^2 + 1 + 2\varepsilon^2\right] \tag{2.97c}$$

$$k'_{yy} = \frac{4\varepsilon}{\left(1-\varepsilon^2\right)^3}\left[(4B\varepsilon)^2 + 1 + 2\varepsilon^2\right] \tag{2.97d}$$

$$C'_{xx} = \frac{2\pi}{\left(1-\varepsilon^2\right)^{5/2}}\left[(\pi B)^2\left(1-\varepsilon^2\right)\left(2+\varepsilon^2\right)-1+\varepsilon^2\right] \tag{2.97e}$$

$$C'_{xy} = C'_{yx} = \frac{8\varepsilon}{\left(1-\varepsilon^2\right)^3}\left[(\pi B)^2\left(1-\varepsilon^2\right)\left(2+\varepsilon^2\right)-1+\varepsilon^2\right] \tag{2.97e}$$

$$C'_{yy} = \frac{2\pi}{\left(1-\varepsilon^2\right)^{5/2}}\left[(4\pi B)^2\left(1-\varepsilon^2\right)\left(2+\varepsilon^2\right)-1+\varepsilon^2\right] \tag{2.97f}$$

The above stiffness and damping expressions will be used for simulations of the system and comparison of system response using the above expressions to using the system model with eccentricity modeled as dynamic parameter and fluid film inertia included.

2.11 FINITE ELEMENT MODEL ASSEMBLY

The shaft, disk and bearing global matrices are given in the equations below. A simple MATLAB program was used to generate the integral constants and the matrices, which is given in the Appendix B. Defining

$$[M_s] = \int_0^{\ell} \rho [N]^T [m_1][N] dz \tag{2.98}$$

$$[G_s] = \int_0^{\ell} \rho [N]^T [g_1][N] dz \tag{2.99}$$

$$[k_s] = \int_0^{\ell} \rho [N']^T [k_1][N'] dz + \int_0^{\ell} \rho [N]^T [k_2][N] dz \tag{2.100}$$

$$[M_b] = \int_0^{\ell} \rho [N_b]^T [m_2][N_b] dz \tag{2.101}$$

$$[k_b] = \int_0^{\ell} \rho [N']^T [k_3][N'] dz \tag{2.102}$$

$$[D_{HS}] = \int_0^{\ell} \rho [N']^T [c_1][N'] dz \tag{2.103}$$

$$[D_{VS}] = \int_0^{\ell} \rho [N]^T [k_4][N] dz \tag{2.104}$$

$$[D_{DS}] = \int_0^{\ell} \rho [N]^T [k_s][N] dz \tag{2.105}$$

The Global Matrices 8X8 are computed as follows :

$$[K_S] = m_0 \begin{bmatrix} 12 & 0 & 0 & 0 & 0 & 0 & 0 & 0 \\ 6l & a_{10} & 0 & 0 & 0 & 0 & 0 & 0 \\ -12 & -6l & 12 & 0 & 0 & 0 & 0 & 0 \\ 6l & a_{11} & -6l & a_{10} & 0 & 0 & 0 & 0 \\ 0 & 0 & 0 & 0 & 12 & 0 & 0 & 0 \\ 0 & 0 & 0 & 0 & 6l & a_{10} & 0 & 0 \\ 0 & 0 & 0 & 0 & -12 & -6l & 12 & 0 \\ 0 & 0 & 0 & 0 & 6l & a_{11} & -6l & a_{10} \end{bmatrix}$$

$a_1 = 156 + 294\Phi + 140\Phi^2$ $\quad a_2 = l(22 + 38.5\Phi + 17.5\Phi^2)$ $\quad a_3 = 54 + 126\Phi + 70\Phi^2$

$a_4 = -l(13 + 31.5\Phi + 17.5\Phi^2)$ $\quad a_5 = l^2(4 + 7\Phi + 3.5\Phi^2)$ $\quad a_6 = -l^2(3 + 7\Phi + 3.5\Phi^2)$

$a_7 = l(3 - 15\Phi)$ $\quad a_8 = l^2(4 + 5\Phi + 10\Phi^2)$ $\quad a_9 = l^2(-1 - 5\Phi + 5\Phi^2)$

$a_{10} = l^2(4 + \Phi)$ $\quad a_{11} = l^2(2 - \Phi)$ $\quad m_0 = \dfrac{EI}{l^3(1 + \Phi)}$

$$[M_S] = \begin{bmatrix} a_{12} & 0 & 0 & 0 & 0 & 0 & 0 & 0 \\ a_{13} & a_{16} & 0 & 0 & 0 & 0 & 0 & 0 \\ a_{14} & a_{17} & a_{12} & 0 & 0 & 0 & 0 & 0 \\ a_{15} & a_{18} & -a_{13} & a_{16} & 0 & 0 & 0 & 0 \\ 0 & 0 & 0 & 0 & a_{12} & 0 & 0 & 0 \\ 0 & 0 & 0 & 0 & a_{13} & a_{16} & 0 & 0 \\ 0 & 0 & 0 & 0 & a_{14} & a_{17} & a_{12} & 0 \\ 0 & 0 & 0 & 0 & a_{15} & a_{18} & -a_{13} & a_{16} \end{bmatrix}$$

$a_{12} = a_1 m1 + 36m2$ $\quad a_{16} = a_5 m1 + a_8 m2$

$a_{13} = a_2 m1 + a_7 m2$ $\quad a_{17} = -a_4 m1 - a_7 m2$

$a_{14} = a_3 m1 - 36m2$ $\quad a_{18} = a_6 m1 + a_9 m2$

$a_{15} = a_4 m1 + a_7 m2$

$m1 = \dfrac{\rho A l}{420(1 + \Phi)^2}$ $\quad m2 = \dfrac{\rho I}{30(1 + \Phi)^2}$

$$[G_S] = m3 \begin{bmatrix} 0 & 0 & 0 & 0 & 36 & 0 & 0 & 0 \\ 0 & 0 & 0 & 0 & a_7 & a_8 & 0 & 0 \\ 0 & 0 & 0 & 0 & -36 & -a_7 & 36 & 0 \\ 0 & 0 & 0 & 0 & a_7 & a_9 & -a_7 & a_8 \\ -36 & 0 & 0 & 0 & 0 & 0 & 0 & 0 \\ -a_7 & -a_8 & 0 & 0 & 0 & 0 & 0 & 0 \\ 36 & a_7 & -36 & 0 & 0 & 0 & 0 & 0 \\ -a_7 & -a_9 & a_7 & -a_8 & 0 & 0 & 0 & 0 \end{bmatrix}$$

$$m3 = \frac{\omega J \rho}{30(1+\Phi)^2}$$

In the system matrices sing Lagrange will introduce a new matrix $[D_{HS}]\{q\}$

Let m4$= \frac{\mathrm{EI}\sin\gamma}{l^2(1+\Phi)^3}$, then the hysteresis non-conservative work matrix becomes

$$[\mathrm{D_{HS}}] = \begin{bmatrix} 0 & 0 & 0 & 0 & 12m4 & 0 & 0 & 0 \\ 0 & 0 & 0 & 0 & 6lm4 & a_{19}m4 & 0 & 0 \\ 0 & 0 & 0 & 0 & -12m4 & -6lm4 & 12m4 & 0 \\ 0 & 0 & 0 & 0 & 6lm4 & a_{20}m4 & -6lm4 & a_{19}m4 \\ -12m4 & 0 & 0 & 0 & 0 & 0 & 0 & 0 \\ -6lm4 & -a_{19}m4 & 0 & 0 & 0 & 0 & 0 & 0 \\ 12m4 & 6lm4 & -12m4 & 0 & 0 & 0 & 0 & 0 \\ -6lm4 & -a_{20}m4 & 6lm4 & -a_{19}m4 & 0 & 0 & 0 & 0 \end{bmatrix}$$

$a_{19} = l^2(4+2\Phi+\Phi^2)$ $\qquad$ $\mathrm{a_{20}} = l^2(2-2\Phi-\Phi^2)$

Calculation gives the internal viscous damping matrices

$$m5 = \frac{lc_d}{420(1+\Phi)^2}$$

$$[D_{VS}]\{\dot{q}\} = m5 \begin{bmatrix} a_1 & 0 & 0 & 0 & 0 & 0 & 0 & 0 \\ a_2 & a_5 & 0 & 0 & 0 & 0 & 0 & 0 \\ a_3 & -a_4 & a_1 & 0 & 0 & 0 & 0 & 0 \\ a_4 & a_6 & -a_2 & a_5 & 0 & 0 & 0 & 0 \\ 0 & 0 & 0 & 0 & a_1 & 0 & 0 & 0 \\ 0 & 0 & 0 & 0 & a_2 & a_5 & 0 & 0 \\ 0 & 0 & 0 & 0 & a_3 & -a_4 & a_1 & 0 \\ 0 & 0 & 0 & 0 & a_4 & a_6 & -a_2 & a_5 \end{bmatrix} \{\dot{q}\}$$

$$m6 = \frac{lc_d\omega}{420(1+\Phi)^2}$$

$$[D_{DS}]\{q\} = m6 \begin{bmatrix} 0 & 0 & 0 & 0 & a_1 & 0 & 0 & 0 \\ 0 & 0 & 0 & 0 & a_2 & a_5 & 0 & 0 \\ 0 & 0 & 0 & 0 & a_3 & -a_4 & a_1 & 0 \\ 0 & 0 & 0 & 0 & a_4 & a_6 & -a_2 & a_5 \\ -a_1 & 0 & 0 & 0 & 0 & 0 & 0 & 0 \\ -a_2 & -a_5 & 0 & 0 & 0 & 0 & 0 & 0 \\ -a_3 & a_4 & -a_1 & 0 & 0 & 0 & 0 & 0 \\ -a_4 & -a_6 & a_2 & -a_5 & 0 & 0 & 0 & 0 \end{bmatrix} \{q\}$$

In the study, the rigid disk was located at Node 3. This will imply that half of the mass and gyroscopic matrices are added to shaft elements 2 and 3 as follows :

$$[M_{S2}] + \begin{bmatrix} 0 & & & & & & & \\ & 0 & & & & & & \\ & & 0.5m_d & & & & & \\ & & & 0.5I_d & & & & \\ & & & & 0 & & & \\ & & & & & 0 & & \\ & & & & & & 0.5m_d & \\ & & & & & & & 0.5I_d \end{bmatrix}$$

$$[G_{S2}]+\begin{bmatrix} 0 & & & & & & \\ & 0 & & & & & \\ & & 0 & & & & \\ & & & 0 & & & -\omega I_d \\ & & & & 0 & & \\ & & & & & 0 & \\ & & & & & & 0 \\ & & & -\omega\ I_d & & & \end{bmatrix}$$

For Shaft Element 3

$$[M_{S3}]=\begin{bmatrix} 0.5m_d & & & & & & \\ & 0.5I_d & & & & & \\ & & 0 & & & & \\ & & & 0 & & & \\ & & & & 0.5m_d & & \\ & & & & & 0.5I_d & \\ & & & & & & 0 \\ & & & & & & & 0 \end{bmatrix}$$

$$[G_{S3}]=\begin{bmatrix} 0 & & & & & & \\ & 0 & & & & & -\omega I_d \\ & & 0 & & & & \\ & & & 0 & & & \\ & & & & 0 & & \\ & -\omega I_d & & & & 0 & \\ & & & & & & 0 \\ & & & & & & & 0 \end{bmatrix}$$

Unbalance force will affect shaft elements 2 and 3 as follows :

$$\{Q_2\}=\begin{Bmatrix} 0 \\ 0 \\ 0.5e_x\cos\omega t-0.5e_x\sin\omega t \\ 0 \\ 0 \\ 0 \\ 0.5e_y\cos\omega t+0.5e_y\sin\omega t \\ 0 \end{Bmatrix} \text{ and } \{Q_3\}=\begin{Bmatrix} 0.5e_x\cos\omega t-0.5e_x\sin\omega t \\ 0 \\ 0 \\ 0 \\ 0.5e_y\cos\omega t+0.5e_y\sin\omega t \\ 0 \\ 0 \\ 0 \end{Bmatrix}$$

using Lagrange principle, $L = T - V$

$$\frac{d}{dt}\left(\frac{\partial L}{\partial \dot{q}}\right) - \frac{\partial L}{\partial q} = F_q \tag{2.106}$$

$$L_s = \frac{1}{2}\{\dot{q}\}^T [M_s]\{\dot{q}\} + \Omega^2 J M_t + 2J\Omega\{\dot{q}\}^T [G_s]\{\dot{q}\} - \frac{1}{2}\{q\}^T [k_s]\{q\} \tag{2.107}$$

Using Lagrange formulation gives the equation of motion for shaft, bearing housing and Disk. The effect of the bearing housing on shaft and disk equations will be included. with

$$Q_s = -EI\alpha\{q\}^T [D_{HS}]\{q\} - \frac{c_t}{\rho A}\{\dot{q}\}^T [D_{vS}] - \frac{c_t \Omega}{\rho A}\{\dot{q}\}^T [D_{DS}]$$

Shaft: $M_s|_{8\times 8}\,\ddot{q}_s + G_s|_{8\times 8}\,\dot{q}_s + k_s|_{8\times 8}\,q_s = Q_s$

Disk: $M_d\ddot{q}_d + G_d\dot{q}_d + k_d q_d = Q_d$

Bearing housing: $M_b\ddot{q}_b + G_b\dot{q}_b + k_b q_b = Q_b$

Number of degrees of freedom as $N = 4(n+1) + 2(b)$

Where n is number of elements, b is number of bearings

$\{q_a\} = \begin{Bmatrix} q_s \\ q_d \\ q_b \end{Bmatrix}$, a indicates absolute shaft movement

To account for the bearing effect, as indicated in the equation of motion the bearing will add the following :

1- At Beginning node shaft element 1 :

$$\begin{bmatrix} -c_{xx} & 0 & 0 & 0 & -c_{xy} & 0 & 0 & 0 \\ 0 & 0 & 0 & 0 & 0 & 0 & 0 & 0 \\ 0 & 0 & 0 & 0 & 0 & 0 & 0 & 0 \\ 0 & 0 & 0 & 0 & 0 & 0 & 0 & 0 \\ -c_{yx} & 0 & 0 & 0 & -c_{yy} & 0 & 0 & 0 \\ 0 & 0 & 0 & 0 & 0 & 0 & 0 & 0 \\ 0 & 0 & 0 & 0 & 0 & 0 & 0 & 0 \\ 0 & 0 & 0 & 0 & 0 & 0 & 0 & 0 \end{bmatrix} \begin{Bmatrix} r_x^1 \\ \theta^1 \\ r_x^2 \\ \theta^2 \\ r_y^1 \\ \psi^1 \\ r_y^2 \\ \psi^2 \end{Bmatrix} \quad \text{and} \quad \begin{bmatrix} -k_{xx} & 0 & 0 & 0 & -k_{xy} & 0 & 0 & 0 \\ 0 & 0 & 0 & 0 & 0 & 0 & 0 & 0 \\ 0 & 0 & 0 & 0 & 0 & 0 & 0 & 0 \\ 0 & 0 & 0 & 0 & 0 & 0 & 0 & 0 \\ -k_{yx} & 0 & 0 & 0 & -k_{yy} & 0 & 0 & 0 \\ 0 & 0 & 0 & 0 & 0 & 0 & 0 & 0 \\ 0 & 0 & 0 & 0 & 0 & 0 & 0 & 0 \\ 0 & 0 & 0 & 0 & 0 & 0 & 0 & 0 \end{bmatrix} \{q_1\}$$

2- At the end node shaft element 4 :

$$\begin{bmatrix} 0 & 0 & 0 & 0 & 0 & 0 & 0 & 0 \\ 0 & 0 & 0 & 0 & 0 & 0 & 0 & 0 \\ -c_{xx} & 0 & 0 & 0 & -c_{xy} & 0 & 0 & 0 \\ 0 & 0 & 0 & 0 & 0 & 0 & 0 & 0 \\ 0 & 0 & 0 & 0 & 0 & 0 & 0 & 0 \\ 0 & 0 & 0 & 0 & 0 & 0 & 0 & 0 \\ -c_{yx} & 0 & 0 & 0 & -c_{yy} & 0 & 0 & 0 \\ 0 & 0 & 0 & 0 & 0 & 0 & 0 & 0 \end{bmatrix} \{\dot{q}_4\} \quad \text{and} \quad \begin{bmatrix} 0 & 0 & 0 & 0 & 0 & 0 & 0 & 0 \\ 0 & 0 & 0 & 0 & 0 & 0 & 0 & 0 \\ -k_{xx} & 0 & 0 & 0 & -k_{xy}0 & 0 & 0 & 0 \\ 0 & 0 & 0 & 0 & 0 & 0 & 0 & 0 \\ 0 & 0 & 0 & 0 & 0 & 0 & 0 & 0 \\ 0 & 0 & 0 & 0 & 0 & 0 & 0 & 0 \\ -k_{yx} & 0 & 0 & 0 & -k_{yy}0 & 0 & 0 & 0 \\ 0 & 0 & 0 & 0 & 0 & 0 & 0 & 0 \end{bmatrix} \{q$$

The assembly process starts with the assemblage of shaft elements including the rigid disk and the bearing effects. This will be in the form $[M]\{\ddot{q}^m\}+[C]\{\dot{q}^m\}+[K]\{q^m\}=\{F^m\}$ where the superscript m indicate Model (Global). The model coordinates will be composed of four different coordinates (two translational and two rotational) at each node. The MATLAB program is constructed such that number of elements can be varied. For the purpose of this study, four shaft elements are used. This gives twenty coordinates, adding two more coordinates for each bearing creates twenty-four coordinates for our model coordinate matrix. The Shaft element mass,

damping and stiffness matrices will have some inclusion (elements added to each other) at the nodes shared between elements. Shaft element one end node associated parameters will be added to shaft element two beginning node associated parameters and so on. This will give 24 X 24 matrices for the mass, stiffness and damping model matrices. The force vector is given below

$$\left\{F^m\right\} = \begin{Bmatrix} F_{bx1} \\ -m^{b1}g + F_{by1} \\ 0 \\ 0 \\ 0 \\ 0 \\ FB1 \\ 0 \\ 0 \\ 0 \\ 0 \\ 0 \\ 0 \\ 0 \\ 0 \\ 0 \\ FB2 \\ 0 \\ 0 \\ 0 \\ 0 \\ 0 \\ F_{bx2} \\ -m^{b2}g + F_{by2} \end{Bmatrix}$$

The Shaft Element Equation takes the form

$$[M_S]\{\ddot{q}^m\} + ([G_S] + [D_{VS}])\{\dot{q}^m\} + ([K_S] + [D_{HS}] + [D_{DS}])\{q^m\} = \{Q\}$$

Shaft element one beginning node have the bearing added matrices, shaft element two and three have the disk matrices, shaft element four have the end bearing matrices. The following pages have the complete system mass, stiffness and damping matrices.

$$[M_S] = \begin{bmatrix}
a_{12} & & & & & & & \\
a_{13} & a_{16} & & & & & & \\
a_{14} & a_{17} & & & a_{12} + [m^d] & & & \\
a_{15} & a_{18} & & & -a_{13} & a_{16} + [I^d] & & \\
 & & a_{12} & & & & & \\
 & & a_{13} & a_{16} & & & & \\
 & & a_{14} & a_{17} & & & a_{12} + [m^d] & \\
 & & a_{15} & a_{18} & & & -a_{13} & a_{16} + [I^d]
\end{bmatrix}
\begin{Bmatrix}
\ddot{u}_{x1} \\ \ddot{\alpha}_1 \\ \ddot{u}_{y1} \\ -\ddot{\beta}_1 \\ \ddot{u}_{x2} \\ \ddot{\alpha}_2 \\ \ddot{u}_{y2} \\ -\ddot{\beta}_2
\end{Bmatrix}$$

[ ] *Applies to element 2 only*

$$[G_S]=\begin{bmatrix} g_1-(c_{xx}) & & -g_7-(c_{xy}) & & & & & & \\ g_2 & g_3 & -g_8 & -g_9 & & & & & \\ g_5 & -g_4 & g_7 & g_8 & g_1-\{c_{xx}\} & & -g_7-\{c_{xy}\} & & \\ g_4 & g_6 & -g_8 & -g_{10} & -g_2 & g_3 & g_8 & -g_9 & \\ g_7-(c_{yx}) & & g_1-(c_{yy}) & & & & & & \\ g_8 & g_9 & g_2 & g_3 & & & & & \left[-2\omega I^d\right] \\ -g_7 & -g_8 & g_5 & -g_4 & g_7-\{c_{yx}\} & & g_1-\{c_{yy}\} & & \\ g_8 & g_{10} & g_4 & g_6 & -g_8 & g_9-\left[2\omega I^d\right] & -g_2 & g_3 & \end{bmatrix}\begin{Bmatrix} \dot{u}_{x1} \\ \dot{\alpha}_1 \\ \dot{u}_{y1} \\ -\dot{\beta}_1 \\ \dot{u}_{x2} \\ \dot{\alpha}_2 \\ \dot{u}_{y2} \\ -\dot{\beta}_2 \end{Bmatrix}$$

$g_1 = a_1 m5 \quad g_2 = a_2 m5 \quad g_3 = a_5 m5 \quad g_4 = a_4 m5 \quad g_5 = a_3 m5$

$g_6 = a_6 m5 \quad g_7 = -36m3 \quad g_8 = -a_7 m3 \quad g_9 = -a_8 m3 \quad g_{10} = -a_9 m3$

( ) *Applies to element 1 only* { } *Applies to element 4 only*

$$[K_S]=\begin{bmatrix} k_1-(k_{xx}) & & -k_5-(k_{xy}) & & & & & & \\ k_2 & k_3 & -k_7 & -k_9 & & & & & \\ -k_1 & -k_2 & -k_6 & k_8 & k_1-\{k_{xx}\} & & -k_5-\{k_{xy}\} & & \\ k_2 & k_4 & -k_8 & -k_{10} & -k_2 & k_3 & k_7 & -k_9 & \\ k_5-(k_{yx}) & & k_1-(k_{yy}) & & & & & & \\ k_7 & k_9 & k_2 & k_3 & & & & & \\ k_6 & -k_8 & -k_1 & -k_2 & k_5-\{k_{yx}\} & & k_1-\{k_{yy}\} & & \\ k_8 & k_{10} & k_2 & k_4 & -k_7 & k_9 & -k_2 & k_3 & \end{bmatrix}\begin{Bmatrix} u_{x1} \\ \alpha_1 \\ u_{y1} \\ -\beta_1 \\ u_{x2} \\ \alpha_2 \\ u_{y2} \\ -\beta_2 \end{Bmatrix}$$

$k_1 = 12m0 \quad k_2 = 6lm0 \quad k_3 = a_{10}m0$

$k_4 = a_{11}m0 \quad k_5 = -12m4 - a_1 m6 \quad k_6 = 12m4 - a_3 m6$

$k_7 = -6lm4 - a_2 m6 \quad k_8 = -6m4 - a_4 m6 \quad k_9 = -a_{19}m4 - a_5 m6 \quad k_{10} = -a_{20}m4 - a_6 m6$

Figure 2.20 below shows how elements are fit to each other

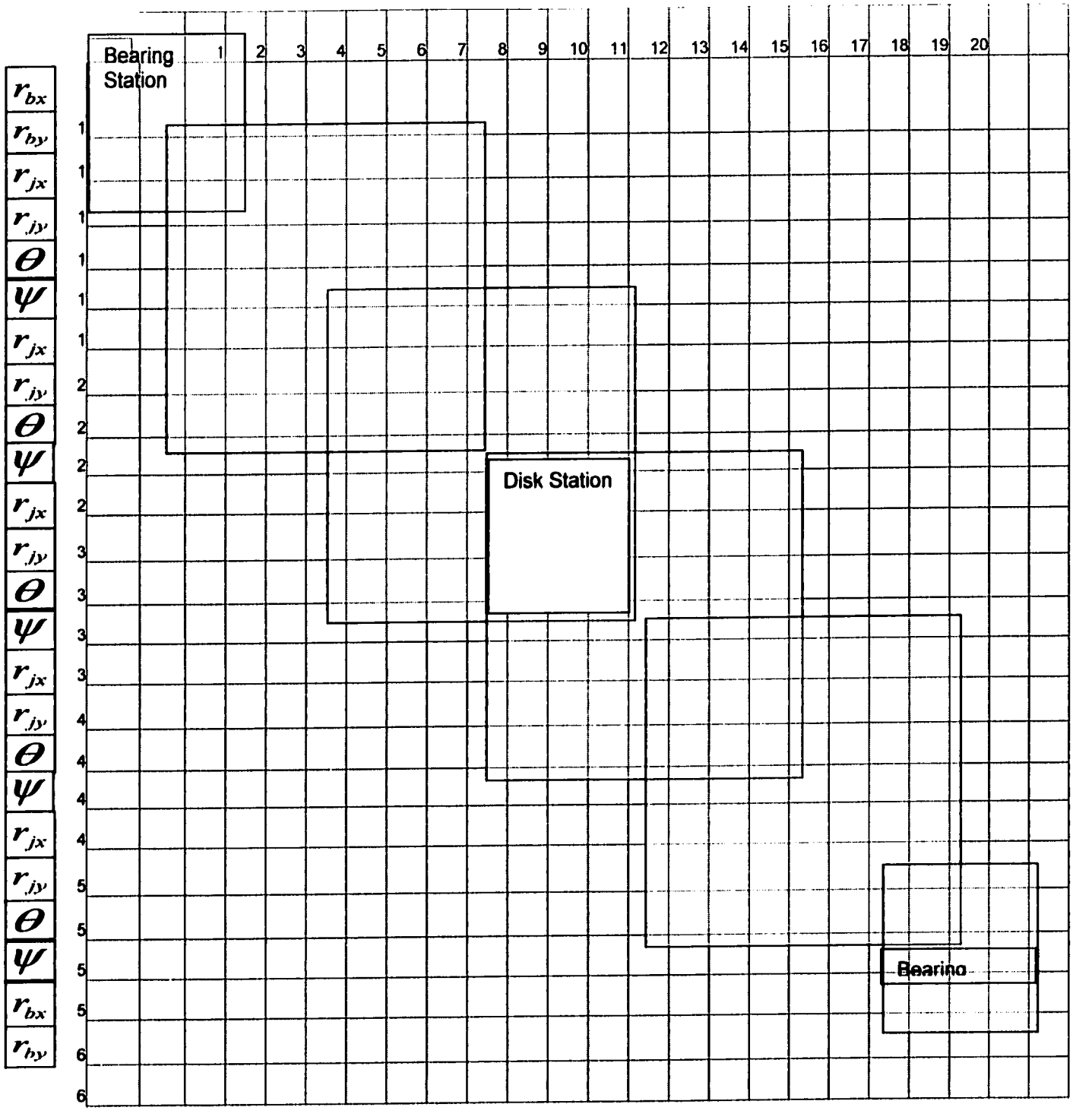

Figure 2.20 Global Matrices Build Up

CHAPTER 3

SHAFT DYNAMIC ECCENTRICITY

Load on machines varies in both magnitude and direction often cyclically, for example reciprocating machinery and out-of-balance rotating machinery. Bearings are generally dynamically loaded. Journal bearings are not inherently stable, for certain combinations of steady-state operating parameters, self-excited whirl orbit, the whirl orbit will increase rapidly until rub occurs. In this chapter the classical solution for a fluid film bearing will be developed such that it addresses the dynamic load factor. In Chapter 2, the General Reynolds equation was given as

$$\frac{\partial}{\partial x}\left(\frac{\rho_f h^3}{12\mu}\frac{\partial P}{\partial x}\right)+\frac{\partial}{\partial y}\left(\frac{\rho_f h^3}{12\mu}\frac{\partial P}{\partial y}\right)=\frac{\partial}{\partial x}\left[\frac{\rho_f h(U_1+U_2)}{2}\right]+\frac{\partial}{\partial y}\left[\frac{\rho_f h(V_1+V_2)}{2}\right] + \rho_f(W_1-W_2)-\rho_f U_1\frac{\partial h}{\partial x}-\rho_f V_1\frac{\partial h}{\partial y}+h\frac{\partial \rho_f}{\partial t} \tag{3.1}$$

From *Figure 3.1* Φ_t is the time independent direction of the load with respect to fixed coordinate system. X-axis should be oriented in the direction of the steady-state part of the load in order to match the attitude angle, which is measured from the x-axis. In the general Reynolds equation, the x-coordinate is in the direction of the unwrapped film thickness. Hence the film thickness will be described in this section from $\theta = 0$ to $\theta = 2\pi$ where $\theta = \phi + \Phi$. The relation indicates the position in the film thickness relative to the fixed coordinate system and independent of the immediate attitude angle.

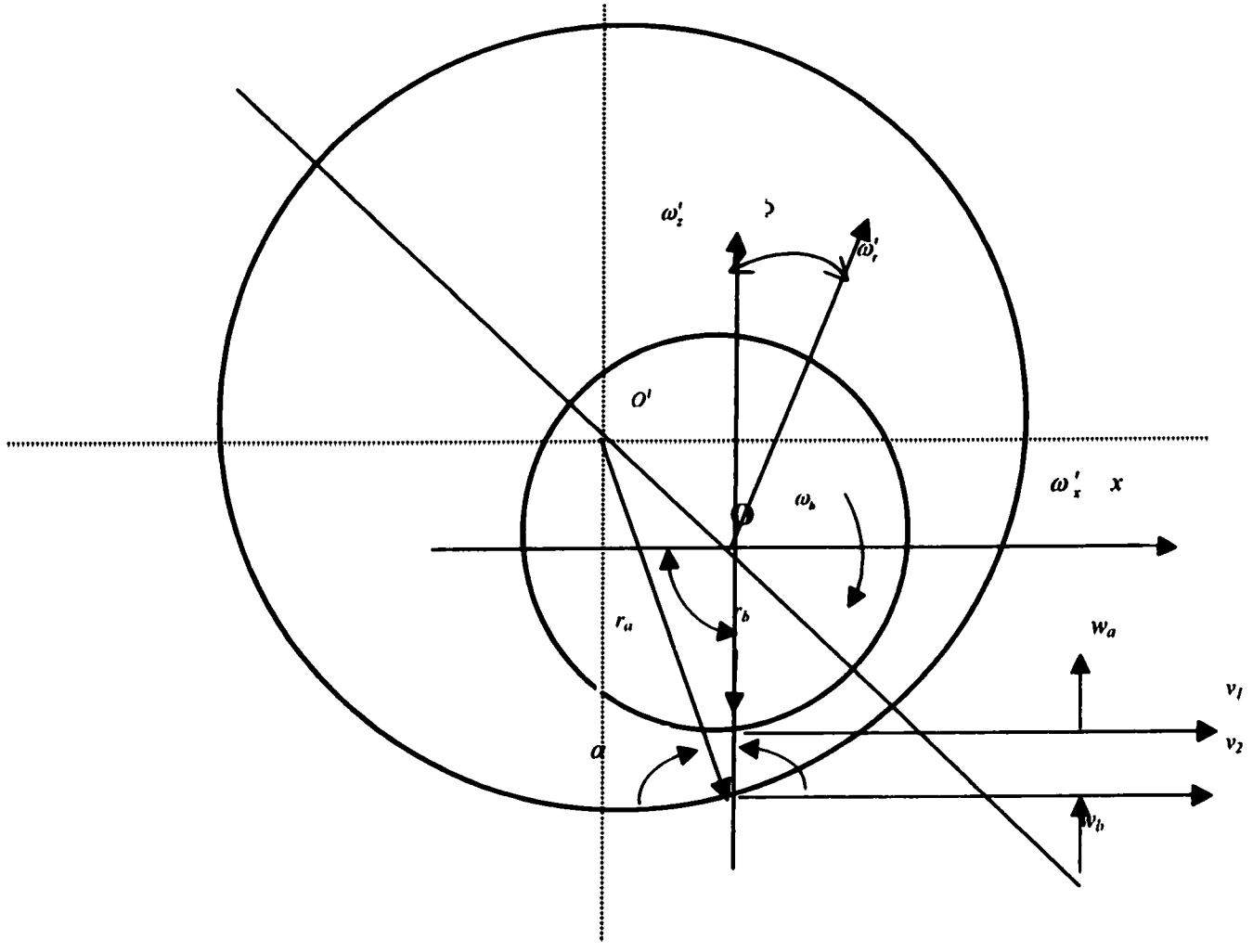

Figure 3.1 – Dynamically Loaded Bearings

In Appendix A, for the dynamically loaded bearing case, fluid film thickness is given as $h = c + e\cos(\theta - \Phi)$, and $h = c(1 + \varepsilon\cos\phi)$ in the static case. From Appendix A, the following expressions for the velocities in the General Reynolds Equation (3.1) is obtained

$$x = r_a\theta, \qquad dx = r_a d\theta \tag{3.2a}$$

$$\begin{aligned} U_1 &= \omega_a r_a, \\ U_2 &= \omega_b r_b \cos(\theta - \alpha') + u_{cb}\sin\theta - \omega_{cb}\cos\theta \end{aligned} \tag{3.2b}$$

$$V_1 = V_2 = 0 \text{ no momentum in y-direction} \tag{3.2c}$$

$$\omega_a = 0 \text{ sleeve rotates about its own center} \tag{3.2d}$$

$$W_2 = -\omega_b \sin(\theta - \Phi) + \dot{e}\cos(\theta + \Phi) + e\dot{\Phi}\sin(\theta - \Phi) \tag{3.2e}$$

$$U_2 = \omega_b r_b + \dot{e}\sin(\theta - \Phi) - e\dot{\Phi}\cos(\theta - \Phi) \tag{3.2f}$$

Substituting (3.2 a-f) into the general Reynolds equation and retaining first order terms

$$\frac{1}{r_a^2}\frac{\partial}{\partial\theta}\left(\frac{h^3}{12\mu}\frac{\partial P}{\partial\theta}\right) + \frac{\partial}{\partial y}\left(\frac{h^3}{12\mu}\frac{\partial P}{\partial y}\right) = \frac{1}{2}(\omega_a + \omega_b)\frac{\partial h}{\partial\theta} + \frac{\partial e}{\partial t}\cos(\theta - \Phi) + e\frac{\partial\Phi}{\partial t}\sin(\theta - \Phi) \tag{3.3}$$

$\omega = \dfrac{d\Phi}{dt}$ rotational velocity of journal about sleeve center when eccentricity ratio is constant.

For $\dfrac{de}{dt} = \dfrac{d\Phi}{dt} = 0$, i.e. steady state loading,

$$\frac{1}{r_a^2}\frac{\partial}{\partial\theta}\left(\frac{h^3}{12\mu}\frac{\partial P}{\partial\theta}\right) + \frac{\partial}{\partial y}\left(\frac{h^3}{12\mu}\frac{\partial P}{\partial y}\right) = \frac{1}{2}(\omega_a + \omega_b)\frac{\partial h}{\partial\theta} \tag{3.4}$$

This is the same equation that was in static load analysis except that side leakage term was neglected. Using full Sommerfeld substitution, $\theta = \phi + \Phi$

$$\frac{\partial}{\partial\phi}\left(\frac{h^3}{\mu}\frac{\partial P}{\partial\phi}\right)=12r_a^2\left[\left(\frac{\omega_a+\omega_b}{2}-\omega\right)\frac{\partial h}{\partial\theta}+\frac{dP}{dt}\cos(\theta-\Phi)\right] \quad (3.5)$$

With constant viscosity in circumferential direction, and integrating

$$P=12\mu_0\left(\frac{r_a}{c}\right)^2\int\left\{\frac{\left(\partial\varepsilon/\partial t\right)\sin\phi-\varepsilon\cos\phi\left(\omega-\frac{\omega_a+\omega_a}{2}\right)-A}{(1+\varepsilon\cos\phi)^3}\right\}d\phi+const \quad (3.6)$$

Using Sommerfeld substitution

$$P=12\mu_0\left(\frac{r_a}{c}\right)^2\left\{\frac{\left(\partial\varepsilon/\partial t\right)\sin\phi}{2\varepsilon(1+\varepsilon\cos\phi)^2}-\left(\omega-\frac{\omega_a+\omega_a}{2}\right)\left[\frac{\gamma-\varepsilon\sin\gamma}{(1-\varepsilon^2)^{3/2}}-\frac{\left(\frac{2+\varepsilon^2}{2}\right)\gamma-2\varepsilon\sin\gamma+\frac{\varepsilon^2}{4}\sin 2\gamma}{(1-\varepsilon^2)^{5/2}}\right]A\right.$$
$$\left.-\frac{A\left[\left(\frac{2+\varepsilon^2}{2}\right)-2\varepsilon\sin\gamma+\frac{\varepsilon^2}{4}\sin 2\gamma\right]}{(1-\varepsilon^2)^{5/2}}+B\right\}$$

Boundary conditions for full Sommerfeld (no cavitation) $P_\phi = P_{\phi+2\pi}$ $\quad P_{\phi=0}=P_{\phi=2\pi}=P_0$

while converting γ to ϕ, give pressure profile as

$$P-P_0=6\mu_0\left(\frac{r_a}{c}\right)^2\left\{\frac{\partial\varepsilon/\partial t}{\varepsilon}\left[\frac{1}{(1+\varepsilon\cos\phi)^2}-\frac{1}{(1+\varepsilon)^2}\right]+(\omega_a+\omega_a-2\omega)\frac{\varepsilon\sin\phi(2+\varepsilon\cos\phi)}{(2+\varepsilon^2)(1+\varepsilon\cos\phi)^2}\right\} \quad (3.7)$$

For half Sommerfeld, the above equation is made valid for $P>0$ and $P=0$ $\quad P<0$

When $\partial\varepsilon/\partial t$, ω_a, ω_b and $\omega=\frac{d\Phi}{dt}$ are known P for any ε given as

$$\omega_x'=12\pi\eta_0 r_a\left(\frac{r_a}{c}\right)^2\frac{\varepsilon(\omega_a+\omega_b-2\omega)}{(2+\varepsilon^2)(1-\varepsilon^2)^{1/2}}=\frac{\omega_r}{b}\sin\Phi_\ell \quad (3.8a)$$

$$\omega_z' = 12\pi\eta_0 r_a \left(\frac{r_a}{c}\right)^2 \frac{\partial\varepsilon/\partial t}{\left(1-\varepsilon^2\right)^{3/2}} = \frac{\omega_r}{b} cos\Phi_\ell \tag{3.8b}$$

With Rotor of mass $2m_a$, in matrix forms

$$\begin{bmatrix} m_a & 0 \\ 0 & m_a \end{bmatrix} \frac{\partial^2}{\partial t^2} \begin{bmatrix} e\cos\Phi \\ e\sin\Phi \end{bmatrix} = \begin{bmatrix} \omega_r \cos\Phi_\ell \\ \omega_r \sin\Phi_\ell \end{bmatrix} - \begin{bmatrix} \omega_x \\ \omega_z \end{bmatrix} \tag{3.9}$$

From *Figure 3.2* when there is small disturbances around the center of bearings, Using first order Taylor series expansion, x-axis direction such that $\omega_z|_0 = 0$

$$\omega_x = \omega_x|_0 + \left.\frac{\partial\omega_x}{\partial x}\right|_0 \Delta x + \left.\frac{\partial\omega_x}{\partial z}\right|_0 \Delta z + \left.\frac{\partial\omega_x}{\partial \dot{x}}\right|_0 \Delta\dot{x} + \left.\frac{\partial\omega_x}{\partial \dot{z}}\right|_0 \Delta\dot{z}$$

$$\omega_z = \omega_z|_0 + \left.\frac{\partial\omega_z}{\partial x}\right|_0 \Delta x + \left.\frac{\partial\omega_z}{\partial z}\right|_0 \Delta z + \left.\frac{\partial\omega_z}{\partial \dot{x}}\right|_0 \Delta\dot{x} + \left.\frac{\partial\omega_z}{\partial \dot{z}}\right|_0 \Delta\dot{z}$$

or In matrix format,

$$\begin{bmatrix} \omega_x \\ \omega_z \end{bmatrix} = \begin{bmatrix} \omega_x|_0 \\ \omega_z|_0 \end{bmatrix} + \begin{bmatrix} \left.\frac{\partial\omega_x}{\partial x}\right|_0 & \left.\frac{\partial\omega_x}{\partial z}\right|_0 \\ \left.\frac{\partial\omega_z}{\partial x}\right|_0 & \left.\frac{\partial\omega_z}{\partial z}\right|_0 \end{bmatrix} \begin{bmatrix} \Delta x \\ \Delta z \end{bmatrix} + \begin{bmatrix} \left.\frac{\partial\omega_x}{\partial \dot{x}}\right|_0 & \left.\frac{\partial\omega_x}{\partial \dot{z}}\right|_0 \\ \left.\frac{\partial\omega_z}{\partial \dot{x}}\right|_0 & \left.\frac{\partial\omega_z}{\partial \dot{z}}\right|_0 \end{bmatrix} \begin{bmatrix} \Delta\dot{x} \\ \Delta\dot{z} \end{bmatrix} \tag{3.10}$$

The same can be applied to pressure field , using linearized Taylor expansion

$$P = P|_0 + \left.\frac{\partial P}{\partial x}\right|_0 \Delta x + \left.\frac{\partial P}{\partial z}\right|_0 \Delta z + \left.\frac{\partial P}{\partial \dot{x}}\right|_0 \Delta\dot{x} + \left.\frac{\partial P}{\partial \dot{z}}\right|_0 \Delta\dot{z}$$

$$\begin{bmatrix} \omega_x \\ \omega_z \end{bmatrix} = \int_y \int_\theta P \begin{bmatrix} \cos\theta \\ \sin\theta \end{bmatrix} r_a d\theta dy \tag{3.11}$$

with load resultant $\omega_r = \omega_{r0} + \Delta\omega_r$

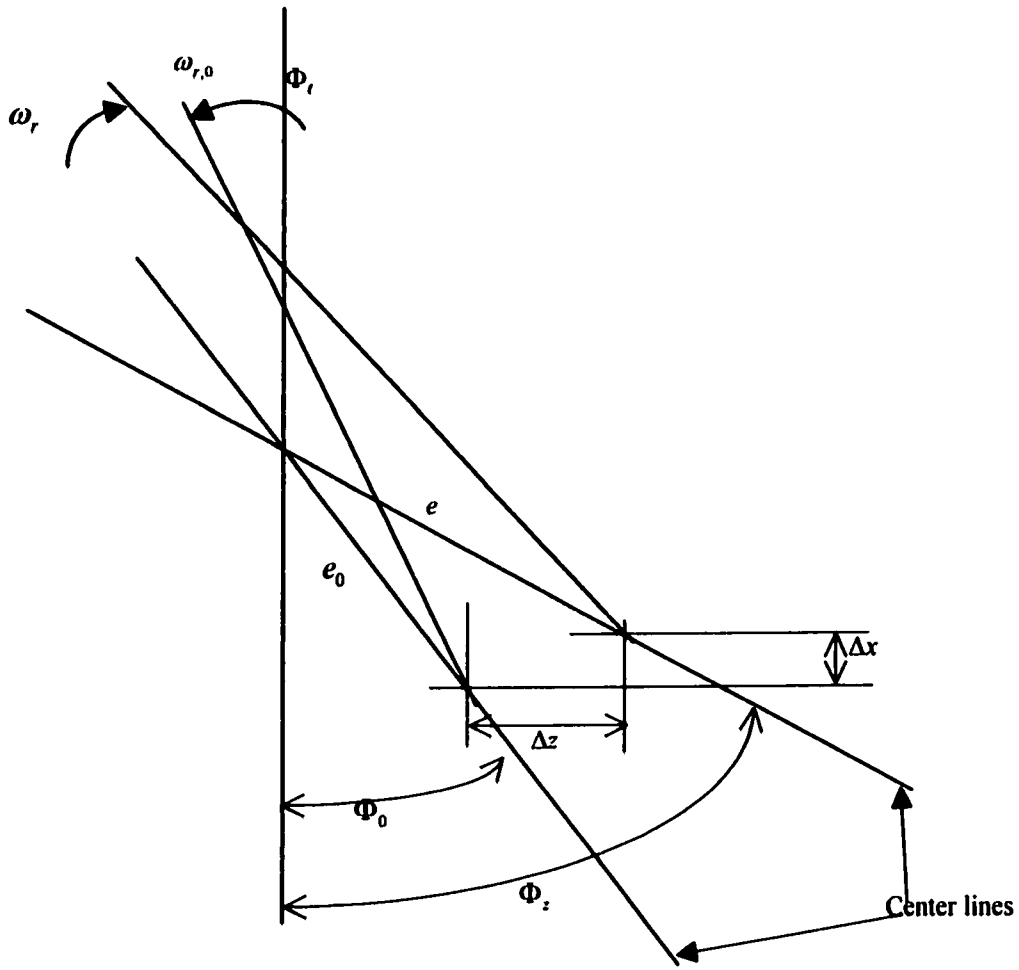

Figure 3.2 – Dynamic Loading Conditions

From steady state solution $e_o \quad \Phi_o$

$$\begin{aligned} e_0\cos\Phi_0 + \Delta x &= e\cos\Phi \\ e_0\sin\Phi_0 + \Delta z &= e\sin\Phi \end{aligned} \tag{3.12}$$

$$h = h_0 + \Delta x\cos\theta + \Delta z\sin\theta, \qquad h_0 = c + e_0\cos(\theta - \Phi_0) \tag{3.13}$$

$$\frac{dh}{dt} = \frac{de}{dt}\cos(\theta-\Phi) + e\frac{d\Phi}{dt}\sin(\theta-\Phi_0) = \Delta\dot{x}\cos\theta + \Delta\dot{z}\sin\theta$$

with no misalignment $h \neq f(y)$ and incompressible fluid $\omega_a = 0$

$$\frac{\partial}{\partial x}\left(\frac{\rho_f h^3}{12\mu}\frac{\partial P}{\partial x}\right) + \frac{\partial}{\partial y}\left(\frac{\rho_f h^3}{12\mu}\frac{\partial P}{\partial y}\right) = \frac{\partial}{\partial x}\left[\frac{\rho_f h(U_1+U_2)}{2}\right] + \frac{\partial}{\partial y}\left[\frac{\rho_f h(V_1+V_2)}{2}\right] + \frac{\partial}{\partial t}(\rho_f h)$$

This equation becomes

$$\boxed{\frac{1}{r_a^2}\frac{\partial}{\partial\theta}\left(\frac{h^3}{12\mu}\frac{\partial P}{\partial\theta}\right) + h^3\frac{\partial}{\partial y}\left(\frac{1}{12\mu}\frac{\partial P}{\partial y}\right) = \frac{\omega_b}{2}\frac{\partial h}{\partial\theta} + \frac{\partial h}{\partial t}} \tag{3.14}$$

Which is Reynolds for dynamic loading conditions with $\omega_a = 0$.

Making use of $\frac{dh}{dt}$ and $P'|_0 = P_x\Delta x + P_z\Delta z + P_{\dot{x}}\Delta\dot{x} + P_{\dot{z}}\Delta\dot{z}$

$$\frac{1}{r_a^2}\frac{\partial}{\partial\theta}\left(\frac{(h_0+\Delta x\cos\theta+\Delta z\sin\theta)^3}{12\mu}\frac{\partial P'}{\partial\theta}\right) + (h_0+\Delta x\cos\theta+\Delta z\sin\theta)^3\frac{\partial}{\partial y}\left(\frac{1}{12\mu}\frac{\partial P'}{\partial y}\right)$$
$$= \frac{\omega_b}{2}\frac{\partial}{\partial\theta}(h_0+\Delta x\cos\theta+\Delta z\sin\theta) + \Delta\dot{x}\cos\theta + \Delta\dot{z}\sin\theta$$

Collecting terms of like order gives

$$\text{O(1)}: \qquad \frac{1}{r_a^2}\frac{\partial}{\partial\theta}\left(\frac{h_0^3}{12\mu}\frac{\partial P_0}{\partial\theta}\right) + h_0^3\frac{\partial}{\partial y}\left(\frac{1}{12\mu}\frac{\partial P_0}{\partial y}\right) = \frac{\omega_b}{2}\frac{\partial h_0}{\partial\theta} \tag{3.15a}$$

$$O(\Delta x): \quad \frac{1}{r_a^2}\frac{\partial}{\partial\theta}\left(\frac{h_0^3}{12\mu}\frac{\partial P_x}{\partial\theta}\right)+h_0^3\frac{\partial}{\partial y}\left(\frac{1}{12\mu}\frac{\partial P_x}{\partial y}\right)=$$
$$-\frac{\omega_b}{2}\sin\theta-\left[\frac{1}{r_a^2}\frac{\partial}{\partial\theta}\left(\frac{h_0^2}{12\mu}\cos\theta\frac{\partial P_0}{\partial\theta}\right)+3h_0^2\cos\theta\frac{\partial}{\partial y}\left(\frac{1}{12\mu}\frac{\partial P_0}{\partial y}\right)\right] \tag{3.15b}$$

$$O(\Delta z): \quad \frac{1}{r_a^2}\frac{\partial}{\partial\theta}\left(\frac{h_0^3}{12\mu}\frac{\partial P_z}{\partial\theta}\right)+h_0^3\frac{\partial}{\partial y}\left(\frac{1}{12\mu}\frac{\partial P_z}{\partial y}\right)=$$
$$\frac{\omega_b}{2}\cos\theta-\left[\frac{1}{r_a^2}\frac{\partial}{\partial\theta}\left(\frac{3h_0^2}{12\mu}\sin\theta\frac{\partial P_0}{\partial\theta}\right)+\frac{h_0^2}{4}\frac{\partial}{\partial y}\left(\frac{\sin\theta}{\mu}\frac{\partial P_0}{\partial y}\right)\right] \tag{3.15c}$$

$$O(\Delta\dot{x}): \quad \frac{1}{r_a^2}\frac{\partial}{\partial\theta}\left(\frac{h_0^3}{12\mu}\frac{\partial P_{\dot{x}}}{\partial\theta}\right)+h_0^3\frac{\partial}{\partial y}\left(\frac{1}{12\mu}\frac{\partial P_{\dot{x}}}{\partial y}\right)=\cos\theta \tag{3.15d}$$

$$O(\Delta\dot{z}): \quad \frac{1}{r_a^2}\frac{\partial}{\partial\theta}\left(\frac{h_0^3}{12\mu}\frac{\partial P_{\dot{z}}}{\partial\theta}\right)+h_0^3\frac{\partial}{\partial y}\left(\frac{1}{12\mu}\frac{\partial P_{\dot{z}}}{\partial y}\right)=\sin\theta \tag{3.15e}$$

Expanding $O(\Delta x)$ second and third terms on the right hand side

$$\frac{1}{r_a^2}\frac{\partial}{\partial\theta}\left(\frac{3h_0^2}{12\mu}\sin\theta\frac{\partial P_0}{\partial\theta}\right)+\frac{h_0^2}{4}\frac{\partial}{\partial y}\left(\frac{\sin\theta}{\mu}\frac{\partial P_0}{\partial y}\right)=\frac{3\cos\theta}{h_0}\left[\frac{1}{r_a^2}\frac{\partial}{\partial\theta}\left(\frac{h_0^3}{12\mu}\frac{\partial P_0}{\partial\theta}\right)+h_0^3\frac{\partial}{\partial y}\left(\frac{1}{12\mu}\frac{\partial P_0}{\partial y}\right)\right]$$
$$+\frac{h_0^3}{12\mu}\left[\frac{3}{r_a^2}\frac{\partial P_0}{\partial\theta}\left(\frac{\cos\theta}{h_0}\right)\right]$$

$O(\Delta x)$ becomes

$$\frac{1}{r_a^2}\frac{\partial}{\partial\theta}\left(\frac{h_0^3}{12\mu}\frac{\partial P_x}{\partial\theta}\right)+h_0^3\frac{\partial}{\partial y}\left(\frac{1}{12\mu}\frac{\partial P_x}{\partial y}\right)=-\frac{\omega_b}{2}\left(\sin\theta+\frac{3\cos\theta}{h_0}\frac{\partial h_0}{\partial\theta}\right)-\frac{h_0^3}{4\mu r_a^2}\frac{\partial P_0}{\partial y}\frac{\partial}{\partial\theta}\left(\frac{\cos\theta}{h_0}\right)$$

Valid for $\lambda_k=\frac{2r_b}{b}>2$. It is independent of perturbation pressure P_0

$$h_0^3 \frac{\partial}{\partial y}\left(\frac{1}{12\mu}\frac{\partial}{\partial y}\right)\begin{bmatrix} P_0 \\ P_x \\ P_z \\ P_{\dot{x}} \\ P_{\dot{z}} \end{bmatrix} = \begin{bmatrix} \frac{\omega_b}{2}\frac{\partial h_0}{\partial \theta} \\ -\frac{\omega_b}{2}\left(\sin\theta + \frac{3\cos\theta}{h_0}\frac{\partial h_0}{\partial \theta}\right) \\ \frac{\omega_b}{2}\left(\cos\theta - \frac{3\sin\theta}{h_0}\frac{\partial h_0}{\partial \theta}\right) \\ \cos\theta \\ \sin\theta \end{bmatrix} \tag{3.16}$$

With no misalignment (pressure profile is symmetric about the center plane)

$\left.\frac{\partial P}{\partial y}\right|_{y=0} = 0, \qquad P|_{y=b/2} = 0$, which implies, $\frac{\partial P_0}{\partial y} = \frac{\partial P_x}{\partial y} = \frac{\partial P_z}{\partial y} = \frac{\partial P_{\dot{x}}}{\partial y} = \frac{\partial P_{\dot{z}}}{\partial y} = 0$ at $y = 0$

$$\begin{bmatrix} P_0 \\ P_x \\ P_z \\ P_{\dot{x}} \\ P_{\dot{z}} \end{bmatrix} = \frac{b\mu_0}{h_0^3}\left(y^2 - \frac{b^2}{4}\right)\begin{bmatrix} \frac{\omega_b}{2}\frac{\partial h_0}{\partial \theta} \\ -\frac{\omega_b}{2}\left(\sin\theta + \frac{3\cos\theta}{h_0}\frac{\partial h_0}{\partial \theta}\right) \\ \frac{\omega_b}{2}\left(\cos\theta - \frac{3\sin\theta}{h_0}\frac{\partial h_0}{\partial \theta}\right) \\ \cos\theta \\ \sin\theta \end{bmatrix} \tag{3.17}$$

Once the steady state pressure is obtained, perturbation pressure and hence dynamic coefficients are derived as follows

$$\begin{bmatrix} k_{xx} & k_{xz} \\ k_{zx} & k_{zz} \end{bmatrix} = \begin{bmatrix} \int_y\int_\theta P_x \cos\theta r_a d\theta dy & \int_y\int_\theta P_z \cos\theta r_a d\theta dy \\ \int_y\int_\theta P_x \sin\theta r_a d\theta dy & \int_y\int_\theta P_z \sin\theta r_a d\theta dy \end{bmatrix} \tag{3.18a}$$

$$\begin{bmatrix} C_{xx} & C_{xz} \\ C_{zx} & C_{zz} \end{bmatrix} = \begin{bmatrix} \int_y\int_\theta P_{\dot{x}} \cos\theta r_a d\theta dy & \int_y\int_\theta P_{\dot{z}} \cos\theta r_a d\theta dy \\ \int_y\int_\theta P_{\dot{x}} \sin\theta r_a d\theta dy & \int_y\int_\theta P_{\dot{z}} \sin\theta r_a d\theta dy \end{bmatrix} \tag{3.18b}$$

Taking double derivatives of (3.12)

$$\frac{\partial^2}{\partial t^2}\begin{bmatrix} e\cos\Phi \\ e\sin\Phi \end{bmatrix} = \begin{bmatrix} \Delta\ddot{x} \\ \Delta\ddot{z} \end{bmatrix}$$

$$\begin{bmatrix} m_a & 0 \\ 0 & m_a \end{bmatrix}\begin{bmatrix} \Delta\ddot{x} \\ \Delta\ddot{z} \end{bmatrix} + \begin{bmatrix} C_{xx} & C_{xz} \\ C_{zx} & C_{zz} \end{bmatrix}\begin{bmatrix} \Delta\dot{x} \\ \Delta\dot{z} \end{bmatrix} + \begin{bmatrix} k_{xx} & k_{xz} \\ k_{zx} & k_{zz} \end{bmatrix}\begin{bmatrix} \Delta x \\ \Delta z \end{bmatrix} = \begin{bmatrix} \omega_r \cos\Phi_l \\ \omega_r \sin\Phi_l \end{bmatrix} - \begin{bmatrix} \omega_x|_0 \\ 0 \end{bmatrix} \quad (3.19)$$

Using half Sommerfeld boundary conditions for short width journal bearing gives

$$\frac{1}{W_r \lambda_k^2} = \frac{\left(1-\varepsilon_0^2\right)^2}{\varepsilon\left[16\varepsilon_0^2 + \pi^2\left(1-\varepsilon_0^2\right)\right]^{1/2}} \quad (3.20)$$

$$\tan\Phi_0 = \frac{\pi\left(1-\varepsilon_0^2\right)^{1/2}}{4\varepsilon_0} \quad (3.21)$$

$$\frac{\partial h_0}{\partial\theta} = -e_0 \sin\left(\theta - \Phi_0\right) \quad (3.22)$$

$$P_x = \left.\frac{\partial P}{\partial x}\right|_0 = \frac{-3\eta_0\omega_b}{c^3}\frac{y^2 - b^2/4}{\left[1+\varepsilon_0\cos\left(\theta-\Phi_0\right)\right]^3}\left[\sin\theta - \frac{3\varepsilon_0\cos\theta\sin\left(\theta-\Phi_0\right)}{1+\varepsilon_0\cos\left(\theta-\Phi_0\right)}\right] \quad (3.23)$$

When integrating as in equation (3.18a,b) the dynamically loaded short bearing parameters are obtained with half Sommerfeld boundary conditions as given below while Going back to ϕ coordinate $\theta = \phi + \Phi$ and integrating with respect to dy and using non-dimensionalizing

$$\begin{bmatrix} K_{xx} & K_{xz} \\ K_{zx} & K_{zz} \end{bmatrix} = \frac{c}{\omega_r}\begin{bmatrix} k_{xx} & k_{xz} \\ k_{zx} & k_{zz} \end{bmatrix}, \qquad \begin{bmatrix} C_{xx} & C_{xz} \\ C_{zx} & C_{zz} \end{bmatrix} = \frac{c\omega_b}{\omega_r}\begin{bmatrix} C_{xx} & C_{xz} \\ C_{zx} & C_{zz} \end{bmatrix} \quad (3.24)$$

Such that the parameters are given by,

$$K_{xx} = \frac{4}{W_r \lambda_k^2}\left[\frac{\varepsilon_0 \sin^2\Phi_0}{\left(1-\varepsilon_0^2\right)^2} + \frac{3\pi\varepsilon_0 \cos\Phi_0 \sin\Phi_0}{4\left(1-\varepsilon_0^2\right)^{5/2}} + 2\frac{\varepsilon_0\left(1+\varepsilon_0^2\right)\cos^2\Phi_0}{\left(1-\varepsilon_0^2\right)^3}\right] \quad (3.25a)$$

$$K_{xz} = \frac{4}{W_r \lambda_k^2}\left[\frac{\pi\left(1+2\varepsilon_0^2\right)}{4\left(1-\varepsilon_0^2\right)^{5/2}}\sin^2\Phi_0 + \frac{\varepsilon_0\left(1+3\varepsilon_0^2\right)}{\left(1-\varepsilon_0^2\right)^3}\sin\Phi_0\cos\Phi_0 + \frac{\pi\cos^2\Phi_0}{4\left(1-\varepsilon_0^2\right)^{3/2}}\right] \quad (3.25b)$$

$$K_{zx} = \frac{4}{W_r \lambda_k^2}\left[-\frac{\pi\sin^2\Phi_0}{4\left(1-\varepsilon_0^2\right)^{3/2}} + \frac{\varepsilon_0\left(1+3\varepsilon_0^2\right)}{\left(1-\varepsilon_0^2\right)^3}\sin\Phi_0\cos\Phi_0 - \frac{\pi\left(1+2\varepsilon_0^2\right)}{4\left(1-\varepsilon_0^2\right)^{5/2}}cos^2\Phi_0\right] \quad (3.25c)$$

$$K_{zz} = \frac{4}{W_r \lambda_k^2}\left[\frac{2\varepsilon_0\left(1+2\varepsilon_0^2\right)}{\left(1-\varepsilon_0^2\right)}\sin^2\Phi_0 - \frac{3\pi\varepsilon_0^2}{4\left(1-\varepsilon_0^2\right)^{5/2}}\sin\Phi_0\cos\Phi_0 + \frac{\varepsilon_0\cos^2\Phi_0}{4\left(1-\varepsilon_0^2\right)^2}\right] \quad (3.25d)$$

$$C_{xx} = \frac{4}{W_r \lambda_k^2}\left[\frac{\pi\sin^2\Phi_0}{2\left(1-\varepsilon_0^2\right)^{3/2}} + \frac{4\varepsilon_0}{\left(1-\varepsilon_0^2\right)^2}\sin\Phi_0\cos\Phi_0 + \frac{\pi\left(1+2\varepsilon_0^2\right)}{2\left(1-\varepsilon_0^2\right)^{5/2}}cos^2\Phi_0\right] \quad (3.25e)$$

$$C_{xz} = C_{zx} = \frac{4}{W_r \lambda_k^2}\left[-\frac{4\varepsilon_0\sin^2\Phi_0}{\left(1-\varepsilon_0^2\right)^2} + \frac{3\pi\varepsilon_0^2}{2\left(1-\varepsilon_0^2\right)^{5/2}}\sin\Phi_0\cos\Phi_0 - \frac{\varepsilon_0}{2\left(1-\varepsilon_0^2\right)^2}cos^2\Phi_0\right] \quad (3.25f)$$

$$C_{zz} = \frac{4}{W_r \lambda_k^2}\left[\frac{\pi\left(1+2\varepsilon_0^2\right)\sin^2\Phi_0}{2\left(1-\varepsilon_0^2\right)^{5/2}} - \frac{4\varepsilon_0}{\left(1-\varepsilon_0^2\right)^2}\sin\Phi_0\cos\Phi_0 + \frac{\pi}{2\left(1-\varepsilon_0^2\right)^{3/2}}cos^2\Phi_0\right] \quad (3.25g)$$

The expressions above will be used to simulate the dynamic eccentricity short bearing solution. Dynamic eccentricity will be derived from the instantaneous shaft position within the bearing clearance as will be shown in the MATLAB program flow chart.

CHAPTER 4

FLUID FILM INERTIA

The work of Muszynska (1986) and early works of Smith (1965) show that there is an appreciable added mass to rotors due to fluid inertia in journal bearings. Reinhardt and Lund (1975) used perturbation solution valid for small Reynolds number and reported the effect of fluid inertia. Work in the area of Squeeze Film Dampers (SFD) conducted by Texas A&M Turbomachinery Lab through San Andres and Vance (1986) gave a good start for researchers to obtain the fluid inertia forces using circular centered orbits. Elshafei (1992) provided energy approximation technique to model inertia in SFD's valid for any orbits of the journal. Elshafei approach was to multiply the momentum equation of N-S with approximate velocity profile and integrate over the film thickness, resulting pressure is integrated to obtain inertia forces. Inertia-less velocity profiles are obtained from Reynolds pressure profile and then inserted in the axial momentum equation of N-S. Fluid inertia is shown to introduce non-linear radial acceleration in addition to the standard radial, centripetal, tangential and Coriolis accelerations as well as provide additional stiffness and damping coefficients. Below is a listing of some shortfalls of the Reynolds Equation is addition to all the approximations made in Chapter two to derive Reynolds from Navier-Stockes (Eight approximations listed),

1. Integration of fluid pressure to get fluid dynamic forces; in order to more adequately calculate the fluid dynamic forces to;
    a. calculate the stresses on the shaft surface

b. integrate the stresses over the surface of the shaft.

2. In the course of developing Reynolds equation, the stresses component that consists of two parts (pressure and velocity gradient), omission of the velocity gradient means that the physical mechanism which forces fluid into rotation with the journal was neglected.
3. Integration is one over an imaginary surface positioned concentrically with the bearing. It should be done over a real shaft surface, eccentric to the bearing. this integration limits shortfall results in discrepancies in the resulting force expressions when the shaft is not in the vicinity of the center of the bearing. Some researchers as big as 20% have reported such errors.
4. Bearing coefficients calculated from fluid dynamic forces gave deficiencies
5. They do not reflect any correlations between the models and observable rotor bearing physical models, which is governed by non-linearities.
6. The Bearing coefficients are evaluated through a displacement response to a static loading of the shaft. The Bearing coefficients obtained here do not take into account additional stiffness terms created by internal motion of the shaft inside the fluid. The solution to this issue is to derive values of bearing fluid film stiffness coefficient analytically through displacement response to a dynamic loading of the shaft .
7. In Data Reduction, system linear behavior is assumed which causes loses of data. This is presented in the form of ratios of fluid force in radial and tangential directions to constant shaft displacement orbit amplitudes. Dynamic stiffness format does not contain any assumption about system linearity, it also allows easier stability analysis.

The neglected viscous terms also in deriving Reynolds from N.S (Inertia terms) can be important in a number of cases some of which are listed below

1. If fluid velocity and inertia are high, they create pressure component $\frac{1}{2}\rho_f u^2$ Comparable to Bearing pressure $\frac{T}{r_o}$ where T is the foil bearing tension.

   This have been reported by El-Shafei [24] to be of significance for Reynold numbers > 50.

2. When separation bubble exists when flow enters the film around a sharp edge corner. This is similar to Vena Contara in sharp edge orifices
3. AS operational speed increases, inertia effects become more important.
4. When there is a solid particle in the path of the fluid flow

The current chapter will adopt a different method for modeling bearing forces in order to avoid all the shortfalls of the Reynolds equation and accommodate the fluid inertia effect into the system under study. The method is based on rotor-disk-bearing model developed by BRDRC, [14,15,16,20]. The model which will be detailed in section 4.2 is based on the fact that the linearized bearing forces from which the stiffness and damping coefficients is derived assumes that the fluid is stagnant! While in reality the approach is to derive the equations and then multiplying by the rotation transformation matrix that represent the fluid film. This will address the fact that fluid is rotating at an average velocity in the circumferential direction and hence this has to be accounted for while developing the equations of motion. The developed model using Reynolds equation with infinite series solution will accommodate the fluid inertia terms as well as use the shaft instantaneous position & velocity used to derive the dynamic eccentricity parameter.

4.1 ROTATING FLUID DYNAMIC MODEL

Due to friction, the lubricating fluid that fills the bearing clearance is dragged into rotation. The fluid layer next to the shaft will have the same sped as the shaft, the fluid layer next to the bearing wall will have zero circumferential velocity. This variation will give the fluid an average circumferential velocity. This term is referred to in literature as fluid average circumferential velocity of the fluid and usually assumed at $\omega/2$ where ω is the shaft speed.

In a bearing system, the volume of the liquid entering the slot per unit time is $LR\omega\frac{(R-r-a)}{2}$ Where L is the length of the bearing. The output volume per unit time is $LR\omega\frac{(R-r+a)}{2}$ The pressure difference is what enables the shaft to carry the loads. However if the center of the rotor rotates at speed Ω about the center of the bearing, the volume of the liquid will increase by $2LRa\Omega$ equating this to the difference in volume entering and leaving the system gives that $\Omega=\omega/2$. This was the base behind the assumption that the fluid average circumferential velocity is $\omega/2$. This approximation is what is normally used in text books and publications up to now.

BRDRC [14], found through their experimental research that λ varies according to bearing design parameters, more specifically it is a function of bearing eccentricity as shown in *Figure 4.1*. Curve fit done by BRDRC gave an experimental value as

$$\lambda=0.48(1-e^2)^{1/5} \qquad (4.1)$$

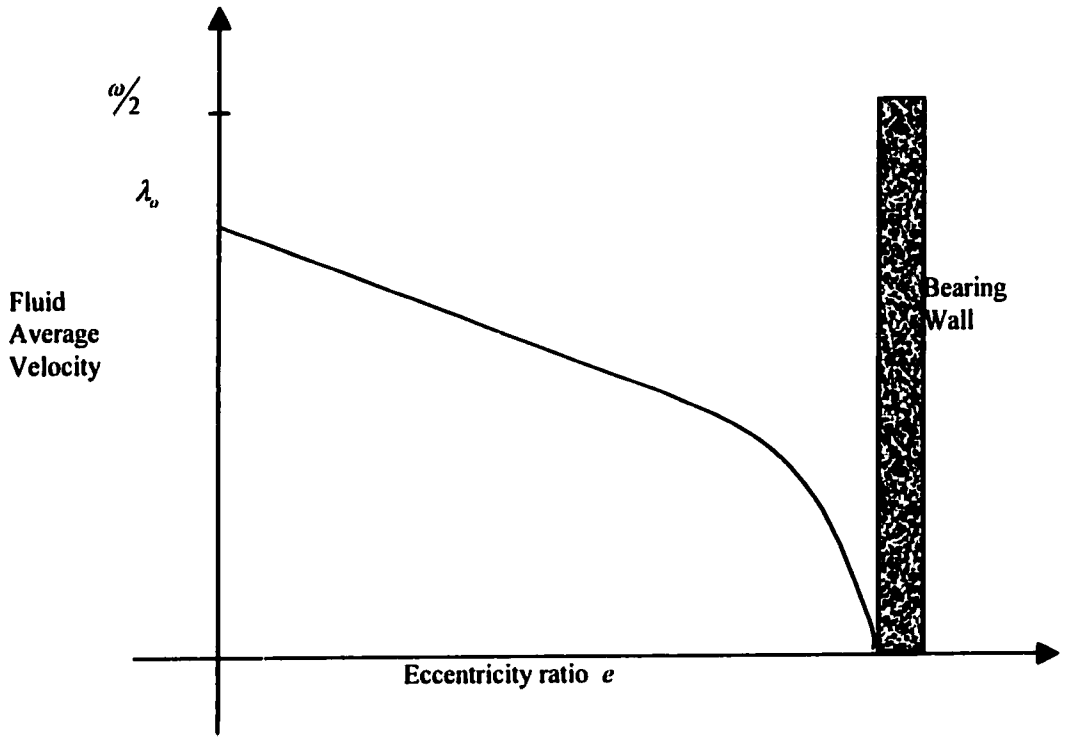

Figure 4.1 – Fluid Average Circumferential Flow

In mechanical systems $Motion = \frac{Force}{Stiffness}$ when rotors are loaded they possess direct stiffness and cross stiffness which acts perpendicular to the input load, this is as a result of the fluid wedge support term. Another way of explaining this is that the fluid support term is formed as a result of the rotor moving sideways to the applied load. This is so the rotor can close the clearance to form a wedge, which in turn supports the applied load. When radial clearance between the bearing center and the shaft center differ (Shaft is moved from concentric to eccentric position) fluid average velocity decreases. during one cycle of rotation, fluid pattern changes, pressure distribution is modified and a wedge is created in front of the narrow fluid gap. λ decreases in this case due to friction losses, axial flow and backward flow/vortices generated in the fluid high pressure regions. Radial load and dynamic stiffness of the system cause the shaft to operate at a specific eccentricity position, this creates a restriction gate and fluid wedge forms in front of the gate. Total fluid wedge support force is equal and opposite to the applied load in order to balance the shaft. The above system description is a simple feedback control system, which under certain condition can go unstable. If a shaft rotates in a plain bearing the oil between the shaft and the sleeve bearing do participate in the rotation forming a stream. The internal surface of the oil firm will be loaded by the friction forces acting in the direction of the motion, the surface of the journal is loaded with forces that will act in the opposite direction. When fluid flow in such a fashion a dynamic effect that creates a rotating force is established. These forces in feedback act on the shaft and cause lateral precesional motion. These forces rotate at the fluid circular speed.

4.2 FLUID FILM FORCE IN ROTATING COORDINATES

4.2.1 ROTOR/BEARING MATHEMATICAL MODELING

In the standard research and text books, bearing systems were modeled as

$$\begin{bmatrix} F_x \\ F_y \end{bmatrix} = \begin{bmatrix} K_{xx} & K_{xy} \\ -K_{yx} & K_{yy} \end{bmatrix} \begin{bmatrix} x \\ y \end{bmatrix} + \begin{bmatrix} D_{xx} & D_{xy} \\ -D_{yx} & D_{yy} \end{bmatrix} \begin{bmatrix} \dot{x} \\ \dot{y} \end{bmatrix} + \begin{bmatrix} M_x & 0 \\ 0 & M_y \end{bmatrix} \begin{bmatrix} \ddot{x} \\ \ddot{y} \end{bmatrix} \qquad (4.2)$$

The above equations hold for a laterally isotropic system (Laterally symmetric). The above system as explained is de-composed in BRDRC [16] work into the following elements:

1) Direct (radial) spring stiffness. This is the sum of liquid film hydrodynamic stiffness with hydrostatic (externally pressurized) stiffness. Both are fluidic inertia terms.
2) Cross Damping and Direct Mass
3) Fluid film Quadrature dynamic stiffness which contains:
   - Cross spring, being the product of direct damping, circumferential average fluid velocity ration and rotative speed.
   - Direct (Radial) damping
   - Cross Mass

For a simple spring damper mass system the system complex form of the dynamic stiffness is given as [14]

$$\text{System Dynamic Stiffness } K - M\omega^2 + j\omega D \qquad (4.2)$$

Fluid in bearings is a major source of damping in rotating equipment. This damping is a function of the length, diameter and clearance (coefficients of Sommerfeld number).

$$\text{Sommerfeld Number } S = 2L\mu R\left(\frac{R}{c}\right)^2 \frac{\Omega}{P} \qquad (4.3)$$

Where: L: Length of Bearing, P: Applied Load, R: Bearing Radius, c: Radial Clearance, Ω: Shaft Speed, μ: Lubricant Viscosity

Shaft rotation as described above with the fluid participating in this circumferential motion will generate a force known in literature as "cross-coupled stiffness" or fluid wedge support which opposes the stabilizing damping force generated by the shaft and pushing on the fluid (passive term). Damping X angular speed = stiffness term, this stiffness which acts tangentially "Quadrature stiffness " have the following parts as shown in *Figure 4.2*:

- Part due to rotor pushing on the fluid = Angular velocity of the push X damping of the bearing = $j\omega D$, j indicate a perpendicular action of the applied force.
- Part due to the fluid pushing on the shaft which acts as a rate of $\lambda\Omega$ and equals = $-j\lambda\Omega D$ and acts opposite to ω D.
- Part due to external viscous damping = $j\omega D_s$

Hence, Quadrature stiffness as part of the system dynamic stiffness is given as

$$\text{Quadrature Stiffness } K_Q = j\omega D - j\lambda\Omega D + j\omega D_s \qquad (4.4)$$

Direct Dynamic stiffness, which constitutes the other part of the system dynamic stiffness is simply as stated earlier:

$$\text{Direct Dynamic Stiffness } K_D = K - \omega^2 M + K_B \qquad (4.5)$$

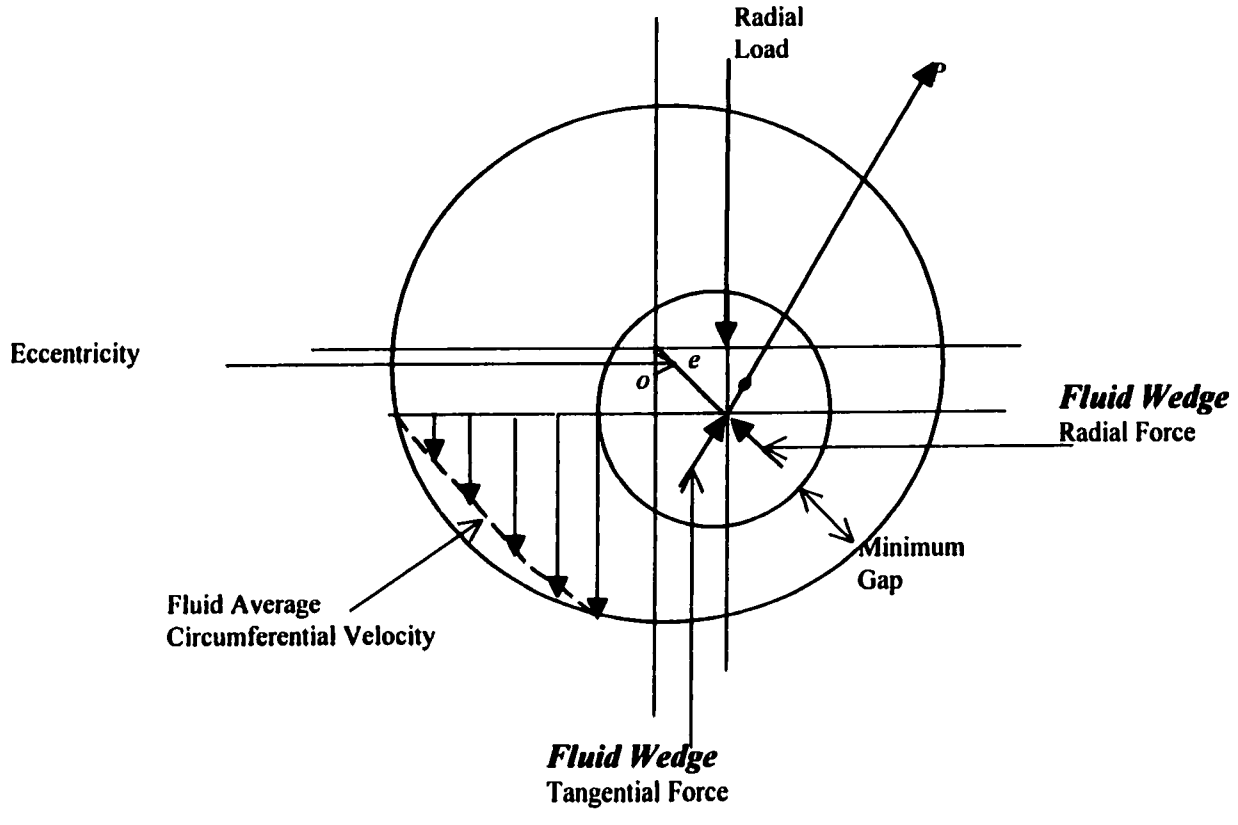

Figure 4.2 – Fluid Wedge and Fluid Average Circumferential Velocity

Where K_B is fluid film direct radial stiffness, which is the fluid film direct radial stiffness, direct dynamic stiffness was found to be a non-linear function of eccentricity experimentally as well as proved analytically in this study. When the shaft at constant rotating speed undergo radial side load *P*, it will react by moving its position from the centerline at a position away from the direction of the load normally perpendicular to the load in the direction of the rotation. The shaft movement inside the bearing from its static load (at rest) to dynamic load position at initial start-up will be studied in details in the following chapters.

4.2.2 CARTESIAN TO ROTATING COORDINATES SYSTEM REPRESENTATION

The Spring and dashpot ends are not attached either to the bearing or to the rotor surfaces, but slide with velocity $\lambda\Omega(R+C)$ on the bearing and $(1-\lambda)\lambda\Omega$ on the rotor as shown in *Figure 4.3* below

Rotor model using z = x +iy

$$M\ddot{x} + D_s\dot{x} + Kx = 0$$

$$M\ddot{y} + D_s\dot{y} + Ky = 0$$

$$M\ddot{z} + D_s\dot{z} + Kz = 0, \qquad (4.6)$$

Using

$$X_J = X_{J3}\cos\lambda\Omega t + Y_{J3}\sin\lambda\Omega t \qquad (4.7a)$$

$$Y_J = X_J\cos\lambda\Omega t - Y_J\sin\lambda\Omega t \qquad (4.7b)$$

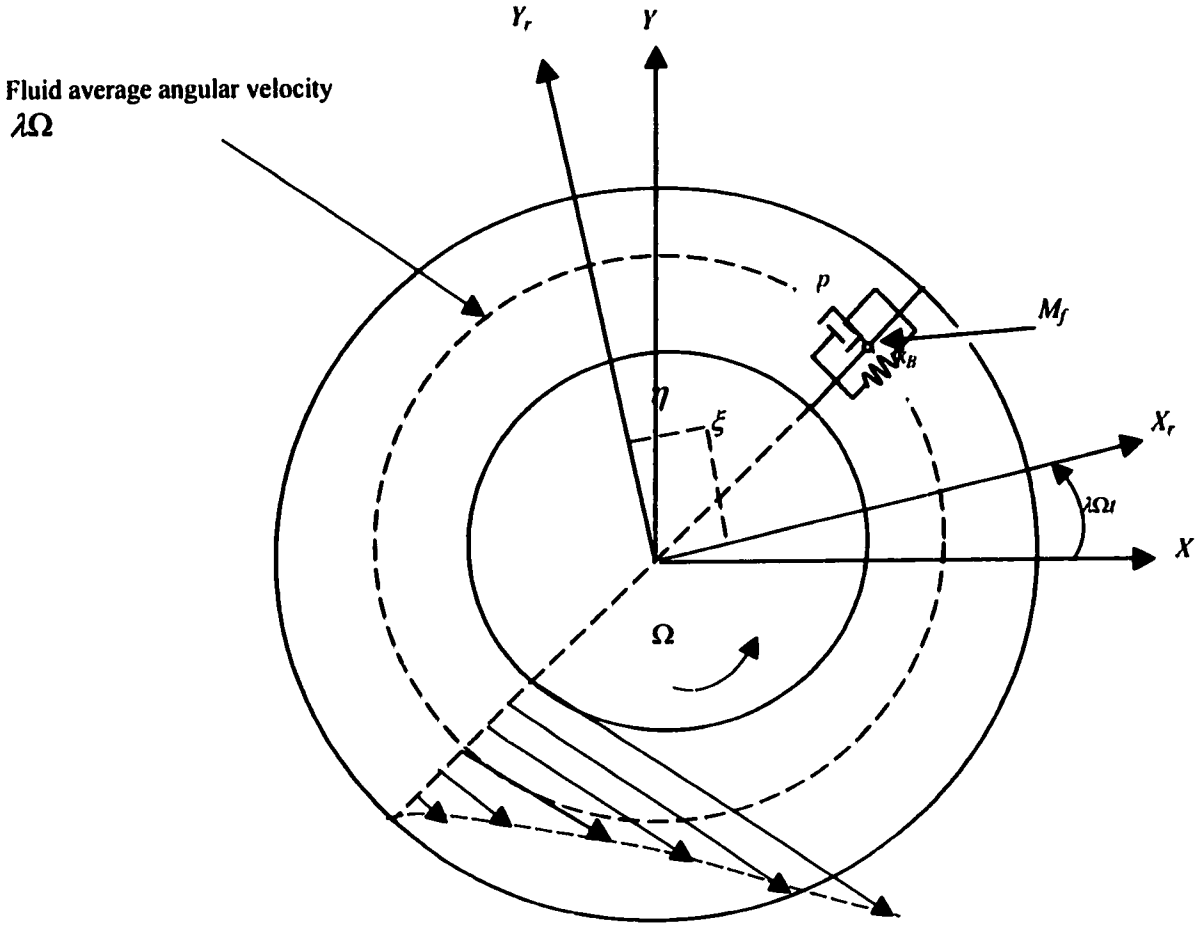

Figure 4.3 – Rotating Fluid Model

Applying Euler identity $e^{j\alpha} = \cos\alpha + j\sin\alpha$

$$z = \zeta e^{j\lambda\Omega t}, \quad z = x + jy, \quad \zeta = \zeta + j\eta$$

$$\dot{z} = \left(\dot{\zeta} + j\lambda\Omega\zeta\right)e^{j\lambda\Omega t}$$

$$\ddot{z} = \left(\ddot{\zeta} + zj\lambda\Omega\dot{\zeta} - \lambda^2\Omega^2\zeta\right)e^{j\lambda\Omega t}$$

Rotor model coordinate rotating at the rate $\lambda\Omega$ will have the form

$$M\left(\ddot{\zeta} + 2j\lambda\Omega\dot{\zeta} - \lambda^2\Omega^2\zeta\right) + D_s\left(\dot{\zeta} + j\lambda\Omega\zeta\right) + K\zeta = 0 \qquad (4.8)$$

Relative inertia force

Coriolis Inertia Force

Centripetal inertia force

Model of rotor with fluid interaction;

$$M\left(\ddot{\zeta} + 2j\lambda\Omega\dot{\zeta} - \lambda^2\Omega^2\zeta\right) + D_s\left(\dot{\zeta} + j\lambda\Omega\zeta\right) + K\zeta + D\dot{\zeta} + K_B\zeta = 0 \qquad (4.9)$$

Fluid effect

To transform to stationary coordinates, the inverse information $\zeta = ze^{-j\lambda\Omega t}$

The model becomes;

$$M\ddot{z} + D_s\dot{z} + Kz + \underbrace{D\left(\dot{z} - j\lambda\Omega t\right)}_{\text{Rotating fluid force}} + K_B z = 0 \tag{4.10}$$

Splitting back to Cartesian displacements

$$X_J = x$$
$$Y_J = y$$
$$Z_J = z$$

$$M\ddot{x} + D_s\dot{x} + Kx + D\left(\dot{x} + \lambda\Omega y\right) + K_B x = 0 \tag{4.11a}$$

$$M\ddot{y} + D_s\dot{y} + Ky + D\left(\dot{y} - \lambda\Omega x\right) + K_B y = 0 \tag{4.11b}$$

In matrix format

$$\begin{bmatrix} M & 0 \\ 0 & M \end{bmatrix}\begin{bmatrix} \ddot{x} \\ \ddot{y} \end{bmatrix} + \begin{bmatrix} D_s + D & 0 \\ 0 & D_s + D \end{bmatrix}\begin{bmatrix} \dot{x} \\ \dot{y} \end{bmatrix} + \underbrace{\begin{bmatrix} K + K_B & \lambda\Omega D \\ -\lambda\Omega D & K + K_B \end{bmatrix}}_{\text{cross coupled stiffness}}\begin{bmatrix} x \\ y \end{bmatrix} \tag{4.12}$$

The forces in coordinate rotating at $\lambda\Omega$ rate

$$F\zeta = M_f\ddot{\zeta} + D\dot{\zeta} + K_B\zeta \tag{4.13}$$

The whole system in stationary coordinates

$$M\ddot{z} + D_s\dot{z} + Kz + \underbrace{\boxed{M_f\left(\ddot{z} - 2j\lambda_f\Omega\dot{z} - \lambda_f^2\Omega^2 z\right) + D\left(\dot{z} - j\lambda\Omega z\right) + K_B z}}_{\text{Fluid Model in Stationary Coordinates}} = 0 \tag{4.14}$$

In matrix format

$$\begin{bmatrix} M+M_f & 0 \\ 0 & M+M_f \end{bmatrix}\begin{bmatrix} \ddot{x} \\ \ddot{y} \end{bmatrix}+\begin{bmatrix} D_S+D & 2M_f\lambda\Omega \\ -2M_f\lambda\Omega & D_S+D \end{bmatrix}\begin{bmatrix} \dot{x} \\ \dot{y} \end{bmatrix}+\begin{bmatrix} K+K_B-M_f\lambda^2\Omega^2 & \lambda\Omega D \\ -\lambda\Omega D & K+K_B-M_f\lambda^2\Omega^2 \end{bmatrix}\begin{bmatrix} x \\ y \end{bmatrix}$$

(4.15)

Skew symmetric "gyroscopic"-like terms due to coriolis acceleration of the rotating fluid

Notice that fluid damping rotate at rate $\lambda\Omega$ while fluid inertia rotate at $\lambda_f\Omega$. Results of experiments show that λ_f is 10% larger λ.

4.2.3 MODEL SOLUTION USING INFINITE SERIES

Using the general Reynolds equation developed in Chapter 2, Reynolds in cylindrical coordinates $\dot{\beta}=\omega$ ω frequency of journal precision as shown in *Figure 4.4*

$$\frac{\partial}{\partial z}\left(\frac{h^3}{\mu}\frac{\partial^2 P}{\partial z}\right)+\frac{1}{r^2}\frac{\partial}{\partial \gamma}\left(\frac{h^3}{\mu}\frac{\partial P}{\partial \gamma r}\right)=12e\left[\left(\frac{\Omega}{2}-\dot{\beta}\right)\frac{\partial h}{\partial \gamma}-c\dot{e}\cos(\gamma-\beta)\right] \qquad (4.16)$$

Using the following dimensionalizing relations

$$H=\frac{h}{c} \qquad \square=\frac{d}{d\Omega t} \qquad P=p\frac{c^2}{\eta\Omega R^2} \qquad Z=\frac{z}{R} \qquad L=\frac{\ell}{R}$$

The general Reynolds equation can be written as

$$H^3\frac{\partial^2 P}{\partial z}+\frac{\partial}{\partial \phi r}\left(H^3\frac{\partial P}{\partial \gamma}\right)=12\left[(1/2-\dot{\beta})\frac{\partial H}{\partial \gamma}-\dot{\varepsilon}\cos(\phi r-\beta)\right] \qquad (4.17)$$

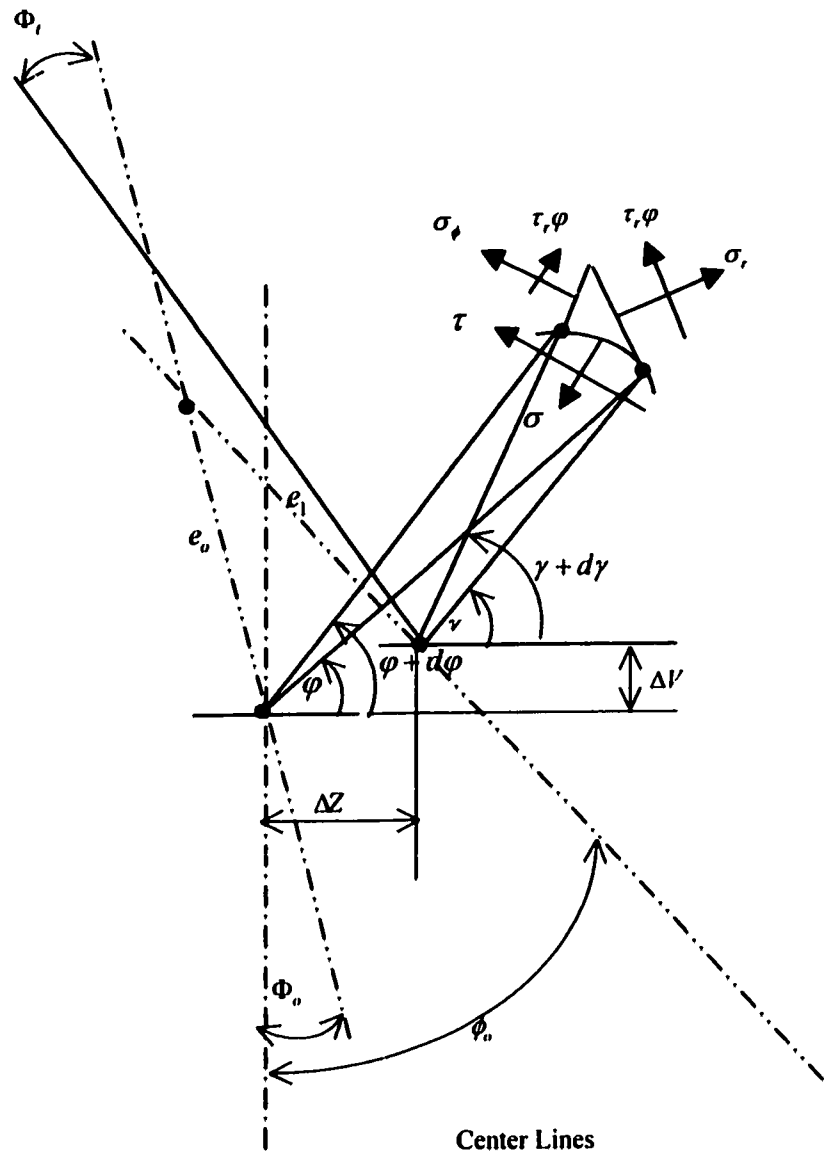

Figure 4.4 – Shaft Center Dynamic motion in Rotating Coordinates

The non-dimensionalized form of Reynolds equation can be solved using the following series as have been suggested by a number of research papers [14, 28], solution of the form

$$P = P_a\left(1-\frac{Z}{L}\right) + P_b\frac{Z}{L} + Z(Z-L)\sum_{n=0}^{\infty}\sum_{n=0}^{\infty} a_{kn}(\gamma)Z^k L^{n-k} \tag{4.18}$$

$$P_a|_{Z=0} = P\,, \qquad P_b|_{Z=L} = P$$

$$\bar{Z} = \frac{Z}{L} = \frac{Z}{R}\frac{R}{\ell} = \frac{Z}{\ell} \text{ Restricted as } 0 < \bar{Z} < L \text{ and } {}^{\ell}/_{R} < 1 \quad or \quad \ell < R$$

In order for the series solution to converge, the condition when substituted into Reynolds

$$\frac{\partial^2 P}{\partial \bar{Z}^2} + L^2\frac{\partial^2 P}{\partial \gamma^2} + L^2\frac{3}{H}\frac{\partial H}{\partial \gamma}\frac{\partial P}{\partial \gamma} = 12\frac{L^2}{H^3}\left[\left({}^{1}/_{2}-\dot{\beta}\right)\frac{\partial H}{\partial \phi} - \dot{\varepsilon}\cos(\gamma-\beta)\right]$$

Should satisfy

$$P = P_a\,(1-\bar{Z}) + P_b\,\bar{Z} + L^2\,\bar{Z}(\bar{Z}-1)\sum_{n=0}^{\infty} L^n\sum_{k=0}^{\infty} a_{kn}\gamma Z^k \tag{4.19}$$

$$P = P_a\frac{\ell-z}{\ell} + P_b\frac{z}{\ell} + \frac{\eta\Omega}{c^2}\,z(z-\ell)\sum_{n=0}^{\infty}\sum_{k=0}^{n} a_{kn}\left(\frac{z}{R}\right)^k\left(\frac{\ell}{R}\right)^{n-k} \tag{4.20}$$

$$\sum_{n=0}^{\infty} 2L^n\sum_{k=0}^{n} a_{kn}\bar{Z}^k + 2\left(2\bar{Z}-1\right)L^{n+1}\sum_{k=1}^{n+1} a_{kn+1}{}^{k}\bar{Z}^{k-1} + \bar{Z}(\bar{Z}-1)L^{n+2}\sum_{k=2}^{n+2} a_{kn+2}k(k+1)\bar{Z}^{k-2} + \frac{3}{H}\frac{\partial H}{\partial \gamma}\bar{Z}(\bar{Z}-1)L^{n+2}\sum_{k=0}^{n}\frac{\partial a_{kn}}{\partial \gamma}\bar{Z}^k$$
$$+\bar{Z}(\bar{Z}-1)L^{n+2}\sum_{k=0}^{n}\frac{\partial^2 a_{kn}}{\partial \gamma^2}\bar{Z}^k = \frac{12}{H^3}(1/2-\dot{\beta})\frac{\partial H}{\partial \gamma} + \frac{12}{H^3}\dot{\varepsilon}cos(\gamma-\beta) \tag{4.21}$$

Using (See Appendix A)

$$H = 1-\varepsilon cos(\gamma-\beta) \tag{4.22}$$

And equating balancing terms having same order of magnitude

$$\frac{\partial H}{\partial \gamma} = \varepsilon\,\sin(\gamma-\beta) \tag{4.23}$$

Collecting terms of order zero, one and onwards

$$a_{00}=\frac{6}{H^3}\left(\tfrac{1}{2}-\dot{\beta}\right)\frac{\partial H}{\partial\gamma}+\frac{6}{H^3}\dot{\varepsilon}\cos(\gamma-\beta) \tag{4.24}$$

$$a_{00}=\left[6\varepsilon\left(\tfrac{1}{2}-\frac{\omega}{\Omega}\right)\sin(\gamma-\beta)-6\frac{d\varepsilon}{d\Omega t}\cos(\gamma-\beta)\right]\left(\frac{c}{n}\right)^3$$

Order one

$$2(a_{01}+a_{11}\,\bar{Z})+2(2\,\bar{Z}\text{-}1)\,a_{11}=0 \Rightarrow a_{01}=a_{11}=0 \tag{4.25}$$

Second order

$$2(a_{02}+a_{12}\bar{Z}+a_{22}\,Z^2)+2(2\bar{Z}\text{-}1)(a_{12}+2\,a_{22}\,\bar{Z})$$
$$+2\,a_{22}\bar{Z}\,(\bar{Z}\text{-}1)+\bar{Z}\,(\bar{Z}\text{-}1)\frac{3}{H}\frac{\partial H}{\partial\gamma}\frac{\partial a_{00}}{\partial\gamma}+\bar{Z}\,(2\,\bar{Z}\text{-}1)\frac{\partial^2 a_{00}}{\partial\gamma^2}=0 \tag{4.26}$$

$-a_{02}=-a_{12}=a_{22}$

$$=\frac{1}{2}\left(\frac{1}{2}-\dot{\beta}\right)\frac{1}{H^5}\frac{\partial H}{\partial\gamma}[1-3\varepsilon^2+2\cos(\gamma-\beta)]+\frac{\dot{\varepsilon}}{2H^5}[\varepsilon-4\varepsilon\sin^2(\gamma-\beta)+$$
$$\cos(\gamma-\beta)[2\varepsilon^2\sin(\gamma-\beta)-2\varepsilon^2+1]$$

Ignore odd second indices $a_n=0$ n: odd

Order three

$$2(a_{03}+a_{13}\bar{Z}+a_{23}\bar{Z}^2+a_{33}\bar{Z}^3)+2(2\bar{Z}\text{-}1)(a_{13}+2\,a_{23}\bar{Z}+3\,a_{33}\,Z^2)+\bar{Z}(\bar{Z}\text{-}1)(6\,a_{23}+12\,a_{33}\bar{Z})$$
$$+\bar{Z}(\bar{Z}\text{-}1)\frac{3}{H}\frac{\partial H}{\partial\gamma}\left[\frac{\partial a_{01}}{\partial\gamma}+\frac{\partial a_{11}}{\partial\gamma}\bar{Z}\right]+\bar{Z}(\bar{Z}\text{-}1)\left[\frac{\partial^2 a_{01}}{\partial\gamma^2}+\frac{\partial^2 a_{11}}{\partial\gamma^2}\bar{Z}\right]=0$$

(4.27)

$a_{03}=a_{13}=a_{23}=a_{33}$

Equation (4.21) is written as

$$2a_{00}+2L\left[(a_{01}+a_{11}\overline{Z})-(2\overline{Z}-1)\,a_{11}\right]+\sum_{n=2}^{\infty}L^{n}\left[(n+1)(n+2)\,a_{nn}\overline{Z}^{n}+\sum_{k=0}^{n-1}(k+1)(k+2)\,[a_{kn}-a_{kn+1}]\overline{Z}^{k}\right.$$

$$\left.-\phi_{0n-2}\overline{Z}+\phi_{n-2n-2}\overline{Z}^{n}+\sum_{k=2}^{n-1}(\phi_{k-2n-2}-\phi_{k-1n-2})\right]=\frac{12}{H^{3}}\left(\frac{1}{2}-\dot{\beta}\right)\frac{\partial H}{\partial\gamma}+\frac{12}{H^{3}}\dot{\varepsilon}\cos(\gamma-\beta)$$

(4.28)

Where

$$\Phi_{kn}=\frac{3\varepsilon}{H}\frac{\partial H}{\partial\gamma}\frac{\partial a_{kn}}{\partial\gamma}+\frac{\partial^{2}a_{kn}}{\partial\gamma^{2}}$$

(4.29)

for n>2

$$\sum_{k=0}^{n-1}(k+1)(k+2)[a_{kn}-a_{kn+1}]\overline{Z}^{k}+(n+1)(n+2)a_{nn}Z^{n}=\overline{\Phi}_{0n-2}\overline{Z}+\sum_{k=2}^{n-1}(\overline{\Phi}_{k-1n-2}-\overline{\Phi}_{k-2n-2})Z^{n}-\Phi_{n-2n-2}Z^{n}$$

$$a_{nn}=\frac{1}{(n+1)(n+2)}\Phi_{n-2n-2}$$

$$\vdots$$

$$a_{kn}=a_{kn+1}+\frac{1}{(k+1)(k+2)}(\Phi_{k-1n-2}-\Phi_{k-2n-2})$$

$$\vdots$$

$$1<k<n$$

$$a_{1n}=a_{2n}+\frac{1}{6}\Phi_{0n-2}$$

$$a_{0n}=a_{1n}$$

$$A_{kn-2}=\left(\frac{c}{h}\right)^{3}\frac{\partial}{\partial\theta}\left(\frac{h}{c}\right)^{3}\frac{\partial a_{kn-2}}{\partial\theta}$$

$$a_{0n}=a_{1n}=a_{2n}+\frac{A_{0n-2}}{6}\qquad\qquad a_{nn}=\frac{A_{n-2n-2}}{(n+1)(n+2)}$$

$$2 \le k \le n \qquad a_{kn} = a_{kn+1} + \frac{A_{k-1n-2} - A_{k-2n-2}}{(k+1)(k+2)}$$

Fourth order

$$\phi_{02} = \phi_{12} = -\phi_{22} =$$

$$\phi_{02} = \phi_{12} = \phi_{22}$$
$$= \frac{-1}{2H^7}\left[\varepsilon\left(\frac{1}{2} - \dot{\beta}\right)\frac{\partial H}{\partial \gamma}\left[(-1+6\varepsilon^2-33\varepsilon^4)+(26\varepsilon^2-12\varepsilon^4)\sin^2(\gamma-\beta)+(-18\varepsilon+46\varepsilon^2)\cos((\gamma-\beta)\right]\right.$$
$$\dot{\varepsilon}\left[(-11\varepsilon+5\varepsilon^3)+(\sin^2(\gamma-\beta)(16\varepsilon^2-4\varepsilon^4\cos(\gamma-\beta))+\cos(\gamma-\beta)+\cos(\gamma-\beta)(30\varepsilon^2+8\varepsilon^4)\right.$$
$$\left.\left.+(26\varepsilon-56\varepsilon^3))(-1+11\varepsilon^2+4\varepsilon^4\right]\right]$$

(4.30)

$$a_{44} = -\frac{1}{30}\phi_{22}$$

$$a_{34} = a_{24} = \frac{1}{15}\phi_{22}$$

$$a_{14} = a_{04} = \frac{1}{10}\phi_{22}$$

Fifth order

$$a_{05} = a_{15} = a_{15} = a_{35} = a_{45} = a_{55} \qquad (4.31)$$

Neglect sixth order which introduce $\left(\frac{\ell}{R}\right)^6$ error.

$$P = P_a\left(1 - \overline{Z}/L\right) + P_b\,\overline{Z}/L + \overline{Z}(\overline{Z}-L)(a_{00} + a_{02}L^2 + a_{12}L\overline{Z} + +a_{22}\overline{Z}^2 + a_{04}L^4 + a_{14}L^3\overline{Z} + a_{24}L^2\overline{Z}^2 + a_{34}L\overline{Z}^3 + a_{44}\overline{Z}^4$$

(4.32)

Velocity calculation

$$\sigma_r = -p + 2\mu \frac{\partial V_r}{\partial r} \tag{4.33}$$

$$\sigma_z = -p + 2\mu \frac{\partial V_r}{\partial Z} \tag{4.34}$$

$$\sigma_\gamma = -\mathrm{p} + 2\mu \left[\frac{1}{\mathrm{r}} \frac{\partial V_\gamma}{\partial \gamma} + \frac{\partial V_r}{\partial r} \right]$$

$$\tau_{r\gamma} = \mu \left(\frac{1}{r} \frac{\partial V_r}{\partial \phi} + \frac{\partial V_\gamma}{\partial r} - \frac{V_\gamma}{r} \right) \tag{4.35}$$

$$\tau_{\phi z} = \mu \left[\frac{\partial V_\gamma}{\partial z} + \frac{1}{r} \frac{\partial V_z}{\partial \gamma} \right] \tag{4.36}$$

$$\tau_{zr} = \mu \left[\frac{\partial V_z}{\partial r} + \frac{\partial V_r}{\partial z} \right] \tag{4.37}$$

With short bearing approximation

$$\frac{\partial P}{\partial r} = 0 \quad \text{and} \quad \frac{1}{\mu r} \frac{\partial P}{\partial r} - \frac{\partial^2 V}{\partial r^2} = 0$$

$$\frac{1}{\mu} \frac{\partial P}{\partial z} - \frac{\partial^2 V_z}{\partial r^2} = 0 \tag{4.38}$$

Non dimensionalizing

$$r = R + cQ \qquad z = Rz \qquad \delta = c/R \qquad V_\gamma = \Omega R V_\gamma \qquad V_z = \Omega R V_z \quad V_r = C\Omega V_r$$

$$p = \mu \Omega \delta^{-2} P \qquad \bar{t} = \Omega t$$

Q, Z dimensionless radial and axial coordinates

$$\frac{\partial P}{\partial Q} = f\left(\delta^2\right) =$$

$$\frac{\partial^2 V_\gamma}{\partial Q^2} = \frac{\partial P}{\partial \gamma} = f(\delta) \tag{4.39}$$

$$\frac{\partial Vr}{\partial Q} + \frac{\partial V\gamma}{\partial \gamma} + \frac{\partial Vz}{\partial z} = f(\delta)$$

$$\frac{\partial (rV_r)}{\partial r} + \frac{\partial V_\gamma}{\partial \gamma} + \frac{\partial (rV_z)}{\partial z} = 0 \tag{4.40}$$

With boundary conditions

$$V_r = V_\gamma = V_z = 0 \quad \text{at Q} = 1 \qquad \text{Bearing wall.}$$

$$V_z = 0, \; V_\gamma = 1, \; V_r = \dot{\varepsilon}\cos(\gamma - \beta) + \varepsilon(\dot{\beta} - 1)\sin(\gamma - \beta)$$

$$\dot{\varepsilon} = \frac{d\varepsilon}{dt} \qquad \dot{\beta} = \frac{d\beta}{dt'} \text{ at Q} = \varepsilon\cos(\gamma - \beta) = \left(\frac{h}{c} - 1\right)$$

$$\frac{\partial P}{\partial Q} = f\left(\delta^2\right) = 0$$

P = const(Q)

Integrating to get

$$V_r = \frac{1}{2}\frac{\partial P}{\partial \gamma}Q^2 + B_1 Q + B_2 \tag{4.41}$$

$$V_z = \frac{1}{2}\frac{\partial P}{\partial z}Q^2 + B_3 Q + B_4 \tag{4.42}$$

$$V_r = -\frac{1}{6}\left(\frac{\partial^2 P}{\partial \gamma} + \frac{\partial^2 P}{\partial z}\right) Q^3 - \frac{1}{2}\left(\frac{\partial B_1}{\partial \gamma} + \frac{\partial B_3}{\partial z}\right) Q^2 - \left(\frac{\partial B_2}{\partial \gamma} + \frac{\partial B_4}{\partial z}\right) Q + B_5 \tag{4.43}$$

Using BC's.

$$B_2 = \frac{1}{2}\frac{\partial P}{\partial \gamma}(1 - H) + \frac{1}{H}$$

$$B_4 = \frac{1}{2}\frac{\partial P}{\partial z}(1-H)$$

$$B_1 = \frac{1}{2}\frac{\partial P}{\partial \gamma}(H-2) - \frac{1}{H}$$

$$B_3 = \frac{1}{2}\frac{\partial P}{\partial z}(H-2)$$

$$\mathrm{B}_5 = \frac{1}{6}\left[\frac{\partial^2 P}{\partial^2 \gamma} + \frac{\partial^2 P}{\partial^2 z}\right] + \frac{1}{2}\left[\frac{\partial B_1}{\partial \gamma} + \frac{\partial B_3}{\partial z}\right] + \left[\frac{\partial B_2}{\partial \phi} + \frac{\partial B_1}{\partial z}\right]$$

$$V_\phi = \frac{1-Q}{H} + \frac{1}{2}\frac{\partial P}{\partial \gamma}(1-Q)[1-H-Q]$$

$$V_z = \frac{1}{2}\frac{\partial P}{\partial z}(1-Q)[1-H-Q]$$

$$V_r = \frac{(1-Q)^2}{2H^2}\frac{\partial H}{\partial \gamma} + \frac{(1-Q)^2}{12}\left\{\left(\frac{\partial^2 P}{\partial^2 \gamma} + \frac{\partial^2 P}{\partial z^2}\right)(2-3H-2Q) - 3\frac{\partial P}{\partial \gamma}\frac{\partial H}{\partial \gamma}\right\} \quad (4.44)$$

B.C's

$$V_r = \dot{\varepsilon}\cos(\gamma-\beta) + \varepsilon(\dot{\beta}-1)\sin(\gamma-\beta)$$

For $Q = \varepsilon\cos(\gamma-\beta)$)

$$\frac{\partial^2 P}{\partial^2 \gamma} + \frac{\partial^2 P}{\partial^2 z} + \frac{3}{H}\frac{\partial H}{\partial \gamma}\frac{\partial P}{\partial \gamma} = \frac{12}{H^3}\frac{\partial H}{\partial \gamma}\left(\frac{1}{2} - \dot{\beta}\right) - \dot{\varepsilon}\cos(\gamma-\beta) \quad (4.45)$$

$$V_r = \left[1 - \frac{r/R-1}{\delta}\right]\left\{\frac{1}{2}\frac{\partial P}{\partial \gamma}\left[\varepsilon\cos(\gamma-\beta) - \frac{r/R-1}{\delta}\right] + \frac{1}{1-\varepsilon\cos(\gamma-\beta)}\right\} \quad (4.46)$$

$$V_z = \left[1 - \frac{r/R-1}{\delta}\right]\left\{\frac{1}{2}\frac{\partial P}{\partial \gamma}\left[\varepsilon\cos(\gamma-\beta) - \frac{r/R-1}{\delta}\right]\right\} \quad (4.47)$$

$$V_r = \left[1 - \frac{r/R - 1}{\delta}\right]^2 \left\{\left[\frac{1}{4H}\frac{\partial H}{\partial r}\frac{\partial P}{\partial \gamma} + \frac{1}{H^3}\left(\frac{1}{2} - \dot{\beta}\right)\frac{\partial H}{\partial \gamma} + \frac{1}{H^3}\dot{\varepsilon}\cos(\gamma - \beta)\right] \times \right.$$

$$\left. \left[3\varepsilon\cos(\gamma - \beta) - 1 + 2\frac{r/R - 1}{\delta}\right] - \frac{1}{4}\frac{\partial P}{\partial \gamma}\varepsilon\sin(\gamma - \beta) - \frac{\varepsilon\sin(\gamma - \beta)}{2[1 - \varepsilon\cos(\gamma - \beta)]^2}\right\}$$

$$V_r = (R_B - r)2\left[-\frac{\varepsilon c\sin\theta}{2h^2} + \left(\frac{1}{R^2}\frac{\partial^2 P}{\partial \theta^2} + \frac{\partial^2 P}{\partial z^2}\right)\frac{2R_B - 2r - 3h}{12\eta} - \frac{\varepsilon c\sin\theta}{4\eta R^2}\frac{\partial P}{\partial \theta}\right]$$

$$V_\gamma = (R_B - r)\left[\frac{\Omega R}{\eta} + \left(\frac{\varepsilon\cos\theta - r + R}{2R\eta}\right)\frac{\partial P}{\partial \theta}\right]$$

$$V_z = \frac{R_B - r}{2\eta}(c\varepsilon\cos\theta - r + R)\frac{\partial P}{\partial z}$$

Where $\theta = (\gamma - \beta)$

Transformation

$$V_\gamma = \frac{\upsilon_\gamma}{\Omega R} \qquad V_z = \frac{\upsilon_z}{\Omega R} \qquad V_r = \frac{\upsilon_r}{\Omega R}$$

$$P = \frac{p\delta^2}{\eta\Omega} \qquad \delta = \frac{c}{R}$$

$$\sigma_r = \frac{\eta\Omega}{\delta^2}\left[-P + 2\delta^3\frac{\partial V_r}{\partial r/R}\right]$$

$$\sigma_\gamma = \frac{\eta\Omega}{\delta^2}\left[-P + 2\frac{1}{r/R}\delta^2\frac{\partial V_r}{\partial \gamma} + 2\delta^3\frac{\partial V_r}{\partial r/R}\right]$$

$$\tau_{r\gamma} = \frac{\eta\Omega}{\delta^2}\left[\frac{1}{r/R}\delta^3\frac{\partial V_r}{\partial \gamma} + \delta^2\frac{\partial V_\gamma}{\partial r/R} - \delta^2\frac{V_\gamma}{r/R}\right]$$

To calculate σ_r, σ_γ, $\tau_{r\gamma}$ on the surface of the journal, Cylindrical coordinate with original in journal and not bearing center

$$\gamma = R\left\{\frac{c}{R}\varepsilon\cos(\gamma - \beta) + \sqrt{1 - \delta^2\varepsilon^2\sin^2(\gamma - \beta)}\right\} \qquad (4.48)$$

$$d_A = Rd_z d_\theta ; = Rd_z\,[1+\varepsilon\frac{c}{R}\cos\theta+...]d_\theta$$

near A1 point on the journal surface, the volume is restricted by $-dr$ segment and $rd\gamma$, $Rd\varphi$ arcs. Volume equilibrium conditions are

$$\sigma(A_1A_3)-\sigma_r(A_1A_2)\cos\zeta-\tau_{r\gamma}(A_2A_3)\cos\zeta-\sigma_\gamma(A_2A_3)\sin\zeta-\tau_{r\gamma}(A_2A_3)\sin\zeta=0$$

$$\tau(A_1A_3)-\tau_{r\gamma}(A_1A_2)\cos\zeta\ -\sigma_r(A_2A_3)\cos\zeta\ +\sigma_\gamma(A_1A2)\sin\zeta+\tau_{r\gamma}(A_2A_3)\sin\zeta=0$$

$$\sigma Rd\varphi+(-\sigma_r rdr+\tau_{r\gamma}dr)\sqrt{1-\frac{e^2}{R^2}\sin^2(\gamma-\beta)}+(\sigma_\gamma d\gamma-\tau_{r\gamma}rd\gamma)\frac{e}{R}\sin(\gamma-\beta)=0 \quad (4.49)$$

$$\tau Rd\varphi+(-\tau_{r\gamma}rd\gamma+\sigma_\gamma dr)\sqrt{1-\frac{e^2}{R^2}\sin^2(\gamma-\beta)}+(\sigma_r rd\gamma-\tau_{r\gamma}dr)\frac{e}{R}\sin(\gamma-\beta)=0 \quad (4.50)$$

$$\frac{dr}{d\gamma}=R\left[-\delta\varepsilon\sin(\gamma-\beta)-\frac{\delta^2\varepsilon^2\sin(\gamma-\beta)\cos(\gamma-\beta)}{\sqrt{1-\delta^2\varepsilon^2\sin^2(\gamma-\beta)}}\right]$$

$$=-r\frac{\delta\varepsilon\sin(\gamma-\beta)}{\sqrt{1-\delta^2\varepsilon^2\sin^2(\gamma-\beta)}}$$

Since $Rd\varphi\approx\sqrt{(rd\gamma)^2+(dr)^2}$

$$d\varphi\approx \mathrm{d}\gamma\left[1+\frac{\delta\varepsilon\cos(\gamma-\beta)}{\sqrt{1-\delta^2\varepsilon^2\sin^2(\gamma-\beta)}}\right] \quad (4.51)$$

Equations (4.49) and (4.50) can be expressed as;

$$\sigma=\sigma_r[1-\delta^2\varepsilon^2\sin^2(\gamma-\beta)]+2\delta\varepsilon\tau_{r\gamma}\sin(\gamma-\beta)\sqrt{1-\delta^2\varepsilon^2\sin^2(\gamma-\beta)}+\delta^2\varepsilon^2\sigma_\gamma\sin^2(\gamma-\beta) \quad (4.52)$$

$$\tau=\delta\varepsilon(\sigma_\gamma+\sigma_r)\sin(\gamma-\beta)\sqrt{1-\delta^2\varepsilon^2\sin^2(\gamma-\beta)}+\delta^2\varepsilon^2\tau_{r\gamma}\sin^2(\gamma-\beta) \quad (4.53)$$

Which transforms the stress tensor from the surface of a concentric cylinder (σ_r, $\tau_{r\gamma}$) to eccentric stresses.

Calculation of forces

Force model in rotating coordinates is given by

$$\begin{bmatrix} F_r \\ F_t \end{bmatrix} = \int_0^L dz \int_0^{2\pi} \begin{bmatrix} \sigma\cos\theta - \tau\sin\theta \\ \tau\cos\theta + \sigma\sin\theta \end{bmatrix} R d\theta, \qquad (4.54)$$

For a small segment on the shaft,

$$dF_r = R^2[\sigma\cos(\gamma-\beta) - \tau\sin(\gamma-\beta)]d\varphi dz \qquad (4.55)$$

$$dF_t = R^2[\tau\cos(\gamma-\beta) - \sigma\sin(\gamma-\beta)]d\varphi dz \qquad (4.56)$$

$$F_r = \int_0^L dz \int_0^{2\pi} R[\upsilon\cos(\gamma-\beta) - \tau\sin(\gamma-\beta)]\left[1 + \frac{\delta\varepsilon\cos(\gamma-\beta)}{\sqrt{1-\delta^2\varepsilon^2\sin(\gamma-\beta)}}\right]d\gamma$$

$$F_t = \int_0^L dz \int_0^{2\pi} R[\tau\cos(\gamma-\beta) - \tau\sin(\gamma-\beta)]\left[1 + \frac{\delta\varepsilon\cos(\gamma-\beta)}{\sqrt{1-\delta^2\varepsilon^2\sin(\gamma-\beta)}}\right]d\gamma$$

Using the equations of stress developed for the surface of the journal,

$$\sigma = \sigma_r[1-\delta^2\varepsilon^2\sin^2(\gamma-\beta)] + 2\delta\varepsilon\tau_{r\gamma}\sin(\gamma-\beta)\sqrt{1-\delta^2\varepsilon^2\sin^2(\gamma-\beta)} + \delta^2\varepsilon^2\sigma_\gamma\sin^2(\gamma-\beta)$$

$$\tau = \delta\varepsilon(\sigma_r+\sigma_\gamma)\sin(\gamma-\beta)\sqrt{1-\delta^2\varepsilon^2\sin(\gamma-\beta)} + \delta^2\varepsilon^2\tau_{r\gamma}\sin^2(\gamma-\beta)$$

$$\sigma = \sigma_r + 2\varepsilon\tau_{r\theta}\frac{c}{R}\sin\theta + \ldots\ldots \qquad \tau = \tau_{r\theta} + \varepsilon(\sigma_\theta - \sigma_r)\frac{c}{R}\sin\theta + \ldots\ldots \qquad (4.57a, b)$$

The radial and tangential components are given using 4.57

$$\sigma_r = \frac{\eta\Omega}{\delta^2}\left[\text{-P+2}\ \delta^3 \frac{\partial V_r}{\partial r/R}\right] \approx \text{-P+...}$$

$$\sigma_\gamma = \frac{\eta\Omega}{\delta^2}\left[-P + 2\frac{1}{r/R}\delta^2 \frac{\partial V_\gamma}{\partial \gamma} + 2\delta^3 \frac{\partial V_r}{\partial r/R}\right] \approx -P + \ldots \tag{4.58}$$

$$\tau_{r\gamma} = \frac{\eta\Omega}{\delta^2}\left[\frac{1}{r/R}\delta^3 \frac{\partial V_r}{\partial \gamma} + \delta^2 \frac{\partial V_\gamma}{\partial r/R} - \delta^2 \frac{V_\gamma}{r/R}\right] \approx \frac{\eta \partial V_\theta}{\partial r} + \ldots \tag{4.59}$$

$$V_\gamma = \frac{V_\gamma}{\Omega R} \qquad V_z = \frac{\upsilon_z}{\Omega R} \qquad P = \frac{P\delta^2}{\eta\Omega} \qquad \delta = \frac{c}{R} \qquad V_r = \frac{V_r}{\Omega c}$$

$$V_\gamma = \left(1 - \frac{r/R - 1}{\delta}\right)\left\{\frac{1}{2}\frac{\partial P}{\partial \gamma}\left[\varepsilon\cos(\gamma-\beta) - \frac{r/R - 1}{\delta}\right] + \frac{1}{\varepsilon\cos(\gamma-\beta)}\right\}$$

$$V_z = \left(1 - \frac{r/R - 1}{\delta}\right)\left\{\frac{1}{2}\frac{\partial P}{\partial z}\left[\varepsilon\cos(\gamma-\beta) - \frac{r/R - 1}{\delta}\right]\right\} \tag{4.60}$$

$$V_r = \left(1 - \frac{r/R - 1}{\delta}\right)^2 \left\{\left[\frac{1}{4H}\frac{\partial H}{\partial \gamma}\frac{\partial P}{\partial \gamma} + \frac{1}{H^3}\left(\frac{1}{2} - \dot{\beta}\right)\frac{\partial H}{\partial \gamma} + \frac{1}{H^3}\dot{\varepsilon}\cos(\gamma-\beta)\right]\times \right.$$
$$\left.\left[3\varepsilon\cos(\gamma-\beta)\text{-1+2}\frac{r/R - 1}{\delta}\right] - \frac{1}{4}\frac{\partial P}{\partial \gamma}\varepsilon\sin(\gamma-\beta) - \frac{\varepsilon\sin(\gamma-\beta)}{z[1-\varepsilon\cos(\gamma-\beta)]^2}\right\} \tag{4.61}$$

Back to the pressure equation to evaluate the series constants

$$P = P_a\left(1 - Z/L\right) + P_b\, Z/L + Z(Z\text{-1})(a_{00} + a_{02}L^2 + a_{12}LZ + a_{a22}Z^2 + a_{04}L^4 + a_{a14}L^3Z + a_{24}L^2Z^2 + a_{a34}LZ^3 + a_{a44}Z^4)$$

$$a_{00} = \frac{6\varepsilon(1/2 - \dot{\beta})\sin(\gamma-\beta)}{[1-\varepsilon\cos(\gamma-\beta)]^3} - \frac{6\dot{\varepsilon}\cos(\gamma-\beta)}{[1-\varepsilon\cos(\gamma-\beta)]^3} \tag{4.62}$$

$$-a_{02} = a_{12} = a_{22} = \frac{1}{2}\frac{\varepsilon(1/2-\beta)}{[1-\varepsilon\cos(\gamma-\beta)]^5} *$$

$$\left[\begin{array}{l}[(1-3\varepsilon^2)(\sin(\gamma-\beta)+2\varepsilon\sin(\gamma-\beta)\cos(\gamma-\beta)) \\ \quad +\frac{1}{2}\frac{\dot{\varepsilon}}{[1-\varepsilon\cos(\gamma-\beta)]^5}[\varepsilon-4\varepsilon\sin^2(\gamma-\beta)+2\varepsilon^2\cos(\gamma-\beta)\sin^2(\gamma-\beta) \\ \quad +(1-2\varepsilon^2)\cos(\gamma-\beta)]\end{array}\right] \tag{4.63}$$

$$a_{04} = a_{14} = \frac{1}{10}\Phi_{22} \tag{4.64}$$

$$a_{24} = a_{34} = \frac{1}{15}\Phi_{22} \tag{4.65}$$

$$a_{44} = \frac{1}{15}\Phi_{22} \tag{4.66}$$

$$-\Phi_{22} = \frac{-\frac{1}{2}\varepsilon(1/2-\dot{\beta})}{[1-\varepsilon\cos(\gamma-\beta)]^7} *$$

$$\left[\begin{array}{l}(-1+6\varepsilon^2-33\varepsilon^4)\sin(\gamma-\beta)+(26\varepsilon^2-12\varepsilon^4)\sin^3(\gamma-\beta) \\ \quad +(-18\varepsilon+46\varepsilon^2)\sin(\gamma-\beta)\cos(\gamma-\beta)\end{array}\right]$$

$$-1/2\frac{\dot{\varepsilon}}{[1-\varepsilon\cos(\gamma-\beta)]^7} *$$

$$\left[\begin{array}{l}[(-11\varepsilon-5\varepsilon^3) \\ \quad +(26\varepsilon-56\varepsilon^3)\sin^2(\gamma-\beta)+16\varepsilon^3\sin^4(\gamma-\beta)+(-1+21\varepsilon^2-4\varepsilon^4)\cos(\gamma-\beta) \\ \quad +(30\varepsilon^2+8\varepsilon^4)\sin^2(\gamma-\beta)\cos(\gamma-\beta)-4\varepsilon^4\sin^4(\gamma-\beta)\cos(\gamma-\beta)\end{array}\right] \tag{4.67}$$

Which in general can be written as

$$a_{kn} = \left(\frac{1}{2}-\frac{\omega}{\Omega}\right)f_1(\varepsilon,\cos\theta)\sin\theta + \frac{d\varepsilon}{d\Omega t}f_2(\varepsilon,\cos\theta) \tag{4.77}$$

$$P = p_a\left(1-\frac{z}{\ell}\right) + p_b\frac{z}{\ell} + p_{\sin} + p_{\cos} \tag{4.78}$$

Using the rotating Rotor-Bearing model

$$M\ddot{s} + D_s s + Ks = F_x + jF_y + m_u r_u \omega^2 e^{-j\omega t} \tag{4.79}$$

$$s = x + jy$$

$\overline{X}$ and $\overline{Y}$ stationary axes for bearing center ω perturbation frequency

Carrying out the integration of pressure using MATLAB,

$$F_r = 2\pi R\ell\delta\varepsilon P_0 + \ldots \tag{4.80}$$

$$F_t = \frac{\varepsilon\pi\eta\Omega}{\delta^2}\left\{\frac{(1/2-\dot{\beta})}{(1-\varepsilon^2)^{3/2}}\left[1-\frac{(\ell/R)^2}{40(1-\varepsilon^2)^3}\left(8+88\varepsilon^2+105\varepsilon^4+9\varepsilon^6\right)\right.\right.$$
$$\left.\left.-\frac{17(\ell/R)^4}{13440(1-\varepsilon^2)^5}\left(16+824\varepsilon^2-166\varepsilon^4-2311\varepsilon^6+1344\varepsilon^8+153\varepsilon^{10}\right)\right]-\delta^3\ell R\left[\frac{1}{1+\sqrt{1-\varepsilon^2}}\right]\right. \tag{4.81}$$

Which will be used to calculate the rotating fluid parameters

$$\lambda = \tfrac{1}{2} - \frac{\delta^3 R^2}{l^2}\left(1+\frac{1}{1+\sqrt{1-\varepsilon^2}}\right)\left(1-\varepsilon^2\right)^{3/2}\left[1-\frac{(\ell/R)^2}{40(1-\varepsilon^2)^3}\left(8+88\varepsilon^2+105\varepsilon^4+9\varepsilon^6\right)\right.$$
$$\left.-\frac{17(\ell/R)^4}{13440(1-\varepsilon^2)^5}\left(16+824\varepsilon^2-166\varepsilon^4-2311\varepsilon^6+1344\varepsilon^8+153\varepsilon^{10}\right)\right]^{-1} \tag{4.82}$$

It is worth mentioning that using zeroth approximation gives the standard "short bearing solution" developed in chapter 2 $P \square P_a\left(1-\frac{z}{\ell}\right)+P_b\frac{z}{\ell}+\eta\Omega c^{-2}z\left(z-\ell\right)a_{00}$

Transferring back to Cartesian coordinates,

$$F_x = -\pi\eta\frac{l^3R}{c^2}\dot{\varepsilon}\frac{1+2\varepsilon^2}{(1-\varepsilon^2)^{5/2}}\frac{x}{c\varepsilon} - \pi\eta\frac{l^3R}{c^2}\left(\frac{1}{2}\Omega-\dot{\beta}\right)\frac{\varepsilon}{(1-\varepsilon^2)^{3/2}}\frac{y}{c\varepsilon} \tag{4.83}$$

$$F_y = -\pi\eta\frac{l^3R}{c^2}\dot{\varepsilon}\frac{1+2\varepsilon^2}{(1-\varepsilon^2)^{5/2}}\frac{y}{c\varepsilon} - \pi\eta\frac{l^3R}{c^2}\left(\frac{1}{2}\Omega - \dot{\beta}\right)\frac{\varepsilon}{(1-\varepsilon^2)^{3/2}}\frac{x}{c\varepsilon} \qquad (4.84)$$

The forces will be used to derive the system stiffness and damping as well as fluid average velocity as follows

$$K_B = \pi\ell P_0 \qquad (4.85)$$

$$\lambda = \tfrac{1}{2} - 2cR\ell^{-2}(1-\varepsilon^2)\left(1+\sqrt{1-\varepsilon^2}\right) \qquad (4.86)$$

$$\mathrm{D} = D = \frac{\pi\ell^3 R\eta}{c^3}\left[\frac{1}{(1-\varepsilon^2)^{3/2}} - \frac{2c}{\varepsilon^2 R} + \frac{c(2-6\varepsilon^2+5\varepsilon^4)}{\varepsilon^2 R(1-\varepsilon^2)^{5/2}}\right] \qquad (4.87)$$

Where $P_0 = \dfrac{P_a + P_b}{2}$, To accommodate dynamic eccentricity the equation below is used

$$\varepsilon = \frac{\sqrt{x^2+y^2}}{c} \qquad (4.88)$$

The effective system artificial viscosity is re-calculated [16] using

$$\eta = \eta_0\left[1 - \frac{\left(\ell/R\right)^2}{40(1-\varepsilon^2)^3}\left(8+88\varepsilon^2+105\varepsilon^4+9\varepsilon^6\right) - \frac{17\left(\ell/R\right)^4}{13440(1-\varepsilon^2)^5}\left(16+824\varepsilon^2-166\varepsilon^4-2311\varepsilon^6+1344\varepsilon^8+153\varepsilon^{10}\right)+\ldots.\right] \qquad (4.89)$$

The above equations are used to simulate the system incorporating the effects of fluid inertia and dynamic eccentricity. The artificial viscosity is still constant as the correction introduced in terms of dynamic eccentricity produce very small correction factor on the constant viscosity.

CHAPTER 5

SIMULATION AND DISCUSSION

The simulation results show that the basic model with Timoshenko beam theory formulation which includes gyroscopic effects, disk, structural damping and static eccentricity short bearing module do match a couple of the references of this thesis. In particular rotor parameters shown in *Figure 5.1* below adopted from [13]. Following below also the flow chart of the program to simulate the rotor, disk and bearing system using various bearing parameters simulation schemes.

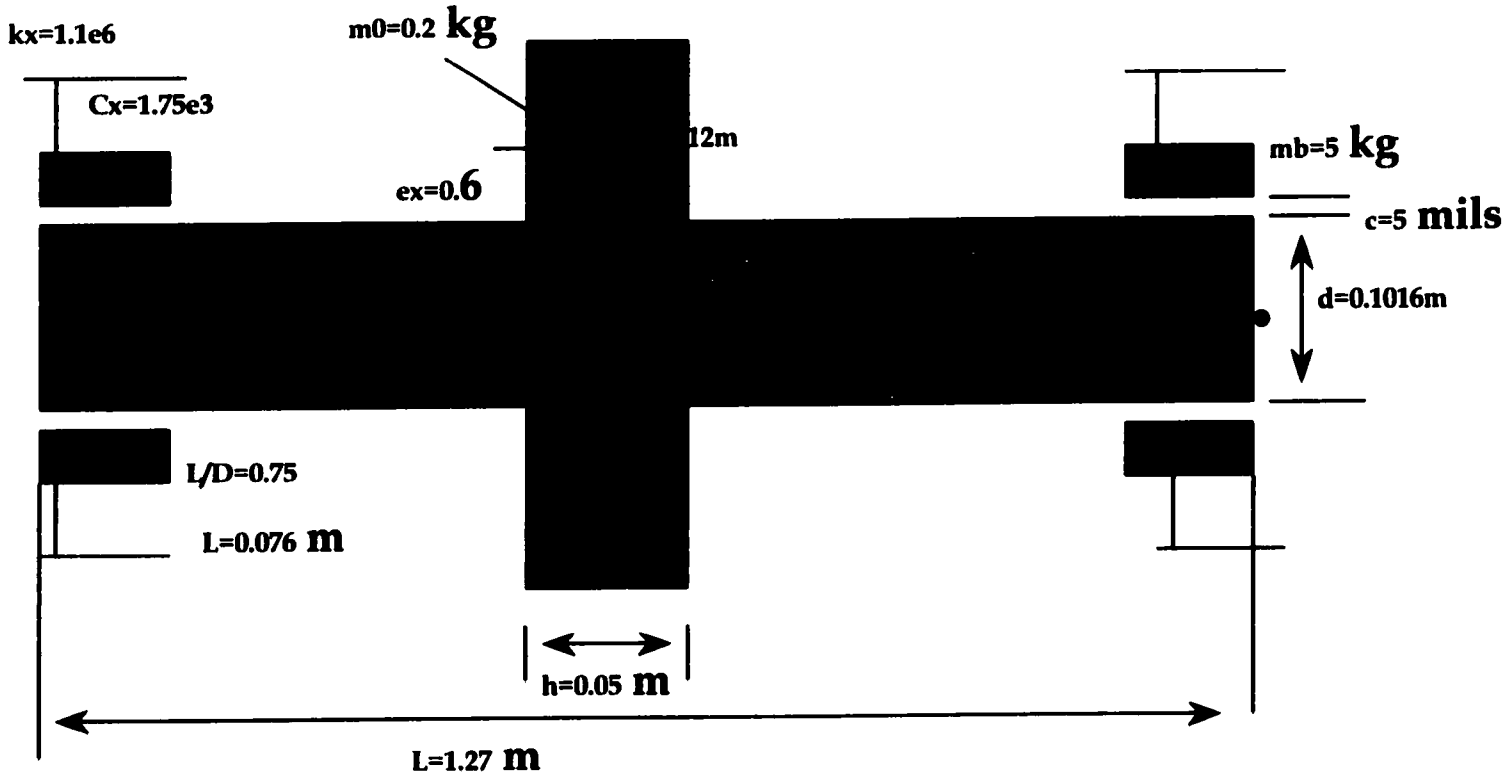

Material : Alloy Steels

E=2.068 e11	ρ=7850 Kg/M3	Cx=2.1e7=Cy
G=0.84 e11	Cv=2.25 e8 Ns/M	kx=.79 e11 = Ky
V= 0.27	η = 0.3 Ns/m2	Mb=15 kg
ηh=0.1e3		

Figure 5.1a - Rotor System under study

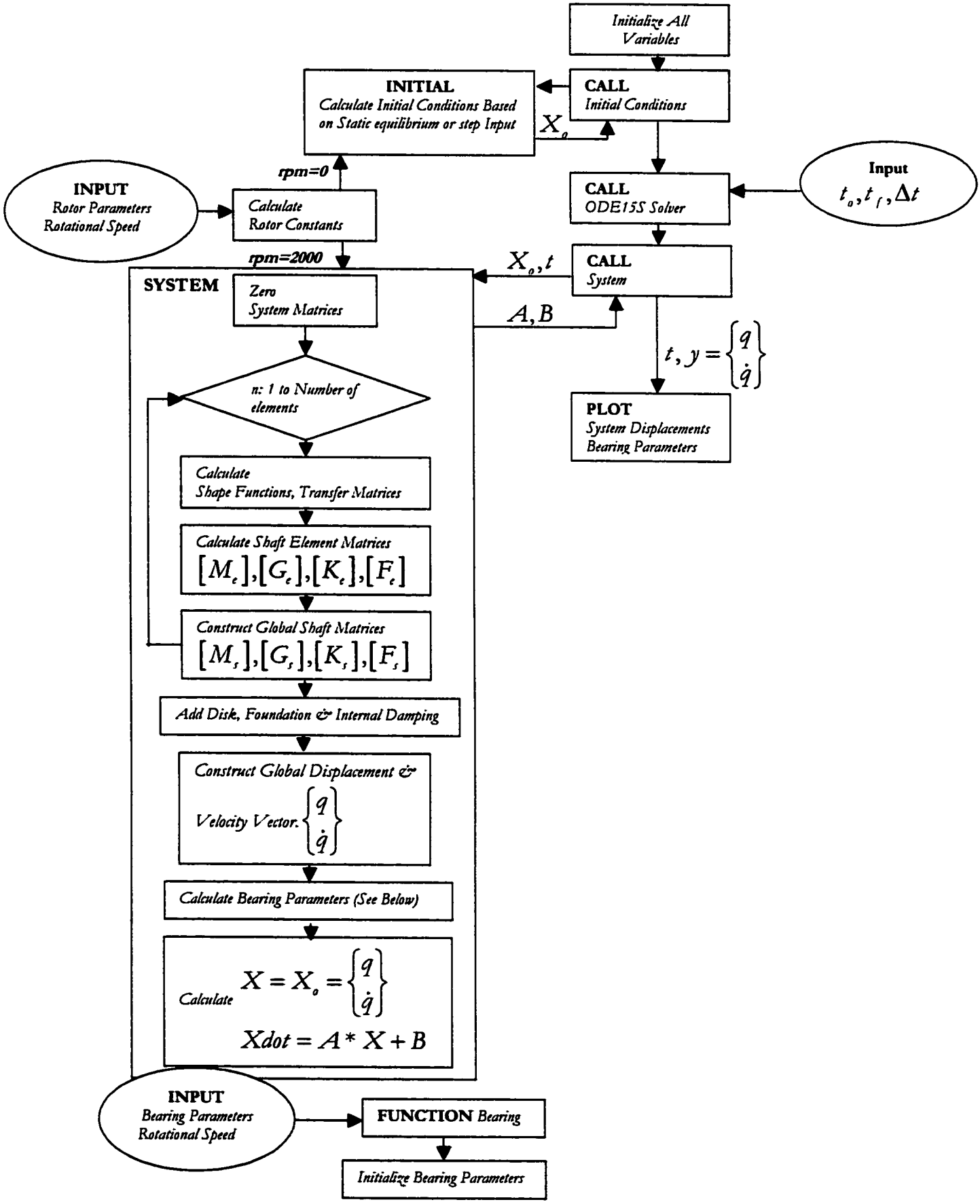
Initialize All Variables
CALL Initial Conditions
INITIAL Calculate Initial Conditions Based on Static equilibrium or step Input
X_o
rpm=0
INPUT Rotor Parameters Rotational Speed
Calculate Rotor Constants
rpm=2000
CALL ODE15S Solver
Input $t_o, t_f, \Delta t$
X_o, t
CALL System
A, B
SYSTEM
Zero System Matrices
$t, y = \begin{Bmatrix} q \\ \dot{q} \end{Bmatrix}$
PLOT System Displacements Bearing Parameters
n: 1 to Number of elements
Calculate Shape Functions, Transfer Matrices
Calculate Shaft Element Matrices
$[M_e],[G_e],[K_e],[F_e]$
Construct Global Shaft Matrices
$[M_s],[G_s],[K_s],[F_s]$
Add Disk, Foundation & Internal Damping
Construct Global Displacement & Velocity Vector. $\begin{Bmatrix} q \\ \dot{q} \end{Bmatrix}$
Calculate Bearing Parameters (See Below)
Calculate $X = X_o = \begin{Bmatrix} q \\ \dot{q} \end{Bmatrix}$
$Xdot = A * X + B$
INPUT Bearing Parameters Rotational Speed
FUNCTION Bearing
Initialize Bearing Parameters

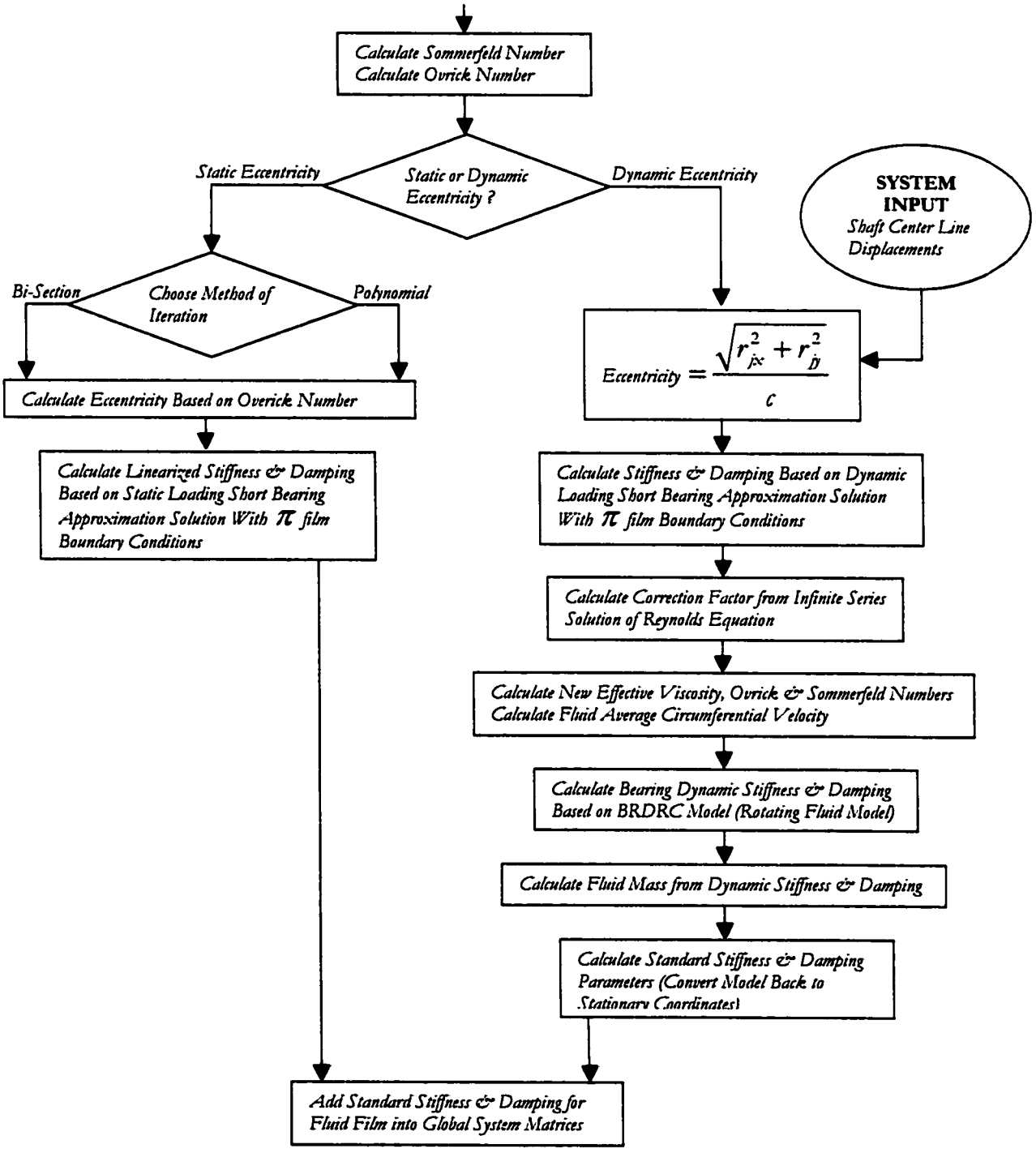

Figure 5.1 b – MATLAB Program Flow Chart

5.1 STNADARD ROTOR AND BEARING SYSTEM COMPARISON

To prove that the basic system developed is accurate, a run was made which included all effects of translational, rotational inertia as well as internal damping, disk and short bearing Reynolds solution. The model as developed from Abduljabar, et al [7] and Hashish [12] did not include foundation elasticity as well as the corrected matrices due to re-integration of the shape functions. The results are given in *figure 5.2* below in terms of nodal displacements which when compared to reference results, they did agree. It worth noting that the system has different response characteristics in the X and Y planes and that the bearing nodes displacements decay for Y at 0.035 seconds and for X at 0.04 seconds. There is a more evident phase lag for the disk in X plane compared with the Y plane. Next the system was simulated using initial conditions of $X_0 = \left[K^{-1}\right]Q$ and including the foundation elasticity. Corrections were implemented on the matrices to match the shape function integrals obtained by Symbolic MATLAB. The system response is shown in *Figures 5.3 and Figure 5.4*. The reader would notice that in the system without foundation and initial static balance conditions, the decay time for bearing displacements were 0.035 and 0.04 seconds in the X and Y directions, and that different system response when considering X or Y at the disk and bearings are exhibited. In the new system with foundation effects, the decay time was found to be 0.003 sec, the X and Y were both in phase. While the disk, nodes 2 and 4 exhibited clearer effects of disk unbalance in their responses.

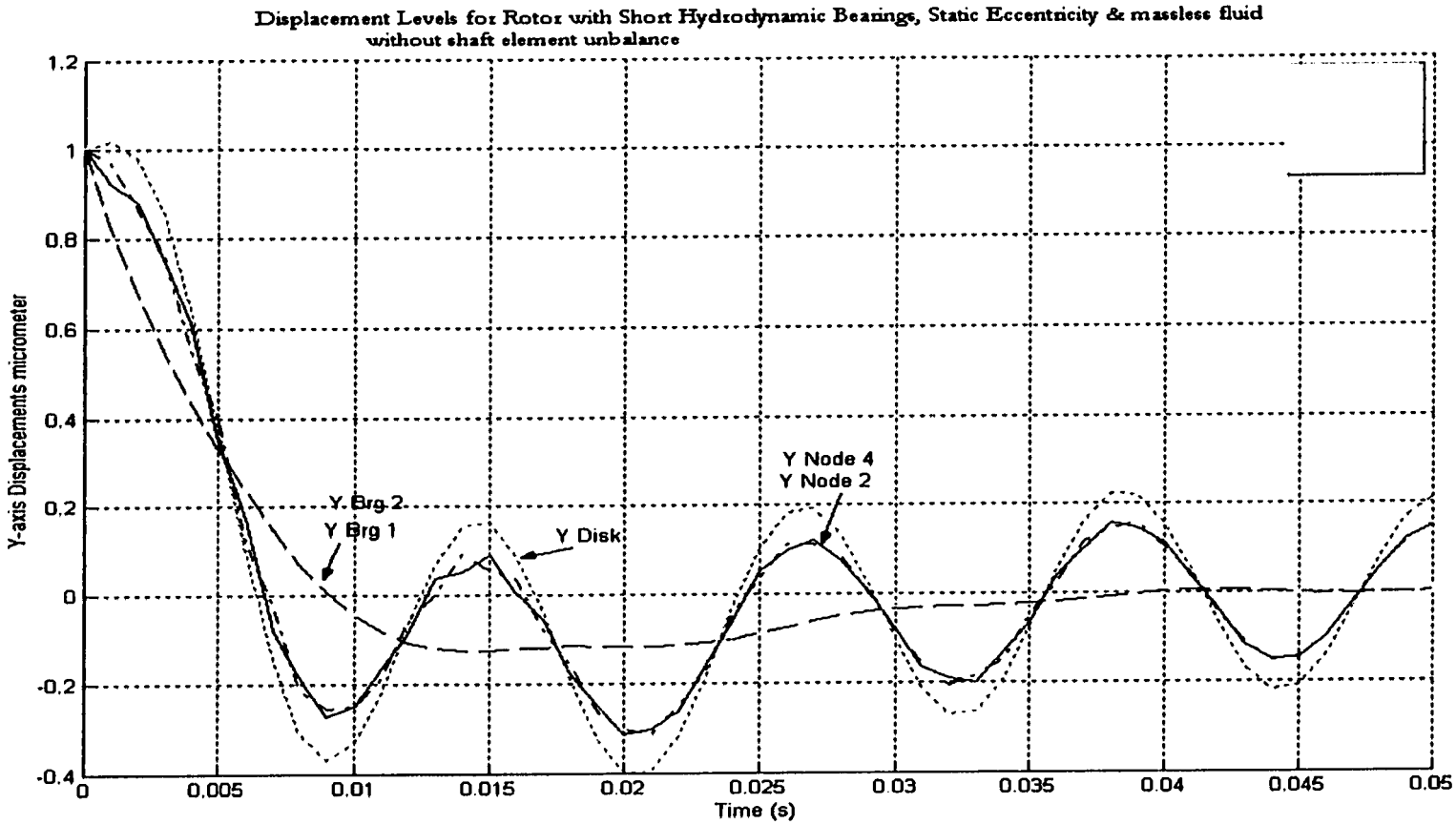

Figure 5.2a – Standard System Y Displacements response

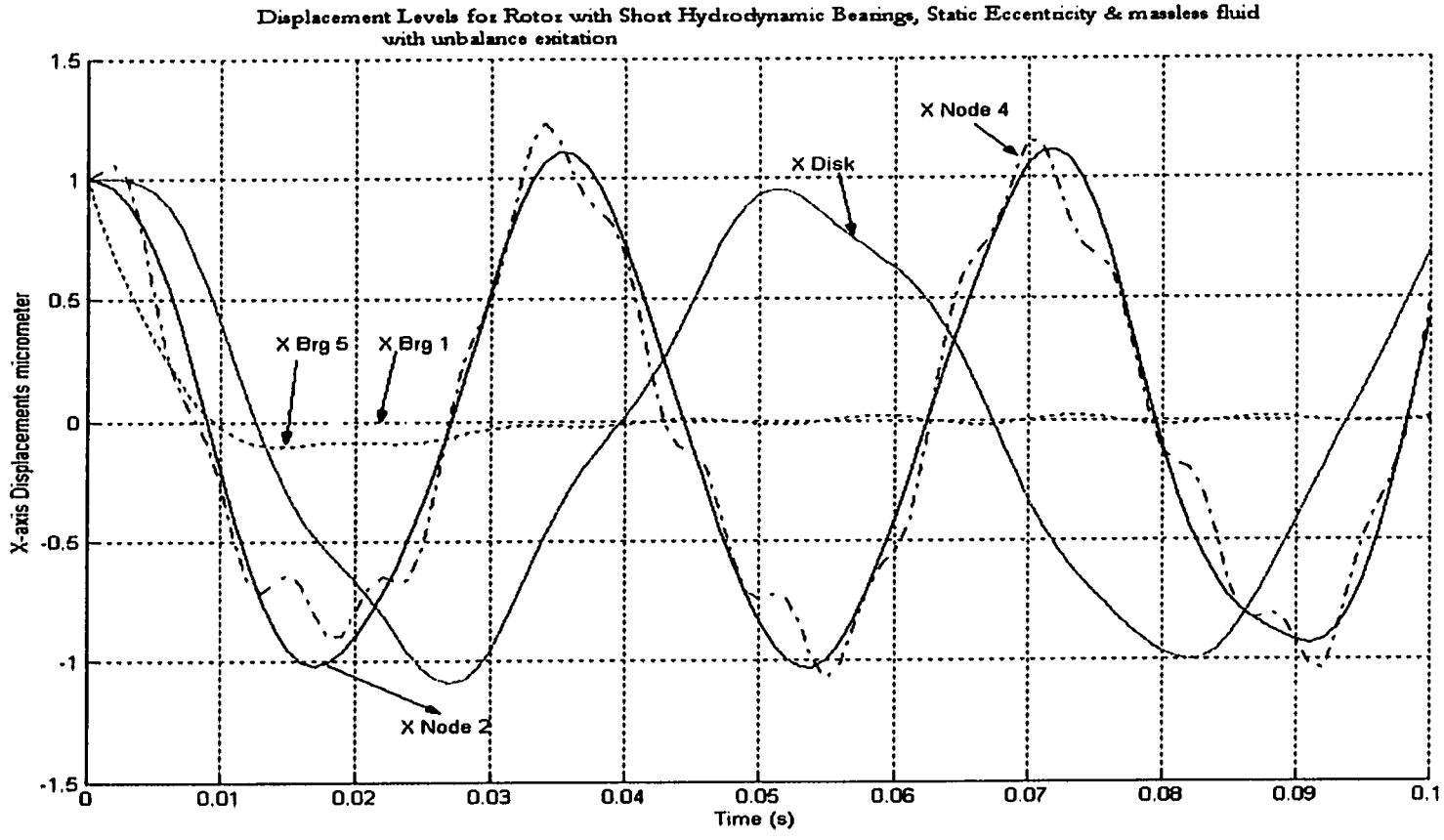

Figure 5.2b – Standard System X Displacements response

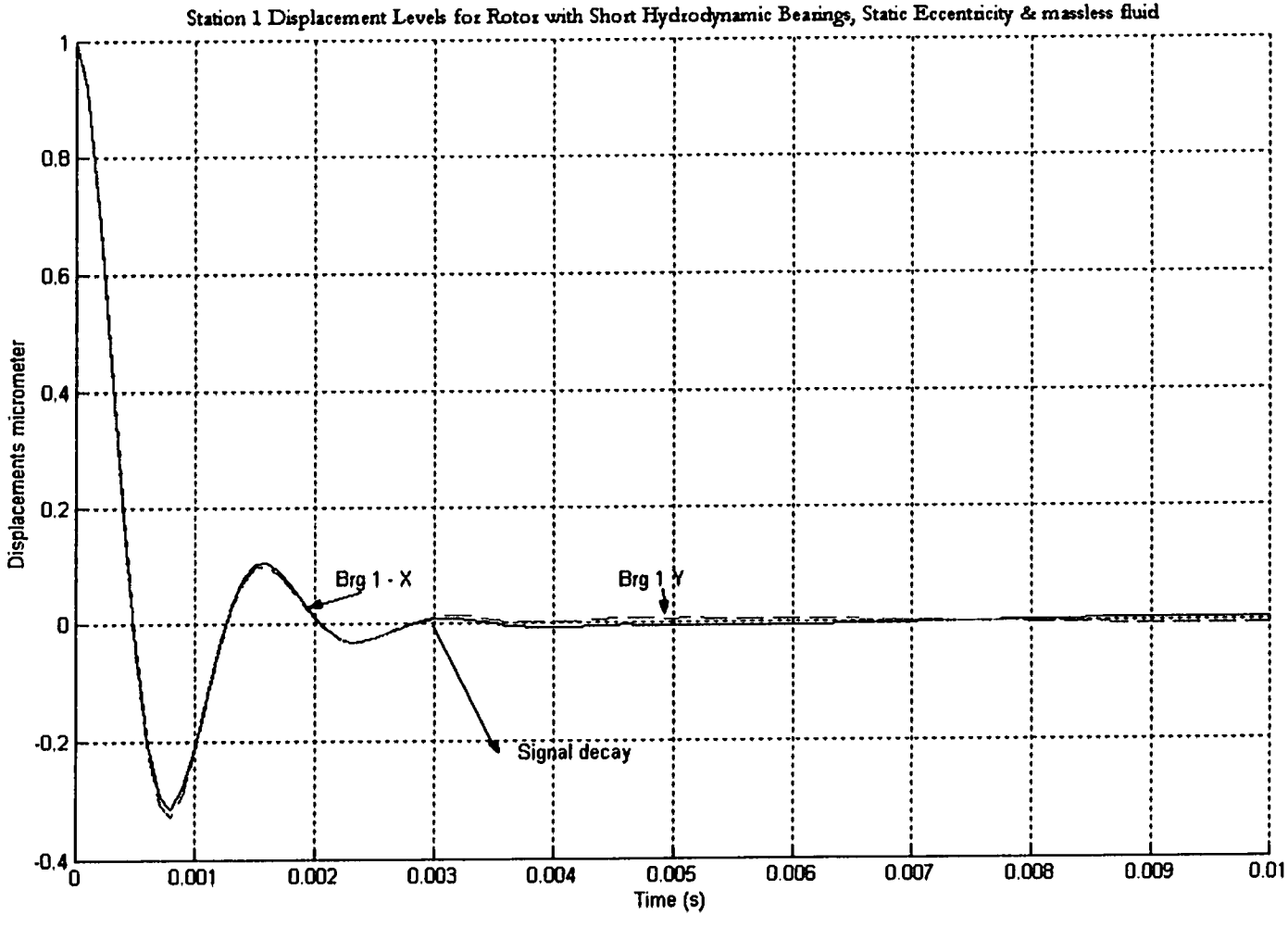

Figure 5.3 – New System with Foundation effects and initial condition – Bearing 1 X and Y

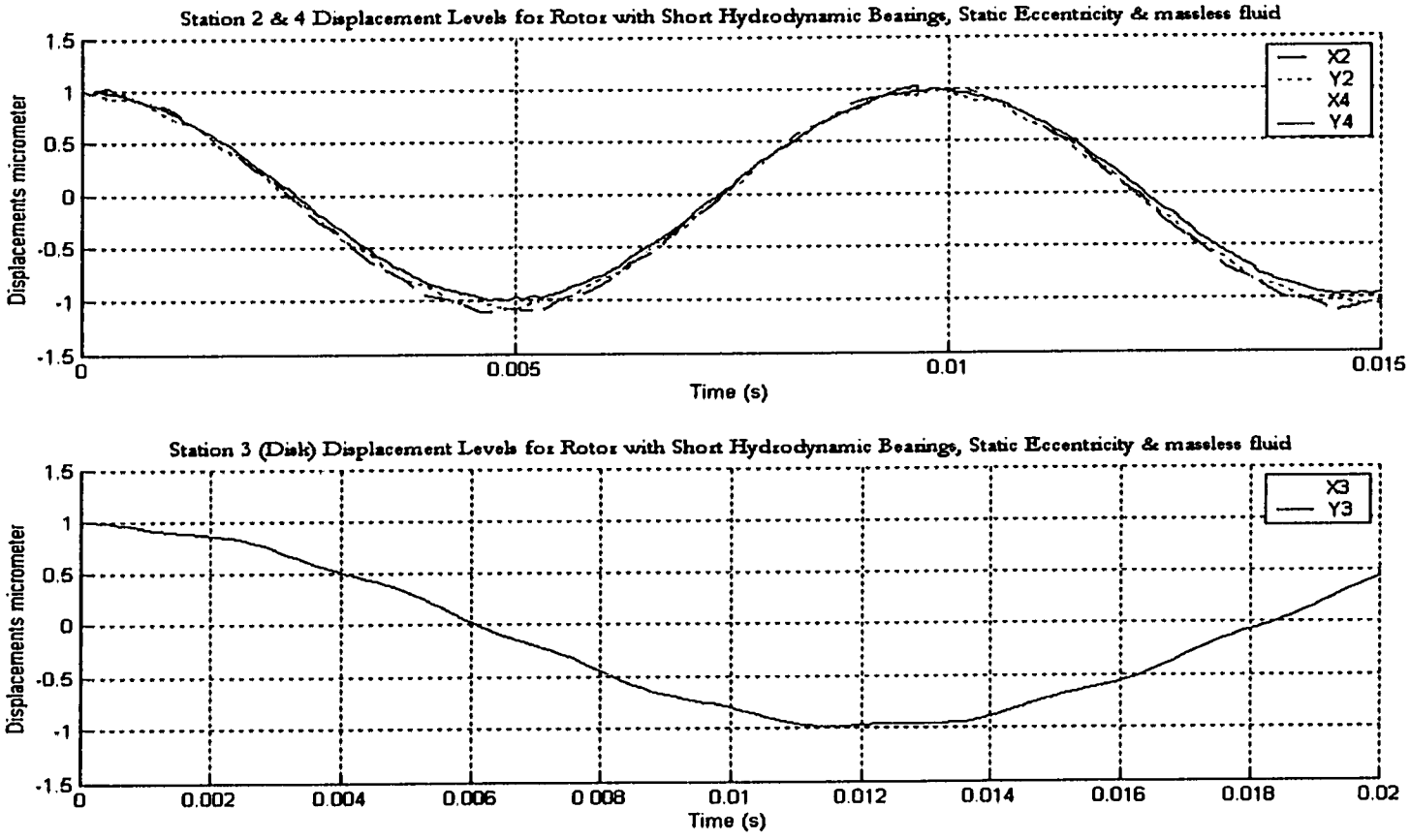

Figure 5.4 – New System with Foundation effects and initial condition – Disk and nodes 2 and 4 X and Y

The bearing (short bearing approximation) characteristics plot is included in *Figure 5.5* which is used for comparison with the cases when dynamic eccentricity is used and fluid inertia is included.

5.2 BEARING DIRECT AND CROSS COUPLED STIFFNESS AND DAMPING COMPARISONS

In this part simulation run was conducted for the bearing separately for speeds 0 – 20,000 rpm to get the bearing characteristics. The comparison is made between Eccentricity value obtained using Bisection method, Polynomial solution method (Chapter 2) and Dynamic Eccentricity simulated from a hypothetical complex signal given below. You would notice comparing the bi-section to polynomial zero that there are distinct differences, hence the accuracy of eccentricity value is controlled by which method you use to solve the Sommerfeld/Eccentricity equation. However what is more evident is that using a hypothetical system response, the eccentricity value taken dynamically gave a more realistic picture expecting the shaft centerline to position itself with increasing speed.

Figure 5.8 was produced to verify that the bearing response do match classical text book bearing response which is shown above using the bi-section iteration method. The bearing simulation exercise was conducted then for the following cases

- BRDRC Fluid model without fluid inertia using Static eccentricity Bi-section method
- Standard Reynolds solution for short bearings incorporating Dynamic Eccentricity
- BRDRC Fluid Model with fluid inertia and Static Eccentricity Solution
- BRDRC Fluid Model with fluid inertia and Dynamic Eccentricity.

The results are shown in *Figures 5.9 – 5.12* respectively. From *Figure 5.9* reader can observe (considering the values in the Direct and Quadrature) parameters that the BRDRC model do match standard Reynolds solutions yet there was no comparison made as to which one is more accurate when considering real machinery data.

Looking at *Figure 5.10* one can observe that there is a considerable effect especially at low eccentricity where the shaft position do affect the small values of stiffness and damping expected at the center of the sleeve. Comparing the BRDRC model, which includes fluid inertia in case with static eccentricity and with dynamic eccentricity the reader will notice the same effect of dynamic eccentricity present at positions in the middle of the sleeve

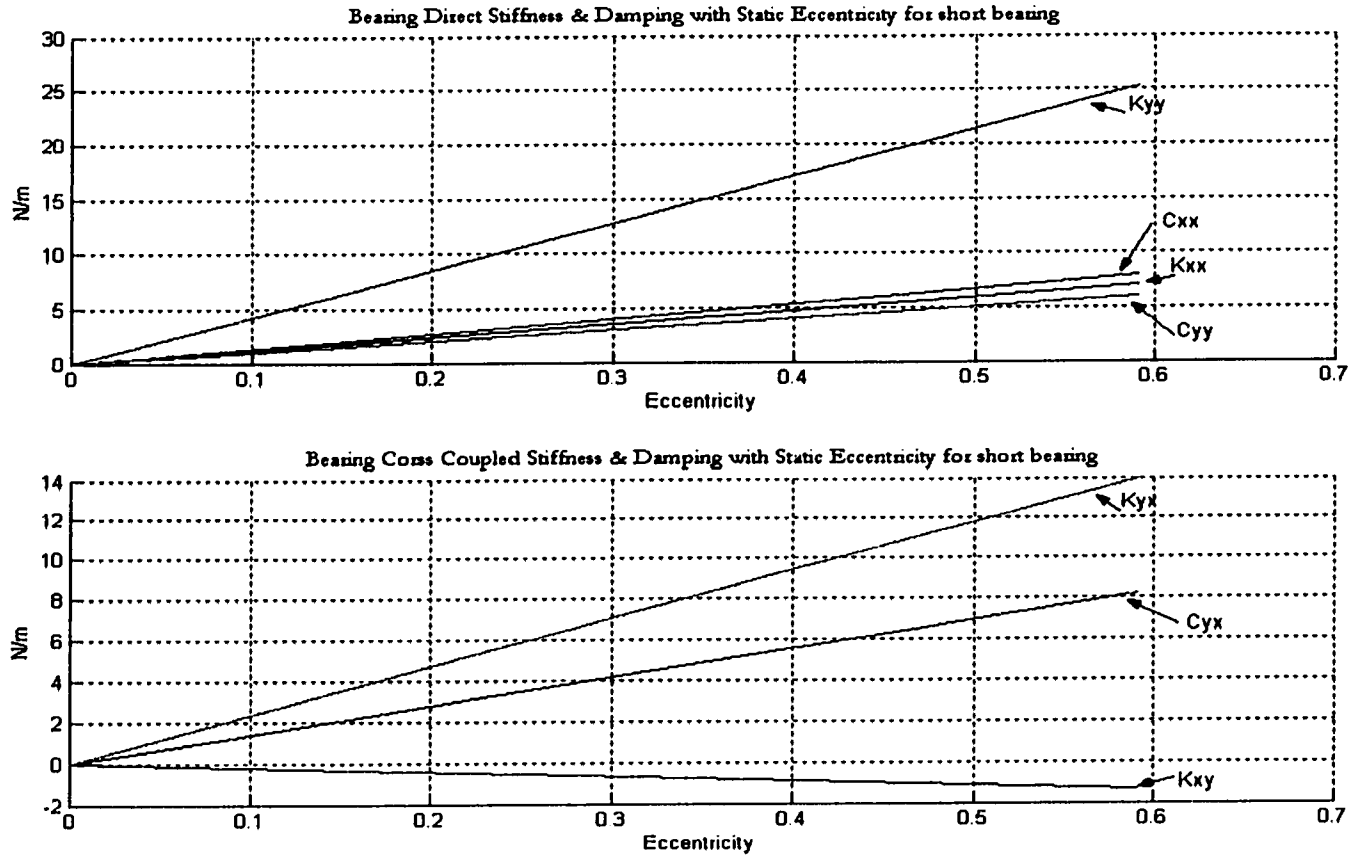

Figure 5.5 –System with Foundation Short Bearing using Reynolds Solution Parameters (2000 rpm)

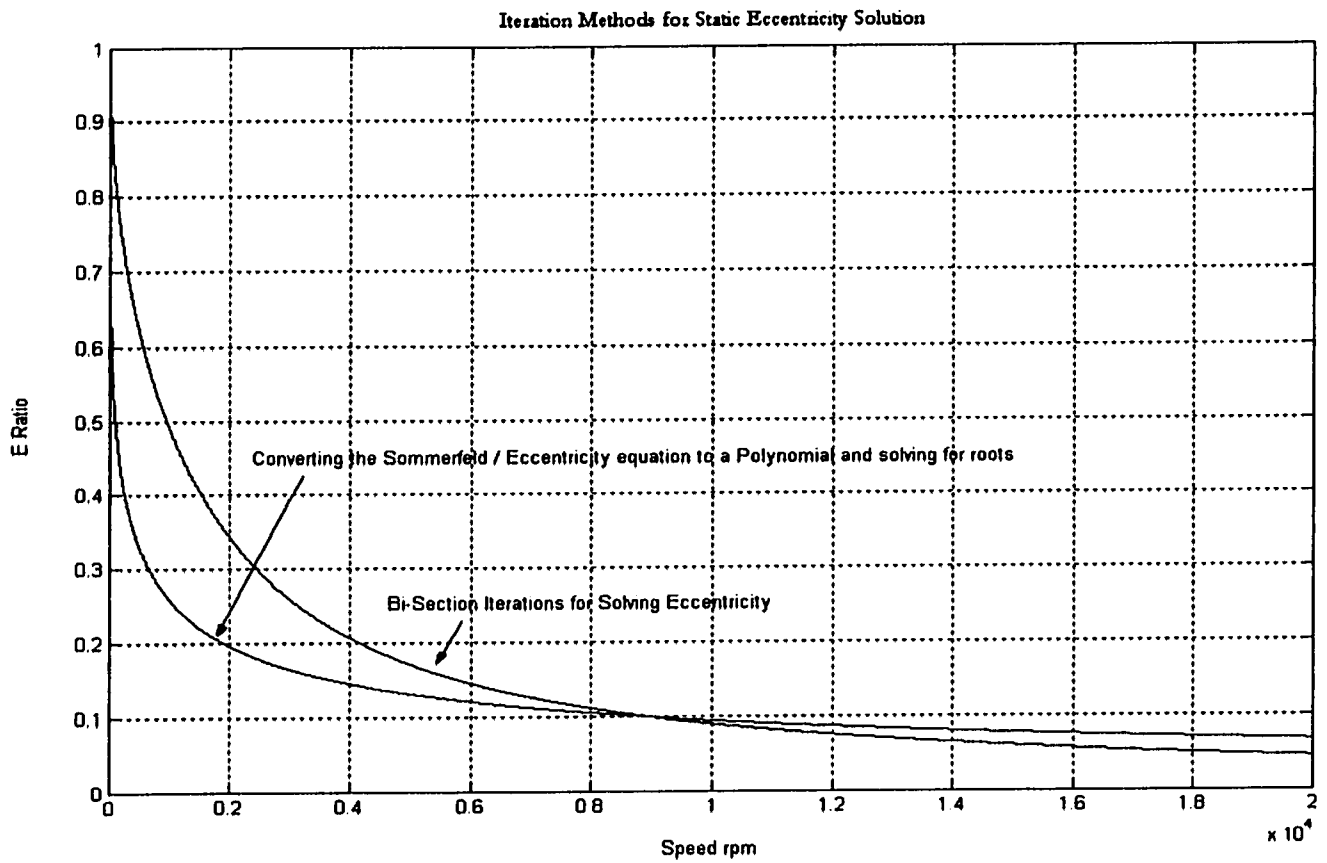

Figure 5.6 – Eccentricity versus speed obtained from static solution using Bi-section and Polynomial zeros

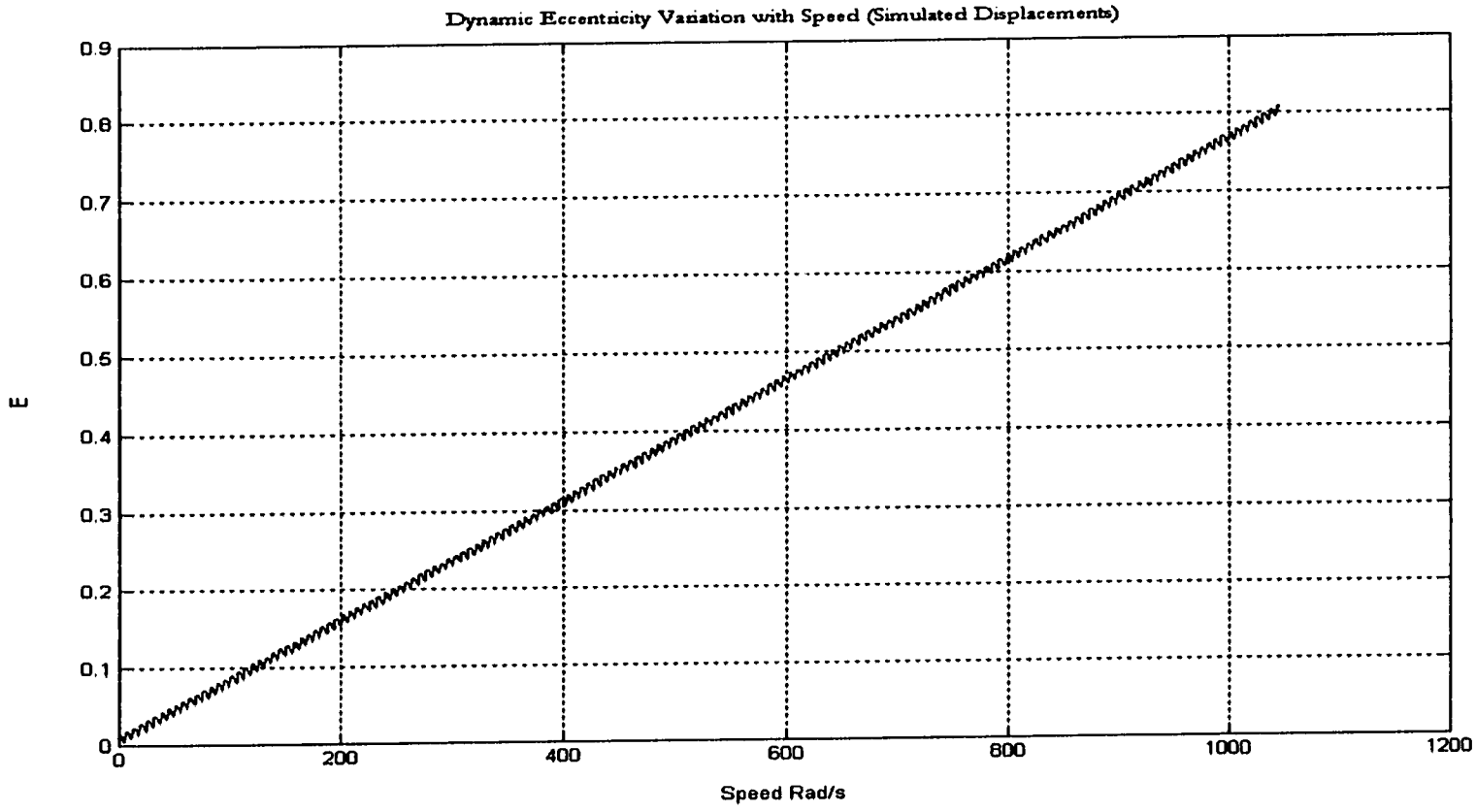

Figure 5.7 – Eccentricity versus speed from a hypothetical shaft displacement simulation

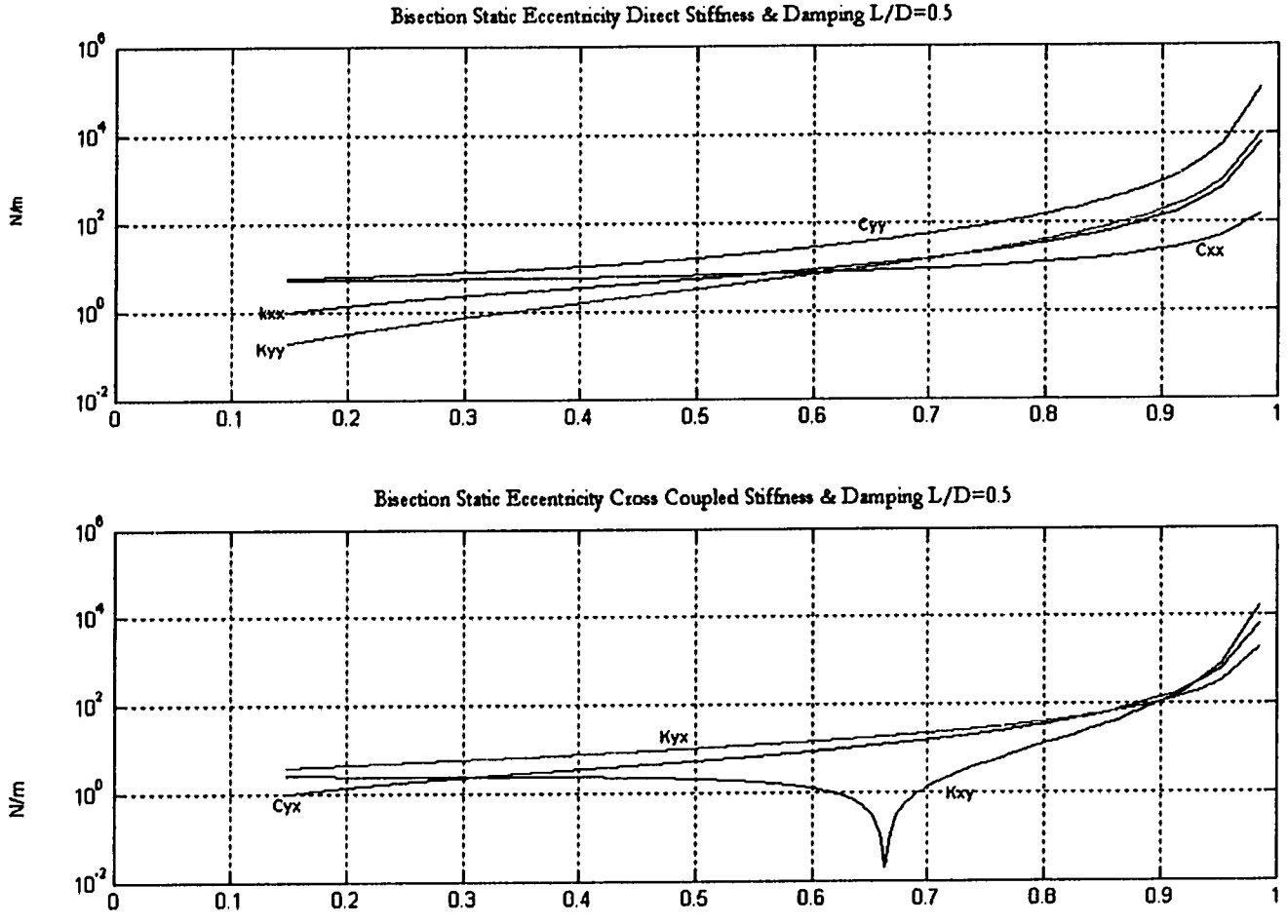

Figure 5.8 – Direct and cross coupled stiffness and damping using short bearing approximation solution

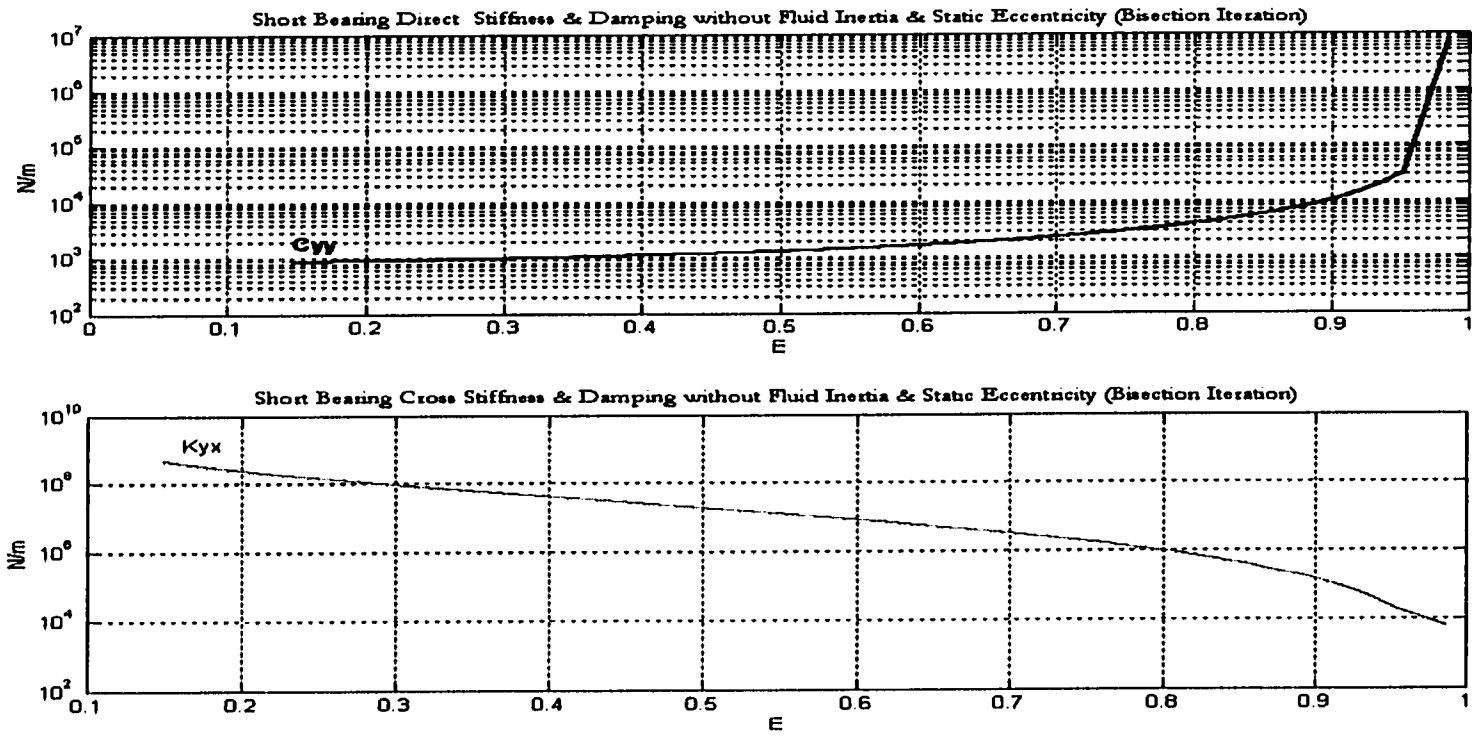

Figure 5.9 – Direct and Quadrature fluid parameters using rotating fluid model with no fluid inertia or dynamic eccentricity.

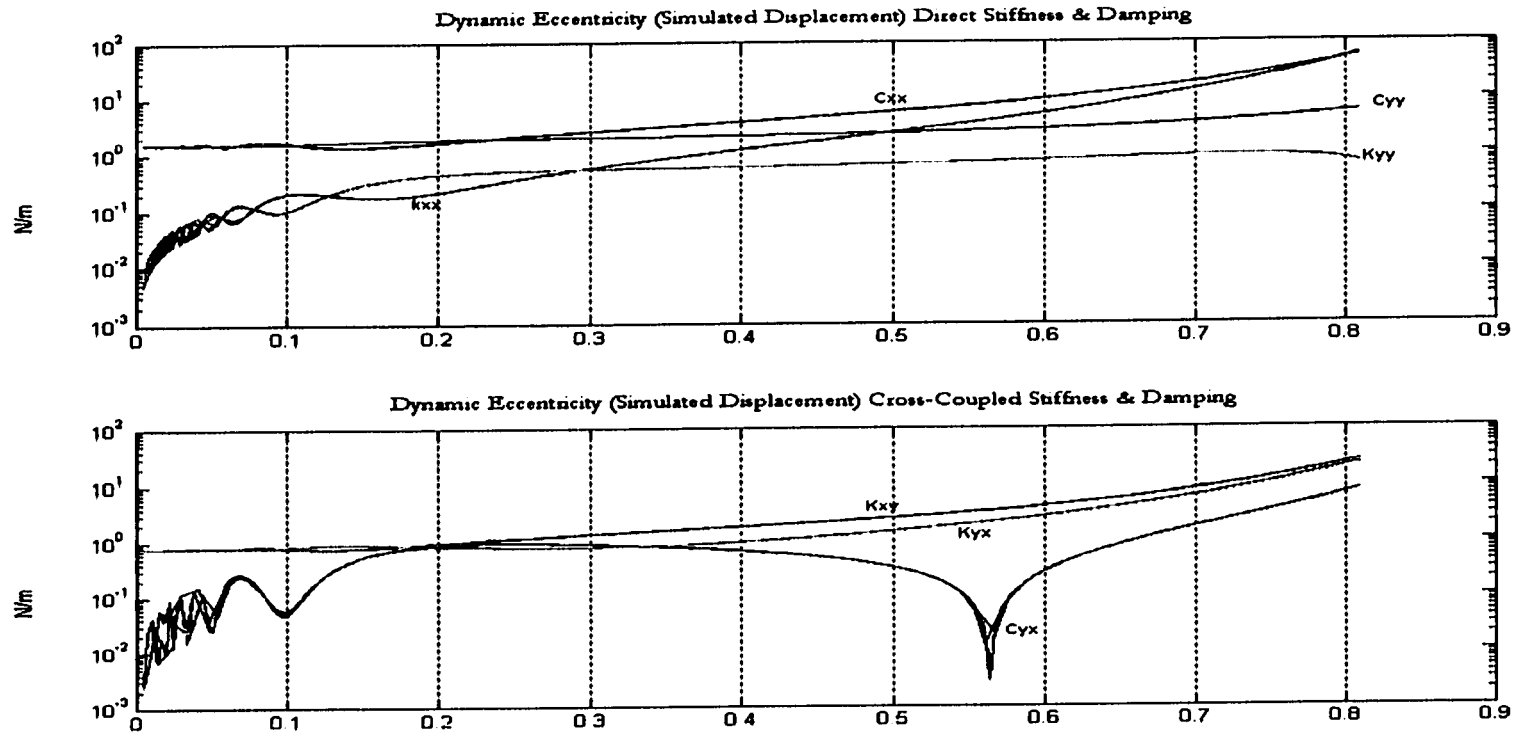

Figure 5.10 – Standard Reynolds Model with simulated dynamic eccentricity.

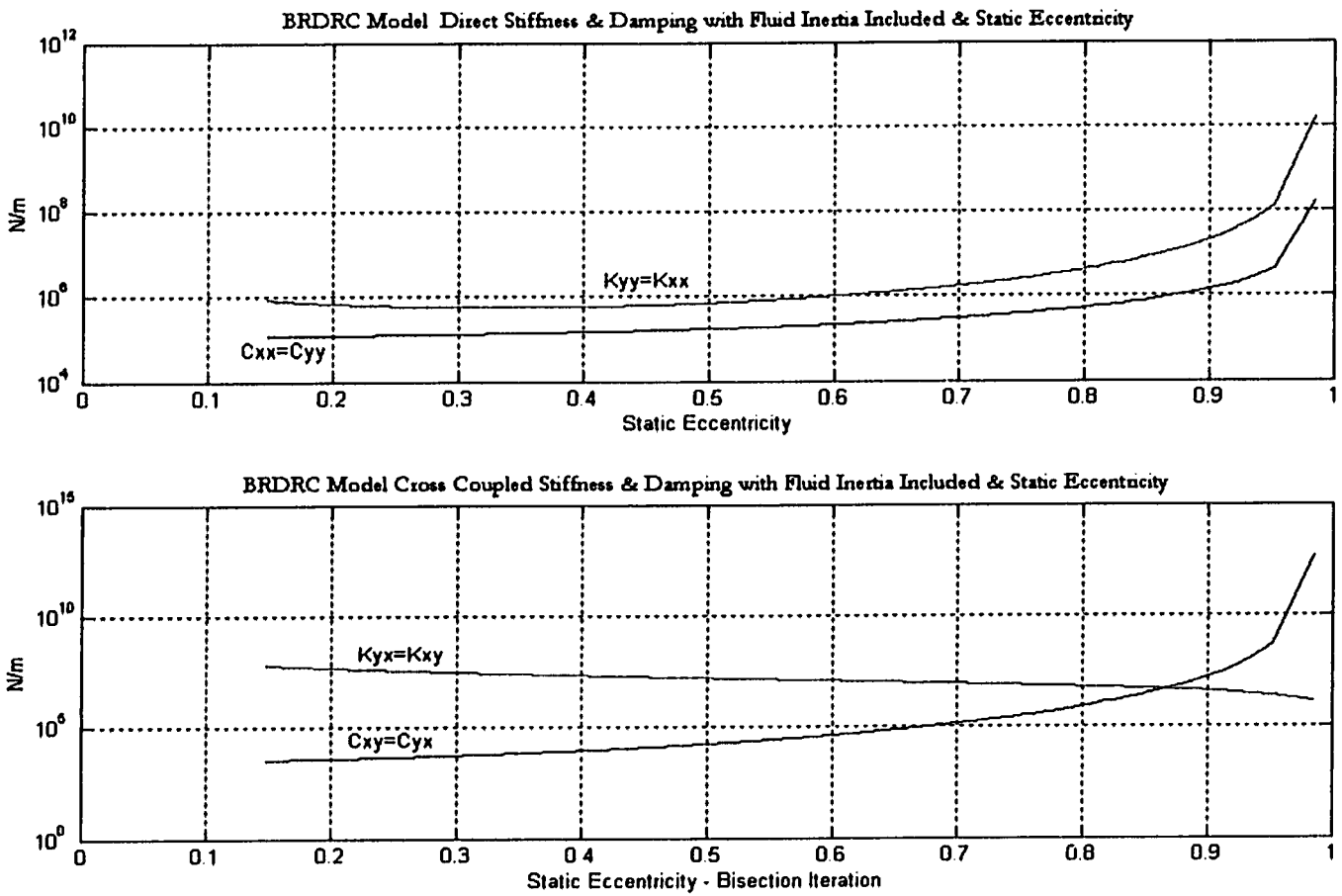

Figure 5.11 – Rotating Fluid model with Fluid Inertia and Static Eccentricity

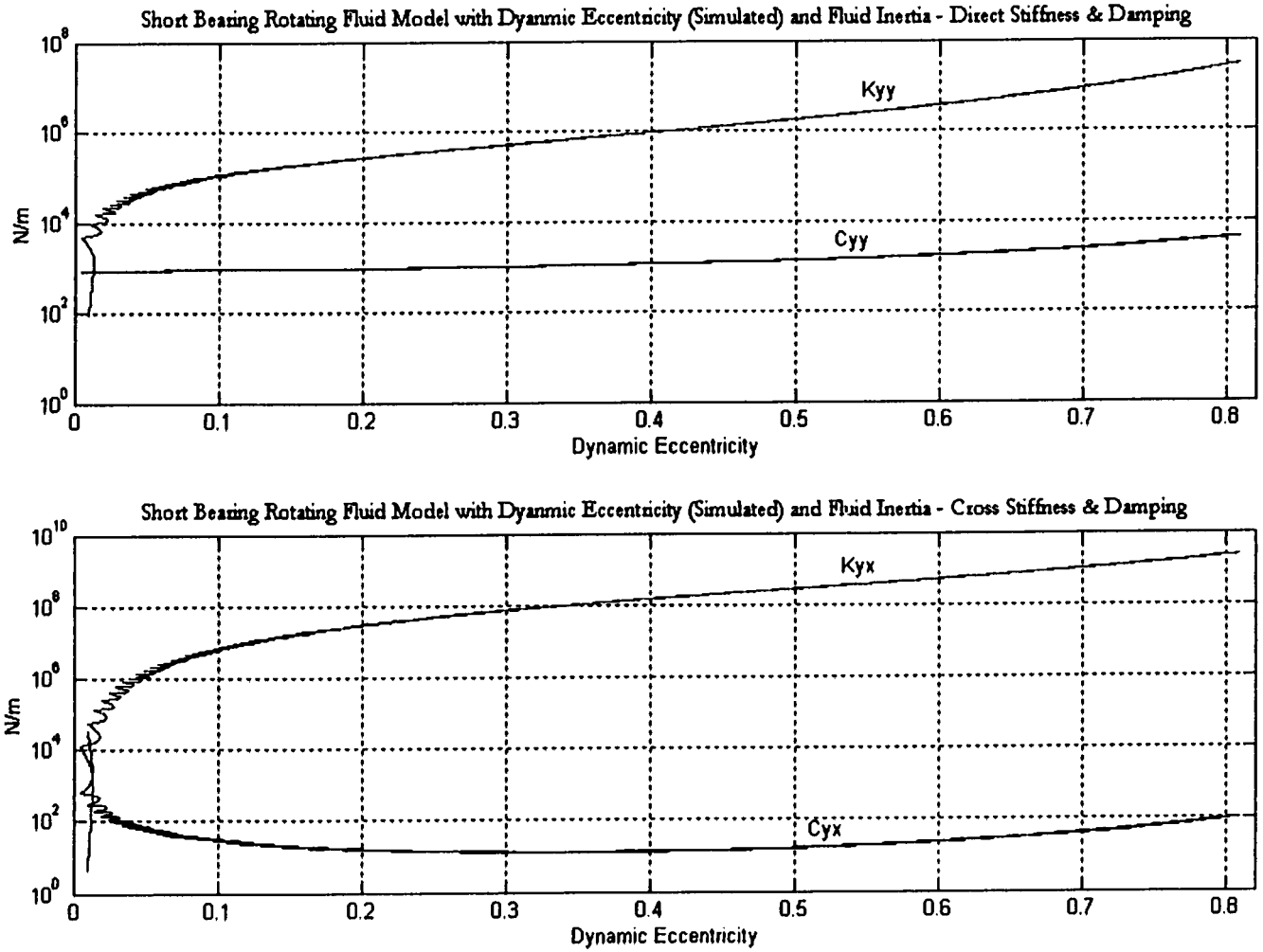

Figure 5.12 – Rotating Fluid Model with Fluid Inertia and Simulated Dynamic Eccentricity

5.3 SYSTEM SIMULATION WITH DYNAMIC ECCENTRICITY AND FLUID INERTIA

In section 5.3 the bearing behavior under dynamic eccentricity and fluid inertia using a simulated system response were compared. In this section the system response with dynamic eccentricity as a feedback is compared to the system and with fluid inertia using the BRDRC bearing model. The use of dynamic eccentricity when comparing figure 6 and figure 9, gives us an idea that bearing stiffness and damping parameters will actually vary to the variation of shaft position within the bearing.

Also comparison of system response to unbalance with time span 0 to 1 seconds shows that the bearing station X and Y displacements will have 0.003 sec decay time in the case of static eccentricity while it will have 0.45 seconds in the case of using shaft dynamic position or dynamic eccentricity. As for fluid inertia the simulation results do prove that the cases specified in the thesis are of significant effect, namely surface irregularities, solid particles or air bubbles in the fluid circumferential flow path. The case that was tried is lowering effective viscosity such that the rotor is driven into an oil whirl instability which shows in figures 14 and 15 that the system unbalance response will start decaying compared with the case of no fluid inertial included. It was found that some of the constants given in papers made in 1970's and used till date are not accurate and a comparison of whirl frequencies proved that this would introduce a 5% error at speed beyond 20,000 rpm as detailed in Chapter 2.

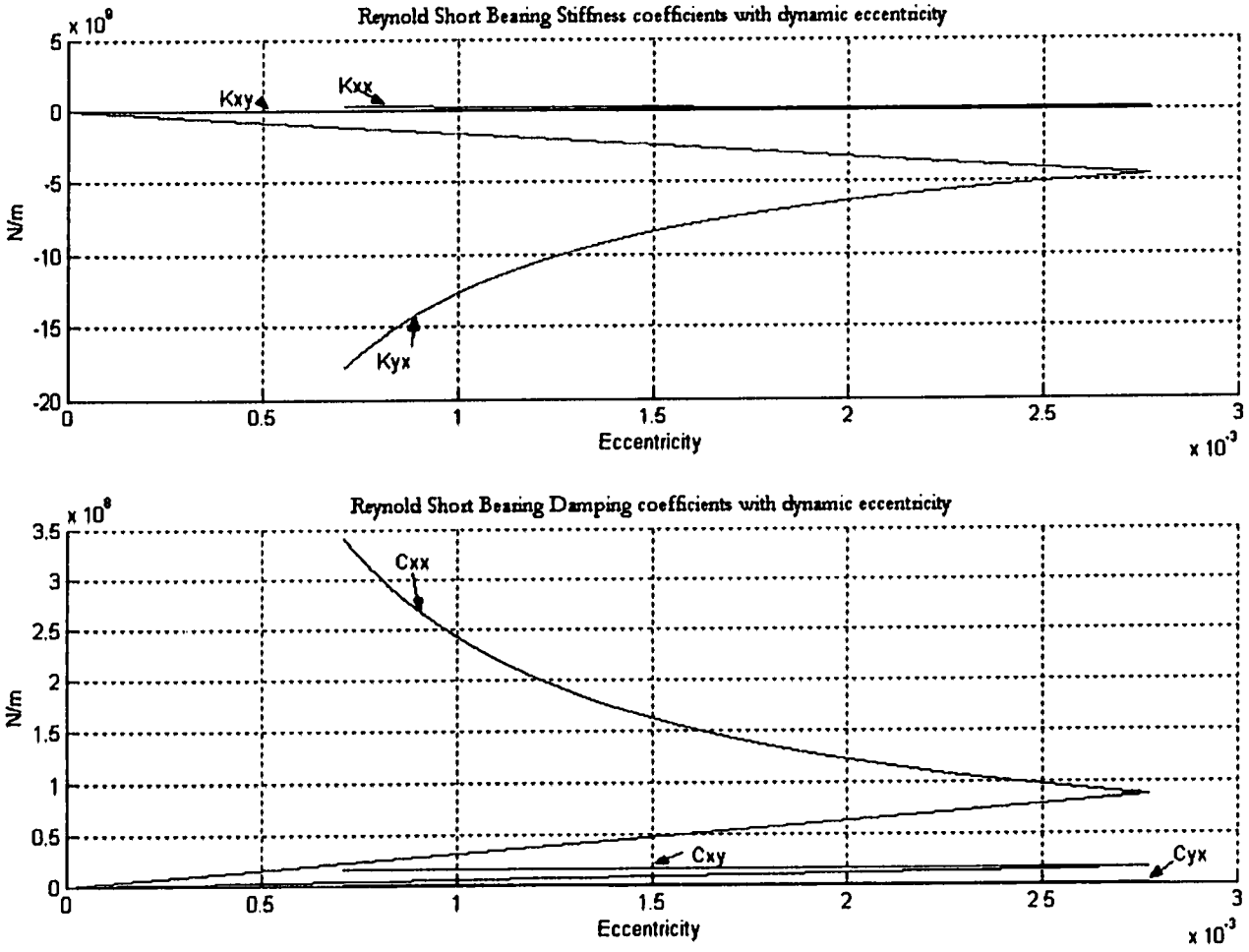

Figure 5.13 – Reynolds Short bearing with system simulation using dynamic eccentricity

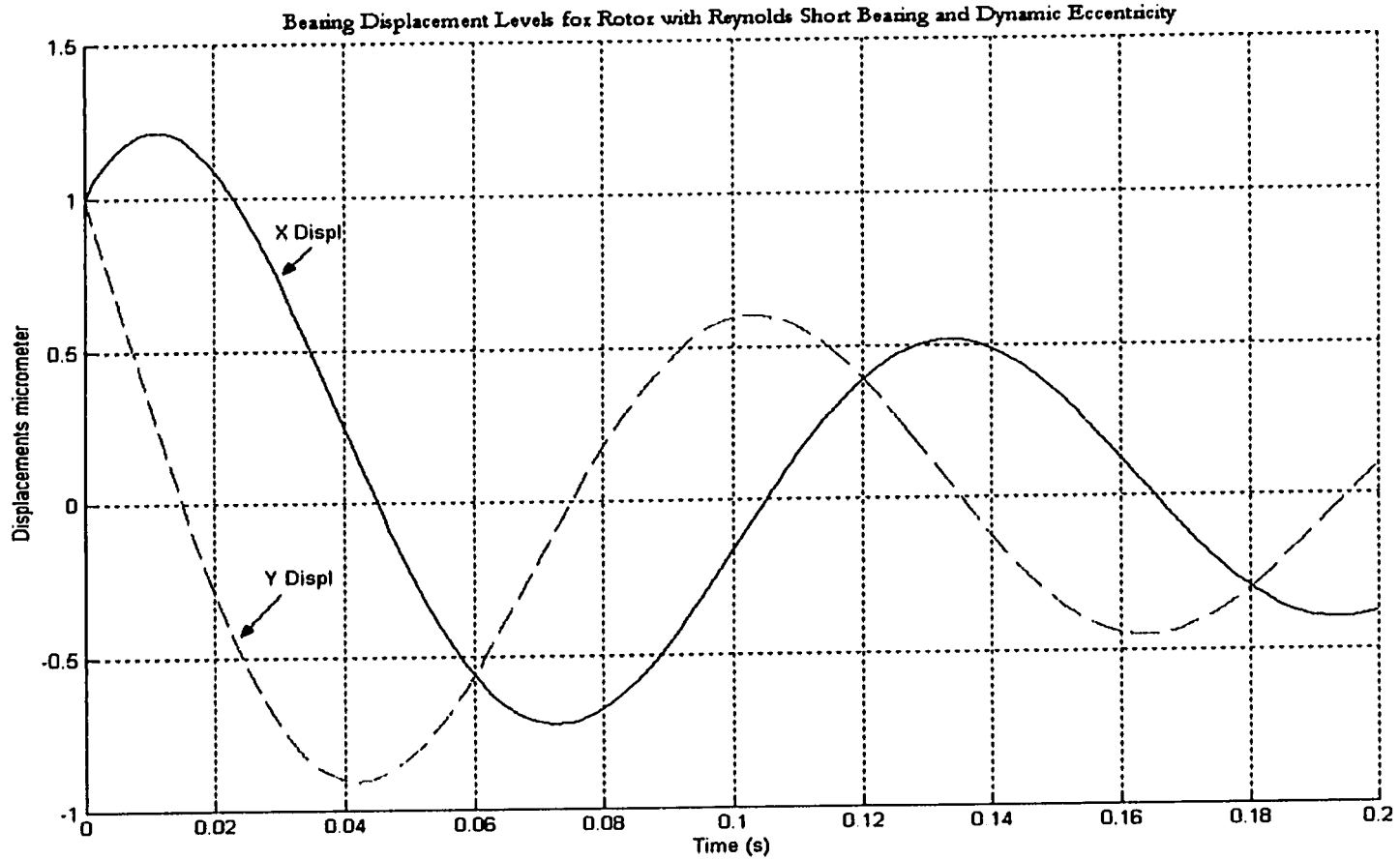

Figure 5.14 –System Bearing displacement response with Reynolds short bearing simulation using dynamic eccentricity

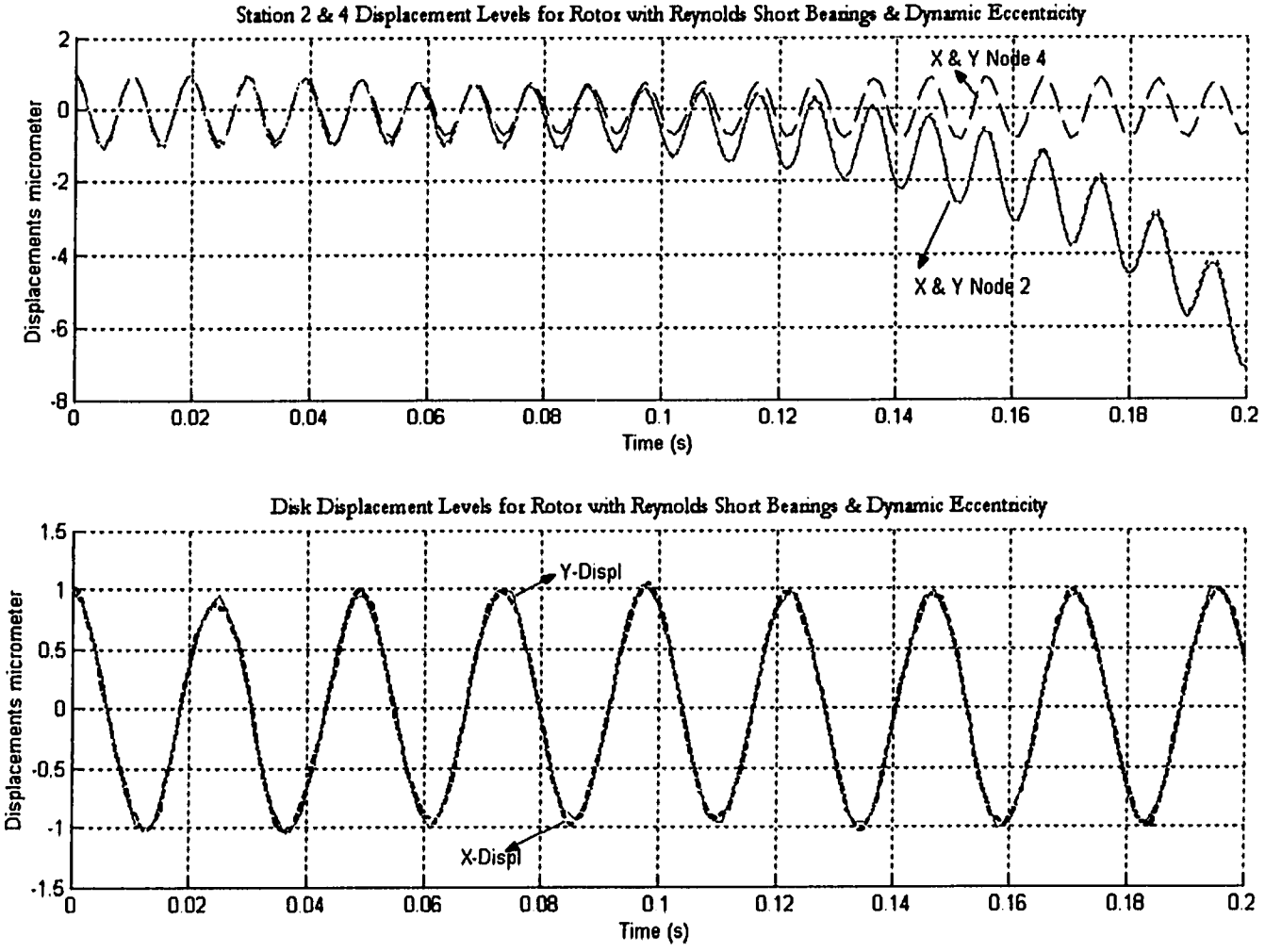

Figure 5.15 –System Disk and Nodes 2/4 displacement response with Reynolds short bearing simulation using dynamic eccentricity

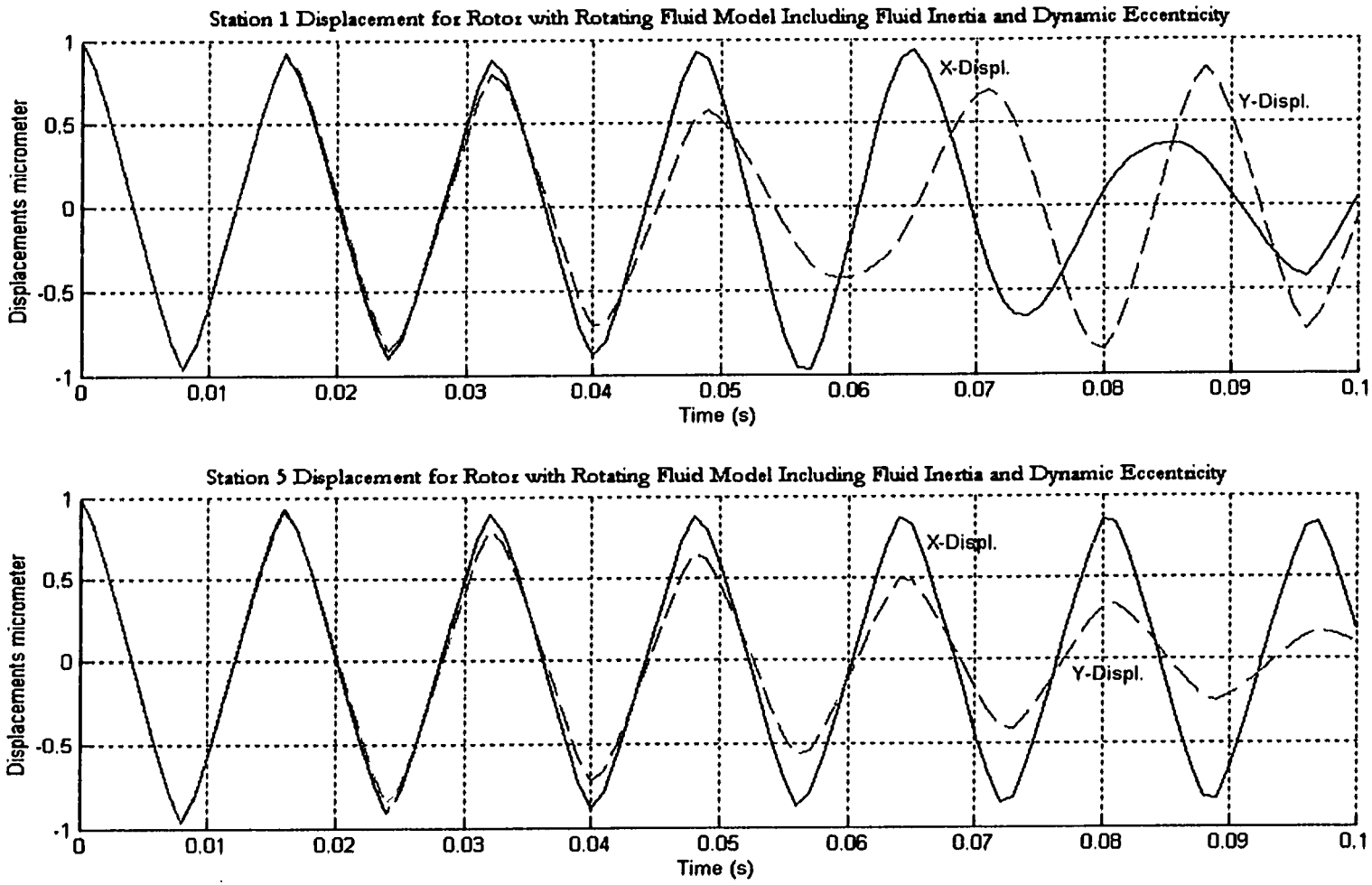

Figure 5.16 –System Bearing displacement response with BRDRC Model including dynamic eccentricity and Fluid Inertia

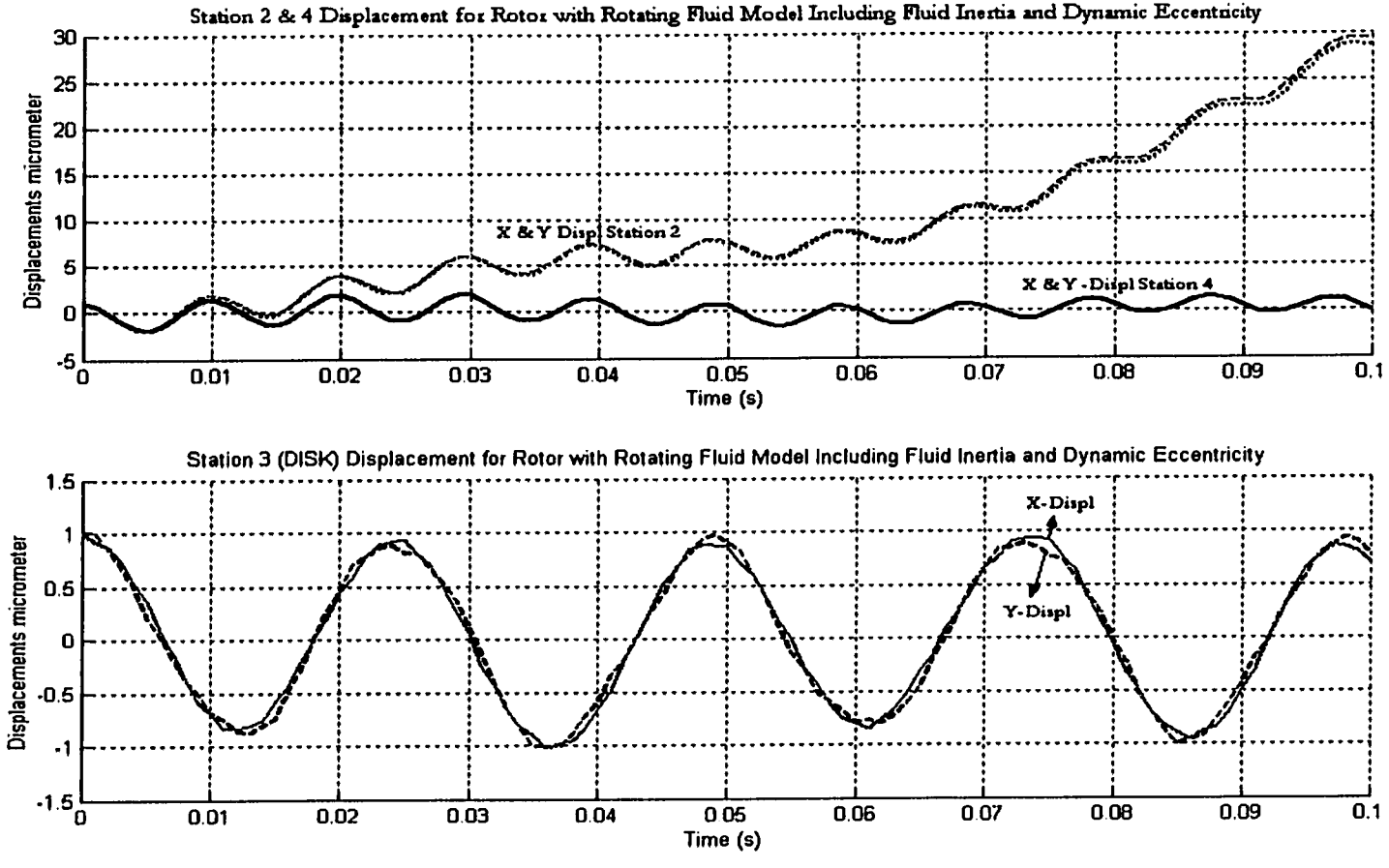

Figure 5.17 –System Disk, Nodes 2 and 4Bearing displacement response with BRDRC Model including dynamic eccentricity and Fluid Inertia

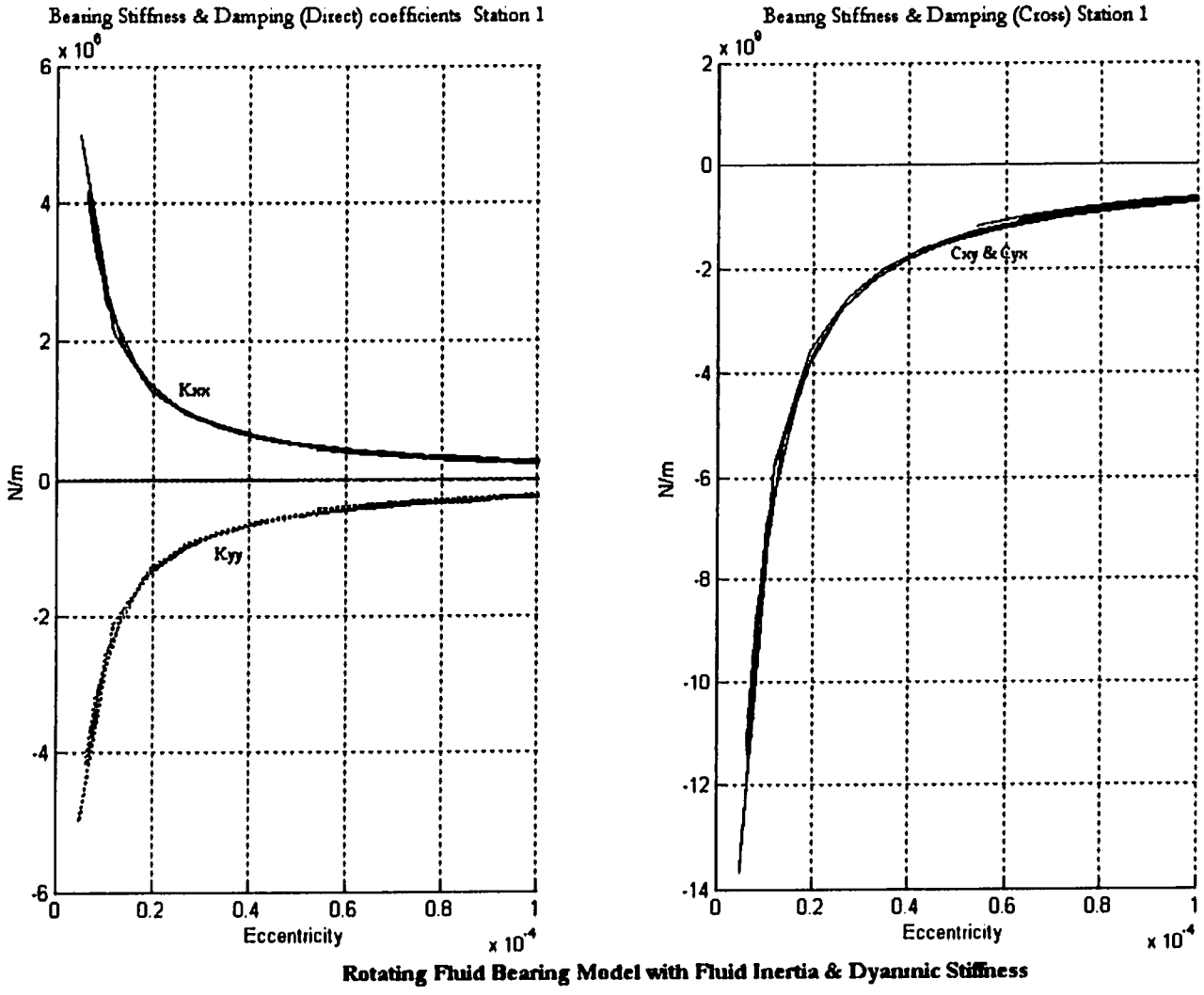

Figure 5.18 – BRDRC bearing with system simulation using dynamic eccentricity and Fluid Inertia

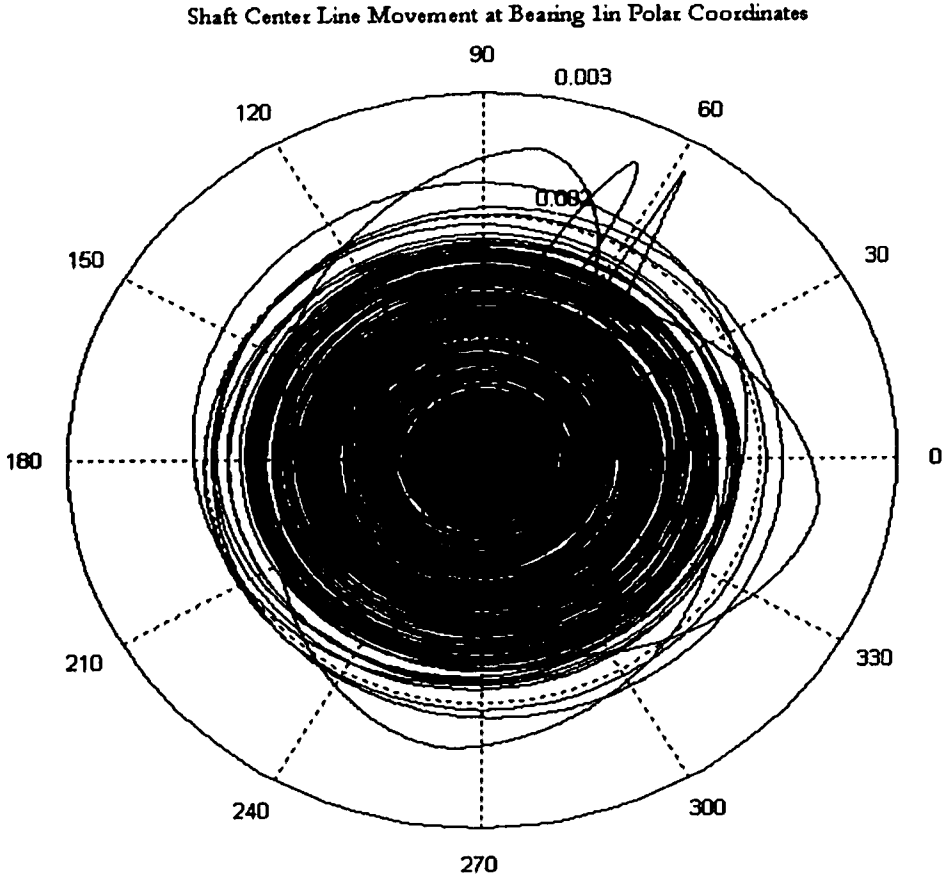

Figure 5.19 – BRDRC bearing used with fluid inertia and dynamic eccentricity loop, shows shaft centerline

CHAPTER 6

CONCLUSION & FUTURE RESEARCH

Based on chapter 5 results, the inclusion of foundation flexibility do introduce significant system response effects which basically reduced the decay time on the nodes which are affected by this. The effect of corrected shape function integrals did reduce the phase lag between X & Y in the disk and other nodes. As for the dynamic eccentricity, it was shown that including the feedback mechanism into the system equations whether using the standard Reynolds short bearing equations or the rotating fluid model equations did actually introduce slower decay into the bearing nodes and made the effect of shaft and disk unbalance clear. In the disk and other nodes, the effect was minimal.

When fluid inertia and dynamic eccentricity were both included utilizing the rotating fluid model, the system response exhibited a slower decay, which was apparent in opposing ends of the shaft. The unbalance was clear in the signals, however the node 2 & 4 went into instability, which is expected in this case as fluid inertia, is a de-stabilizing force. The shaft centerline plot showed that the shaft movement was in the middle of the sleeve in full elliptical orbit mode. This showed that using static eccentricity which when simulated by iteration techniques; do not match what one would expect in reality. The effect of fluid inertia was apparent as low viscosity oil was used, which would make Reynolds numbers high and hence increase the effect of inertia terms in the standard Navier-Stockes equations.

6.1 RECOMMENDATIONS

For future research, the system should be solve for more accuracy using pressure profiles developed in this study, however the half Sommerfeld condition should be avoided as it does not account for cavitation and would not produce an accurate prediction of positive pressures in the assumed 0-π film. For time transient rotordynamic simulations which were not addressed in this study, cavitated bearing do definitely need to address the Gumbel conditions can be applied by finding the positive pressure region from the pressure equation and then perform integration to obtain the fluid film forces using the limits devised from actual pressure profile. Also worth mentioning that π film assumption is valid for only small perturbations about the static equilibrium position, which is anyway the case in this study but might not be in real applications.

LIST OF REFERENCES

[1] Ruhl, R., et al, *A Finite Element Model for Distributed Parameter Turbo-rotor Systems*, pp.126-132, Journal of Engineering for Industry, Feb 1972.

[2] Nelson, H., McVaugh, J., *The Dynamics of Rotor-Bearing Systems Using Finite Elements*, pp. 593-599, Journal of Engineering for Industry, May 1976.

[3] Lund, J., *Stability and Damped Critical Speeds of a Flexible Rotor in Fluid Film Bearings*, pp. 509-517, Journal of Engineering for Industry, May 1974.

[4] Nelson, H., *A Finite Rotating Shaft Element Using Timoshenko Beam Theory*, Vol. 102, pp. 793-803, Journal of Mechanical Design, Oct. 1980.

[5] Abduljabbar, Z., et al, *Active Vibration Control of a Flexible Rotor*, Vol.58, pp.499-511, Computers and Structures, 1996.

[6] Mohiuddin, M., Khulief, Y., *Coupled Bending Torsional Vibration of Rotors Using Finite Element*, Vol.223(2), pp.297-316, Journal of Sound and Vibration, 1998.

[7] Mohiuddin, M., Khulief, Y., *Modal Characteristics of Rotors Using a Conical Shaft Finite Element*, Vol.115, pp.125-144, Computer Methods in Applied Mechanics and Engineering, 1994.

[8] Dubois, G., et al, *Analytical Derivation and Experimental Evaluation of Short-Bearing Approximation for Full Bearing*, Report 1157, National Advisory Committee for Aeronautics, 1953.

[9] Hori, Y., *A Theory of Oil Whip*, pp. 189-198, Journal of Applied Mechanics, June 1959.

[10] Kirk, R., Gunter, E., *Stability and Transient Motion of a Plain Journal Mounted in Flexible Damped Supports*, pp. 576-592, Journal of Engineering for Industry, May 1976.

[11] Zorzi, E., Nelson, H., *Finite Element Simulation of Rotor/Bearing Systems with Internal Damping*, pp. 71-76, Journal of Engineering for Power, Jan 1977.

[12] Hanish, E., et al, *Finite Journal Bearing with Nonlinear Stiffness and Damping Parts I & II,* Vol.104, pp.397-411, Journal of Mechanical Design, April 1982.

[13] Hashish, E., Sankar, T.l, *Finite Element and Modal Analysis of Rotor/Bearing Systems Under Stochastic Loading Conditions,* Vol. 106, pp. 80-89, Journal of Vibration, Acoustics, Stress and Reliability in Design, Jan 1984.

[14] Bently, D., et al, *Role of Circumferential Flow in the Stability of Fluid Handling Machine Rotors,* Texas A&M 5th Workshop on Rotordynamics Instability Problems in High Performance Turbomachinery, May 1988.

[15] Muszynska, A., *Whirl and Whip – Rotor/Bearing Stability Problems,* Vol. 110(3), pp. 443-462, Journal of Sound and Vibration, 1986.

[16] Muszynska, A., *Improvements in Lightly Loaded Rotor / Bearing and Rotor / Seal Models,* Vol.110, pp.129-136, Journal of Vibration, Acoustics, Stress and Reliability in Design, April 1988.

[17] Muszynska, A., Bently, D., *Anti Swirl Arrangements Prevent Rotor/Seal Instability,* pp. 156-161, Journal of Vibration, Acoustics, Stress and Reliability in Design, April 1989.

[18] Muszynska, A., Bently, D., *Frequency Swept Rotating Input Perturbation Techniques and Identification of the Fluid Force Model in Rotor / Bearing / Seal Systems and Fluid Handling Machines,* Vol. 143(1), pp. 103-124, Journal of Sound and Vibration, 1990.

[19] Muszynska, A., et al, *Stability of a Two Mode Rotor Supported by Two Fluid Lubricated Bearings,* Vol.113, pp.316-, Journal of Vibration and Acoustics, July 1991.

[20] Muszynska, A., *Modal Testing of Rotors with Fluid Interaction,* Vol.1 #2, pp. 83-116, International Journal of Rotating Machinery, 1995.

[21] Muszynska, A., *Dynamics of Anistropically Supported Rotors,* 6th International Symposium on Transport Phenomena and Dynamics of Rotating Machinery, 1996.

[22] Tam, L., et al, *Numerical and Analytical Study of Fluid Dynamic Forces in Seals and Bearings,* Vol.110, pp.315-, Journal of Vibration, Acoustics, Stress and Reliability in Design, July 1988.

[23] BRDRC, ISCORMA discussions.

[24] Elshafei, A., *Modeling Fluid Inertia Forces of Short Journal Bearing for Rotordyanmic Application*, Vol.117, pp.462-, Journal of Vibration and Acoustics, Oct. 1995.

[25] Barret, T., et al, *Active Vibration Control of Rotating Machinery Using Piezoelectric Actuators Incorporating Flexible Casing Effects*, Vol.117, pp. 176- , Journal of Engineering for Gas Turbines and Power, Jan 1995.

[26] Berger, S., et al, *Influence of Axial Thrust Bearing on the Dynamic Behavior of an Elastic Shaft: Coupling Between the Axial Dynamic Behavior and the Bending Vibrations of a Flexible Shaft*, Vol.123, pp.145-149, Journal of Vibration and Acoustics, April 2001.

[27] Rieger, N., Zhou, S., *An Instability Analysis Procedure for Three Level Multi Bearing Rotor Foundation Systems*, Vol.120, pp. 753-762, Journal of Vibration and Acoustics, July 1998.

[28] Shabanah, N., Zu, W., *Dynamic Analysis of Rotor-Shaft Systems with Viscoelastically Supported Bearings*, Vol.35, pp.1313-1330, Mechanism and Machine Theory – Elsevier Science Ltd, 2000.

[29] Wong, E., Zu, J., *Dynamic Response of a Coupled Spinning Timoshenko Shaft System*, Vol.121, pp.110-113, Journal of Vibrations and Acoustics, Jan 1999.

APPENDIX A

ECCENTRICITY & FILM THICKNESS RELATION

Consider Figure A.1, bearing center O, journal center C, OC is eccentricity e, CO line to hit bearing surface at E (Maximum clearance) where angular co-ordinates θ is measured, the extension of this line hits the bearing at F (Minimum clearance).

OA radius of bearing R_1, CA is $(R_2 + h)$, radial clearance c $(R_1 - R_2)$. Minimum oil film thickness is (c-e) at F and maximum is (c+e) at E. Angle ECA is θ and OAC is α. Drop from O to CA perpendicular at D Where R_1 bearing radius and R_2 as shaft radius, $c = R_1 - R_2$ is the radial clearance. $c_{max} = c + e$ at E and $c_{min} = c - e$ at F. One can define the following

$$\overline{O_2A} = R_2 + h = \overline{O_2D} + \overline{DA} = e\cos\theta + R_1\cos\alpha$$

In triangle ΔO_1O_2A, $\quad \dfrac{e}{\sin\alpha} = \dfrac{R_1}{\sin\theta} \Rightarrow \sin\alpha = \dfrac{e}{R_1}\sin\theta$

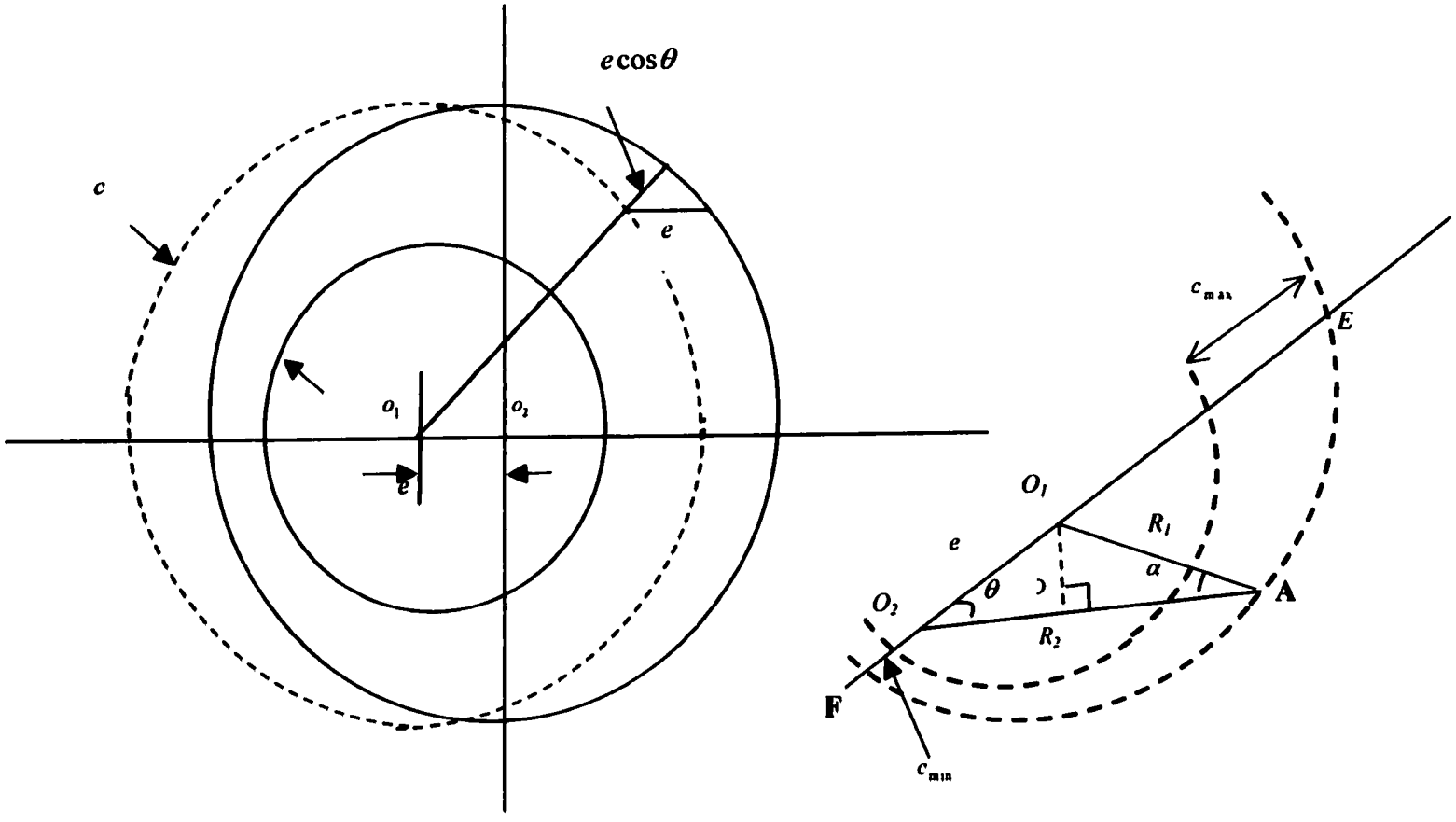

Figure A.1 Film thickness and eccentricity geometric relations

$$\cos\alpha = \sqrt{1-\sin^2\alpha} = \sqrt{1-\left(\frac{e}{R_1}\sin\theta\right)^2}$$

since $\frac{e}{R_1} << 1, \qquad \cos\alpha \approx 1 - \frac{e^2\sin^2\alpha}{2R_1^2}$

$$\overline{O_2A} = e\cos\theta + R_1\left(1 - \frac{e^2\sin^2\alpha}{2R_1^2}\right) \approx e\cos\theta + R_1$$

$$h = (R_1 - R_2) + e\cos\theta = c + e\cos\theta$$

If you roll out the film as shown in Figure A.2, the relation derived for fluid film thickness becomes

$$h = c + e\cos\theta = c(1+\varepsilon\cos\theta), \qquad \varepsilon = \frac{e}{c}$$

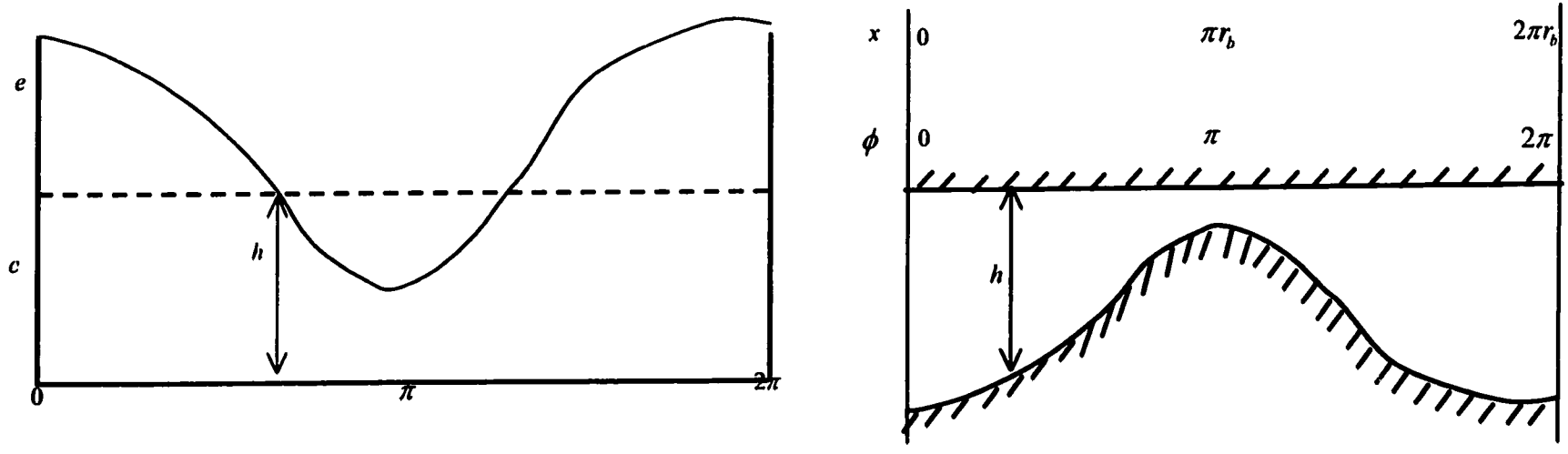

Figure A.2 Fluid Film Roll out

When considering a Load where the bearing will assume an attitude angle as shown in Figure A.3, we have the segment $Rd\theta dy$ with P we have

$$W_x = \int_0^{\pi} \int_{-l/2}^{l/2} PR\cos\theta dy d\theta$$

$$W_y = \int_0^{\pi} \int_{-l/2}^{l/2} PR\sin\theta dy d\theta$$

$$\tan\varphi = \frac{-W_y}{W_x} = \frac{\pi}{4}\frac{\left(1-\varepsilon^2\right)^{1/2}}{\varepsilon} \approx \frac{\sin\varphi}{\cos\varphi} \approx \frac{\left(1-\varepsilon^2\right)^{1/2}}{\varepsilon} \Rightarrow \cos\varphi \square\ \varepsilon$$

Plot of ε and φ in polar coordinates gives semicircle

$$c = r_a - r_b$$

$$\cos\alpha = \frac{1}{r_a}\left[h + r_b + e\cos(\pi - \phi)\right]$$

$$h = r_a\cos\alpha - r_b + e\cos\phi$$

$$\frac{e}{\sin\alpha} = \frac{r_a}{\sin\phi}, \qquad \sin\alpha = \frac{e\sin\phi}{r_a}$$

$$\cos\alpha = \sqrt{1-\sin^2\alpha} = \left(1 - \left(\frac{e\sin\phi}{r_a}\right)^2\right)^{1/2} = 1 - \frac{1}{2}\left(\frac{e}{r_a}\right)^2\sin^2\phi - \frac{1}{8}\left(\frac{e}{r_a}\right)^4\sin^4\phi + \ldots$$

$$h = r_a\left(1 - \left(\frac{e\sin\phi}{r_a}\right)^2\right)^{1/2} - r_b + e\cos\phi$$

$$h = c + e\left[\cos\phi - \frac{1}{2}\frac{e}{r_a}\sin^2\phi - \frac{1}{8}\left(\frac{e}{r_a}\right)^3\sin^4\phi + \ldots\right]$$

$\frac{e}{r_a}$ is of the order of 10^{-3}, $\quad \cos\alpha \approx 1, \quad h = c\left(1 + \varepsilon\cos\phi\right), \quad \varepsilon = \frac{e}{c}$

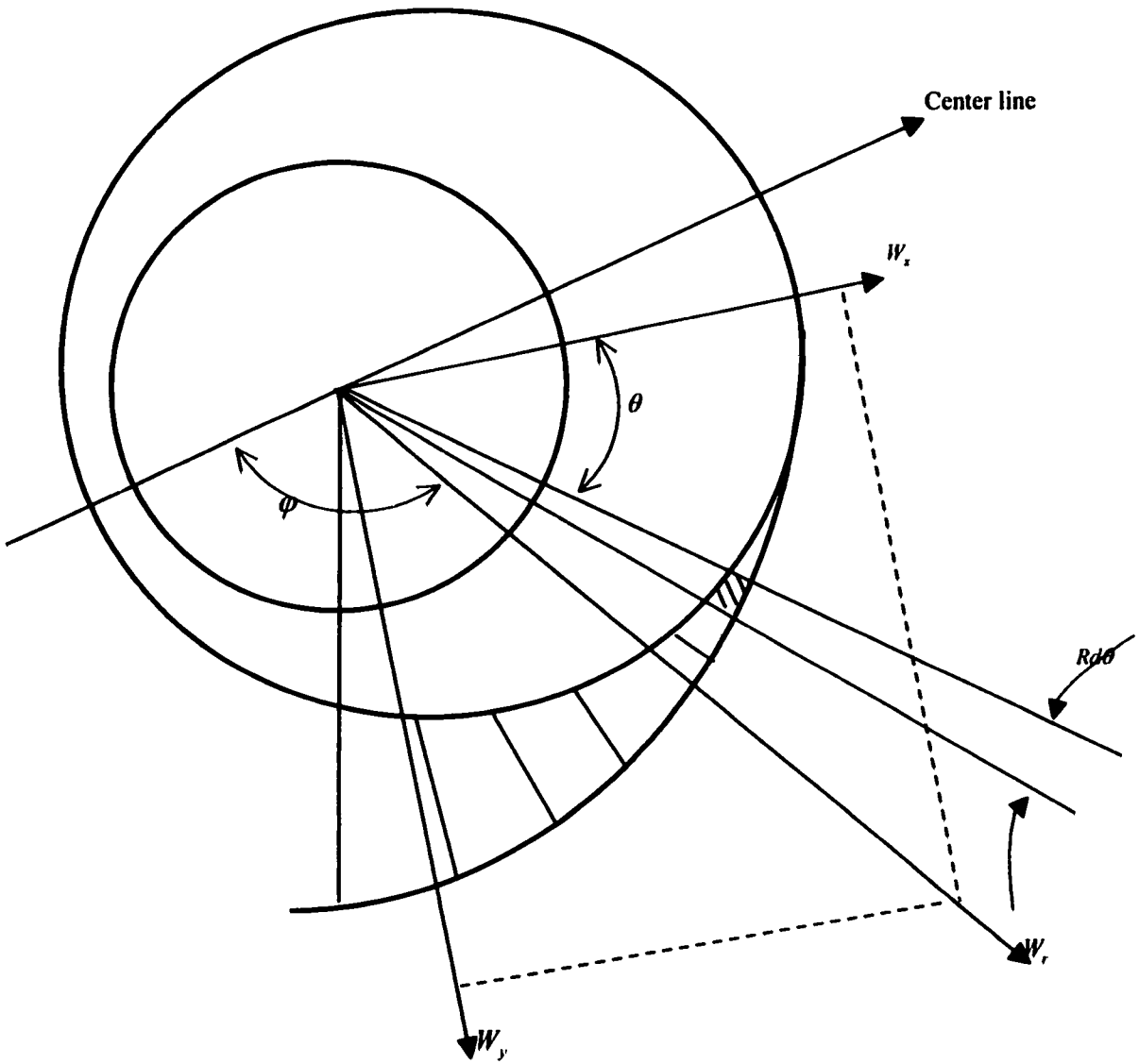

Figure A.3 Shaft Load & Attitude Angle

For the case of dynamic shaft loading the film thickness to eccentricity equation assumes that Film thickness<< shaft radius. Curvature of film can be neglected. neglecting curvature of the film gives x coordinate in the unwrapped film

$$x = r_a\theta, \qquad dx = r_a d\theta \tag{1}$$

$$u_1 = \omega_a r_a, \qquad u_2 = \omega_b r_b \cos(\theta - \alpha') + u_{cb}\sin\theta - \omega_{cb}\cos\theta \tag{2}$$

$v_1 = v_2 = 0$ no momentum in y-direction (3)

$\omega_a = 0$ sleeve rotates about its own center (4)

$$\omega_b = \omega_b r_b \sin(\theta - \alpha') + u_{cb}\cos\theta + \omega_{cb}\cos\theta$$

u_{cb} is the velocity at journal center parallel to x-axis

ω_{cb} is the velocity at journal center perpendicular to x-axis

$$u_{cb} = \frac{de}{dt}\cos\Phi - e\frac{d\Phi}{dt}\sin\Phi$$

$$\omega_{cb} = \frac{de}{dt}\sin\Phi + e\frac{d\Phi}{dt}\cos\Phi$$

$$r_b\cos\alpha' = e\cos\Phi + |c_a a|\cos\theta$$

$$r_b\sin\alpha' = e\sin\Phi + |c_a a|\sin\theta$$

$r_b\sin(\theta - \alpha') = e\sin(\theta - \Phi)$ substitute with u_{cb} and ω_{cb} into u_2 and ω_b

$$u_2 = \omega_b r_b\left[1 - \frac{e^2}{r_b^2}\sin^2(\theta - \Phi)\right]^{1/2} + \frac{de}{dt}\sin(\theta - \Phi) - e\frac{d\Phi}{dt}\cos(\theta - \Phi)$$

$$w_b = -\omega_b\sin(\theta - \Phi) + \frac{de}{dt}\cos(\theta + \Phi) + e\frac{d\Phi}{dt}\sin(\theta - \Phi) \tag{5}$$

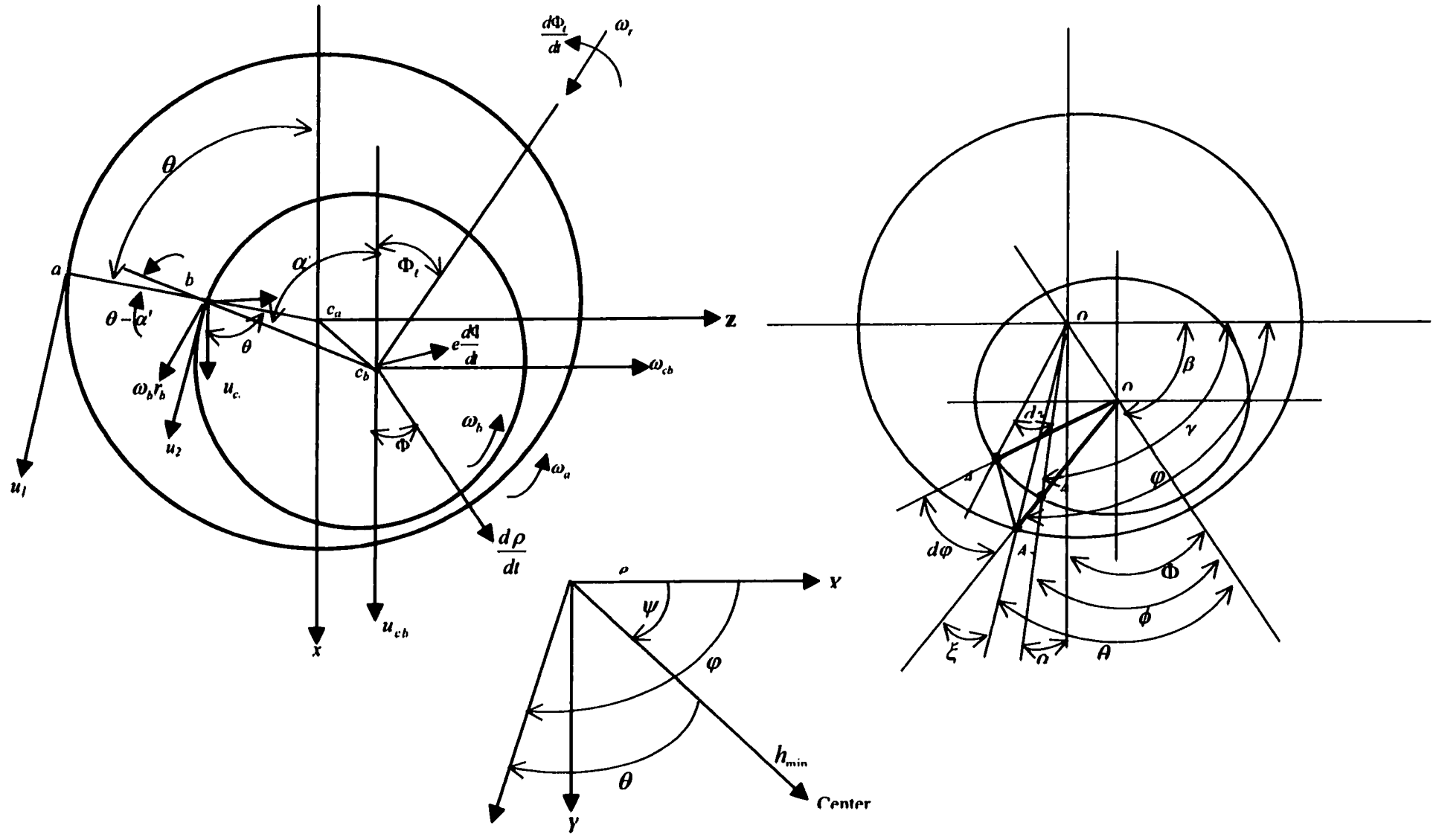

Figure A.4 Dynamic Loading Film Thickness-Eccentricity Geometric Diagram with Angul Details

$$h = c + e\cos(\theta - \Phi), \qquad h = c(1 + \varepsilon\cos\phi)$$

neglecting $\frac{e^2}{r_b^2}$ in u_2

$$u_2 = \omega_b r_b + \frac{de}{dt}\sin(\theta - \Phi) - e\frac{d\Phi}{dt}cos(\theta - \Phi) \tag{6}$$

$$A_1A_3 = \sqrt{(A_1A_2)^2 + (A_2A_3)^2} \qquad Rd\varphi = \sqrt{(rd\gamma)^2 + (dr)^2}$$

$$h = c + e\cos\theta \approx c + e\cos\phi$$

$\gamma - \beta = \phi$ with respect to stationary coordinates

$$h = c + e\cos(\theta - \Phi)$$

$$h = c - e\cos(\gamma - \beta)$$

$$-\cos(\gamma - \beta) = \cos(\alpha + \Phi) = \cos\phi$$

$$\zeta = \gamma - \varphi$$

$$\sin\zeta = \frac{e}{R}\sin(\gamma - \beta) \qquad \cos\zeta = \sqrt{1 - \left(\frac{e}{R}\sin(\gamma - \beta)\right)^2}$$

$$h = c + e\cos\theta, \qquad \theta = \varphi - \phi$$

$$\frac{1}{R}\frac{\partial}{\partial\varphi}\left(\frac{h^3}{\mu R}\frac{\partial P}{\partial\varphi}\right) + \frac{\partial}{\partial z}\left(\frac{h^3}{\mu}\frac{\partial P}{\partial z}\right) = -6\left[e(2\dot{\psi} - \Omega)\sin\theta + 2\dot{e}\cos\theta\right]$$

At A1 the small volume is restricted by segment $[A_2A_3]$

$$= [O_1A_2] - [O_1A_3] = [O_1A_1] - [O_1A_3] = \gamma - (r + dr) = -dr = [O_1A_2] - [O_1A_3]$$

and two arcs

$$(A_1A_2) = rd\gamma$$

$$(A_1A_3) = Rd\varphi$$

APPENDIX B

MATLAB LISTING

MAIN PROGRAM

```
clear all
global dat dat1 dat2 dof logdat dirdat eigdat eigvec fn;

logdat=[];
dirdat=[];
eigdat=[];
eigvec=[];
fn=[];
dat=zeros(1,11);
dat1=zeros(1,11);
dat2=zeros(1,11);
%[X0]=Initial
X0=ones(1,40);
%for t=0:4
   %[M,C,K,Q] = Syshm8(t,X0);
   %end
%u=1;
%[eta,yim]=fediresp(M,K,Q,u,t,C,X0);
%end
Tspan = [0:0.01:0.1];
%OPTIONS=ODESET('RelTol',1,'AbsTol',1e-1)
OPTIONS=odeset('OutputSel',[1 5 9 13 17]);
%[t,y]=ode15s('SYSH8',Tspan,X0,OPTIONS);
[t,y]=ode15s('Sysh8',Tspan,X0,OPTIONS);

figure
subplot(211)
hold
grid
xlabel('Time (s)')
ylabel('Displacements micrometer')
title('Station 1 Displacement Levels for Rotor with Short Hydrodynamic Bearings, Static Eccentricity & massless
fluid')
plot(t,y(:,1),'r-',t,y(:,2),'g--')
subplot(212)
hold
grid
xlabel('Time (s)')
ylabel('Displacements micrometer')
title('Station 5 Displacement Levels for Rotor with Short Hydrodynamic Bearings, Static Eccentricity & massless
fluid')
plot(t,y(:,17),'r-',t,y(:,18),'g--')

figure
subplot(211)
hold
```

```
grid
xlabel('Time (s)')
ylabel('Displacements micrometer')
title('Station 2 & 4 Displacement Levels for Rotor with Short Hydrodynamic Bearings, Static Eccentricity &
massless fluid')
plot(t,y(:,5),'r.',t,y(:,6),'go',t,y(:,13),'yx',t,y(:,14),'b+')
subplot(212)
hold
grid
xlabel('Time (s)')
ylabel('Displacements micrometer')
title('Station 3 (Disk) Displacement Levels for Rotor with Short Hydrodynamic Bearings, Static Eccentricity &
massless fluid')
plot(t,y(:,9),'r.',t,y(:,10),'g-')

figure
grid
xlabel('Speed rpm')
ylabel('Eccentricity')
title('Speed vs. Eccentricity for Bisection iteration methods')
plot (dat(:,10),dat(:,1))

figure
subplot(121)
hold
grid
xlabel('Eccentricity')
ylabel('N/m')
title('Bearing Direct Stiffness & Damping with Static Eccentricity for short bearing')
semilogy (dat(:,1),dat(:,2),dat(:,1),dat(:,3),dat(:,1),dat(:,6),dat(:,1),dat(:,7))
subplot(122)
hold
grid
xlabel('Eccentricity')
ylabel('N/m')
title('Bearing Corss Coupled Stiffness & Damping with Static Eccentricity for short bearing')
semilogy (dat(:,1),dat(:,4),dat(:,1),dat(:,5),dat(:,1),dat(:,8),dat(:,1),dat(:,9))

figure
grid
polar(dat1(:,11),dat1(:,1))

figure
subplot(121)
hold
grid
xlabel('Eccentricity')
ylabel('N/m')
title('Bearing Stiffness coefficients for short bearing Station 1')
semilogy (dat1(:,1),dat1(:,2),dat1(:,1),dat1(:,3),dat1(:,1),dat1(:,6),dat1(:,1),dat1(:,7))
subplot(122)
hold
grid
xlabel('Eccentricity')
ylabel('N/m')
title('Bearing Damping coefficients for short bearing Station 1')
semilogy (dat1(:,1),dat1(:,4),dat1(:,1),dat1(:,5),dat1(:,1),dat1(:,8),dat1(:,1),dat1(:,9))
```

```
figure
subplot(121)
hold
grid
xlabel('Eccentricity')
ylabel('N/m')
title('Bearing Stiffness coefficients for short bearing Station 5')
semilogy (dat2(:,1),dat2(:,2),dat2(:,1),dat2(:,3),dat2(:,1),dat2(:,6),dat2(:,1),dat2(:,7))
subplot(122)
hold
grid
xlabel('Eccentricity')
ylabel('N/m')
title('Bearing Damping coefficients for short bearing Station 5')
semilogy (dat2(:,1),dat2(:,4),dat2(:,1),dat2(:,5),dat2(:,1),dat2(:,8),dat2(:,1),dat2(:,9))

save bearcoef1 dat1 -ascii
save bearcoef2 dat2 -ascii
save displ_1 t y –ascii
```

FUNCTION SYSTEM MATRICIES BUILD UP

```
function Xdot = Sysh8(t,X0)

global dat dat1 dat2 smd csa ym mi md bhm logdat dirdat eigdat eigvec fn;

disp('')
disp('Please wait !! - The System Matricies are being constructed')
% ************************** Input Constants ****************************
noe=4;                                  % Number of Elements
dof=(noe+1)*4;   % Degrees of Freedom
ym=2.07e11;                     % Young's Modulus (N/m)     - Lee E=2e11 N/m2, density=8000 kg/m3,
rs=0.04m, ls=1 m,
sr=0.0508;                              % Shaft Radius (m)
csa=pi*sr^2;                    % Shaft Element - Cross Sectional Area
mi=(pi*sr^4)/4;                 % Shaft Element - Moment of Inertia
smd=7800;               % Shaft Mass Density (Kg/m^3)
sem=smd*csa;                    % Shaft mass per unit length
jt=sem*sr^2/4;
jz=jt/2;
shm=0.79e10;                    % Shear Modulus (N/m)       -
pr=-0.5;                        % Poisson's Ratio
cf=6*(1+pr)/(7+6*pr);                           % Shape function (Correction Factor)
%shm=ym/(2*(1+pr));
ex1=0.04;          % Shaft Element Imbalance Distibution
ex2=0.04;          % Shaft Element Imbalance Distibution
ey1=0.04;          % Shaft Element Imbalance Distibution
ey2=0.04;          % Shaft Element Imbalance Distibution
%mo=0.01;
len=[0.3175 0.3175 0.3175 0.3175];                                      % Shaft Element - Length
for rpmm=2000:2000;
   M=zeros(dof,dof);
   C=zeros(dof,dof);
   K=zeros(dof,dof);
```

```
Q=zeros(dof,1);
rs=rpmm*2*pi/60;
for n=1:noe;
   L=len(n);
   sdc=12*ym*mi/(cf*csa*shm*L^2);        % Shear Deformation Coefficient

   h11=156+294*sdc+140*sdc^2;
   h12=L*(22+38.5*sdc+17.5*sdc^2);       % 10*sdc^2
   h22=L^2*(4+7*sdc+3.5*sdc^2);
   h13=54+126*sdc+70*sdc^2;
   h23=L*(13+31.5*sdc+17.5*sdc^2);  %10*sdc^2 also multiplied by -1
   h24=-L^2*(3+7*sdc+3.5*sdc^2);
   mt=L/(420*(1+sdc)^2)*[h11 0 0 0;h12 h22 0 0;h13 h23 h11 0;-h23 h24 -h12 h22];
   mt=mt'+tril(mt,-1);

   %h55=(1/L^2)*36;  % *L^2
   %h56=(1/L)*(3-15*sdc); % L*
   %h66=4+5*sdc+10*sdc^2; % L^2
   %h58=(1/L)*(30-42*sdc);
   %h68=5-18.5*sdc+12.5*sdc^2;  %L^2(-1-5*sdc+5*sdc^2)
   %h88=40-130*sdc+109*sdc^2;
   %mr=1/(30*(1+sdc)^2)*[h55 0 0 0;h56 h66 0 0;-h55 -h56 h55 0;h58 h68 -h58 h88];
   % jt/(30*L*(1+sdc)^2)*[h55 0 0 0;-h56 h66 0 0;-h55 h56 h55 0;-h56 h68 h56 h66];
   %mr=mr'+tril(mr,-1);

   h55=36;
   h56=L*(3-15*sdc);
   h66=L^2*(4+5*sdc+10*sdc^2);
   h68=L^2*(-1-5*sdc+5*sdc^2);
   mr=1/(30*L*(1+sdc)^2)*[h55 0 0 0;h56 h66 0 0;-h55 -h56 h55 0;h56 h68 -h56 h66];
   mr=mr'+tril(mr,-1);

   %k55=(1/L^2)*12; %*L^2
   %k56=(1/L)*6;   % L^2
   %k66=4+2*sdc+sdc^2; %L^2*(4+sdc)
   %k58=(1/L)*6*sdc;
   %k68=2-sdc-4*sdc^2;  %L^2*(2-sdc)
   %k88=4-16*sdc+19*sdc^2;
   %dmr=(1/(1+sdc)^2)*[k55 0 0 0;k56 k66 0 0;-k55 -k56 k55 0;k58 k68 -k58 k88];
   % ym*mi/L^3/(1+sdc)*[k55 0 0 0;-k56 k66 0 0;-k55 k56 k55 0;-k56 k68 k56 k66]
   %dmr=dmr'+tril(dmr,-1);

   k55=12;
   k56=6*L;
   k66=L^2*(4+2*sdc+sdc^2);
   k58=(1/L)*6*sdc;
   k68=L^2*(2-sdc-4*sdc^2);
   k88=4-16*sdc+19*sdc^2;
   dmr=1/(1+sdc)^2*[k55 0 0 0;k56 k66 0 0;-k55 -k56 k55 0;k56 k68 -k56 k66];
   % ym*mi/L^3/(1+sdc)*[k55 0 0 0;-k56 k66 0 0;-k55 k56 k55 0;-k56 k68 k56 k66]
   dmr=dmr'+tril(dmr,-1);

   k11=36+60*sdc+30*sdc^2;
   k12=3*L;
   k22=L^2*(4+5*sdc+2.5*sdc^2);
   k14=2*k12;
   k24=L^2*(-1-5*sdc-2.5*sdc^2);
```

```
dmt=1/(30*L*(1+sdc)^2)*[k11 0 0 0;k12 k22 0 0;-k11 -k12 k11 0;2*k12 k24 -k12 k22];
dmt=dmt'+tril(dmt,-1);

m1=42*L+40*L*sdc;
m2=18*L+20*L*sdc;
m3=-6*L^2+5*L^2*sdc;
m4=-40*L^2-5*L^2*sdc;
m5=40*L^2-5*L^2*sdc;
m6=6*L^2+5*L^2*sdc;
m7=-42*L+40*L*sdc;
m8=-18*L+20*L*sdc;
cgt=[ex1 ex2 ey1 ey2]';
Mac=[m1 m2 0 0;0 0 m1 m2;0 0 m3 m4;-m3 -m4 0 0;m2 m1 0 0;0 0 m2 m1;0 0 m5 m6;-m5 -m6 0 0]*cgt;
Mas=[0 0 m7 m8;m1 m2 0 0;m3 m4 0 0;0 0 m3 m4;0 0 -m2 -m1;m2 m1 0 0;m5 m6 0 0;0 0 m5 m6]*cgt;

grv=[0 -6*L L^2 0 0 -6*L -L^2 0];

ze=zeros(4,4);
% ******** Transformation Matrix Computed Integrals **********************************
% 'Following Matrices coordinates are (Nelson with coordinates interchanged) to be
% | ux1 theta1 ux2 theta2 uy1 epsi1 uy2 epsi2 |T
Mt=[mt ze;ze mt];       % Translational Transformation Matrix X & Y Direction
Mr=[mr ze;ze mr];       % Rotational Transformation Matrix Y-Direction
DMt=[dmt ze;ze dmt];    % Differential (wrt Z) Translational Transformation Matrix X-Direction
DMr=[dmr ze;ze dmr];    % Differential (wrt Z) Rotational Transformation Matrix Y-Direction
%Hg=[ze ze;mr ze];      % Rotational X-axis / Rotational Y-axis Transformation Matrix
%Mg=Hg-Hg';
Mg=[ze mr;-mr ze];     % Revised according to Hanish
Cid=[ze mt;mt ze];      % Rotational Transformation Matrix X-Direction
% ************************** Coordinates Change to be **********************************
% | ux1 uy1 theta1 epsi1 ux2 uy2 theta2 epsi2 |T
cnt1=[1 5 6 5 6 7 8 8];
for j=1:8
   cj=cnt1(j);
   temp=Mt(:,j);   Mt(:,j)=Mt(:,cj);      Mt(:,cj)=temp;
   temp=Mr(:,j);   Mr(:,j)=Mr(:,cj);      Mr(:,cj)=temp;
   temp=DMt(:,j);  DMt(:,j)=DMt(:,cj);    DMt(:,cj)=temp;
   temp=DMr(:,j);  DMr(:,j)=DMr(:,cj);    DMr(:,cj)=temp;
   temp=Mg(:,j);   Mg(:,j)=Mg(:,cj);      Mg(:,cj)=temp;
   temp=Cid(:,j);  Cid(:,j)=Cid(:,cj);    Cid(:,cj)=temp;
end
for i=1:8
   ri=cnt1(i);
   temp=Mt(i,:);   Mt(i,:)=Mt(ri,:);      Mt(ri,:)=temp;
   temp=Mr(i,:);   Mr(i,:)=Mr(ri,:);      Mr(ri,:)=temp;
   temp=DMt(i,:);  DMt(i,:)=DMt(ri,:);    DMt(ri,:)=temp;
   temp=DMr(i,:);  DMr(i,:)=DMr(ri,:);    DMr(ri,:)=temp;
   temp=Mg(i,:);   Mg(i,:)=Mg(ri,:);      Mg(ri,:)=temp;
   temp=Cid(i,:);  Cid(i,:)=Cid(ri,:);    Cid(ri,:)=temp;
end
% ********************** Shaft Element Matrices ************************************
Me=smd*csa*Mt+smd*mi*Mr;                % Shaft Element Mass Matrix
Ge=2*rs*smd*mi*Mg;                      % Shaft Element Gyroscopic Matrix
%Ge=jz*rs*Mg;
Ke=(cf*csa*shm*(DMt+Mr))+(ym*mi*DMr);           % Shaft Element Stiffness
%Ke=ym*mi*DMr;
```

```
    Fu=-(rs^2*smd*csa*cos(rs*t)*Mac)-(rs^2*smd*csa*sin(rs*t)*Mas);  % Shaft Element Imbalance Force Vector
smd*csa
    %Fu=0;
    % ********** Start Loop for Assembly of System Mass, Stiffness, Gyro & Force Matricies
**********************
    cnt4=[4*n-3  4*n  4*(n+1)-3  4*(n+1)  4*n-2  4*n-1  4*(n+1)-2  4*(n+1)-1];
    for i=1:8
      ri=cnt4(i);
      Q(ri)=Fu(i);
      for j=1:8
        cj=cnt4(j);
        M(ri,cj)=M(ri,cj)+Me(i,j);
        C(ri,cj)=C(ri,cj)+Ge(i,j);
        K(ri,cj)=K(ri,cj)+Ke(i,j);
      end
    end
  end
  q=X0(1:dof);
  qv=X0(dof+1:2*dof);
  X=[q;qv];

  [M,C,Q]=disk(rs,t,M,C,Q);
  [M,C,K,Q]=Foundation(M,C,K,Q,noe);
  [C,K,Q]=Structure(C,K,Q,Mt,Cid,DMr,grv,rs);

  %[C,K,dat]=SbrgSEccNMf(rs,C,K,dat);
  %[C,K,dat]=SbrgSEccNMfPoly(rs,C,K,dat);
  %[C,K,dat1,dat2]=SbrgDEccNMf(rs,X,C,K,dat1,dat2);
  %[C,K,dat]=SbrgSEccNMfShf(rs,t,C,K,dat);
  %[C,K,dat]=BRDBrgSEccNMfXfrm(rs,C,K,dat);
  %[C,K,dat]=BRDBrgSEccMf(rs,C,K,dat);
  [M,C,K,dat1,dat2]=BRDBrgDEccMf(rs,X,M,C,K,dat);


  invm=inv(M);
  A=[ zeros(dof) eye(dof);-invm*K  -invm*C];
  B=[zeros(dof,1); invm*Q];
  Xdot=A*X+B;
  % ********** Eigen Values & Vector Calculation ******************************


  [V,W]=eig(K,M);
  [lam,k]=sort(diag(W));
  V=V(:,k);
  Factor=diag(V'*M*V);
  Vnorm=V*inv(sqrt(diag(Factor)));       % Normalizing Eigenvectors
  Omega=diag(sqrt(Vnorm'*K*Vnorm));     % Natural Frequencies
  eigvec=[eigvec Vnorm'];
  fn=[fn Omega'];

  [v,w1]=eig(A);
  wii=abs(w1);
  zetai=-real(w1)/wii;
  wi=diag(wii);
  zeta=diag(zetai);
  logdec=2*pi*zeta;
  nn=dof;
```

```
  for j=1:nn,
    jj=2*j;
    if det([real(v(nn+1,jj)) -imag(v(nn+1,jj)) ; real(v(nn+2,jj)) -imag(v(nn+2,jj))]) > 0
      wdir(j)='F';
    elseif det([real(v(nn+1,jj)) -imag(v(nn+1,jj)) ; real(v(nn+2,jj)) -imag(v(nn+2,jj))]) < 0
      wdir(j)='B';
    else
      wdir(j)=' ';
    end
    eigen(j)=wi(jj);
    logdc(j)=logdec(jj);
  end
  dirdat=[dirdat wdir'];
  eigdat=[eigdat eigen'];
  logdat=[logdat logdc'];

end          % end of the loop for w
```

FUNCTION DISK

```
function [M,C,Q]=disk(rs,t,M,C,Q)

global md;
numd=1;
r=.12;
ex=r/2;                    % Disk Unbalance Eccentricity - X Direction
ey=r/2;                    % Disk Unbalance Eccentricity - Y Direction
md=50;
mo=0.2;
it=md*r^2/4;
ip=md*r^2/2;
Q(9)=-ex*mo*rs^2*cos(rs*t)+ey*mo*rs^2*sin(rs*t);
Q(10)=-md*9.81;
Q(11)=-ey*mo*rs^2*cos(rs*t)-ex*mo*rs^2*sin(rs*t);
M(9,9)=M(9,9)+md;
M(10,10)=M(10,10)+md;
M(11,11)=M(11,11)+it;
M(12,12)=M(12,12)+it;
C(11,12)=C(11,12)-rs*ip;
C(12,11)=C(12,11)+rs*ip;
```

FUNCTION STRUCTURAL DAMPING

```
function [C,K,Q]=Structure(C,K,Q,Mt,Cid,DMr,grv,rs)

global smd csa ym mi noe;
sd=2.2e7;          %100    % Shaft Viscous Damping (Ns/m)
lf=0.3; %100;              % Loss Factor
hdf=lf/sqrt(1+lf^2);                    % Hysteresis Damping Factor [sin(gamma)]

% ********************** Shaft Element Matrices ************************************
Dv=(sd/(smd*csa))*Mt;   % Shaft Element Internal Viscous Damping Matrix Velocity Related
```

```
Dd=((sd/(smd*csa))*rs*Cid); % Shaft Element Internal Viscous Damping Displacement related
Dh=(0.5*ym*mi*hdf*DMr); % Shaft Element Hysteresis damping matrix
Fg=(smd*csa*9.81/12*grv'); % Shaft Element Gravity Force Vector
% ********** Start Loop for Assembly of System Mass, Stiffness, Gyro & Force Matricies
**********************
for n=1:noe;
 cnt4=[4*n-3  4*n  4*(n+1)-3  4*(n+1)  4*n-2  4*n-1  4*(n+1)-2  4*(n+1)-1];
 for i=1:8
  ri=cnt4(i);
  Q(ri)=Fg(i);
  for j=1:8
   cj=cnt4(j);
   C(ri,cj)=C(ri,cj)+Dv(i,j);
   K(ri,cj)=K(ri,cj)+Dd(i,j)+Dh(i,j);
  end
 end
end
```

FUNCTION INITIAL CONDITIONS

```
function [X0]=Initial

global rs dat smd csa ym mi md bhm;


% ************************** Input Constants ***************************
noe=4;                                  % Number of Elements
dof=(noe+1)*4;   % Degrees of Freedom
ym=2.07e11;                     % Young's Modulus (N/m)     - Lee E=2e11 N/m2, density=8000 kg/m3,
rs=0.04m, ls=1 m,
sr=0.0508;                              % Shaft Radius (m)
csa=pi*sr^2;                    % Shaft Element - Cross Sectional Area
mi=(pi*sr^4)/4;                 % Shaft Element - Moment of Inertia
smd=7800;               % Shaft Mass Density (Kg/m^3)
sem=smd*csa;                    % Shaft mass per unit length
jt=sem*sr^2/4;
jz=jt/2;
shm=0.79e10;                    % Shear Modulus (N/m)       -
pr=-0.5;                        % Poisson's Ratio
cf=6*(1+pr)/(7+6*pr);                           % Shape function (Correction Factor)
%shm=ym/(2*(1+pr));
ex1=0.04;          % Shaft Element Imbalance Distibution
ex2=0.04;          % Shaft Element Imbalance Distibution
ey1=0.04;          % Shaft Element Imbalance Distibution
ey2=0.04;          % Shaft Element Imbalance Distibution
ls=1.27;                        % Shaft Length (m)
sm=sem*ls;
len=[0.3175 0.3175 0.3175 0.3175];                                      % Shaft Element - Length
M=zeros(dof,dof);
C=zeros(dof,dof);
K=zeros(dof,dof);
Q=zeros(dof,1);
rpmm=0;
t=0;
```

```
X0 = zeros(1,2*dof);
rs=rpmm*2*pi/60;
for n=1:noe;
   L=len(n);
   sdc=12*ym*mi/(cf*csa*shm*L^2);          % Shear Deformation Coefficient

      h11=156+294*sdc+140*sdc^2;
      h12=L*(22+38.5*sdc+17.5*sdc^2);      % 10*sdc^2
      h22=L^2*(4+7*sdc+3.5*sdc^2);
      h13=54+126*sdc+70*sdc^2;
      h23=L*(13+31.5*sdc+17.5*sdc^2);  %10*sdc^2 also multiplied by -1
      h24=-L^2*(3+7*sdc+3.5*sdc^2);
      mt=L/(420*(1+sdc)^2)*[h11 0 0 0;h12 h22 0 0;h13 h23 h11 0;-h23 h24 -h12 h22];
      mt=mt'+tril(mt,-1);

      h55=36;
      h56=L*(3-15*sdc);
      h66=L^2*(4+5*sdc+10*sdc^2);
      h68=L^2*(-1-5*sdc+5*sdc^2);
      mr=1/(30*L*(1+sdc)^2)*[h55 0 0 0;h56 h66 0 0;-h55 -h56 h55 0;h56 h68 -h56 h66];
      mr=mr'+tril(mr,-1);

      k55=12;
      k56=6*L;
      k66=L^2*(4+2*sdc+sdc^2);
      k58=(1/L)*6*sdc;
      k68=L^2*(2-sdc-4*sdc^2);
      k88=4-16*sdc+19*sdc^2;
      dmr=1/(1+sdc)^2*[k55 0 0 0;k56 k66 0 0;-k55 -k56 k55 0;k56 k68 -k56 k66];
      % ym*mi/L^3/(1+sdc)*[k55 0 0 0;-k56 k66 0 0;-k55 k56 k55 0;-k56 k68 k56 k66]
      dmr=dmr'+tril(dmr,-1);

      k11=36+60*sdc+30*sdc^2;
      k12=3*L;
      k22=L^2*(4+5*sdc+2.5*sdc^2);
      k14=2*k12;
      k24=L^2*(-1-5*sdc-2.5*sdc^2);
      dmt=1/(30*L*(1+sdc)^2)*[k11 0 0 0;k12 k22 0 0;-k11 -k12 k11 0;2*k12 k24 -k12 k22];
      dmt=dmt'+tril(dmt,-1);

      m1=42*L+40*L*sdc;
      m2=18*L+20*L*sdc;
      m3=-6*L^2+5*L^2*sdc;
      m4=-40*L^2-5*L^2*sdc;
      m5=40*L^2-5*L^2*sdc;
      m6=6*L^2+5*L^2*sdc;
      m7=-42*L+40*L*sdc;
      m8=-18*L+20*L*sdc;
      cgt=[ex1 ex2 ey1 ey2]';
      Mac=[m1 m2 0 0;0 0 m1 m2;0 0 m3 m4;-m3 -m4 0 0;m2 m1 0 0;0 0 m2 m1;0 0 m5 m6;-m5 -m6 0 0]*cgt;
      Mas=[0 0 m7 m8;m1 m2 0 0;m3 m4 0 0;0 0 m3 m4;0 0 -m2 -m1;m2 m1 0 0;m5 m6 0 0;0 0 m5 m6]*cgt;

      grv=[0 -6*L L^2 0 0 -6*L -L^2 0];

      ze=zeros(4,4);
      % ******** Transformation Matrix Computed Integrals **********************************
      % *Following Matrices coordinates are (Nelson with coordinates interchanged) to be
```

```
    % | ux1 theta1 ux2 theta2 uy1 epsi1 uy2 epsi2 |T
    Mt=[mt ze;ze mt];       % Translational Transformation Matrix X & Y Direction
    Mr=[mr ze;ze mr];       % Rotational Transformation Matrix Y-Direction
    DMt=[dmt ze;ze dmt];    % Differential (wrt Z) Translational Transformation Matrix X-Direction
    DMr=[dmr ze;ze dmr];    % Differential (wrt Z) Rotational Transformation Matrix Y-Direction
    %Hg=[ze ze;mr ze];      % Rotational X-axis / Rotational Y-axis Transformation Matrix
    %Mg=Hg-Hg';
    Mg=[ze mr;-mr ze];      % Revised according to Hanish
    Cid=[ze mt;mt ze];      % Rotational Transformation Matrix X-Direction
    % ************************* Coordinates Change to be ********************************
    % | ux1 uy1 theta1 epsi1 ux2 uy2 theta2 epsi2 |T
    cnt1=[1 5 6 5 6 7 8 8];
    for j=1:8
      cj=cnt1(j);
      temp=Mt(:,j);   Mt(:,j)=Mt(:,cj);     Mt(:,cj)=temp;
      temp=Mr(:,j);   Mr(:,j)=Mr(:,cj);     Mr(:,cj)=temp;
      temp=DMt(:,j);  DMt(:,j)=DMt(:,cj);   DMt(:,cj)=temp;
      temp=DMr(:,j);  DMr(:,j)=DMr(:,cj);   DMr(:,cj)=temp;
      temp=Mg(:,j);   Mg(:,j)=Mg(:,cj);     Mg(:,cj)=temp;
      temp=Cid(:,j);  Cid(:,j)=Cid(:,cj);   Cid(:,cj)=temp;
    end
    for i=1:8
      ri=cnt1(i);
      temp=Mt(i,:);   Mt(i,:)=Mt(ri,:);     Mt(ri,:)=temp;
      temp=Mr(i,:);   Mr(i,:)=Mr(ri,:);     Mr(ri,:)=temp;
      temp=DMt(i,:);  DMt(i,:)=DMt(ri,:);   DMt(ri,:)=temp;
      temp=DMr(i,:);  DMr(i,:)=DMr(ri,:);   DMr(ri,:)=temp;
      temp=Mg(i,:);   Mg(i,:)=Mg(ri,:);     Mg(ri,:)=temp;
      temp=Cid(i,:);  Cid(i,:)=Cid(ri,:);   Cid(ri,:)=temp;
    end
    % ********************* Shaft Element Matrices ***********************************
    Me=smd*csa*Mt+smd*mi*Mr;                    % Shaft Element Mass Matrix
    Ge=2*rs*smd*mi*Mg;                          % Shaft Element Gyroscopic Matrix
    %Ge=jz*rs*Mg;
    Ke=(cf*csa*shm*(DMt+Mr))+(ym*mi*DMr);       % Shaft Element Stiffness
    %Ke=ym*mi*DMr;
    Fu=-(rs^2*smd*csa*cos(rs*t)*Mac)-(rs^2*smd*csa*sin(rs*t)*Mas); % Shaft Element Imbalance Force Vector
smd*csa
    %Fu=0;
    % ********** Start Loop for Assembly of System Mass, Stiffness, Gyro & Force Matricies
**********************
    cnt4=[4*n-3 4*n 4*(n+1)-3 4*(n+1) 4*n-2 4*n-1 4*(n+1)-2 4*(n+1)-1];
    for i=1:8
      ri=cnt4(i);
      Q(ri)=Fu(i);
      for j=1:8
        cj=cnt4(j);
        M(ri,cj)=M(ri,cj)+Me(i,j);
        C(ri,cj)=C(ri,cj)+Ge(i,j);
        K(ri,cj)=K(ri,cj)+Ke(i,j);
      end
    end
  end
  q=X0(1:dof);
  qv=X0(dof+1:2*dof);
  X=[q;qv];
```

```
  [M,C,Q]=disk(rs,t,M,C,Q);
  [M,C,K,Q]=Foundation(M,C,K,Q,noe);
  [C,K,Q]=Structure(C,K,Q,Mt,Cid,DMr,grv,rs);
  [M,C,K,dat1,dat2]=BRDBrgDEccMf(rs,X,M,C,K,dat);
  Fi=(sm+md+bhm)*9.81;          % Initial Force (N)
  Q(10)=Fi;       % **** Adding initial force
  % *************** Computing Initial Conditions using Static Equilibrium **************
  x0=inv(K)*Q;
  v0=zeros(dof,1);
  X0=[x0;v0];
end
```

FUNCTION FOUNDATION ELASTICITY

```
function [M,C,K,Q]=Foundation(M,C,K,Q,noe)

global bhm;

cx=1.75e5;                    % Bearing Housing Support Damping  - X Direction
cy=1.75e5;                    % Bearing Housing Support          - Y Direction
kx=1.1e9;                          % Bearing Housing Support Stiffness- X Direction
ky=1.1e9;                          % Bearing Housing Support Stiffness- Y Direction
fbx1=1e2;                          % Bearing1 Housing Support Input Force  - X Direction
fby1=1e2;                          % Bearing Housing Support Input Force  - Y Direction
bhm=50;                              % Bearing Housing Mass (Kg)

Mf(1,1)=bhm; Mf(2,2)=bhm;      % Foundation Mass
Gf(1,1)=cx;  Gf(2,2)=cy;       % Foundation Damping
Kf(1,1)=kx;  Kf(2,2)=ky;       % Foundation Stiffness
Ff(1)=fbx1+bhm*9.81;  Ff(2)=fby1+bhm*9.81;     % Foundation Force Vector

% Adding Support Parameters for Station 1.
for i=1:2
 Q(i)=Q(i)+Ff(i);
 for j=1:2
  M(i,j)=M(i,j)+Mf(i,j);
  C(i,j)=C(i,j)+Gf(i,j);
  K(i,j)=K(i,j)+Kf(i,j);
 end
end
% Adding Support Parameters for Last Station.
num1=4*(noe+1);
cnt2=[num1-3 num1-2];
for i=1:2
 ri=cnt2(i);
 Q(ri)=Q(ri)+Ff(i);
 for j=1:2
  cj=cnt2(j);
  M(ri,cj)=M(ri,cj)+Mf(i,j);
  C(ri,cj)=C(ri,cj)+Gf(i,j);
  K(ri,cj)=K(ri,cj)+Kf(i,j);
 end
end
```

FUNCTION STANDARD SHORT BEARING

```
function [C,K,dat]=SbrgSEccNMf(rs,C,K,dat)

global dat dat1 dat2;
y=max(size(C));
s=y-3;
t=y-2;
kxx=0;, kyy=0;, kxy=0;, kyx=0;, cxx=0;, cyy=0;, cxy=0;, cyx=0;
f=222.5; %50; %417.5;  %50  %Bearing Load
lv=6.9e-3;  %1e-5; %7
br=0.0285; %0.3;
bc=.000051; %0.0005;
bl=0.0285; %0.3;
a=0.01;
b=0.99;
tol=0.0001;
n0=1000;
rps=rs/2/pi;
ovr=lv*rps*br*bl^3/2/f/bc^2;    % Ovrick Number
som=lv*rps*2*br^3*bl/f/bc^2;    % Sommerfeld Number
i=1;
while i <= n0
 p=a + (b - a) / 2;
 qb = (1 - p^2)^2 / pi /p/(pi^2*(1-p^2)+16*p^2)^.5 -ovr;
 if qb == 0 | (b-a)/2 < tol
  e = p;, break
 end
 i = i + 1;
 qb1 = (1 - a ^ 2)^2 / pi/a/(pi^2 *(1-a^2)+16*a^2)^.5-ovr;
 if qb * qb1 > 0
  a = p;
 else
  b = p;
 end
end
if i>n0
 disp ('method failed iteration to find the root')
end
c1=1-e^2;
c2=16*e^2+pi^2*c1;
c3=(bl/2/br)^2;
c4=1+2*e^2;
kxx=c3*4*pi*e*(pi^2+c2)/c1^2/c2;
kxy=c3*pi^2*(16*e^4-pi^2*c1^2)/c1^2.5/c2;
kyx=c3*(32*pi*e*c1+pi^3*c4*c1)*pi*c1^0.5/c1^3/c2;
kyy=c3*4*e*(32*pi*e^2*c1+pi^2*c4*c1)/c1^3/c2;
cxx=c3*2*pi^2*c1*(pi^2*c4-16*e^2)/c1^2/c2;
cxy=c3*8*pi*e*(pi^2+2*e^2*(pi^2-8))/c1^2/c2;
cyx=cxy;
cyy=c3*2*pi^2*(pi^2+2*(24-pi^2)*e^2+pi^2*e^4)/c1^2.5/c2;
da=[e cxx cyy kxx kyy cxy cyx kxy kyx rs som];
dat=[dat;da];
% Assembly of Bearing + Flexible Support Damping and Stiffness Matrices
```

```
K(1,1)=K(1,1)+kxx;
K(2,2)=K(2,2)+kyy;
K(1,2)=K(1,2)+kxy;
K(2,1)=K(2,1)+kyx;
K(s,s)=K(s,s)+kxx;
K(t,t)=K(t,t)+kyy;
K(s,t)=K(s,t)+kxy;
K(t,s)=K(t,s)+kyx;
C(1,1)=C(1,1)+cxx;
C(2,2)=C(2,2)+cyy;
C(1,2)=C(1,2)+cxy;
C(2,1)=C(2,1)+cyx;
C(s,s)=C(s,s)+cxx;
C(t,t)=C(t,t)+cyy;
C(s,t)=C(s,t)+cxy;
C(t,s)=C(t,s)+cyx;
```

FUNCTION STNADARD SHORT BEARING WITH DYNAMIC ECCENTRICITY

```
function [C,K,dat1,dat2]=SbrgDEccNMf(rs,X,C,K,dat1,dat2)

global dat dat1 dat2;
y=max(size(C));
s=y-3;
t=y-2;
lv = 6.9e-3;  %.069;
bl = .0285;   %.0254;
br = .0286;   %.0254;
bc = .000051; %.005 * .0254;
f =  222.5;    %22.68 * 9.81;
rps=rs/2/pi;
ovr=lv*rps*br*bl^3/2/f/bc^2;    % Ovrick Number
som=lv*rps*2*br^3*bl/f/bc^2;    % Sommerfeld Number

kxx1=0;, kyy1=0;, kxy1=0;, kyx1=0;, cxx1=0;, cyy1=0;, cxy1=0;, cyx1=0;
kxx2=0;, kyy2=0;, kxy2=0;, kyx2=0;, cxx2=0;, cyy2=0;, cxy2=0;, cyx2=0;
%  the eight linearized coeffecients calculations
e1=(abs(X(1))^2+abs(X(2))^2)^0.5/(bc*10e6);
q1=(1-e1^2);
Wr1=e1*(16*e1^2+pi^2*q1)^0.5/q1^2/(2*br/bl)^2;
att1=atan(pi*q1^0.5)/4/e1;
kxx1=( (e1/q1^2*sin(att1)^2) + (3*pi*e1^2/4*q1^2.5*sin(att1)*cos(att1)) + (2*e1*(1+e1^2)/q1^3*cos(att1)^2) );
kxy1=( (pi*(1+2*e1^2)/4/q1^2.5*sin(att1)^2) + (e1*(1+3*e1^2)/q1^3*sin(att1)*cos(att1)) +
(pi/4/q1^1.5*cos(att1)^2) );
kyx1=( (-pi/4/q1^1.5*sin(att1)^2) + (e1*(1+3*e1^2)/q1*sin(att1)*cos(att1)) -
(pi*(1+2*e1^2)/4/q1^2.5*cos(att1)^2) );
kyy1=( (2*e1*(1+e1^2)/q1^1.5*sin(att1)^2) - (3*pi*e1^2/4/q1^2.5*sin(att1)*cos(att1)) + (e1/q1^2*cos(att1)^2) );
cxx1=( (pi/2/q1^1.5*sin(att1)^2) + (4*e1/q1^2*sin(att1)*cos(att1)) + (pi*(1+2*e1^2)/2/q1^2.5*cos(att1)^2) );
cxy1=( (-4*e1/q1^2*sin(att1)^2) + (3*pi*e1^2/2/q1^2.5*sin(att1)*cos(att1)) - (e1/2/q1^2*cos(att1)^2) );
cyx1=cxy1;
cyy1=( (pi*(1+2*e1^2)/2/q1^2.5*sin(att1)^2) - (4*e1^2/q1^2*sin(att1)*cos(att1)) + (pi/2/q1^1.5*cos(att1)^2) );
da1=[e1 cxx1 cyy1 kxx1 kyy1 cxy1 cyx1 kxy1 kyx1 rs som];
dat1=[dat1 ; da1];
%  the eight linearized coeffecients calculations
```

```
e2=(abs(X(17))^2+abs(X(18))^2)^0.5/(bc*10e6);
q2=(1-e2^2);
Wr2=e2*(16*e2^2+pi^2*q2)^0.5/q2^2/(2*br/bl)^2;
att2=atan(pi*q2^0.5)/4/e2;
kxx2=4/Wr2/(2*br/bl)^2*( (e2/q2^2*sin(att2)^2) + (3*pi*e2^2/4*q2^2.5*sin(att2)*cos(att2)) +
(2*e2*(1+e2^2)/q2^3*cos(att2)^2) );
kxy2=4/Wr2/(2*br/bl)^2*( (pi*(1+2*e2^2)/4/q2^2.5*sin(att2)^2) + (e2*(1+3*e2^2)/q2^3*sin(att2)*cos(att2)) +
(pi/4/q2^1.5*cos(att2)^2) );
kyx2=4/Wr2/(2*br/bl)^2*( (-pi/4/q2^1.5*sin(att2)^2) + (e2*(1+3*e2^2)/q2*sin(att2)*cos(att2)) -
(pi*(1+2*e2^2)/4/q2^2.5*cos(att2)^2) );
kyy2=4/Wr2/(2*br/bl)^2*( (2*e2*(1+e2^2)/q2^1.5*sin(att2)^2) - (3*pi*e2^2/4/q2^2.5*sin(att2)*cos(att2)) +
(e2/q2^2*cos(att2)^2) );
cxx2=4/Wr2/(2*br/bl)^2*( (pi/2/q2^1.5*sin(att2)^2) + (4*e2/q2^2*sin(att2)*cos(att2)) +
(pi*(1+2*e2^2)/2/q2^2.5*cos(att2)^2) );
cxy2=4/Wr2/(2*br/bl)^2*( (-4*e2/q2^2*sin(att2)^2) + (3*pi*e2^2/2/q2^2.5*sin(att2)*cos(att2)) -
(e2/2/q2^2*cos(att2)^2) );
cyx2=cxy2;
cyy2=4/Wr2/(2*br/bl)^2*( (pi*(1+2*e2^2)/2/q2^2.5*sin(att2)^2) - (4*e2^2/q2^2*sin(att2)*cos(att2)) +
(pi/2/q2^1.5*cos(att2)^2) );
da2=[e2 cxx2 cyy2 kxx2 kyy2 cxy2 cyx2 kxy2 kyx2 rs som];
dat2=[dat2 ; da2];
K(1,1)=K(1,1)+kxx1;    %1.7513E7;
K(2,2)=K(2,2)+kyy1;
K(1,2)=K(1,2)+kxy1;
K(2,1)=K(2,1)+kyx1;
K(s,s)=K(s,s)+kxx2;
K(t,t)=K(t,t)+kyy2;
K(s,t)=K(s,t)+kxy2;
K(t,s)=K(t,s)+kyx2;
C(1,1)=C(1,1)+cxx1;
C(2,2)=C(2,2)+cyy1;
C(1,2)=C(1,2)+cxy1;
C(2,1)=C(2,1)+cyx1;
C(s,s)=C(s,s)+cxx2;
C(t,t)=C(t,t)+cyy2;
C(s,t)=C(s,t)+cxy2;
C(t,s)=C(t,s)+cyx2;
```

FUNCTION ROTATING FLUID MODEL WITH FLUID INERTIA AND DYNAMIC ECCENTRICITY

```
function [M,C,K,dat1,dat2]=BRDBrgDEccMf(rs,X,M,C,K,dat)

global dat dat1 dat2;
y=max(size(C));
s=y-3;
t=y-2;
kxx=0;, kyy=0;, kxy=0;, kyx=0;, cxx=0;, cyy=0;, cxy=0;, cyx=0; e=0;
P0=0;  % Supply Pressure
f=222.5; %50; %417.5;  %50  %Bearing Load
lv=6.9e-3;  %1e-5; %7
br=0.0285; %0.3;
bc=.000051; %0.0005;
bl=0.0285; %0.3;
dl=bc/br;
```

```
rps=rs/2/pi;
e=(abs(X(1))^2+abs(X(2))^2)^0.5/(bc*10e6);
phase=atan(X(2)/X(1))*180/pi;
de=(abs(X(21))^2+abs(X(22))^2)^0.5/(bc*10e6);
Cf=1-bl^2*br^2*(8+88*e^2+105*e^4+96*e^6)/40/(1-e^2)^3-17*bl^2*br^2*(16+824*e^2-166*e^4-
2311*e^6+1344*e^8+153*e^10)/13440/(1-e^2)^5;
elv=lv*Cf;
ovr=elv*rps*br*bl^3/2/f/bc^2;   % Ovrick Number
som=elv*rps*2*br^3*bl/f/bc^2;   % Sommerfeld Number
fv=lv/elv*( 0.5- dl^3*br^2/bl^2* (1+ (1/(1+sqrt(1-e^2)))) * (1-e^2)^1.5 ); % Fluid Average Circumferential Flow
Kb=2*pi*bl*P0;     % Dynamic Stiffness
Db=pi*bl^3*elv/dl^3/br^2/(1-e^2)^1.5;  % Dynamic Damping
C1=-pi*elv*bl^3*br*de*(1+2*e^2)/bc^3/(1-e^2)^2.5/e;   % Force X Component Ignoring Eccentricity Velocity
Mf=-C1/fv^2/rs^2;
W=f/bl; %/bl/2/br;
ww=W*bc^2/br^3/rs/elv;
ww=1/ww;
ck=W/bc;
ck=ww; %/bc;
%ck=1/ck;
cc=W/rs/bc;
cc=ww/rs; %/bc;
%cc=1/cc;
% the eight linearized coeffecients calculations
kxx=ck*(Kb-fv^2*rs^2*Mf);
kyy=kxx;
kxy=ck*(fv*rs*Db);
kyx=-kxy;
cxx=cc*Db;
cyy=cxx;
cxy=cc*(2*Mf*rs*fv);
cyx=-cxy;
da=[e cxx cyy kxx kyy cxy cyx kxy kyx rs phase];
dat1=[dat1;da];
M(1,1)=M(1,1)+Mf;
M(2,2)=M(2,2)+Mf;
K(1,1)=K(1,1)+kxx;    %1.7513E7;
K(2,2)=K(2,2)+kyy;
K(1,2)=K(1,2)+kxy;
K(2,1)=K(2,1)+kyx;
C(1,1)=C(1,1)+cxx;
C(2,2)=C(2,2)+cyy;
C(1,2)=C(1,2)+cxy;
C(2,1)=C(2,1)+cyx;

kxx=0;, kyy=0;, kxy=0;, kyx=0;, cxx=0;, cyy=0;, cxy=0;, cyx=0; e=0;
e=(abs(X(17))^2+abs(X(18))^2)^0.5/(bc*10e6);
phase=atan(X(2)/X(1))*180/pi;
de=(abs(X(37))^2+abs(X(38))^2)^0.5/(bc*10e6);
Cf=1-bl^2*br^2*(8+88*e^2+105*e^4+96*e^6)/40/(1-e^2)^3-17*bl^2*br^2*(16+824*e^2-166*e^4-
2311*e^6+1344*e^8+153*e^10)/13440/(1-e^2)^5;
elv=lv*Cf;
ovr=elv*rps*br*bl^3/2/f/bc^2;   % Ovrick Number
som=elv*rps*2*br^3*bl/f/bc^2;   % Sommerfeld Number
fv=lv/elv*( 0.5- dl^3*br^2/bl^2* (1+ (1/(1+sqrt(1-e^2)))) * (1-e^2)^1.5 ); % Fluid Average Circumferential Flow
Kb=2*pi*bl*P0;     % Dynamic Stiffness
Db=pi*bl^3*elv/dl^3/br^2/(1-e^2)^1.5;  % Dynamic Damping
```

```
C1=-pi*elv*bl^3*br*de*(1+2*e^2)/bc^3/(1-e^2)^2.5/e;   % Force X Component Ignoring Eccentricity Velocity
Mf=-C1/fv^2/rs^2;
W=f/bl; %/bl/2/br;
ww=W*bc^2/br^3/rs/elv;
ww=1/ww;
ck=W/bc;
ck=ww; %/bc;
%ck=1/ck;
cc=W/rs/bc;
cc=ww/rs; %/bc;
%cc=1/cc;
% the eight linearized coeffecients calculations
kxx=ck*(Kb-fv^2*rs^2*Mf);
kyy=kxx;
kxy=ck*(fv*rs*Db);
kyx=-kxy;
cxx=cc*Db;
cyy=cxx;
cxy=cc*(2*Mf*rs*fv);
cyx=-cxy;
da=[e cxx cyy kxx kyy cxy cyx kxy kyx rs phase];
dat2=[dat2;da];
M(s,s)=M(s,s)+Mf;
M(t,t)=M(t,t)+Mf;
K(s,s)=K(s,s)+kxx;
K(t,t)=K(t,t)+kyy;
K(s,t)=K(s,t)+kxy;
K(t,s)=K(t,s)+kyx;
C(s,s)=C(s,s)+cxx;
C(t,t)=C(t,t)+cyy;
C(s,t)=C(s,t)+cxy;
C(t,s)=C(t,s)+cyx;
```

FUNCTION SHAPE MATRICIES

```
syms z a
f1=sym('f1');
f2=sym('f2');
f3=sym('f3');
f4=sym('f4');
f5=sym('f5');
f6=sym('f6');
f7=sym('f7');
f8=sym('f8');
z=zeros(2,4);
a=[f1 f2 f3 f4;f5 f6 f7 f8];
N=[a z;z a]
m1=[1 0 0 0;0 0 0 0;0 0 1 0;0 0 0 0];
g1=[0 0 0 0;0 0 0 1;0 0 0 0;0 0 0 0];
m2=[0 0 0 0;0 1 0 0;0 0 0 0;0 0 0 1];
c1=[0 0 0 0;0 1 0 1;0 0 0 0;0 0 0 1];
k3=[1;0;1;0];
ms1=N'*m1*N
gs1=N'*g1*N
ms2=N'*m2*N
Dc1=N'*c1*N
Dv=N'*k3
```

```
syms z a
sf1=sym(1+a-a*z-3*z^2+2*z^3);
sf2=sym(2*z+a*z-4*z^2-a*z^2+2*z^3);
sf3=sym(a*z+3*z^2-2*z^3);
sf4=sym(-a*z-2*z^2+a*z^2+2*z^3);
sf5=sym(-6*z+6*z^2);
sf6=sym(1+a-4*z-a*z+3*z^2);
sf7=sym(6*z-6*z^2);
sf8=sym(-2*z+a*z+3*a*z^2);
dsf1=sym(-a-6*z+6*z^2);
dsf2=sym(2+a-8*z-2*a*z+6*z^2);
dsf3=sym(a+6*z-6*z^2);
dsf4=sym(-a-4*z+2*a*z+6*z^2);
dsf5=sym(-6+12*z);
dsf6=sym(-4-a+6*z);
dsf7=sym(6-12*z);
dsf8=sym(-2+a+6*a*z);
h11=420*expand(int(sf1*sf1,z,0,1))
h12=210*expand(int(sf1*sf2,z,0,1))
h13=420*expand(int(sf1*sf3,z,0,1))
h14=210*expand(int(sf1*sf4,z,0,1))
h22=105*expand(int(sf2*sf2,z,0,1))
h23=210*expand(int(sf2*sf3,z,0,1))
h24=105*expand(int(sf2*sf4,z,0,1))
h33=420*expand(int(sf3*sf3,z,0,1))
h34=210*expand(int(sf3*sf4,z,0,1))
h44=105*expand(int(sf4*sf4,z,0,1))
h55=30*expand(int(sf5*sf5,z,0,1))
h56=30*expand(int(sf5*sf6,z,0,1))
h57=30*expand(int(sf5*sf7,z,0,1))
h58=30*expand(int(sf5*sf8,z,0,1))
h66=30*expand(int(sf6*sf6,z,0,1))
h67=30*expand(int(sf6*sf7,z,0,1))
h68=30*expand(int(sf6*sf8,z,0,1))
h77=30*expand(int(sf7*sf7,z,0,1))
h78=30*expand(int(sf7*sf8,z,0,1))
h88=30*expand(int(sf8*sf8,z,0,1))
k11=30*expand(int(dsf1*dsf1,z,0,1))
k12=15*expand(int(dsf1*dsf2,z,0,1))
k13=30*expand(int(dsf1*dsf3,z,0,1))
k14=30*expand(int(dsf1*dsf4,z,0,1))
k22=7.5*expand(int(dsf2*dsf2,z,0,1))
k23=15*expand(int(dsf2*dsf3,z,0,1))
k24=7.5*expand(int(dsf2*dsf4,z,0,1))
k33=30*expand(int(dsf3*dsf3,z,0,1))
k34=15*expand(int(dsf3*dsf4,z,0,1))
k44=7.5*expand(int(dsf4*dsf4,z,0,1))
k55=expand(int(dsf5*dsf5,z,0,1))
k56=expand(int(dsf5*dsf6,z,0,1))
k57=expand(int(dsf5*dsf7,z,0,1))
k58=expand(int(dsf5*dsf8,z,0,1))
k66=expand(int(dsf6*dsf6,z,0,1))
k67=expand(int(dsf6*dsf7,z,0,1))
k68=expand(int(dsf6*dsf8,z,0,1))
k77=expand(int(dsf7*dsf7,z,0,1))
k78=expand(int(dsf7*dsf8,z,0,1))
k88=expand(int(dsf8*dsf8,z,0,1))
```

```
n1=12*expand(int(sf1,z,0,1))
n2=6*expand(int(sf2,z,0,1))
n3=12*expand(int(sf3,z,0,1))
n4=6*expand(int(sf4,z,0,1))

N =
[ f1, f2, f3, f4,  0,  0,  0,  0]
[ f5, f6, f7, f8,  0,  0,  0,  0]
[  0,  0,  0,  0, f1, f2, f3, f4]
[  0,  0,  0,  0, f5, f6, f7, f8]

ms1 =
[ (f1)*f1, (f1)*f2, (f1)*f3, (f1)*f4,        0,        0,        0,        0]
[ (f2)*f1, (f2)*f2, (f2)*f3, (f2)*f4,        0,        0,        0,        0]
[ (f3)*f1, (f3)*f2, (f3)*f3, (f3)*f4,        0,        0,        0,        0]
[ (f4)*f1, (f4)*f2, (f4)*f3, (f4)*f4,        0,        0,        0,        0]
[         0,        0,        0,        0, (f1)*f1, (f1)*f2, (f1)*f3, (f1)*f4]
[         0,        0,        0,        0, (f2)*f1, (f2)*f2, (f2)*f3, (f2)*f4]
[         0,        0,        0,        0, (f3)*f1, (f3)*f2, (f3)*f3, (f3)*f4]
[         0,        0,        0,        0, (f4)*f1, (f4)*f2, (f4)*f3, (f4)*f4]

gs1 =
[         0,        0,        0,        0,  (f5)*f5, (f5)*f6, (f5)*f7, (f5)*f8]
[         0,        0,        0,        0,  (f6)*f5, (f6)*f6, (f6)*f7, (f6)*f8]
[         0,        0,        0,        0,  (f7)*f5, (f7)*f6, (f7)*f7, (f7)*f8]
[         0,        0,        0,        0,  (f8)*f5, (f8)*f6, (f8)*f7, (f8)*f8]
[         0,        0,        0,        0,        0,        0,        0,        0]
[         0,        0,        0,        0,        0,        0,        0,        0]
[         0,        0,        0,        0,        0,        0,        0,        0]
[         0,        0,        0,        0,        0,        0,        0,        0]

ms2 =
[ (f5)*f5, (f5)*f6, (f5)*f7, (f5)*f8,        0,        0,        0,        0]
[ (f6)*f5, (f6)*f6, (f6)*f7, (f6)*f8,        0,        0,        0,        0]
[ (f7)*f5, (f7)*f6, (f7)*f7, (f7)*f8,        0,        0,        0,        0]
[ (f8)*f5, (f8)*f6, (f8)*f7, (f8)*f8,        0,        0,        0,        0]
[         0,        0,        0,        0, (f5)*f5, (f5)*f6, (f5)*f7, (f5)*f8]
[         0,        0,        0,        0, (f6)*f5, (f6)*f6, (f6)*f7, (f6)*f8]
[         0,        0,        0,        0, (f7)*f5, (f7)*f6, (f7)*f7, (f7)*f8]
[         0,        0,        0,        0, (f8)*f5, (f8)*f6, (f8)*f7, (f8)*f8]


Dc1 =
[ (f5)*f5, (f5)*f6, (f5)*f7, (f5)*f8,  (f5)*f5, (f5)*f6, (f5)*f7, (f5)*f8]
[ (f6)*f5, (f6)*f6, (f6)*f7, (f6)*f8,  (f6)*f5, (f6)*f6, (f6)*f7, (f6)*f8]
[ (f7)*f5, (f7)*f6, (f7)*f7, (f7)*f8,  (f7)*f5, (f7)*f6, (f7)*f7, (f7)*f8]
[ (f8)*f5, (f8)*f6, (f8)*f7, (f8)*f8,  (f8)*f5, (f8)*f6, (f8)*f7, (f8)*f8]
[         0,        0,        0,        0, (f5)*f5, (f5)*f6, (f5)*f7, (f5)*f8]
[         0,        0,        0,        0, (f6)*f5, (f6)*f6, (f6)*f7, (f6)*f8]
[         0,        0,        0,        0, (f7)*f5, (f7)*f6, (f7)*f7, (f7)*f8]
[         0,        0,        0,        0, (f8)*f5, (f8)*f6, (f8)*f7, (f8)*f8]


Dv =

[ (f1)]
[ (f2)]
```

[(f3)]
[(f4)]
[(f1)]
[(f2)]
[(f3)]
[(f4)]

h11 = 156+294*a+140*a^2
h12 = 22+77/2*a+35/2*a^2
h13 = 54+126*a+70*a^2
h14 = -13-63/2*a-35/2*a^2
h22 = 4+7*a+7/2*a^2
h23 = 13+63/2*a+35/2*a^2
h24 = -3-7*a-7/2*a^2
h33 = 156+294*a+140*a^2
h34 = -22-77/2*a-35/2*a^2
h44 = 4+7*a+7/2*a^2
h55 = 36
h56 = 3-15*a
h57 = -36
h58 = -42*a+30
h66 = 4+5*a+10*a^2
h67 = -3+15*a
h68 = -37/2*a+25/2*a^2+5
h77 = 36
h78 = 42*a-30
h88 = 109*a^2-130*a+40

k11 = 36+60*a+30*a^2
k12 = 3
k13 = -36-60*a-30*a^2
k14 = 6
k22 = 4+5*a+5/2*a^2
k23 = -3
k24 = -1-5*a-5/2*a^2
k33 = 36+60*a+30*a^2
k34 = -3
k44 = 4+5*a+5/2*a^2
k55 = 12
k56 = 6
k57 = -12
k58 = 6*a
k66 = 4+2*a+a^2
k67 = -6
k68 = a-4*a^2+2
k77 = 12
k78 = -6*a
k88 = 19*a^2-16*a+4

n1 = 6+6*a
n2 = 1+a
n3 = 6+6*a
n4 = -1-a

TABLE B.1 – SYMPOLS USED IN MATLAB PROGRAM

File Name		
FRM Analysis.m	a	
FRM Analysis.m	b	
FRM Analysis.m	bc	C Bearing radial clearance
FRM Analysis.m	bhm	M_b Bearing Housing Mass
RotorConst.m	bl	l_b Bearing Length = $L / D \times 2 \times r_b$
RotorConst.m	bld	$L_b = {M_b g}/{2}$ Bearing Load
RotorConst.m	br	r_b Bearing Radius = $C + r_s$
RotorConst.m	bsl	W_r Bearing static load = $\frac{L_b}{2 l_b r_b}$
RotorConst.m	bsm	$M_b = \frac{M_s + M_d}{2}$ Bearing Static mass
FRM.m	C	System Damping Matrix
BearingMat.m	c1	
BearingMat.m	c2	
BearingMat.m	c3	
BearingMat.m	cbxx	
BearingMat.m	cbxy	
BearingMat.m	cbyx	
BearingMat.m	cbyy	
RotorConst.m	cf	κ Shape function correction factor = $\frac{6(1+\nu)}{7+6\nu}$
ShapeMat.m	cgt	
BearingMat.m	Chb	
ShapeMat.m	Cid	
ShapeMat.m	cj	
FoundationMat.m	Cjj	
RotorConst.m	cmu	
ShapeMat.m	cnt1	
FoundationMat.m	cnt2	
RigidModeMat.m	cnt3	
ShaftMat.m	cnt4	
RotorConst.m	cr	
RotorConst.m	crp	
RotorConst.m	csa	A_e Shaft element cross sectional area = πr_s^2
RotorConst.m	ct	
RotorConst.m	ctp	
FRM Analysis.m	cx	C_{fx} Frame (Bearing support) x-dir damping
FRM Analysis.m	cy	C_{fy} Frame (Bearing support) y-dir damping
BearingMat.m	da	
FRM Analysis.m	dat	
IntDampMat.m	Dd	
FRM Analysis.m	dh	d_h Disk thickness

IntDampMat.m	Dh	
RotorConst.m	dit	I_{as} Disk axial moment of inertia=$2\times I_{ds}$
RotorConst.m	dm	M_d Disk mass =$\pi r_d^2 d_h \rho$
ShapeMat.m	DMr	
ShapeMat.m	dmr	
ShapeMat.m	DMt	
ShapeMat.m	dmt	
RotorConst.m	dof	$N=4\times(n_s+1)+2\times n_b$ Degrees of freedom
RotorConst.m	dpi	I_{ds} Disk lateral (diameteral) moment of inertia=$\frac{M_d r_d^2}{2}$
FRM Analysis.m	dr	r_d Disk Radius
FRM Analysis.m	dt	Δt Time step
IntDampMat.m	Dv	
BearingMat.m	e	Static Eccentricity
FRM Analysis.m	ex	e_x Mass Unbalance Location on Disk x-dir
FRM Analysis.m	ex1	e_{x1} Mass unbalance location on shaft element x-dir
FRM Analysis.m	ex2	e_{x2} Mass unbalance location on shaft element x-dir
FRM Analysis.m	ey	e_y Mass unbalance location on disk y-dir
FRM Analysis.m	ey1	e_{y1} Mass unbalance location on shaft element y-dir
FRM Analysis.m	ey2	e_{y2} Mass unbalance location on shaft element y-dir
RigidModeMat.m	Fb	
FRM Analysis.m	fbx	F_{fx} Frame (Bearing support) x-dir force
FRM Analysis.m	fby	F_{fy} Frame (Bearing support) y-dir force
DiskMat.m	Fd	
DiskMat.m	Fda	
DiskMat.m	Fdb	
DiskMat.m	Fdc	
FoundationMat.m	Ff	
IntDampMat.m	Fg	
RotorConst.m	Fi	f_i Static balance force = $M_s g$
ShaftMat.m	Fu	Shaft element force vector
RigidModeMat.m	Gb	
DiskMat.m	Gd	
ShaftMat.m	Ge	Shaft Gyro Matrix
FoundationMat.m	Gf	
ShapeMat.m	grv	
RotorConst.m	h(XX)	$\Psi_x \Psi_x$ Shape functions $x=1,..8$
DiskMat.m	Hd	
RotorConst.m	hdf	$\sin\alpha=\frac{\eta}{\sqrt{1+\eta^2}}$ Hystersis Damping Neutral axis lag
DiskMat.m	Hg	
BearingMat.m	i	

RotorConst.m	indx	
FRM.m	K	System Stiffness Matrix
RotorConst.m	k(XX)	$\Psi'_x\Psi'_x$ Differential Shape functions $x = 1,..8$
RigidModeMat.m	Kb	
BearingMat.m	kbxx	
BearingMat.m	kbxy	
BearingMat.m	kbyx	
BearingMat.m	kbyy	
ShaftMat.m	Ke	Shaft element Stiffness Matrix
FoundationMat.m	Kf	
BearingMat.m	Khb	
FRM Analysis.m	kx	K_{fx} Frame (Bearing support) x-dir stiffness
FRM Analysis.m	ky	K_{fy} Frame (Bearing support) y-dir stiffness
RotorConst.m	l	l_e Shaft element lenght = $\frac{l_s - d_h}{n_s}$
FRM Analysis.m	ld	$L:D$ Ratio for Hydrodynamic Bearings
FRM Analysis.m	lf	η Shaft Material loss factor
FRM Analysis.m	lv	μ Lubricant Dynamic Viscsity
FRM.m	M	System Mass Matrix
RotorConst.m	m(X)	Unbalance force shape transformation coefficients x=1,..8
ShapeMat.m	Mac	
ShapeMat.m	mac	
ShapeMat.m	mas	
ShapeMat.m	Mas	
RigidModeMat.m	Mb	
DiskMat.m	Md	
ShaftMat.m	Me	Shaft element Mass Matrix
FoundationMat.m	Mf	
ShapeMat.m	Mg	
RotorConst.m	mi	I_d Shaft element diameteral moment of inertia = $\frac{\pi r_s^4}{4}$
RotorConst.m	minv	
FRM Analysis.m	mo	m_o Mass unbalance on disk
ShapeMat.m	mr	
ShapeMat.m	Mr	
ShapeMat.m	mt	
ShapeMat.m	Mt	
ShaftMat.m	n	Counter
FRM Analysis.m	n0	
FRM Analysis.m	noe	n_s number of elements in shaft
FoundationMat.m	num1	
RotorConst.m	num2	
BearingMat.m	p	
FRM Analysis.m	P	P Shaft Axial Load
RotorConst.m	pmi	J_d Polar diameteral moment of inertia $=\rho I_d$
FRM Analysis.m	pr	ν Poisson Ratio
FRM.m	Q	System Force Vector

RotorConst.m	q	
BearingMat.m	qb	
BearingMat.m	qb1	
RotorConst.m	qt	
ShapeMat.m	ri	
FoundationMat.m	rii	
FRM.m	rps	Rotations per Second
FRM.m	rs	Ω Shaft speed (rad/s)
FRM Analysis.m	sd	c_i Shaft Internal Viscous Damping
RotorConst.m	sdc	Φ Shear deformation coefficient $= \frac{12EI_d}{\kappa A_e G l_e^2}$
RotorConst.m	sem	M_e Shaft element mass $= \rho A_e$
BearingMat.m	sfn	Sommerfeld Number
FRM Analysis.m	shm	G Shear Modulus
FRM Analysis.m	sl	l Shaft Lenght
RotorConst.m	sm	M_s Shaft mass $= \rho A_e l_s$
FRM Analysis.m	smd	ρ Shaft mass density
FRM Analysis.m	sr	r_s Shaft Radius
FRM.m	sss	Rotational speed (rpm)
FRM.m	t	Time
FRM Analysis.m	tf	t_f Final time
RotorConst.m	tj	
FRM Analysis.m	to	t_0 Initial Time
FRM Analysis.m	tol	
RotorConst.m	ww	
RotorConst.m	X0	
RotorConst.m	x0	
FRM Analysis.m	ym	E Young Modulus of elasticity
ShapeMat.m	ze	

NOMENCLATURE

ε	*Shaft Eccentricity Ratio*
e	*Shaft Eccentricity*
c	*Bearing Radial Clearance*
λ	*Fluid Average Circumferential Velocity*
Ω	*Shaft Spin Velocity "Speed"*
$X_r Y_r Z_r$	*Inertial (Reference) Coordinate System*
$X_j Y_j Z_j$	*Inertial (Reference) Coordinate System*
θ	*Angular Deformation around X-axis*
ψ	*Angular Deformation around Y-axis*
R_{jx}, R_{jy}	*Journal Center Displacements within the Bearing*
ω_j	*Angular Velocity Vector of Journal with respect (wrt) Stationary Body Coordinates*
$\bar{\omega}_j$	*Angular Velocity Vector of Journal with respect (wrt) Rotating Body Coordinates*
$r_j, \dot{r}_j, \ddot{r}_j$	*Position, Velocity & Acceleration Vectors of a Shaft Material Point wrt Reference Frame*
u_j	*Position Vector of a Shaft Material Point wrt Journal Reference Frame in Stationary Coordinates*
$\bar{u}_j$	*Position Vector of a Shaft Material Point wrt Journal Reference Frame in Rotating Coordinates*
A_j, A_j^T	*Transformation Matrices from Stationary to Rotating Coordinates and vise versa*
ω	*Instantaneous Angular Velocity Vector*

M_x, M_y, M_z	*Moments of Shaft Element in Cartesian Coordinates*
I_d	*Diameteral Moment of Inertia*
I_a	*Polar Moment of Inertia*
H_G	*Angular Momentum*
γ_a	*Shear Angle*
V_s	*Shear Force*
κ	*Shear Correction Factor*
A	*Cross Sectional Area*
G	*Shear Modulus*
E	*Young's Modulus*
I	*Moment of Inertia*
m	*Shaft Element Mass*
ρ	*Shaft Element Mass Density*
Φ	*Transverse Shear Correction Constant*
N	*Shape Transformation Matrix*
Ψ_i	*Shape Transformation Functions* $(i = 1,2,..8)$
f_n	*Natural Frequency*
σ	*Stress*
ε	*Strain*
E^*	*Complex Modulus of Elasticity*
η	*Shaft Material Loss Factor*

δ	*Logarithmic Decrement*
$[Dv]$	*Internal Viscous Damping*
c_i	*Internal Viscous Damping Coefficient*
τ	*Shear Stress*
γ	*Shear Strain*
T	*Kinetic Energy*
V	*Potential Energy*
$\{q\}$	*Global Displacements Vector*
$\{d\}$	*Nodal Displacement Vector*
a_x, a_y	*Shaft Element Imbalance Location*
m_s	*Shaft mass*
m_{ud}, m_{us}	*Imbalance Mass (d for Disk & s for Shaft)*
e_x, e_y	*Disk Imbalance Location*
r_f	*Shaft Material Point Position Vector wrt Foundation*
R_b	*Bearing Housing Position Vector*
c_b	*Bearing Center*
c_j	*Journal Center*
c_x, c_y	*Foundation Damping in the X & Y Directions*
k_x, k_y	*Foundation Stiffness in the X & Y Directions*
μ	*Lubricant Viscosity*

$\vec{V}_f$	*Fluid Velocity Vector* $[u, v, w]$ *in X, Y & Z Directions Respectively*
Λ	*Volumetric Dialation of Fluid* $= div\vec{V}$
ρ_f	*Fluid Mass Density*
l_b	*Bearing Length*
h	*Fluid Film Thickness*
R_x, R_y, R_z	*Reynolds Numbers (X, Y & Z Directions)*
σ_s	*Squeeze Number*
b, l, h	*Bearing Length in (X, Y & Z Directions Respectively)*
Φ_l	*Dynamic Load Direction*
Φ	*Attitude Angle*
W_r	*Bearing Load*
λ_k	*Bearing Length/Radius Ration*
k_{xx}, k_{yy}	*Bearing Direct Stiffness Coefficients (Dimensional)*
k_{xy}, k_{yx}	*Bearing Cross Coupled Stiffness Coefficients (Dimensional)*
c_{xx}, c_{yy}	*Bearing Direct Damping Coefficients (Dimensional)*
c_{xy}, c_{yx}	*Bearing Cross Coupled Damping Coefficients (Dimensional)*
m_a	*Bearing Housing Mass*
K_B	*Bearing Radial Stiffness*
S	*Sommerfeld Number*
$[K]$	*Global System Stiffness Matrix*

$[M]$	*Global System Mass Matrix*
$[C]$	*Global System Damping Matrix*
k_Q	*Quadrature Stiffness*
k_D	*Direct Stiffness*

VITA

Akram Awni Mohammed Hamad Rabayah is a graduate of King Fahd University of Petroleum and Minerals, Dhahran, Saudi Arabia in 1991 where he obtained his bachelors degree in Systems Engineering, Automation option. Later he joined Bechtel/CCC an Engineering & Construction consortium to build and commission oil and gas industrial plants in Kingdom of Saudi Arabia. In 1993 Akram joined the industry leader in rotating machinery vibration protection and mechanical condition management systems, Bently Nevada Corporation. He held various positions from applications engineering, product service, solution and sales specialist to services management. His work included the training and joint work with the Bently Rotor Dynamics Research Corp in Nevada, USA on the subjects of fluid film bearing control and stability and other research subjects driven widely by the research company to its parent international company Bently Nevada Corporation. In 1997 Akram started his masters degree in Systems Engineering and after three years in the program transferred to Mechanical Engineering department where he finished course requirements both in undergraduate and graduate programs.